

University of Montana

ScholarWorks at University of Montana

Graduate Student Theses, Dissertations, &
Professional Papers

Graduate School

2011

SYNTHESIS OF N_B-ARYL-ASPARTAMIDES, N_a-ARYLAMIDE- ASPARTATES, AND HYDROXY-L-PROLINE DERIVATIVES AS INHIBITORS OF AMINO ACID TRANSPORT FOR EVALUATING THE GLUTAMINE / GLUTAMATE CYCLE

Brent Russell Lyda
The University of Montana

Follow this and additional works at: <https://scholarworks.umt.edu/etd>

Let us know how access to this document benefits you.

Recommended Citation

Lyda, Brent Russell, "SYNTHESIS OF N_B-ARYL-ASPARTAMIDES, N_a-ARYLAMIDE-ASPARTATES, AND HYDROXY-L-PROLINE DERIVATIVES AS INHIBITORS OF AMINO ACID TRANSPORT FOR EVALUATING THE GLUTAMINE / GLUTAMATE CYCLE" (2011). *Graduate Student Theses, Dissertations, & Professional Papers*. 942.

<https://scholarworks.umt.edu/etd/942>

This Dissertation is brought to you for free and open access by the Graduate School at ScholarWorks at University of Montana. It has been accepted for inclusion in Graduate Student Theses, Dissertations, & Professional Papers by an authorized administrator of ScholarWorks at University of Montana. For more information, please contact scholarworks@mso.umt.edu.

SYNTHESIS OF N_β-ARYL-ASPARTAMIDES, N_α-ARYLAMIDE-ASPARTATES,
AND HYDROXY-L-PROLINE DERIVATIVES AS INHIBITORS OF AMINO ACID
TRANSPORT FOR EVALUATING THE GLUTAMINE / GLUTAMATE CYCLE.

By

BRENT RUSSELL LYDA

Dissertation

presented in partial fulfillment of the requirements
for the degree of

Doctor of Philosophy
in Pharmacology / Pharmaceutical Sciences

The University of Montana
Missoula, MT

May 2011

Approved by:

Graduated School

Dr. Nicholas Natale, Chair
Department of Biomedical and Pharmaceutical Sciences

Dr. Michael Kavanaugh,
Department of Biomedical and Pharmaceutical Sciences

Dr. Richard Bridges
Department of Biomedical and Pharmaceutical Sciences

Dr. Charles Thompson
Department of Biomedical and Pharmaceutical Sciences

Dr. Howard Beall
Department of Biomedical and Pharmaceutical Sciences

Dr. J.B. Alexander (Sandy) Ross
Department of Chemistry and Biochemistry

Acknowledgments

First of all I thank all those who have contributed to this work through their efforts to evaluate and characterize the biological activity of the compounds which I and my advisor have designed and synthesized at the University of Montana, including Ben Seaver and Ran Ye. I thank Dr. Greg Leary for his hard work, enthusiasm, and intellectual input that he has provided towards fulfilling the group's project goal(s); particularly, his involvement in the development of ASCT inhibitors. Thank you to Dr. Dave Holley and Dr. Mike Braden for their assistance involving the computational modeling as well as Professor Gerdes for use of the computational core. Thank you to Beverly Parker for her patience in dealing with all of my LC-MS samples. Thank you to my research advisory committee including but not limited to Professor Kavanaugh and Professor Bridges for their involvement in our group projects, Professor Natale for the synthetic discussions and help regarding organic synthesis, and Professor Thompson for his support and use of his group's LC-MS. I give thanks to the Department of Biomedical and Pharmaceutical Science for their financial support and the Department of Chemistry for the use of their NMR facility.

Most of all I am thankful for the support of my family including my mother, my father, my sister Jennene and above all my wife Rosemary for her patience and fortitude. Lastly, it is with great sorrow to say goodbye to my former advisor Dr. Christopher Sean Esslinger. He was the greatest of mentor's, he was my boss, my colleague and my friend, and I regret that all of our work together ends here. Farewell....

Table of Contents

| | |
|--|------|
| Acknowledgments. | ii |
| Table of Contents. | iii |
| List of Figures. | iv-v |
| List of Tables. | vi |
| List of Schemes. | vii |
| Chapter 1. Introduction: | |
| 1.1 The glutamine / glutamate cycle. | 1 |
| 1.2 System A and ASC glutamine transporters / function / inhibitors. | 6 |
| Manuscripts: | |
| Chapter 2: Synthesis of β -aryl-aspartamides & α -aryl-amide aspartates as pharmacologic tools for evaluating amino acid transporters. | 20 |
| Chapter 3: Derivatives of trans-hydroxy-L-proline: Inhibitors of the neutral amino acid transporters ASCT1 and ASCT2. | 104 |
| References. | 213 |
| Appendix A: NMR spectra of final product β -aryl-aspartamides & α -aryl-amide aspartates. | 221 |
| Appendix B: NMR spectra of hydroxy-L-proline derivatives. | 243 |

List of Figures

Chapter 1. Introduction:

- Figure 1. Glutamatergic neuronal synapse3
- Figure 2. GltPH ligand bound trimer13
- Figure 3. ASCT2 transport regulation of mTOR18

Manuscripts:

Chapter 2: Synthesis of β -aryl-aspartamides & α -aryl-amide aspartates as pharmacologic tools for evaluating amino acid transporters

- Figure 1. Synthesized β -aryl-aspartamides and α -aryl-amide aspartates25
- Figure 2. Alpha and beta isomers produced from nucleophilic addition of an aryl amine (X) to N-tBoc-aspartic-anhydride. 28
- Figure 3. Dose response curves showing fractional block of radiolabeled ^3H -L-alanine uptake at ASCT2 or fractional block of L-glutamine current at EAAT3 by aryl-aspartamides.30
- Figure 4. CSE72 dose response (μM) showing percent block of a 3 μM L-Glu current: hEAAT1 (diamonds), hEAAT2 (squares), and hEAAT3 (circles) @ (-60 mV).30
- Figure 5. Aryl-aspartamides CSE84, CSE79, CSE99 at 30 mg/kg or aryl-glutamide CSE102 tested in rat spinal nerve ligation model over time course of 20 min 32
- Figure 6. CSE67 shows a greater effect than does CSE84 at 20 mg/kg measure by paw withdrawal threshold; A. Rat spinal nerve ligation model; B. CSE84 dose response in rat spinal nerve ligation model. 33

Chapter 3: Derivatives of *trans*-hydroxy-L-proline: Inhibitors of the neutral amino acid transporters ASCT1 and ASCT2.

| | |
|---|-----|
| Figure 1. EAAT inhibitors. | 108 |
| Figure 2. L-[3H]-alanine efflux over 20 minute time course in presence of <i>trans</i> -3-hydroxy-L-proline, L-alanine, or L-glutamine and water injected oocytes. | 115 |
| Figure 3. A. hASCT1 dose response curve for substrate activated anion currents using two-electrode voltage clamp of <i>Xenopus laevis</i> oocytes. B. mASCT2 dose response curve for substrate activated anion currents using two-electrode voltage clamp of <i>Xenopus laevis</i> oocytes. | 117 |
| Figure 4. Synthesized substituted prolinols for biological testing as inhibitors of the ASC transporters. | 120 |
| Figure 5. Hydroxy proline derivative CSE 121 and CSE 122 block a leak current in mASCT2 and hASCT1, opposite the current induced by substrate. | 122 |
| Figure 6. The leak current in hASCT1 and mASCT2 has a saturable block revealed by increasing concentrations of CSE 131, CSE 130, CSE 122, CSE 121, CSE 118, and CSE 115. | 123 |
| Figure 7. CSE121 docked into a mouse ASCT2 homology model. | 131 |
| Figure 8. Crystal structure of GltPH with TBOA bound and intermolecular interactions in yellow dotted lines. | 132 |
| Figure 9. CSE113 and CSE121 overlay in mouse ASCT2 homology model. | 133 |
| Figure 10. CSE130 and CSE131 overlay docked into ASCT2 homology model. | 135 |
| Figure 11. CSE 131 docked in ASCT2 homology model depicting surface density. | 136 |
| Figure 12. Substituted prolinol targets. | 144 |
| Figure 13. Proton and carbon numbering scheme used in ¹ H-NMR & ¹³ C-NMR assignments. | 145 |

| | |
|--|-----|
| Figure 14. gCOSY of CSE 122. | 146 |
| Figure 15. Synthesized ether substituted prolinols. | 162 |
| Figure 16. Regioselective addition and ring opening of protected <i>trans</i> - and <i>cis</i> -3,4-epoxy-L-prolines. | 165 |
| Figure 17. Synthesized alkyl, aryl and phenol-ether prolinols. | 190 |

List of Tables

Manuscripts:

Chapter 2: Synthesis of β -aryl-aspartamides & α -aryl-amide aspartates as pharmacologic tools for evaluating amino acid transporters

Table 1. K_i estimated using the Cheng- Prusoff conversion of IC_{50} values obtained from screening CSE aspartamides across various amino acid transporters. 29

Chapter 3: Derivatives of *trans*-hydroxy-L-proline: Inhibitors of the neutral amino acid transporters ASCT1 and ASCT2.

Table 1. Actual * or estimated K_i in μ M derived from inhibition of tonic anion leak by first and second generation prolinols in *Xenopus* oocytes expressing human ASCT1 or mouse ASCT2. 126

Table 2. Actual K_i 's of third generation prolinols as lead inhibitors of ASCT1 and ASCT2.128

List of Schemes

Manuscripts:

Chapter 2: Synthesis of β -aryl-aspartamides & α -aryl-amide aspartates as pharmacologic tools for evaluating amino acid transporters

Scheme 1. Synthesis of β -aryl-aspartamides and α -arylamide-aspartates. 26

Chapter 3: Derivatives of *trans*-hydroxy-L-proline: Inhibitors of the neutral amino acid transporters ASCT1 and ASCT2.

Scheme 1. Synthesis of N-Cbz-*trans*- and *cis*-3,4-epoxy-proline-benzyl ester. 150

Scheme 2. Synthesis of 3,4-dehydroprolines. 157

Scheme 3. Synthesis of ether substituted prolinols. 163

Scheme 4. Synthesis of alkyl, aryl or phenol-ether prolinols. 191

Scheme 5. Synthesis of 4-substituted-4-hydroxy-prolines. 204

1.1 Glutamine / Glutamate cycle:

The glutamine / glutamate cycle is a highly regulated system found in the central / peripheral nervous system that's function is thought to involve the shuttling of glutamate and glutamine in or out of cells through a diversity of cell membrane spanning amino acid transporters [Bröer and Brookes 2001; Heckel *et al.* 2003; Gegelashvili, G.; and Schousboe 1997]. The cycle's primary role within the central nervous system (CNS) is the recycling of synaptically released L-glutamate, the primary excitatory amino acid involved in neurotransmission [Beryl *et al.* 1968, Danbolt, 2001]. Following vesicular release of L-glutamate at a glutamatergic neuronal synapse, glutamate is free to bind and activate the glutamate gated ionotropic receptors NMDA (N-methyl-D-aspartate), AMPA (alpha-amino-3-hydroxy-5-methyl-4-isoxazole-4-propionic acid receptor) and kainate receptors (KA) or the metabotropic glutamate receptors (mGluR's) that may be locally present. The ionotropic glutamate receptors are first and foremost ligand gated ion channels that are thought to be responsible for mediating excitatory neurotransmission involved in learning and memory, cell-cell communication, and synaptic plasticity. The mGluR's on the other hand are glutamate activated G-protein coupled receptors that are thought to both modulate ionotropic glutamate receptors and function in the regulation of gene expression through downstream activation of protein kinase C or down regulation of adenylyl cyclase. Additionally, mGluRs have also been suggested to affect synaptic plasticity.

Glutamatergic signaling is terminated by rapid sequestering and clearing of L-glutamate via the excitatory amino acid transporters (EAATs (subtypes 1-5)) expressed on peri-synaptic astrocytes or neuron (post or pre-synaptic) [Cousin and Robinson 2000; Danbolt 2001]. At this point there are two divergent paths which L-glutamate may take. L-glutamate may be translocated into the pre-synaptic neuron by EAAT-3 [Nieoullon *et al.* 2006] and shuttled into a glutamate containing vesicle by the vesicular glutamate transporter (VGLUT) [Takamori 2006] therefore ready for the next signaling event. Alternatively, if taken up by glial cell where EAAT1 and EAAT-2 are generally expressed [Arriza *et al.* 1994; Lehre *et al.* 1995; Chaudhry *et al.*, 1995], L-glutamate can be converted to L-glutamine by the enzyme glutamine synthetase. Glutamine, while highly profuse in plasma and cerebral spinal fluid (CSF) at 0.13-0.5 mM [Jacobson *et al.* 1985; ErcinÅska and Silver 1990; Xu *et al.* 1998], is thought to act in the cycle as an intermediate of L-glutamate to be safely shuttled between glial cell to CSF and ultimately back to the neuron where it can be converted to glutamate by the enzyme glutaminase. There are a number of amino acid transporters which are suggested to take part in the shuttling of glutamine between glia (astrocyte) cell and neuron. The neutral amino acid transporters ASCT2, SN1, LAT2, and ATA2 have all been thought to be involved in the transport of glutamine in or out of astrocytes and into the CSF [Bröer and Brookes 2001; Gliddon *et al.* 2009]. Glutamine is then shuttled into the pre-synaptic neuron via ATA1, ATA2, LAT1 / LAT2 or ASCT2 transporter [Heckel *et al.* 2003; Bak *et al.* 2006] where it is converted to glutamate catalyzed by the enzyme glutaminase. Glutamate is then

concentrated into a glutamate containing vesicle by VGLUT, thus completing the cycle (Figure 1).

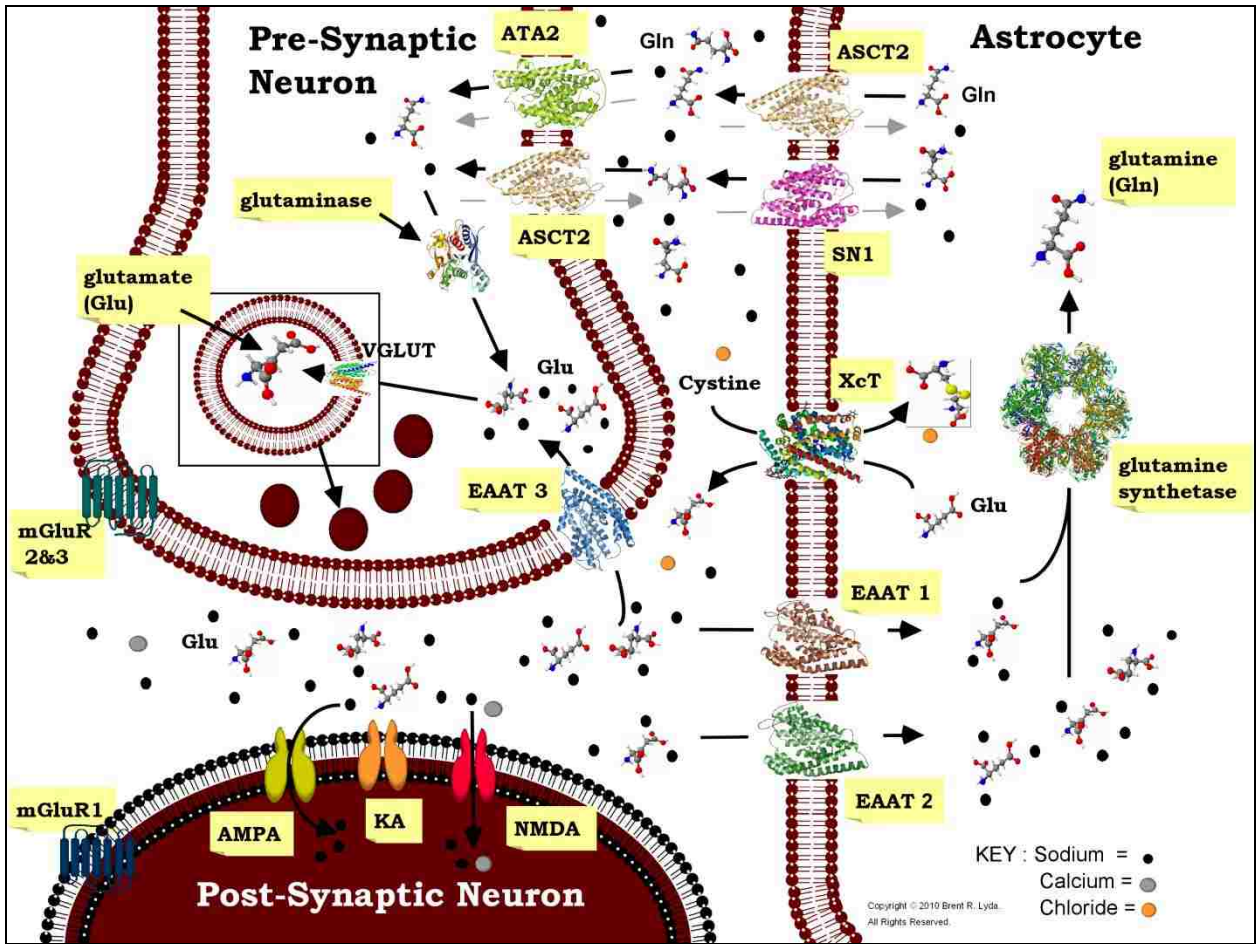


Figure 1: Glutamatergic neuronal synapse – Illustrating the glutamine / glutamate cycle.

Impairment of the glutamate / glutamine cycle's proper functioning has been implicated in the progression of a few pathological disease processes such as neurodegenerative diseases, and even cancer [Albrecht *et al.* 2007]. Dysregulation of the cycle may lead to excessive accumulation of L-glutamate at neuronal synapses or excessive spillage in other extracellular spaces which may lead to cell damage / death. This damage is thought to occur by a mechanism known as excitotoxicity, where prolonged activation of the glutamate activated ionotropic receptors AMPA and NMDA leads to excessive Ca^{2+} and Na^{+} influx that triggers a cascade of intracellular events which in turn leads to cell death by necrosis or apoptosis. The continuing release of glutamate can then lead to the spreading of this process and damage in other parts of the CNS. Therefore the dysfunction of cycle has been suggested to play an integral role in many proposed models of pathologic mechanism or consequent CNS damage that occurs in the neurodegenerative diseases Alzheimer's, Parkinson's, and amyotrophic lateral sclerosis (ALS) [Walton and Dodd 2007]. Though, it is not clear whether dysfunction of the glutamate / glutamine cycle is the pathological cause or a downstream effect resulting in chronic CNS damage that occurs in neurodegenerative diseases. The link between the cycle and glutamate mediated chronic CNS damage as cause of neurodegeneration is still quite valid especially considering that allosteric antagonists of NMDA, such as memantine, are an effective preventative measure and treatment for Alzheimer's related CNS damage [Walton and Dodd 2007]. More directly, the ischemic injury that occurs following stroke or traumatic brain injury is arguably the result of when the Gln / Glu

cycles proper functioning and capacity is overwhelmed. Likewise, the damage that occurs as a result of an epileptic seizure seems also to be dependant upon the proper functioning of the glutamine / glutamate cycle [Tani *et al.* 2010].

Glutamine availability, supplied through the Glu/Gln cycle, has shown to be essential for the growth of some highly prolific cell lines such as tumors [Bode, 2002], Thus indicating a role for its regulation in cancer therapy. The cycle employs ligand selective membrane bound transporters to maintain physiologic concentrations of glutamine needed to grow and proliferate such as found in gliomas over-expressing neutral amino acid transporters LAT1 and ASCT2 [Fuchs *et al.* 2005]. The physiologic need for glutamine is explained by the high demand of rapidly dividing cells for amino acids such as glutamine / glutamate to provide energy via the Krebs cycle of which the transporters involved in the Gln / Glu cycle supply [Baggetto 1992]. Being that Gln is the most abundant amino acid in mammalian plasma, glutamine is in steady supply to be converted by glutaminases to glutamate for production of glutathione a neuroprotective antioxidant, or α -ketoglutarate, a starting material for energy in the Krebs cycle [Medina 2001; Hu *et al.* 2010]. Therefore, specific inhibitors of the Gln / Glu cycle at key points in the cycle may make promising candidates as antimetabolic chemotherapeutic agents. The availability of glutamine via the cycle and cycle dependent transporters also seems to regulate the growth and proliferation of tumor cells as well as acting as an exchanger for other essential amino acids [Nicklin *et al.* 2009]. This is yet another example how dysfunction of the glutamine / glutamate cycle may contribute to pathology, particularly

in gliomas. In order to better understand the mechanisms by which glutamate / glutamine cycle dysfunction may contribute to neurodegenerative diseases and/or cancer, it would be logical to utilize transporter and enzyme specific inhibitors to investigate the role and significance of each molecular participant involved within the cycle. Unfortunately, there exist only a handful of inhibitors to evaluate the role of a few amino acid transporters.

1.2 Glutamine transporters:

A combination of radiolabeled uptake and electrophysiology based experiments has identified an abundance of neutral amino acids transporters which shuttle glutamine in and out of mammalian cells. Most of these transporters were first discovered in the mid 1960's and early 1970's and functionally characterized by radiolabeled uptake in Ehrlich ascite tumor cells and various red blood cells collected from pigeons, and rabbits, common work performed by Halvor N. Christensen [for review see Christensen 1984; or Barker, G.A.; and Ellory, J.C 1990]. These neutral amino acid transporters were classified by their function in transporting preferred amino acids and designated the names system A for alanine preferring, system ASC for alanine, cysteine, serine preferring; system N for nitrogen side chain preferring, and system L for leucine preferring. Worth mentioning, these names do not imply that these transporter systems exclusively transport the amino acid they were named after. System L however, does transport glutamine with low affinity though its expression and/or function as a

transporter of glutamine within the CNS has yet to be found. Cloning has allowed for the identification of subclasses of these transporter systems, most of which transport glutamine as a preferred substrate. These include SN1 of system N, ASCT2 of system ASC, LAT2 and to a lesser extent LAT1 of system L, and ATA1 and ATA2 both of system A. All of these transporters function as bidirectional transporters of glutamine as well other amino acids. Essentially, these transporters may operate by uptake or efflux depending on the substrate (amino acid) concentration gradient and the electrochemical concentration gradient [Bröer and Brookes 2001].

Although not entirely complete, the localization and cellular distribution of these transporters in many mammalian tissues has been determined by immunoblotting and functional radiolabeled uptake competition using known substrates. From initial characterization it has been revealed that there exists a fairly considerable overlap in substrate specificity between the various amino acid transporters, particularly the glutamine transporters. This is suggestive of the versatile physiological roles in which glutamine might play. Pertaining to the CNS, the glutamine transporters that have been detected in astrocytes include the neutral amino acid transporters SN1, LAT2, and ASCT2. Interestingly their expression or overall contribution to the glutamine shuttling greatly depends on the tissue involved. For example SN1 is generally the primary transporter of glutamine in hippocampal astrocytes, where as in reactive astrocytes this transport is shifted to ASCT2 and LAT1. Where as in astrocytes localized to other regions of mouse brain glutamine uptake is well transported by both SN1 and ASCT2.

In neurons, the glutamine transporters ATA2, ATA1, LAT2, and ASCT2, have been detected by both immunohistochemical staining and functional uptake. As with glutamine transporters expressed in astrocytes, the expression of functionally detectable glutamine transporters in neurons also varies depending on the tissue being observed. System A has traditionally been thought of as the primary transporter of L-glutamine near peri-synaptic terminals, though it has been shown to account for only 10% of glutamine uptake [Heckel *et al.* 2003], therefore ~90% of the glutamine uptake that is observed in these primary neurons must be transported by an alternative transport system. Functional analysis using a series of substrates to block glutamine uptake suggested that ~30-40% of glutamine uptake is mediated by system L and another remaining 30% by an unknown D-aspartate sensitive uptake. Until recently ASCT2 had been thought of as an astrocyte specific transporter. However, ASCT2 has now been detected in Purkinje neurons bodies, dendrites, and dendrites in hippocampus, striatum, and cortex from mouse brain slices identified by immunohistochemical staining, and by D-serine radio labeled uptake [Gliddon *et al.* 2009; Shao *et al.* 2009]. This is inconsistent with previous reports in which in situ hybridization or antibodies failed to detect ASCT2 mRNA or protein expression in neuronal cultures. Previous functional assays also failed to detect ASCT2 like transport using radiolabeled uptake within these neuronal cultures. What is clear from the multitude of studies is that expression of glutamine transporters is highly variable with respect to region and tissue type. Glutamine transporter expression is also

highly variable with regard to how the cells were obtained by culture, primary culture or tissue slices.

1.2.1- ATA1 / ATA2:

System A of the solute carrier 38 gene family includes two Na⁺ dependent glutamine / neutral amino acid transporters ATA1 and ATA2 [Varoqui *et al.* 2000; Sugawara *et al.* 2000]. Previously named GlnT / SAT1 for ATA1 and SAT2 for ATA2, these transporters exhibit cotransport of one amino acid substrate coupled to the transport of one sodium ion along its electrochemical gradient. ATA1 and ATA2 transport short chain neutral amino acids alanine, glutamine, serine, asparagine, glycine, proline, cysteine and histidine with affinities ranging between K_m of 0.5-1.5 mM for preferred substrates [Yao *et al.* 2000; Sugawara *et al.* 2000]. Interestingly both ATA1 and ATA2 are pH sensitive and with decreasing pH their rate of transport diminishing quickly from approximately K_m of 3.5 mM at pH 7.4 to 32 mM at pH of 6.0 [Mackenzie and Erickson 2004]. However, with increasing pH the rate of substrate transport by system A transporters increases [Varoqui *et al.* 2000; Sugawara *et al.* 2000]. This change in transport rate is thought to occur by a H⁺ competing for the same binding site that requires Na⁺ binding for translocation of a substrate [Chaudhry *et al.* 2002].

In the CNS, the system A transporters are widely distributed amongst neurons localized in the spinal cord, cerebral cortex, hippocampus and in cerebellar neurons

typically of GABA or glutamatergic neurons. Rarely, these two transporters have been found on astrocyte cultures. The distribution of ATA1 and ATA2 would seem to suggest a possible role for these transporters in the glutamine / glutamate cycle. Currently the only synthetic inhibitor of these transporters is methyl amino isobutyric acid (MeAIB), which acts as a transportable and specific System A inhibitor. The affinity the system A transporters express for MeAIB ranges between $K_m \approx 0.2-0.6$ mM at ATA2 and a $K_m \approx 1-2$ mM at ATA1 [Yao *et al.* 2000; Sugawara *et al.* 2000; Albers *et al.* 2001, Chaudhry *et al.* 2002]. Recent studies in brain slices have used MeAIB to competitively inhibit glutamine transport via system A to probe the contribution of ATA1 and ATA2 in supplying glutamine for production of glutamate have had remarkable results. Neurons treated with MeAIB leads to a measurable decrease of dendritic glutamate containing pools [Jenstad *et al.* 2009]. This may be attributable to blocking of glutamine uptake by neurons resulting in accumulation in extracellular spaces [Kanamori and Ross 2004]. However, there is no evidence to support that MeAIB decreases vesicular glutamate in neurons, though, this is effect is seen when applying histidine [Rae *et al.* 2003].

Application of MeAIB has been observed to decrease amplitude and frequency of miniature EPSP (mEPSP) [Armano *et al.* 2002] in cultured hippocampal neurons and evoked field potential (EFP) in disinhibited neocortical slices [Tani *et al.* 2010], though this effect was rapidly reversible in field excitatory post synaptic potential (fEPSP) recorded in hippocampal slices [Kam and Nicoll 2007]. Little can be concluded from these studies as to the role of the system A transporters in neurons. In the first example

glutamine supplied by system A is suggested to be crucial for glutamatergic signaling. The second example suggests that system A does contribute to neuronal glutamine uptake; however, system A's contribution in glutamine uptake that is destined to be converted to glutamate is negligible. It was thus determined that this function is really an unknown transporter that is inhibited by amino isobutyric acid (AIB) or histidine which accounts for most of the glutamine uptake that is available for glutamatergic signaling, therefore system A transport is not essential. The last example concludes that the Glutamate / Glutamine cycle is not essential for glutamatergic signaling, though it may contribute in part. The irresolute conclusions derived from these numerous studies places emphasis on the need for potent and selective pharmacologic inhibitors of the system A transporters so as to more precisely determine their physiological significance, particularly within the CNS.

1.2.2 - ASCT1 / ASCT2:

Discovery and characterization of system ASC was first accomplished through radiolabeled uptake [Christensen *et al.* 1967]. Expressed ubiquitously in mammals, this neutral amino acid transport system was properly named after its preferred transport of alanine, serine, and cysteine. Though, as with system A, there are other naturally occurring neutral amino acids, such as L-glutamine, that are transported with equivalent or higher affinity. System ASC consists of two transporter types, ASCT1 and ASCT2, which were cloned (SLC1A4 & SLC1A5 respectively) and functionally characterized

[Arriza *et al.* 1993; Utsunomiya-Tate *et al.* 1996; Kekuda *et al.* 1996]. The transporters were classified as Na⁺ dependent solute carrier's type 1 (SLC1) belonging within the same family of amino acid transporters that includes the EAATs. ASCT1 transports a limited number of short chain amino acids including alanine, serine, cysteine and to a lesser extent threonine by an electroneutral Na⁺ dependent obligate amino acid exchange process. ASCT2 by contrast transports a slightly broader range of amino acids which also includes glutamine, asparagine, and threonine. Both transporters express a stoichiometrically uncoupled substrate gated anion conductance that is associated with translocation of a substrate [Zerangue and Kavanaugh 1996; Bröer *et al.* 2000] which is consistent with other transporters found in the SLC1 family. Additionally, transport of L-glutamate mediated by ASCT2 is pH dependant. With increasing acidity L-glutamate is transported with higher efficiency by ASCT2. This observation may in fact be suggestive of conserved homology between system ASC and other members of the SLC1 family which primarily transport L-glutamate the EAATs. The most fundamentally useful information that has arisen from the cloning of the SLC1 family is their homology to a bacterial aspartate transporter *Pyrococcus horikoshii* which has been crystallized [Yernool *et al.* 2004; Boudker *et al.* 2007]. The crystal structure alone has provided invaluable structural understanding into the binding dynamics of the glutamate transporters the EAATs which has fueled the development for inhibitors of glutamate transport. The GltPH homology structure (**Figure 2**) could also be potential used for

computational modeling of the other SLC1 carrier related transporters including system ASC.

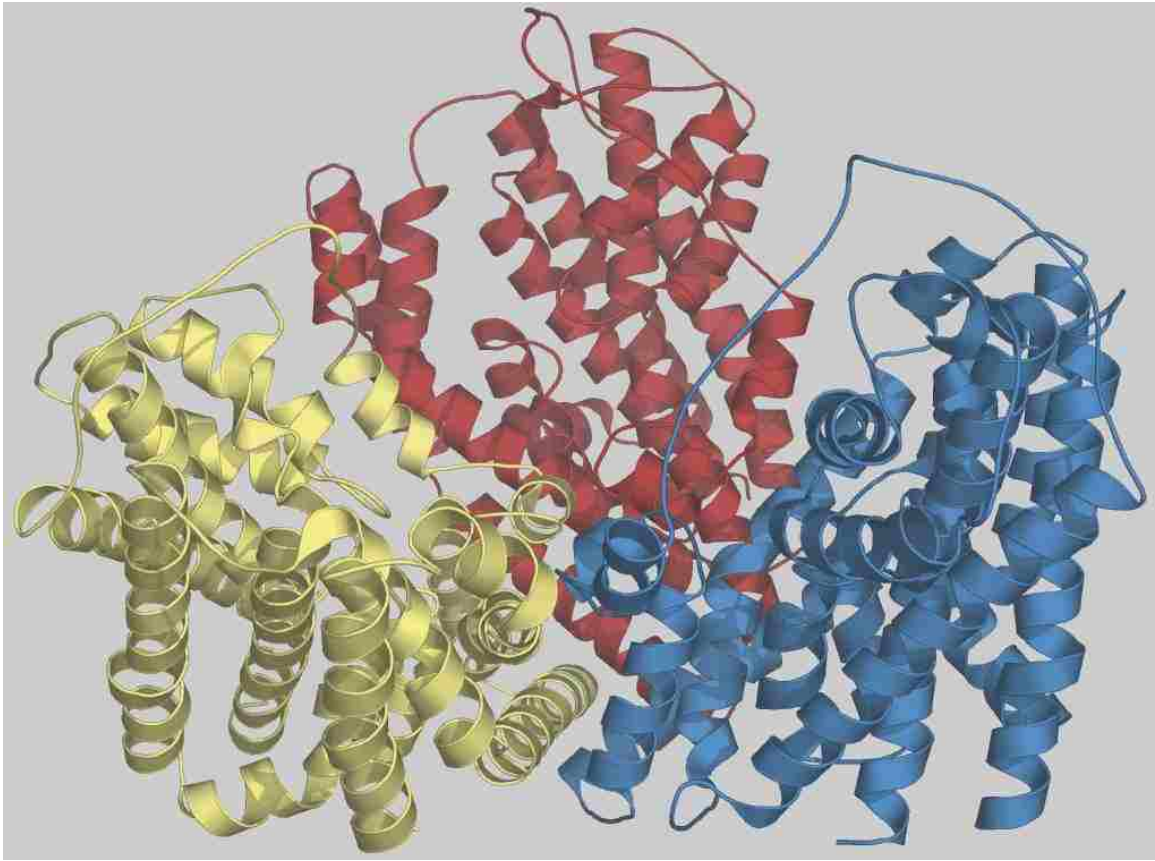


Figure 2: GltPH open form trimer, protein data bank- 2NWW. [Boudker *et al.* 2007]

Within the CNS, both ASCT1 and ASCT2 are widely distributed amongst astrocytes. ASCT2 is thought to be highly concentrative with respect to glutamine efflux from glia / astrocyte in exchange for other amino acid substrates alanine, serine, cysteine [Bröer *et al.* 1999]. Though, the apparent contribution of ASCT2 to pooling of glutamine in the CSF in is unknown. Most of the concentrative effort of glutamine into the CSF may instead be as a result of SN1 mediated transport. ASCT1 has been found

ubiquitously on neurons [Yamamoto *et al.* 2003], though, being that this transporter is an obligate exchanger of amino acids the implications for its function are obscure. ASCT2 has also recently been found on a small subset of neurons in cortex, striatum and cerebellar regions [Gliddon *et al.* 2009; Shao *et al.* 2009]. The significance and function of ASCT2 expressed in these neurons, however has remained elusive. ASCT2 and ASCT1 may function together in neurons to supply essential amino acids or maintain appropriate amino acid reserves. Equally, glutamine may be used as a currency for obligate exchange for recruitment of essential amino acids through ASCT1 or system L transport [Nicklin *et al.* 2009]. It is also probable that glutamine supplied by ASCT2 may be used as an energy source by production α -ketoglutarate which enters into the Krebs cycle, or alternatively converted to glutamate for glutamatergic signaling. Though much work in functional characterization and distribution has been made, the significance and contribution of the ASC transporters in normal physiologic processes such as the glutamate / glutamine cycle and / or pathologic conditions is unknown. Regardless, the transporter ASCT2 may have other more demonstrable physiological implications within the CNS such as by functioning in uptake of D-serine [Shao *et al.* 2009]. D-serine is recognized as a high affinity co-agonist of the glutamate ionotropic receptor NMDA, like that of glycine. D-serine has been suggested to contribute to neuronal damage via activation of NMDA in ischemic induced injury [Katsuki *et al.* 2004; Katsuki *et al.* 2007]. Thus it may be conceivable that under hypoxic circumstances ASCT2 functions

as a scavenger of D-serine at glutamatergic synapses to reduce over stimulation of NMDA receptors which otherwise may result in neuronal injury.

Radiolabeled uptake has identified trans-4-hydroxy-L-proline (4-HP) as a high affinity substrate of ASCT1 while conversely L-proline exhibits low affinity uptake. These results indicate that system ASC may have a preference for recognizing H-bond capable small side chain containing amino acids [Pinilla-Tenas *et al.* 2003]. Importantly, this is the first reporting of a homo-chiral amino acid as a high affinity substrate of ASC transport. The finding also highlights the possibility of a chiral switch or diastereomer selectivity that may exist within this SLC1 family of transporters. This is also consistent with a previous report in which the EAATs, another group of transporters within the SLC1 family of transporters, were shown to transport pyrrolidine-2,4-dicarboxylate with high affinity.

1.2.3 - Synthetic inhibitors of ASCT2

To date there are very few inhibitors that may be capable to discern the physiological function or relevance of the ASC transporters. Benzylserine and benzylcysteine were revealed as non-substrate inhibitors of ASCT2 [Greuer and Grabsch 2004]. The activity of these compounds at ASCT2 is quite low $K_i > 700 \mu\text{M}$. Most interesting is that these inhibitors exposed the presence of a tonic anion current that is uncoupled to ligand binding. They demonstrated that non-substrate inhibitors of ASCT2 block this anion leak with saturable kinetics that is competitive with transportable

substrates. Furthermore, a direct measure of the dissociation constant or K_i was attainable by a relatively straightforward dose response curve. Though, these compounds have not been used to elucidate structure or physiological function of the ASC transporters they still serve as proof of concept to effectively screen and/or establish the activity of non-substrate inhibitors at ASCT2.

N γ -Aryl-glutamine analogues were reported to inhibit uptake of radiolabeled glutamine in C6 rat glioma cell line [Esslinger *et al.* 2005]. Though not very potent $\sim K_i > 800 \mu\text{M}$, these inhibitors indicate a hydrophobic pocket that can accommodate an aromatic ring. Additionally, these aryl-glutamine analogs were used to demonstrate the pH sensitivity of ASCT2. It was observed that the inhibitory activity of these analogs increased with decreasing pH, supporting a hypothesis that the amide functionality participates in a hydrogen bond donating or dipole-dipole interaction. With respect to pKa of the amide however, the effects of electron withdrawing or donating by the various phenyl ring substituents had no detectable influence on activity. Rather, it may have been the lipophilicity of the phenyl substituents which is accountable for the observed change in inhibitory activity. It is therefore reasonable to infer from this study that both lipophilic and hydrogen bonding interactions are important to consider when designing inhibitors of the ASCT2 transporter. Interestingly, the most active analog of this series reported, N- γ -glutamyl-p-nitro-aniline, is the only pharmacologic inhibitor to be used in delineating the physiological role of ASCT2 in proliferating cells [Nicklin *et al.* 2009], even though this compound as an inhibitor of ASCT2 is quite poor.

1.2.4 - ASCT2 relation to proliferating cells

A role for ASCT2 is emerging in relation to regulating growth and proliferation in certain cancerous tumor cell lines [see Fuchs and Bode 2005 for review]. ASCT2 has long been known to be highly expressed and distributed amongst reactive astrocytes and other forms of prolific glial tumor lines such as C6 glioma, as [Dolinska et al. 2001]. Additionally, ASCT2 been seen to be upregulated in a neuroblastoma cell line [Wasa *et al.* 2002]. This transporter has also been shown to be upregulated in a number of other tumor cell lines that are un-related to the CNS. The upregulation of ASCT2 and function as the primary glutamine transporter in prolific cell lines is not limited to CNS tumor lines, ASCT2 has been observed as the primary glutamine transporter in other tumor cell lines such as human hepatoma cells [Bode *et al.* 1995]. Additionally, ASCT2 is thought to be the primary transporter of glutamine in colon carcinoma cells and when inhibited by abundant competing substrates, effectively slows the growth of these cells [Pawlik et al. 2000].

It is thought that ASCT2 may supply rapidly dividing cells with glutamine for converting to energy. This is also consistent with findings in the developing embryonic brain where ASCT2 is highly distributed in an area of high energy demand [Wu and Schwartz 1998]. There is also indication that ASCT2 regulates growth and proliferation of cells indirectly by activation of the mammalian target-of-rapamycin (mTOR) an

energy sensing pathway that mediates growth / proliferation of cells if energy reserves and various conditions are reached (Figure 3) [Fuchs and Bode 2005].

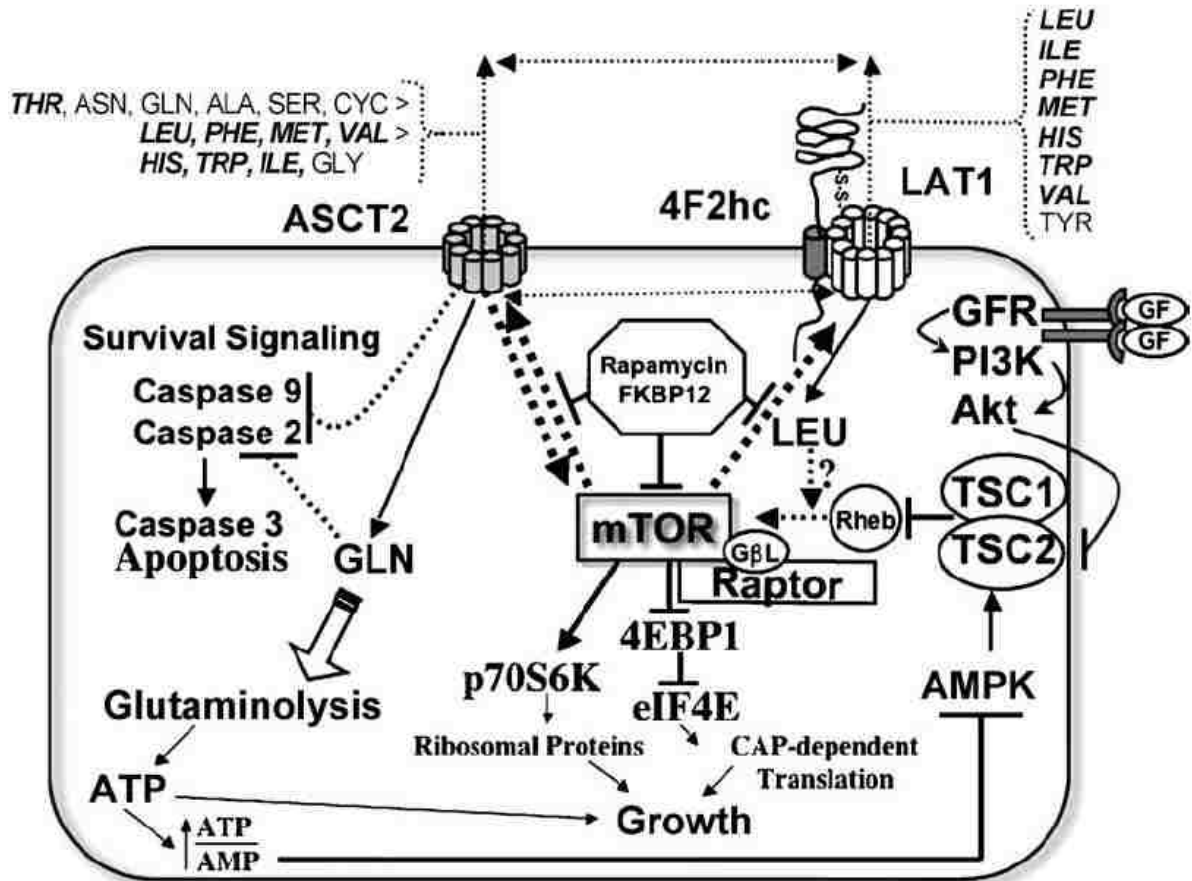


Figure 3: ASCT2 transport indirectly or directly regulates mTOR which is linked to cell growth/proliferation and survival [Fuchs and Bode 2005].

Another mechanism relating ASCT2 to the activation of mTOR has also been proposed whereby ASCT2 functions to concentrate L-glutamine into rapidly dividing cells to be used as an efflux substrate to bring in larger essential amino acids via LAT1, which otherwise cannot be synthesized *ex novo* [Nicklin *et al.* 2009]. The availability of

essential amino acids tryptophan, phenyl-alanine, and valine may then trigger the activation of mTOR. Unfortunately, there are no available inhibitors of ASCT2 to test this concept. The only evidence that would suggest that ASCT2 transport is a valid target to inhibit cell growth within tumors has been by silencing of ASCT2 mRNA expression via RNAi [Fuchs *et al.* 2007]. Silencing of ASCT2 in human derived hepatoma cells resulted in repression of growth followed by induction of apoptosis regulated by mTOR complex-1 (mTORC1). Indeed, it appears that ASCT2 does have a significant role in this cell line; this notion may also be true in other tumor cell lines.

An alternative mechanism yet to emerge in discussion or literature which portrays its novelty is to affect glutathione production by inhibition ASCT2 mediated transport. A rationale that might also explain ASCT2 up-regulation in rapidly dividing cells may be to supply cells with L-glutamine for the production of glutathione. As mentioned before, L-glutamine can be converted to glutamate by glutaminase and glutamate is a precursor for biosynthesis of glutathione. ASCT2 may also function to supply these cells with cysteine, also a precursor of glutathione. Although premature, these suggestions exemplify the need for ASCT2 selective inhibitors to act as probes to examine the biological significance of this transporter within these systems.

Chapter 2.

Synthesis of β -aryl-aspartamides & α -aryl-amide aspartates as pharmacologic tools for evaluating amino acid transporters.

Brent R. Lyda, Nicholas Natale, C. Sean Esslinger.

Department of Biomedical and Pharmaceutical Sci., University of Montana, 32 Campus Dr., Missoula, Montana 59801-1552

***Corresponding authors**

Brent R. Lyda
Dept. of Biomedical and Pharmaceutical Sciences
University of Montana
Missoula MT 59801
Tel: 406-855-7401
Brent.Lyda@umontana.com

Nicholas Natale
Dept. of Biomedical and Pharmaceutical Sciences
University of Montana
Missoula, MT 59801
Tel: 406-243-4132
nicholas.natale@umontana.edu

Abstract

L-Aspartate provides as a synthetically useful starting material for the rapid synthesis and biologic screening of chiral α amino acid analogs to be evaluated as inhibitors of amino acid transporters. A series of β -aryl-aspartamides and α -arylamide-aspartates were synthesized and screened against the amino acid transporters including the excitatory amino acid transporters subtypes 1-3 (EAATs 1-3), and the neutral amino acid transporters ATA2, ASCT2, and SN1 in order to generate new pharmacologic leads. The pharmacologic leads will serve in identifying structure activity relationship (SAR) and may prove useful towards developing transporter subtype selective inhibitors to ultimately delineate the physiological relevance or discover new therapeutic strategies related to these amino acid transporters of interest.

INTRODUCTION

Amino acid transporters are ubiquitously expressed in nearly every mammalian tissue. The capacity of researchers to investigate the physiological function of these various amino acids transporters is limited in scope by the pharmacologic tools as inhibitors that are available. Considering the many diseases that amino acid transporters may be involved in, including cancer and/or neurodegenerative diseases [Allen *et al.* 2004], there remains a need for selective and potent inhibitors to investigate the physiological significance of the numerous amino acid transporters that exist [see Bröer 2002; & Bröer 2008 for review of transporters]. Amongst the various scaffolds available for generating inhibitors of amino acid transport, the α -amino acids, the substrates of the transporters themselves, are often a good starting point.

Naturally occurring α -amino acids have found wide application as molecular scaffolds to synthesize unnatural amino acid inhibitors of both membrane bound receptors, such as those involved in neurotransmission, and membrane spanning amino acid transporters. Incorporation of bulky, hydrophobic groups to an endogenously transported amino acid has led to the discovery of highly potent inhibitors of amino acid transporters. For example, it was discovered that addition of a benzyl, benzyloxy or larger groups such as fluorene to L-aspartate created highly potent and, in some cases, selective inhibitors of the excitatory amino acid transporters (EAATs) [Shimamoto *et al.* 1998; Esslinger *et al.* 2005; Greenfield *et al.* 2005]. Of particular interest to our lab are the L-glutamine transporters SN1, ATA2, and ASCT2 and the L-glutamate transporters,

excitatory amino acid transporters EAAT's (1-5). These transporters are suggested to play a central role in the Glutamate / Glutamine cycle for the recycling of the neurotransmitter L-glutamate near neuronal synapses [Hertz *et al.* 1999; Shank and Aprison 1981]. Interestingly, both system ATA2 and ASCT2 transport have shown to be pH sensitive [Chaudhry *et al.* 2002; Utsunomiya-Tate *et al.* 1996] whereas SN1, an amino acid cotransporter with antiport proton exchange, is pH insensitive [Chaudhry *et al.* 1999], and then of course the glutamate transporters transport an acidic amino acid. In addition to structural differences, we reasoned that dissimilarity between transporters which may account for pH sensitivity versus ligand specificity might also be exploited to create potent transporter selective inhibitors. What was needed was a useful method to quickly synthesize the desired tools or potential inhibitors for biological screening to generate initial pharmacologic leads that may facilitate a developing pharmacophore model. Here we describe an effective synthetic route used to produce a series of β -aryl-aspartamides & α -aryl-amide aspartates as probes for biological evaluation at the Glutamine / Glutamate amino acid transporters.

L-aspartate can be used to synthesize a large variety of aryl substituted derivatives. Of these, aspartyl aryl-amides are readily accessible via aspartyl anhydride [Witiak *et al.* 1971] such as to produce a series of these analogs rapidly and in scalable quantity. In the series reported here (**Figure 1**), we aimed to produce a number of amino acid analogs with varying electron withdrawing / donating properties, various

spatial/geometrical configuration, or finally analogs with fluorescent properties. To preliminarily assess the influence of probable hydrogen bond interactions with the amide functionality, the β or α carboxylic acid of the aspartate scaffold could be coupled to anilines with electron withdrawing groups, such as p-chloro or 2,3-dichloro anilines **8, 9** (Figure 1), which may decrease the pKa of the amide N-H and therefore increase its capacity as an H-bond donating group. Alternatively, electron donating anilines, such as 2,3-methyl aniline **10** (Figure 1), could be coupled to the aspartate scaffold to enhance the H-bond accepting properties of the amide. Analogs for surveying larger hydrophobic binding sites were synthesized by coupling with larger aryl-amines such as biphenyl, naphthyl, or fluorenyl substituent's, **11-14**. The spatial and geometrical limitations of a hydrophobic pocket or other suspected interactions within the binding domain could be assessed in this manner. Lastly, aspartyl aryl-amide analogs intended to function as fluorescent or photoactive inhibitors were also synthesized by L-aspartate coupling with 9-fluorenone **15**, 7-nitro-fluorene **16**, or carbazole **17** (Figure 1).

alpha-arylamide-aspartate beta-aryl-aspartamide

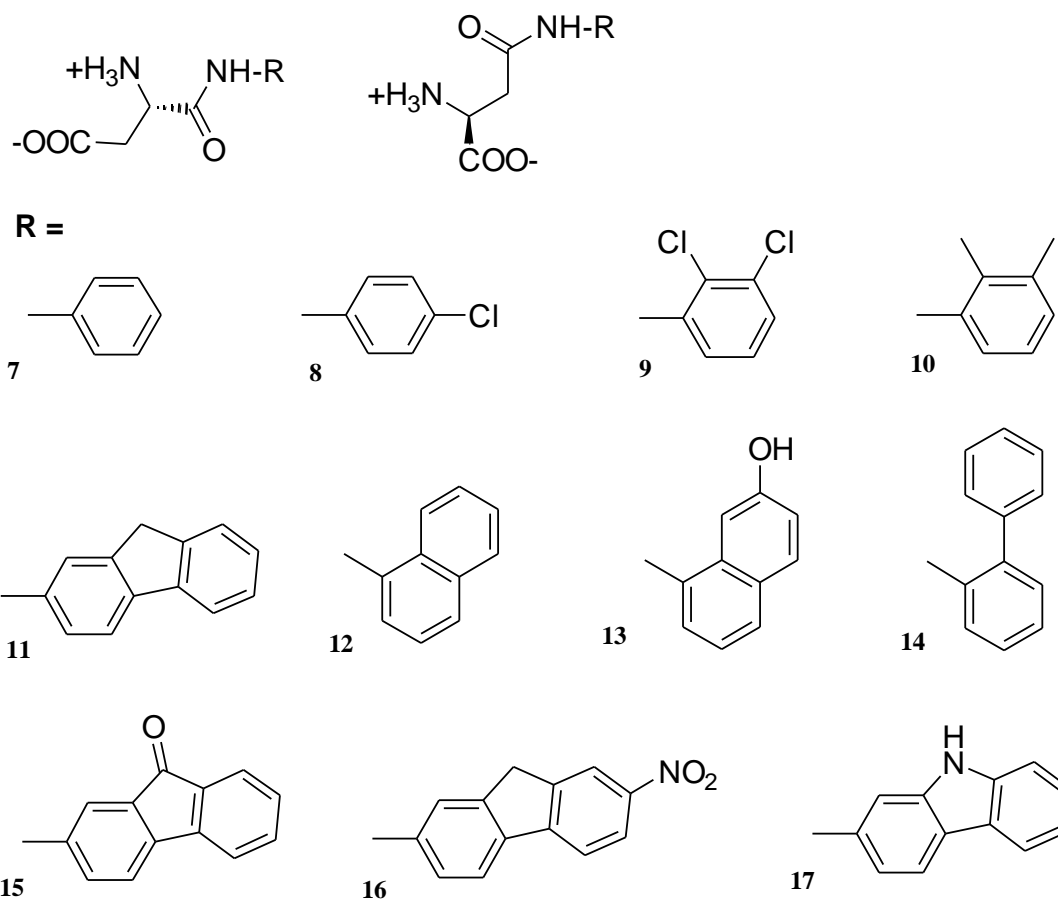
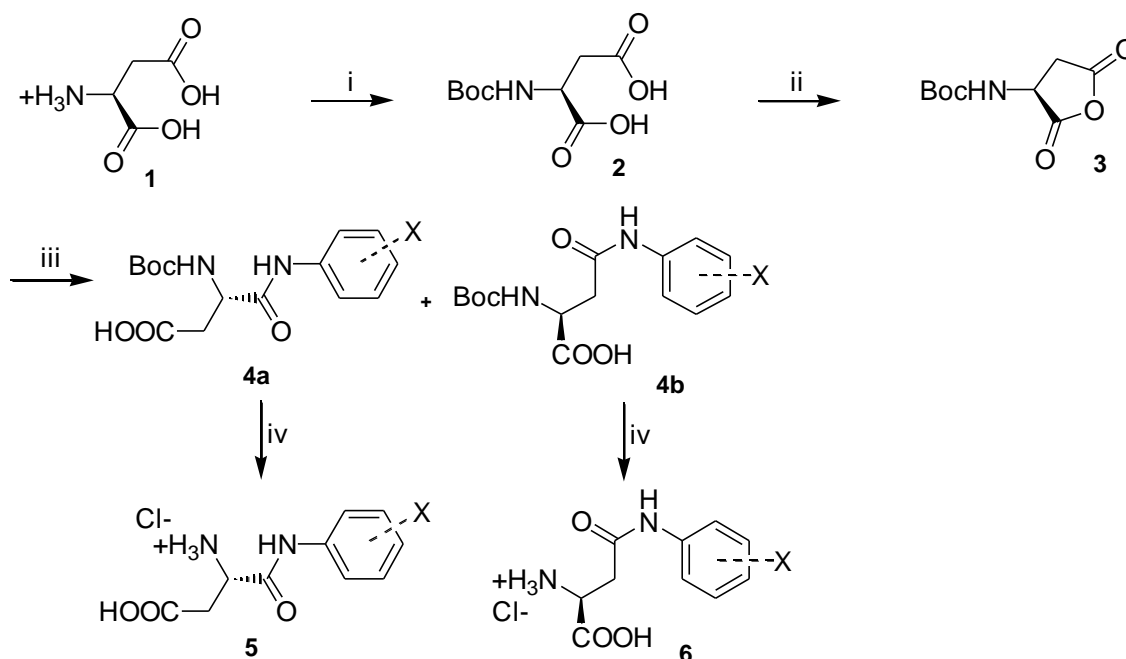


Figure 1: Synthesized β -aryl-aspartamides and α -aryl-amide aspartates

β -Aryl-aspartamides and α -arylamide-aspartates were synthesized from L-aspartate by nucleophilic addition of an aryl amine to an anhydride of the N-protected L-aspartate (**Scheme 1**) [Huang *et al.* 1997; Timko 2005]. Briefly, amine protection of aspartic acid with di-tert-butyl dicarbonate (Boc anhydride) resulted in formation of the tert-butyl carbamate aspartic acid **2** with quantitative yield. After crude workup, the remaining product N-tBoc-protected-aspartate **2** was then dissolved in acetic anhydride to

form the N-tBoc-aspartic-anhydride **3**. The acidic anhydride was removed by vacuum and multiple washes using toluene and hexanes. The remaining aspartic anhydride was immediately used in the following addition reaction to avoid hydrolysis. Addition via a nucleophilic aryl amine to the anhydride **3** was carried out using DMSO or ethyl acetate as the solvent.



Scheme 1: Synthesis of β-aryl-aspartamides and α-arylamide-aspartates. (i) Boc anhydride, 50/50 TEA / methanol at 22°C; (ii) acetic anhydride, 40°C; (iii) aryl-amine in DMSO, 60°C; (iv). 1.) 1:1 TFA and CH₂Cl₂ at 22°C. 2.) 1.2 eq. 0.01 M HCl, lyophilize.

Nucleophilic addition of an aryl amine to the anhydride **3** in 0.05 M DMSO with heating afforded the product N-tBoc protected aryl-aspartamide **4b** in 85-90% yield and

N-tBoc protected α -arylamide-aspartate **4a** accounting for the remaining 5-10%. The two isomers could then be easily separated by silica gel using 94-97% CH₂Cl₂, 2-5% methanol, 1% acetic acid for the mobile phase. Deprotection of the N-tBoc protected aspartic aryl-amide **4a or 4b** to produce the target β -aryl-L-aspartamide **6** or α -arylamide-L-aspartate **5** was accomplished by the addition of excess trifluoroacetic acid (TFA) in dichloromethane, typically 30-50% by volume. The remaining product and TFA salt after aspiration and multiple washes with dichloromethane was then treated with 1.2 equivalents of HCl solution and frozen and lyophilized (freeze dried) to remove the any remaining TFA salt. The remaining pure products **5** or **6** (Scheme 1) were stored as an HCl salt.

Solvent controlled regioselective addition:

Typically, ring opening of the N-protected aspartic anhydride yields two isomers, the β -carbonyl amide and the α -carbonyl amide (**Figure 2**). We have observed in this series that nucleophilic addition by various aryl amines consistently and strongly favors substitution to the β -carbonyl group under dilute conditions in DMSO (0.01-0.025 M). The selectivity ranges between 85-95% β -addition depending upon the aryl amine employed. However, when the addition is accomplished in non-polar or polar-aprotic solvents, such as ethyl-acetate or ethanol, it was observed that the α -addition is favored 8:2, α : β or 80% alpha. The selectivity is thought to occur by an existing H-bond between the carbamate NH and the α -carbonyl of the anhydride in nonpolar solvents. This results

in a more electropositive α -carbon center that is more reactive towards a nucleophilic amine, thus favoring the α -addition. Using DMSO or DMF as the solvent disrupts this H-bond, and therefore nucleophilic substitution is most energetically favored at the β -carbonyl [Yang 1986].

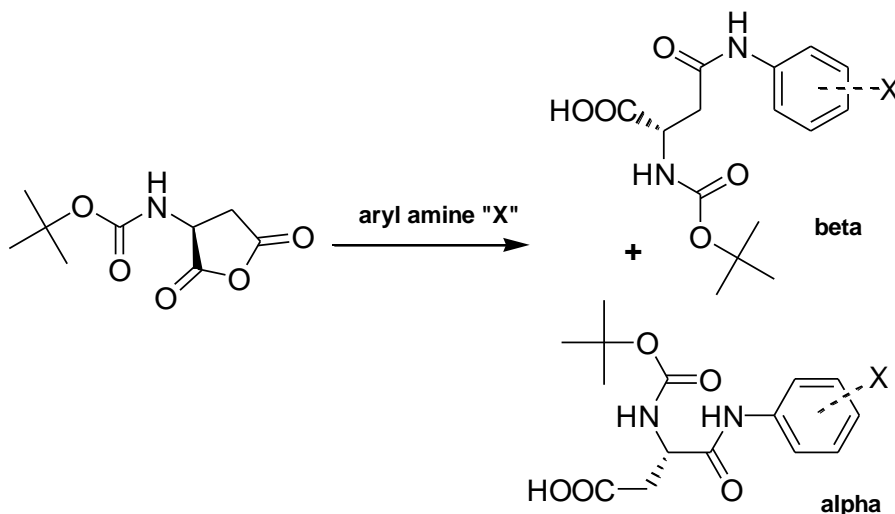


Figure 2: Alpha and beta isomers produced from nucleophilic addition of an aryl amine (X) to N-tBoc-aspartic-anhydride.

Biological Discussion & Conclusions:

The activity of a select aspartyl aryl-amide analogs were screened by radiolabeled uptake competition in C17 neuroprogenitor cells or by electrophysiological recordings of substrate induced current inhibition in *Xenopus laevis* oocytes expressing transgenic ATA2, ASCT-2, SN1 or EAAT 1-3 transporters. The objective here was to identify potential lead inhibitors of the excitatory amino acid transporters (EAATs, subtypes 1-5), or the neutral amino acid transporters ASCT-2, SN1, and ATA2 from the synthetic series

of β -aryl-aspartamides and α -arylamide-aspartates. The estimated K_i of some of these compounds were calculated from a dose response (**Figure 3 & 4**) using non-linear regression to calculate an IC_{50} followed by Cheng-Prusoff [Cheng and Prusoff 1973] conversion which can then be entered into a table to compare activity between the amino acid transporters relative to endogenous substrate in K_m (**Table 1**).

Cheng-Prusoff equation –

$$K_i = \frac{IC_{50}}{1 + \frac{[Substrate]}{K_M}}$$

| | hATA2 | mASCT2 | rSN1 | EAAT1 | EAAT2 | EAAT3 |
|------------------------------|--------------------|--------------------|--------------------|---------------------|---------------------|---------------------|
| Gln or Glu | $K_m = 655 \mu M$ | $K_m = 55 \mu M$ | $K_m = 1884 \mu M$ | $K_m = 20 \mu M$ | $K_m = 20 \mu M$ | $K_m = 20 \mu M$ |
| CSE79 [β -9] | $K_i = 1780 \mu M$ | $K_i = 373 \mu M$ | small effect | $K_i = 280 \mu M$ | $K_i = 69 \mu M$ | $K_i = 13.3 \mu M$ |
| CSE84 [β -12] | $K_i = 2000 \mu M$ | $K_i = 954 \mu M$ | small effect | $K_i = 65 \mu M$ | $K_i = 29 \mu M$ | $K_i = 8.6 \mu M$ |
| CSE99 [β -13] | $K_i = 2900 \mu M$ | $K_i = 2800 \mu M$ | small effect | $K_i = 48 \mu M$ | $K_i = 15 \mu M$ | $K_i = 4.1 \mu M$ |
| CSE67 [β -15] | n/e | n/e | n/e | $K_i = 0.19 \mu M$ | $K_i = 3.5 \mu M$ | $K_i = 0.13 \mu M$ |
| CSE97 [α -11] | | | | $K_i = 11 \mu M$ | $K_i = 18 \mu M$ | $K_i = 6.0 \mu M$ |
| CSE72 / 2-FAA [β -11] | n/e | n/e @ 10 μM | n/e | $K_i = 0.054 \mu M$ | $K_i = 0.059 \mu M$ | $K_i = 0.005 \mu M$ |
| MeAIB | $K_m = 277 \mu M$ | n/e | n/e | n/e | n/e | n/e |

Table 1: K_i estimated using the Cheng- Prusoff conversion of the IC_{50} values obtained from screening CSE aspartamides across various amino acid transporters; n/e = no effect at 1 mM. Where glutamine (Gln) or glutamate (Glu) represent endogenous substrates and MeAIB = methyl amino isobutyric acid, a selective system A inhibitor. Brackets [] designate α or β carboxylic acid coupled to arylamide **R**.

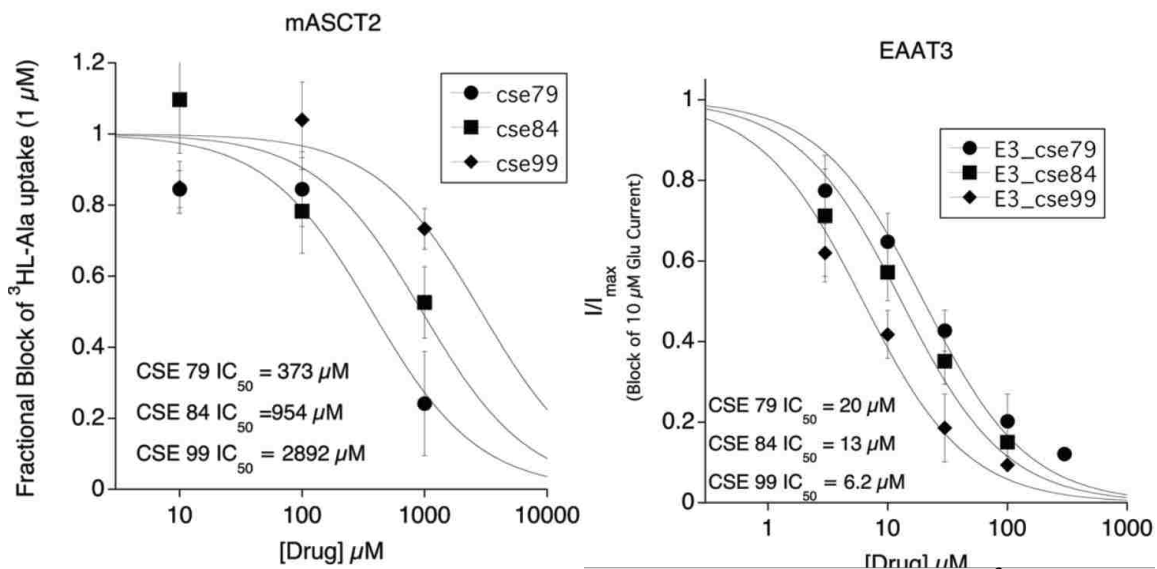


Figure 3: Dose response curves showing fractional block of radiolabeled $^3\text{H-L-alanine}$ uptake at ASCT-2 or fractional block of L-glutamine current at EAAT-3 by aryl-aspartamides CSE79, CSE84, CSE99.

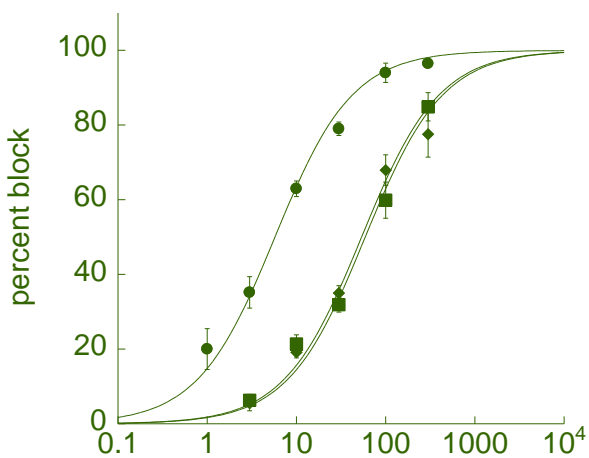


Figure 4: CSE72 dose response (μM) showing percent block of a $3 \mu\text{M}$ L-Glu current: hEAAT1 (diamonds), hEAAT2 (squares), and hEAAT3 (circles) @ (-60 mV).

Analysis of the estimated K_i for a particular aspartyl-aryl-amide across various transporters reveals potential lead inhibitors with limited selectivity. Once completed,

this table will provide an improved perspective to evaluate the selectivity/activity of the aspartyl-aryl-amides at these transporters. More importantly, the generated data will support a developing pharmacophore for each of these transporters to facilitate the discovery of more potent and selective next generation inhibitors. The activity of these aspartyl-aryl-amides compounds across the numerous transporters may also provide a more clear understanding of their biological activity and mechanism of action. For example, CSE79, CSE84, and CSE99 were all tested in a rat spinal nerve ligation model that measures paw withdrawal as an indication of pain mitigation (**Figure 5**). In comparing the *in vivo* activity to the inhibitory activity between these three compounds screened across the 6 amino acid transporters, it would appear that the biological activity of these aryl-aspartamides may be acting through inhibition of the EAATs or ASCT2. Although unlikely, these compounds display a relatively low inhibitory activity towards ASCT2, it is possible that the observed response in rats treated is mediated in part or entirely by inhibition of ASCT2. Therefore, a role for ASCT2 within this model for neuropathic pain cannot be completely ruled out.

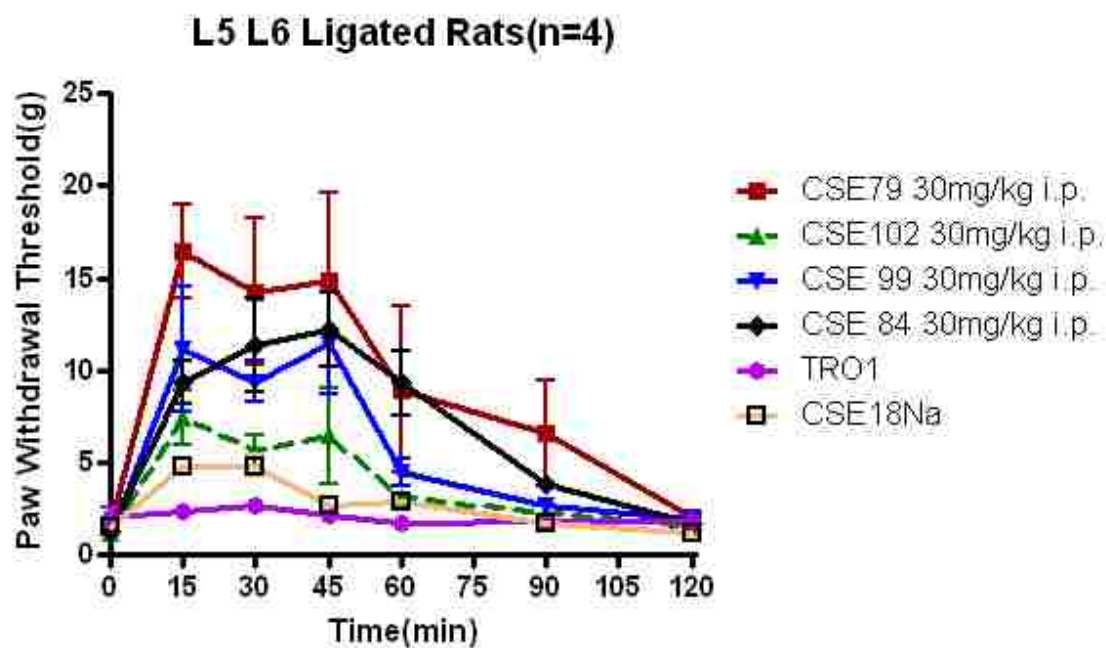
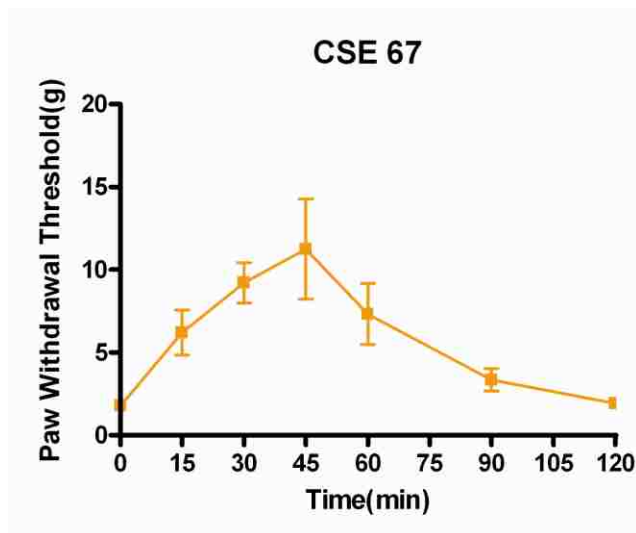


Figure 5: Various aryl-aspartamides CSE84, CSE79, CSE99 at 30 mg/kg or aryl-glutamide CSE102 tested in rat spinal nerve ligation model over time course of 20 minutes. An increased paw withdrawal threshold indicates the rat is less sensitive to pain.

Further examination of this withdrawal effect in rats when using an EAAT specific inhibitor, aryl-aspartamide CSE67 at 20 mg/kg, revealed that the observed biological activity may instead be primarily mediated through the EAATs, particularly EAAT-3 (**Figure 6**). This is indicated by the activity of CSE67 at 20 mg/kg in paw withdrawal threshold vs paw withdrawal threshold with CSE84 at 20 mg/kg. These observations stress the necessity to fully characterize the activity of these aspartyl-aryl-amides at multiple amino acid transporters not only for pharmacologic design to produce novel inhibitors but also to determine a plausible mechanism of action.

A



B

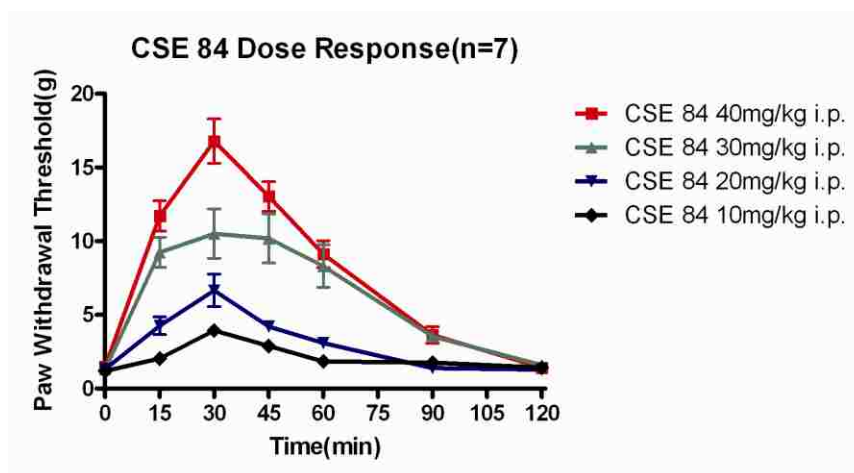


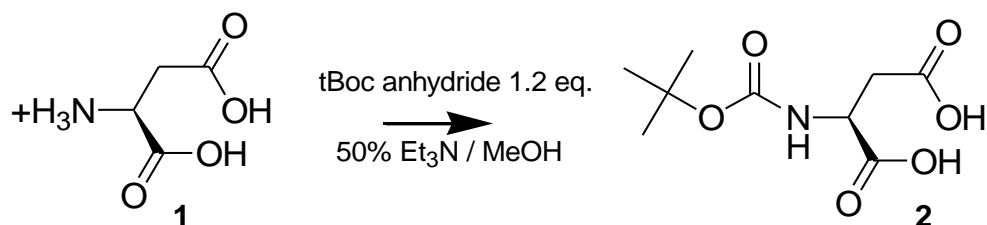
Figure 6: CSE67 shows a greater effect than does CSE84 at 20 mg/kg measure by paw withdrawal threshold; **A.** CSE67 at 20 mg/kg in rat spinal nerve ligation model; **B.** CSE84 dose response in rat spinal nerve ligation model at 40, 30, 20, & 10 mg/kg.

Ultimately the activity of this series of compounds can be placed into a table that will lead to the generation or development of a pharmacophore model for these

transporters of interest. Currently there is already a developing pharmacophore of the EAATs subtypes 1-3. There has also been much effort to design selective inhibitors of EAAT-3 [Esslinger *et al.* 2005; Mavencamp *et al.* 2008]. An efficient synthetic route to rapidly synthesize a large series or library of compounds to facilitate and explore hypothesis driven pharmacological design will be highly beneficial towards discovering selective inhibitors of EAAT-3. The synthetic route we have developed here is quite capable to meet the demands for large screenings for activity and biological evaluation at these various glutamate / glutamine transporters.

Experimental section:

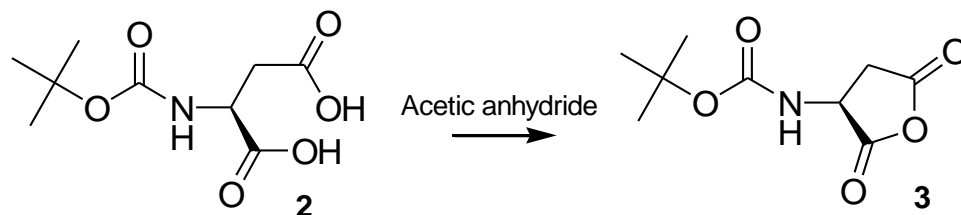
Proton ^1H and carbon ^{13}C nuclear magnetic resonance (NMR) spectra were obtained from Varian VXR 400 MHz or Varian 500 MHz spectrometers as specified. Both ^1H and ^{13}C spectra are reported in parts per million (ppm or δ) downfield from tetramethylsilane as an internal standard. All chemical shifts reported were referenced to residual protonated DMSO solvent peaks at 2.5 ppm for ^1H proton spectra or 39.5 ppm for ^{13}C carbon spectra unless specified otherwise. Multiplicity is reported as doublets (d), doublet of doublets (dd) etc. where Σ represents the sum of all couplings, b = broad. Optical rotations of compounds dissolved in DMSO or methanol, as specified, with concentrations given in g/100 mL were determined via a Perkin-Elmer Model 241 polarimeter in a 1.0 dm glass cell sodium D line. High resolution mass spectra (HRMS) were determined on a Waters LC-MS spectrometer using caffeine or trimethoprim as a mass standard at m/z 195.0882 or 291.1457 respectively for HRMS. All reagents were purchased from Acros Organics and used without further purification. Solvents as well as 40-60 μM silica gel for flash chromatography were obtained from EMD chemicals (Gibbstown, NJ). Intermediates were initially isolated by silica gel and used for the addition step without further purification. A mobile phase consisting of 95% CH_2Cl_2 / 4% MeOH / 1% AcOH was used for TLC and flash chromatography. All final products were isolated by multiple washes with dichloromethane and ethyl acetate to remove organic impurities.



N-tBoc-aspartic-acid: BRL:26

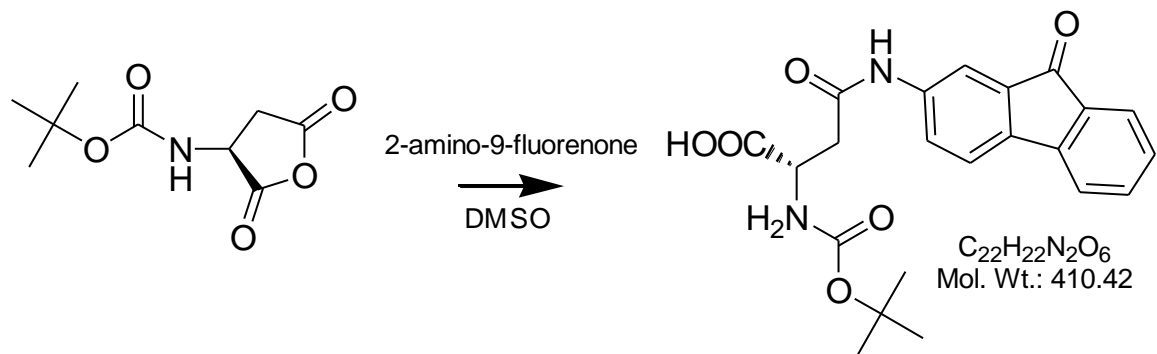
L-Aspartic acid (13.492, 101.4 mmol) was added to a round bottom flask. Cold (~4° C) triethylamine (21.20 mL, 1.5 eq.) and methanol (21 mL) were added followed by the slow addition of tBoc anhydride (26.58 g, 1.2 eq). The reaction solution was then allowed to stir at rt (~23° C) for 24 h, where upon the reaction was determined to be complete by TLC. The reaction solution was then placed on a rotovap to remove all remaining triethylamine and methanol. Water (200 mL) was then added to the remaining residue and the pH was adjusted to ~2 via addition of H₃PO₄ (conc.). The aqueous solution was then saturated with NaCl and extracted with 3 x 200 mL ethyl acetate portions. The ethyl acetate portions were then combined and concentrated by rotovap. The remaining viscous oil was then chased with multiple portions of methylene chloride and concentrated leaving 21.529 g of a white solid, N-tBoc protected L-aspartate, an apparent 91.2% yield. This material was then used in the next synthetic step without further purification.

$^1\text{H-NMR}$ (400 MHz, d_6 -DMSO at 2.5 ppm) δ 7.02 (d, $J = 9.1$ Hz, 1H), 4.24 (ddd, $J = 22.0_\Sigma, 7.3$ Hz, 1H), 2.65 (dd, $J = 21.4_\Sigma, 16.2, 5.2$ Hz, 1H), 2.50 (dd, $J = 24.6_\Sigma, 16.8, 7.8$ Hz, 1H), 1.36 (s, 9H).



N-tBoc-aspartic-anhydride: BRL:22

N-tBoc protected L-aspartate (1.502 g, 6.44 mmol) was added to a round bottom flask followed by added of 15 mL acetic anhydride. The mixture was allowed to stir at $\sim 40^\circ\text{C}$ overnight until N-tBoc-L-aspartate appeared to be completely dissolved. The mixture was then concentrated by rotovap at 50°C . Evaporation of the acetic anhydride took 2-3 h where upon the remaining solid was chased 3-4 times with 20 mL of toluene and placed on rotovap to remove any remaining acetic anhydride from the solid anhydride product. The remaining solid was then chased three times with 20 mL of hexanes in a similar manner and removed by reduced pressure. The product N-tBoc-aspartic anhydride was then used immediately in the amine addition step without further purification.

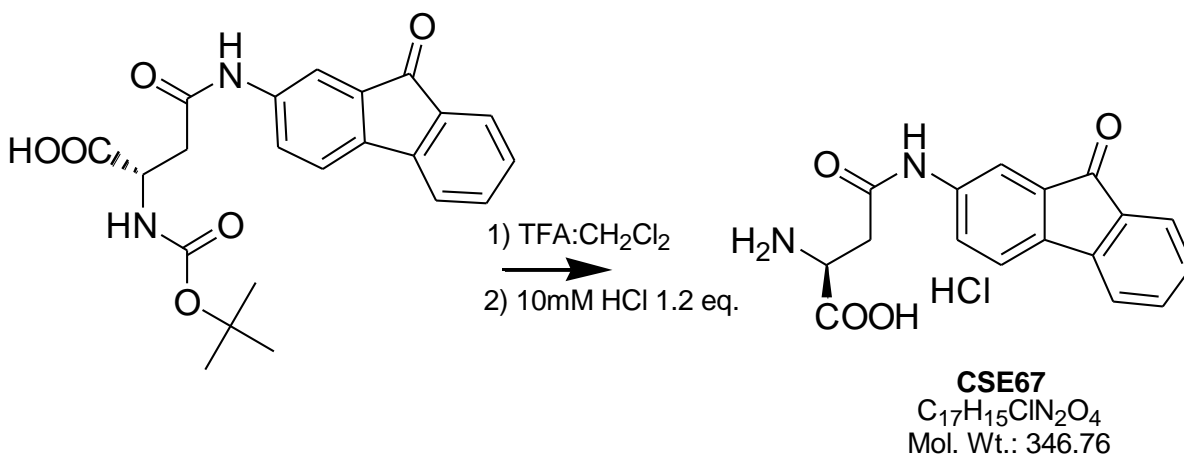


N-tBoc-2-fluoren-9-one-aspartamide: BRL:22

The N-protected aspartate anhydride (1.386 g, 6.44 mmol) was stirred in DMSO (64 mL, to make the final 0.1 M) and to this 2-amino-9-fluorenone (1.132 g, .85 eq.-assuming 85% yield from previous anhydride formation) was added. The solution was allowed to stir for 48 h, when the reaction had reached completion (determined by absence of 2-amino-2-fluoren-9-one by TLC), at ~ 45° C. The product in DMSO was then diluted with CHCl_3 (400 mL) and washed water, 6 x 250 mL aliquots (pH = 2, total 1.5 L) to remove any remaining DMSO. Extracted products, observed by TLC, contained primarily the β -amide addition product; N-tBoc protected 2-fluoren-9-one aspartamide, but also included small amounts of the α -amide addition product and starting material tBoc protected aspartate. The extracted products were then subsequently concentrated by rotovap to a dry solid and separated by silica gel (mobile phase = 95% CH_2Cl_2 / 4% MeOH / 1% acetic acid). The β addition product was then collected and concentrated by rotovap to afford N-tBoc-2-fluoren-9-one-aspartamide (1.460 g, 3.557 mmol, 65% yield), as a

yellow/orange powder, which was used in the next synthetic step without further purification.

$^1\text{H-NMR}$ (400 MHz, d_6 -DMSO at 2.5 ppm) δ 10.42 (s, 1H), 7.92 (s, 1H), 7.68 (m, 3H), 7.56 (m, 2H), 7.30 (dd, $J = 14.9_{\Sigma}$, 7.4 Hz, 1H), 7.01 (d, 7.1 Hz, 1H), 4.32 (ddd, $J = 20.7_{\Sigma}$, 6.9 Hz, 1H), 2.82 (dd, $J = 21.4_{\Sigma}$, 15.5, 5.8 Hz, 1H), 2.64 (dd, $J = 22.6_{\Sigma}$, 7.6 Hz, 1H), 1.36 (s, 9H).



2-Fluoren-9-yl-L-aspartamide: CSE67 / BRL:23

CH₂Cl₂ (1.5 mL) and trifluoroacetic-acid (TFA, 1.5 mL, 8.87 mmol, 17.8 eq) was added to a round bottom flask followed by N-tBoc protected aspartamide-2-fluoren-9-one (0.2044 g, 0.498 mmol) which dissolved immediately and turned a dark orange/brown color. The solution was allowed to stir for 40 min, whereby it was observed that the

reaction had completed as determined by TLC. The solution was then air dried with compressed air to remove the remaining TFA and CH_2Cl_2 . The remaining solid (deprotected product and TFA salt) was then mixed thoroughly with 1.1 equivalents of 0.01 M HCl and sonicated. The solution was then frozen to -80°C and placed on the lyophilizer to freeze dry and remove all the water and remaining TFA leaving a pure yellow/orange powder (0.163 g, 0.47 mmol, 96% yield). The identity and purity of the final product was confirmed by ^1H , ^{13}C NMR, HRMS & rotational analysis.

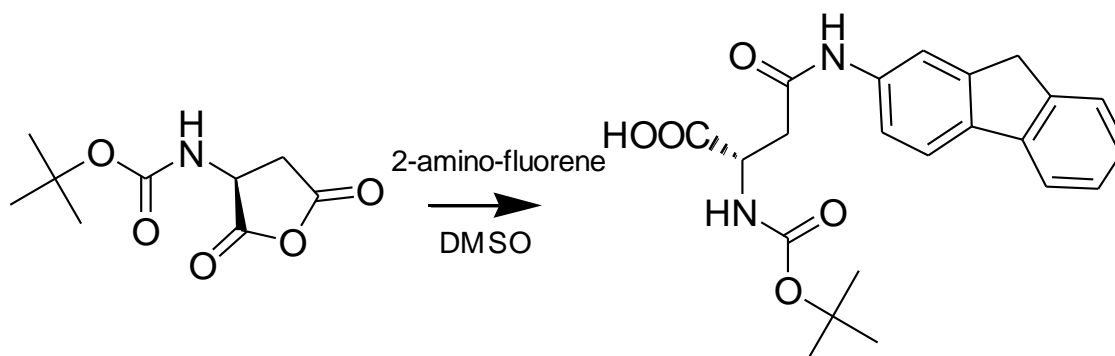
^1H -NMR (400 MHz, d_6 -DMSO at 2.5 ppm) δ 10.79 (s, 1H), 8.43 (b, 2.5H), 7.98 (s, 1H), 7.68 (m, 3H), 7.55 (m, 2H), 7.29 (dd, $J = 14.9_\Sigma$, 7.4 Hz, 1H), 4.28 (dd, $J = 10.4_\Sigma$, 5.2 Hz, 1H), 3.05 (m, $J = 46.0_\Sigma$, Hz, 2H);

^{13}C -NMR (400 MHz, d_6 -DMSO at 39.5 ppm) δ 193.0, 170.3, 167.7, 144.1, 140.0, 138.7, 135.5, 134.0, 133.4, 128.7, 124.8, 124.0, 121.7, 120.7, 114.8, 48.6, 36.0;

CHN analysis for $\text{C}_{17}\text{H}_{15}\text{ClN}_2\text{O}_4 \cdot 2\text{H}_2\text{O}$ calc. C, 53.34; H, 5.00; N, 7.32; O, 25.08; Cl, 9.26. Found: C, 53.29; H, 4.23; N, 6.65;

HRMS m/e calcd. For $\text{C}_{17}\text{H}_{15}\text{N}_2\text{O}_4 = 311.1032$, found 311.1016;

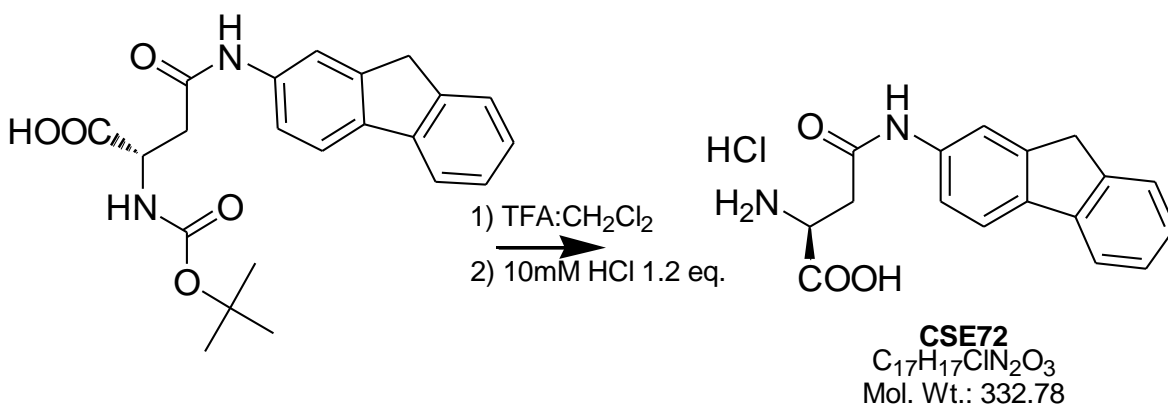
$[\alpha]_D^{22} = +12^\circ$ ($c = 0.23$, DMSO)



N-tBoc-fluorenyl-L-aspartamide: BRL:24

Protected aspartate anhydride (0.936 g, 4.35 mmol) was stirred in DMSO (87 mL, to make the concentration 0.05 M) and to this 2-aminofluorene (0.684 g, 0.85 eq.-assuming 85% yield from previous anhydride formation) was added. The solution was allowed to stir for 24 h, when the reaction had reached completion (as determined by the absence of 2-amino-fluorene via TLC), at 60° C. The product in DMSO was then diluted with CHCl₃ (400 mL) and washed with water, 6 x 250 mL aliquots pH = 2, total of 1.5 L to remove DMSO. Extracted products, observed by TLC, contained primarily the β-amide addition product; tBoc protected 2-fluorenyl-aspartamide, but also included small amounts of α-amide addition product and starting material tBoc protected aspartate. The extracted products were then subsequently concentrated by rotovap to a dry solid and a fraction of this dry solid was separated by silica gel (mobile phase = 95% CH₂Cl₂ / 4% MeOH / 1% acetic acid) The β addition product was then collected and concentrated by rotovap to afford N-tBoc-2-fluorenyl-aspartamide (0.697g, 1.758 mmol) as a white/brown or off-white powder, which was used without further purification.

$^1\text{H-NMR}$ (400 MHz, $\text{d}_6\text{-DMSO}$ at 2.5 ppm) δ 10.15 (s, 1H), 7.93 (s, 1H), 7.78 (d, $J = 8.4$ Hz, 2H), 7.52 (d, $J = 7.1$ Hz, 2H), 7.33 (dd, $J = 14.9_\Sigma$, 7.44 Hz, 1H), 7.24 (dd, $J = 14.9_\Sigma$, 7.4 Hz, 1H), 7.03 (d, $J = 8.4$ Hz, 1H), 4.36 (ddd, $J = 21.4_\Sigma$, 6.9 Hz, 1H), 2.82 (dd, $J = 20.7_\Sigma$, 15.2, 5.5 Hz, 1H), 2.86 (dd, $J = 22.6_\Sigma$, 15.5, 7.1 Hz, 1H), 1.37 (s, 9H).



2-Fluorenyl-L-aspartamide: CSE72 / BRL:25

CH₂Cl₂ (4 mL) and trifluoroacetic-acid (TFA, 4 mL, 23.65 mmol, 13.45 eq) was added to a round bottom flask followed by N-tBoc protected β -fluorenyl-aspartamide (0.697 g, 1.758 mmol) which dissolved immediately and turned a dark brown color. The solution was allowed to stir for 30 min, whereby it was observed that the reaction had completed, determined by TLC. The solution was then aspirated with compressed air (removes the excess TFA and CH₂Cl₂) and washed with 3 x 50 mL CH₂Cl₂ and again aspirated until dry. The remaining residue (product and TFA salt) was then suspended in 0.01M HCl

(193 mL water, 1.1 eq. HCl) and sonicated. The solution was then frozen to -80°C and placed on the lyophilizer to freeze dry / remove all the water and remaining TFA leaving an off-white residue (0.555 g, 1.67 mmol, 95% yield). The identity and purity of the final product was confirmed by ^1H , ^{13}C NMR, and HRMS. Specific rotation was also calculated.

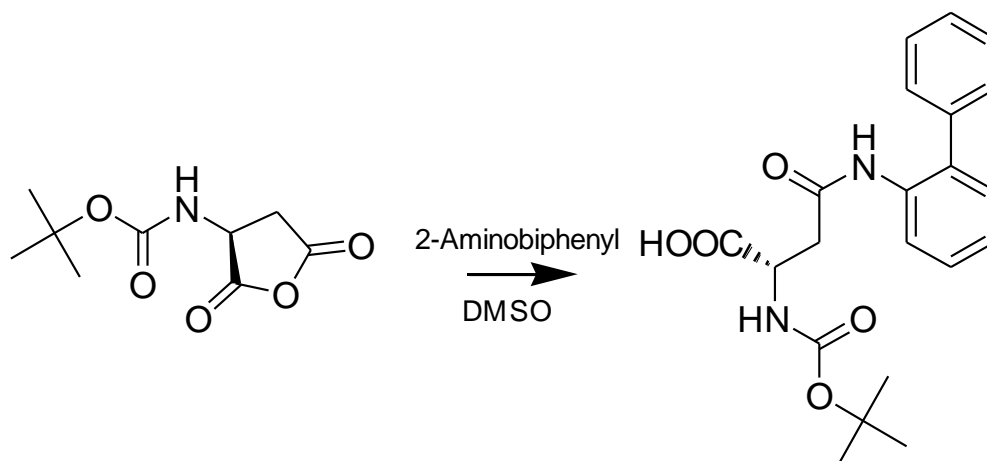
^1H -NMR (400 MHz, d_6 -DMSO at 2.5 ppm) δ 10.65 (s, 1H), 8.47 (s, 3 H), 7.95 (s, 1H), 7.805 (d, $J = 3.9$ Hz, 1H), 7.78 (d, $J = 2.6$ Hz, 1H), 7.59 (d, $J = 8.4$ Hz, 1H), 7.52 (d, $J = 7.8$ Hz, 1H), 7.33 (dd, $J = 14.2_{\Sigma}$, 7.1 Hz, 1H), 7.24 (dd, $J = 14.9_{\Sigma}$, 7.4 Hz, 1H), 4.24 (dd, $J = 10.4_{\Sigma}$, 5.2 Hz, 1H), 3.87 (s, 2H), 3.12 (dd, $J = 22.0_{\Sigma}$, 17.2, 4.9 Hz, 1H), 3.05 (dd, $J = 22.7_{\Sigma}$, 17.2, 5.5 Hz, 1H);

^{13}C -NMR (400 MHz, d_6 -DMSO at 39.5 ppm) δ 170.3, 167.4, 143.7, 142.8, 141.0, 137.9, 136.5, 126.8, 126.2, 125.0, 120.2, 119.6, 118.0, 116.1, 48.8, 36.5, 36.0;

CHN analysis for $\text{C}_{17}\text{H}_{19}\text{ClN}_2\text{O}_3 \cdot \text{H}_2\text{O}$ calc. C, 58.21; H, 5.46; N, 7.99; O, 18.24; Cl, 10.11 Found: C, 59.34; H, 5.02; N, 7.78;

HRMS m/e calcd. For $\text{C}_{17}\text{H}_{17}\text{N}_2\text{O}_3 = 297.1239$, found 297.1227;

$[\alpha]_{\text{D}}^{22} = +20^{\circ}$ ($c = 0.28$, DMSO)

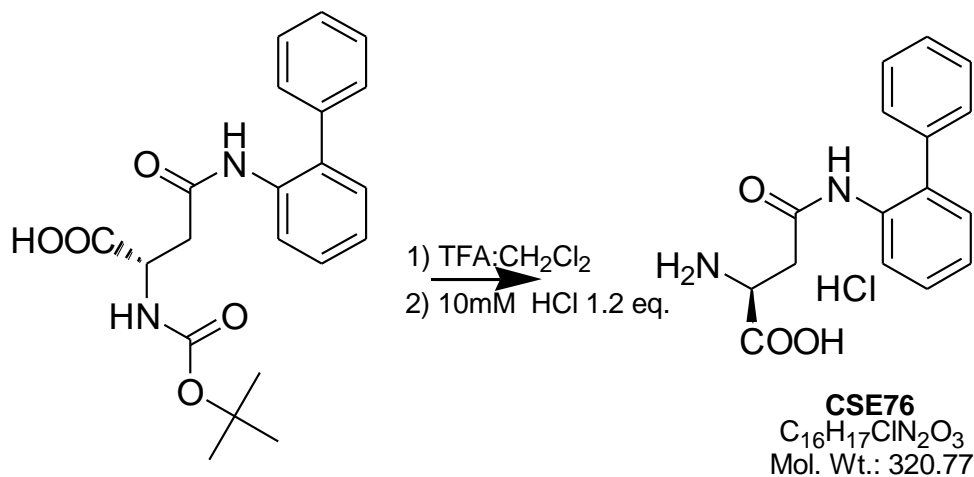


N-tBoc-2-biphenyl-aspartamide: BRL:27

Protected aspartate anhydride (1.41 g, 6.55 mmol) was stirred in DMSO (131 mL, to make the concentration 0.05 M) and to this 2-amino-biphenyl (0.9625 g, 0.85 eq.- assuming 85% yield from previous anhydride formation) was added. The solution was allowed to stir for 24 hours, when the reaction had reached completion (determined by absence of 2-amino-biphenyl by TLC), at ~ 40° C. The product in DMSO was then diluted with CHCl₃ (400 mL) and washed with 6 x 250 mL aliquots of pH 2 brine (adjusted 2M HCl) to remove DMSO. Extracted products, observed by TLC, contained primarily the β-amide addition product; N-tBoc protected aspartamide-biphenyl, but also included small amounts of α-amide product and starting material protected aspartate. The extracted products were then subsequently concentrated by rotovap to a dry solid and a fraction of this dry solid was separated by silica gel (mobile phase = 94% CH₂Cl₂ / 5% MeOH / 1% acetic acid (R_f = 0.2)). The β addition product was then collected and

concentrated by rotovap to afford N-tBoc-2-biphenyl-aspartamide (0.460 g, 1.197 mmol), as a light brown residue and used without further purification.

$^1\text{H-NMR}$ (400 MHz, $\text{d}_6\text{-DMSO}$ at 2.5 ppm) δ 9.3 (s, 1H), 7.53 (d, 1H), 7.25-7.45 (m, 8H), 6.90 (d, $J = 8.4$ Hz, 1H), 4.30 (dd, $J = 20.7_{\Sigma}$, 6.9 Hz, 1H), 2.65 (dd, $J = 20.1_{\Sigma}$, 14.9, 5.2 Hz, 1H), 2.51 (m, 1H overlap with solvent), 1.39 (s, 9H).



2-Biphenyl-L-aspartamide: BRL:28

CH_2Cl_2 (3 mL) and trifluoroacetic-acid (TFA, 3 mL, 17.74 mmol, 14.83 eq) was added to a round bottom flask followed by N-tBoc protected aspartamide-biphenyl (0.460 g, 1.197 mmol) which dissolved immediately and turned a darker almost brown color. The solution was allowed to stir for 40 min. whereby it was observed that the reaction had completed as determined by TLC. The solution was then air dried with compressed air to remove the remaining TFA and CH_2Cl_2 . The remaining solid (deprotected product and TFA salt) was then mixed thoroughly with 0.01M HCl (131 mL water, 1.1 eq. HCl) and sonicated. The solution was then frozen to $-80^\circ C$ and placed on the lyophilizer to freeze dry / remove all the water and remaining TFA leaving a pure light-brown powder (0.36 g, 1.12 mmol, 94% yield). The identity and purity of the final product was confirmed by 1H , ^{13}C NMR, HRMS & rotational analysis.

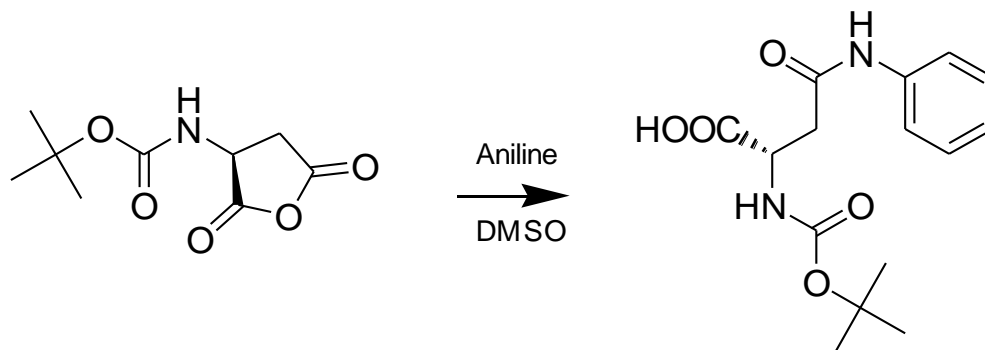
$^1\text{H-NMR}$ (400 MHz, d_6 -DMSO at 2.5 ppm) δ 9.67 (s, 1H), 8.46 (s, 2.5H), 7.27-7.50 (m, 9H), 4.18 (dd, J = undetectable, 1H), 2.92 (dd, J = 22.0 $_{\Sigma}$, 16.8, 5.2 Hz, 1H), 2.83 (dd, J = 22.6 $_{\Sigma}$, 16.8, 5.8 Hz, 1H);

$^{13}\text{C-NMR}$ (400 MHz, d_6 -DMSO at 39.5 ppm) δ 170.3, 168.1, 138.6, 136.4, 134.1, 130.4, 128.9, 128.5, 127.7, 127.4, 126.4, 48.7, 35.0;

CHN analysis for $\text{C}_{16}\text{H}_{20}\text{ClN}_2\text{O}_3 \cdot 1.25 \cdot \text{H}_2\text{O}$ calc. C, 55.74; H, 5.75; N, 8.12; O, 20.11; Cl, 10.28. Found: C, 55.76; H, 4.77; N, 7.45;

HRMS m/e calcd. For $\text{C}_{16}\text{H}_{17}\text{N}_2\text{O}_3$ = 285.1239, found 285.1263;

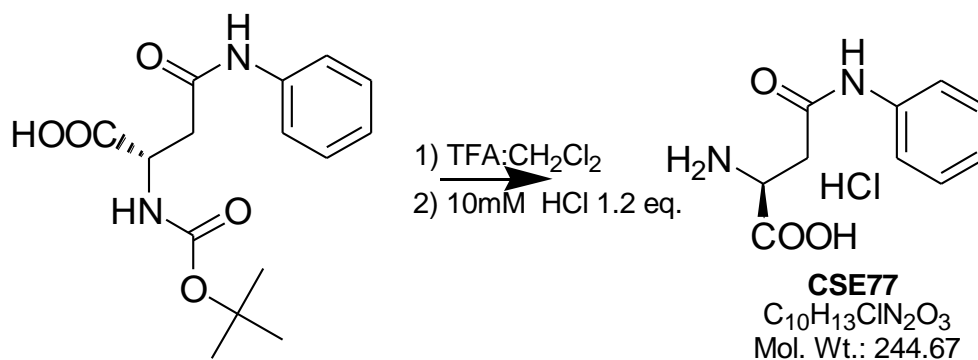
$[\alpha]_{\text{D}}^{22} = +20^\circ$ ($c = 0.31$, DMSO)



N-tBoc-phenyl-aspartamide: BRL:29

Protected aspartate anhydride (1.29 g, 5.99 mmol) was stirred in DMSO (120 mL, to make the concentration 0.05 M) and to this aniline (0.464 mL, 5.08 mmol, 0.85 eq.- assuming 85% yield from previous anhydride formation) was added. The solution was allowed to stir for 24 hours, when the reaction had reached completion (determined by absence of aniline by TLC), at ~ 45° C. The product in DMSO was then diluted with CHCl₃ (400 mL) and washed with 6 x 250 mL aliquots pH = 2 brine (adjusted by 2M HCl) to take up the DMSO. Extracted products, observed by TLC, contained primarily the β-amide addition product; N-tBoc protected-phenyl-L-asparagine, but also included small amounts of α-amide addition product and starting material N-tBoc protected aspartate. The extracted products were then subsequently concentrated by rotovap to a dry solid and a fraction of this dry solid was separated by silica gel (mobile phase = 94% CH₂Cl₂ / 5% MeOH / 1% acetic acid). The β addition product was then collected and concentrated by rotovap to afford N-tBoc-phenyl-aspartamide (0.249g, 0.808 mmol) as a white residue, which was used in the next synthetic step without further purification.

$^1\text{H-NMR}$ (400 MHz, $\text{d}_6\text{-DMSO}$ at 2.5 ppm) δ 9.96 (s, 1H), 7.57 (d, $J = 7.8$ Hz, 2H), 7.27 (dd, $J = 15.5_\Sigma, 7.8$ Hz, 2H), 7.00-7.07 (m, 2H), 4.35 (dd, $J = 21.7_\Sigma, 6.9$ Hz, 1H), 2.79 (dd, $J = 20.7_\Sigma, 15.2, 5.5$ Hz, 1H), 2.64 (dd, $J = 23.3_\Sigma, 15.5, 7.8$ Hz, 1H), 1.36 (s, 9H).



Phenyl-L-aspartamide: CSE77 / BRL:30

CH₂Cl₂ (1.5 mL) and trifluoroacetic-acid (TFA, 1.5 mL, 8.87 mmol, 10.98 eq) were added to a round bottom flask followed by N-tBoc protected aspartamide-phenyl (0.249 g, 0.808 mmol) which dissolved immediately and turned a darker yellow color. The solution was allowed to stir for 45 min, whereby it was observed that the reaction had completed as determined by TLC. The solution was then air dried with compressed air to remove the remaining TFA and CH₂Cl₂. The remaining solid (deprotected product and TFA salt) was then mixed thoroughly with 0.01M HCl (89 mL water, 1.1 eq. HCl) and sonicated. The solution was then frozen to -80° C and placed on the lyophilizer to freeze

dry / remove all the water and remaining TFA leaving a white powder (0.156 g, 0.638 mmol, 80% yield). The identity and purity of the final product was confirmed by ^1H , ^{13}C NMR, HRMS & rotational analysis.

^1H -NMR (400 MHz, d_6 -DMSO at 2.5 ppm) δ 10.58 (s, 1H), 8.34 (s, 3H), 7.62 (d, $J = 7.8$ Hz, 2H), 7.27 (dd, $J = 15.5_\Sigma$, 7.8 Hz, 2H), 7.02 (dd, $J = 14.2_\Sigma$, 7.1 Hz, 1H), 4.09 (app s, 1H), 3.08 (d, $J = 14.2$ Hz, 1H), 2.96 (dd, $J = 20.1_\Sigma$, 16.2, 3.9 Hz, 1H);

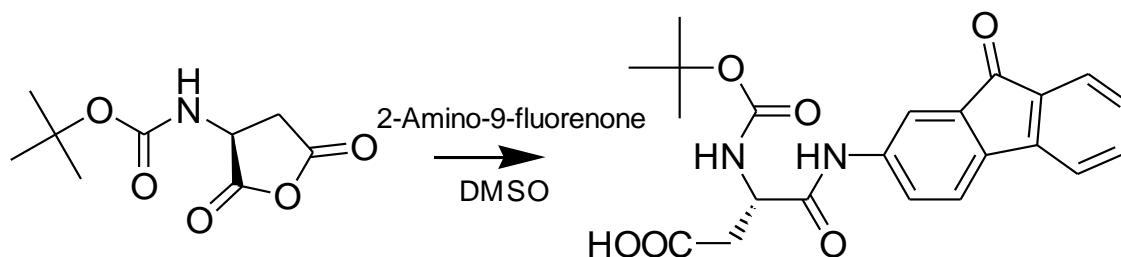
^{13}C -NMR (400 MHz, d_6 -DMSO at 39.5 ppm) δ 170.4, 167.8, 139.0, 128.7, 123.3, 119.2, 49.1, 36.2;

CHN analysis for $\text{C}_{10}\text{H}_{13}\text{ClN}_2\text{O}_3$ calc. C, 49.09; H, 5.36; N, 11.50; O, 19.70; Cl, 14.55

Found: C, 50.39; H, 5.26; N, 11.41;

HRMS m/e calcd. For $\text{C}_{10}\text{H}_{13}\text{N}_2\text{O}_3 = 209.0926$, found 209.0923;

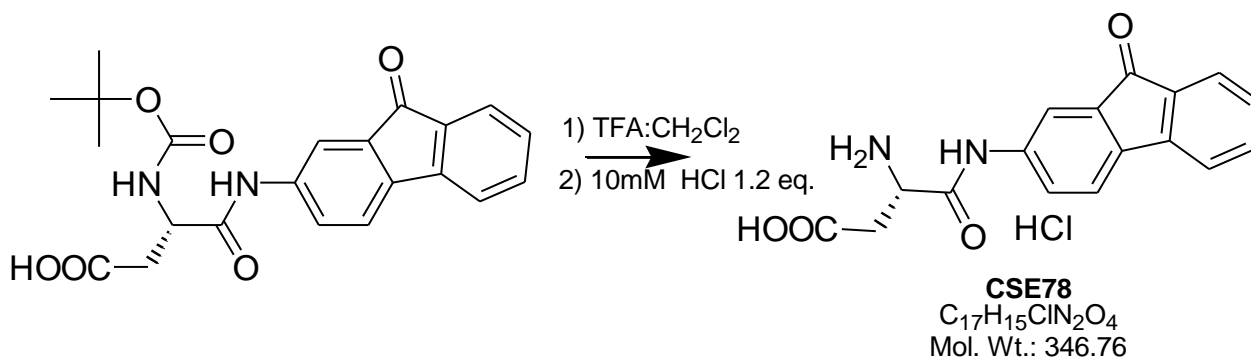
$[\alpha]_D^{22} = +22^\circ$ ($c = 0.23$, DMSO)



N-tBoc-2-fluoren-9-one- α -amide-aspartate: BRL:22

Protected aspartate anhydride (1.379 g, 6.41 mmol) was stirred in DMSO (64 mL, to make the final 0.1 M) and to this 2-amino-9-fluorenone (1.132 g, 0.85 eq.-assuming 85% yield from previous anhydride formation) was added. The solution was allowed to stir for 48 hours, when the reaction had reached completion (determined by absence of 2-amino-9-fluorenone by TLC), at $\sim 45^\circ$ C. The product in DMSO was then diluted with CHCl_3 (400 mL) and washed with 6 x 250 mL aliquots of pH 2 brine (adjusted by 2M HCl) to remove DMSO. Extracted products, observed by TLC, contained primarily the β -amide addition product; N-tBoc protected aspartamide-9-fluorenone, but also included small amounts of α -amide addition product and starting material, N-tBoc protected aspartate. The extracted products were then subsequently concentrated by rotovap to a dry solid and separated by silica gel (mobile phase = 94% CH_2Cl_2 / 5% MeOH / 1% acetic acid). The α addition bi-product was collected from several columns (from 3 reaction preparations), combined and then concentrated by rotovap to afford N-tBoc-fluoren-9-one- α -amide-aspartate (0.260 g, 3.56 mmol) as an orange foam which was used in the next synthetic step without further purification.

$^1\text{H-NMR}$ (400 MHz, d_6 -DMSO at 2.5 ppm) δ 10.33 (s, 1H), 7.96 (s, 1H), 7.69 (m, 3H), 7.56 (m, 2H), 7.30 (dd, $J = 14.9_{\Sigma}$, 7.4 Hz, 1H), 7.25 (d, 7.8 Hz, 1H), 4.43 (dd, $J = 20.1_{\Sigma}$, 6.9 Hz, 1H), 2.72 (dd, $J = 22.0_{\Sigma}$, 16.5, 5.5 Hz, 1H), 2.58 (dd, $J = 24.6_{\Sigma}$, 8.2 Hz, 1H), 1.39 (s, 9H).



2-Fluoren-9-one- α -amide-aspartate: CSE78 / BRL:31

CH₂Cl₂ (1.5 mL) and trifluoroacetic-acid (TFA, 1.5 mL, 8.87 mmol, 14.0 eq) was added to a round bottom flask containing N-tBoc protected 9-fluorenone-aspartamide (0.260 g, 0.633 mmol) which dissolved immediately and turned a dark orange/brown color. The solution was allowed to stir for 40 min, whereby it was observed that the reaction had completed as determined by TLC. The solution was then air dried with compressed air to remove the remaining TFA and CH₂Cl₂. The remaining solid (deprotected product and TFA salt) was then mixed thoroughly with 0.01M HCl (60 mL water, 1.1 eq. HCl) and sonicated. The solution was then frozen to -80° C and placed on the lyophilizer to freeze

dry and remove all the water and remaining TFA leaving an orange powder (0.199 g, 0.574 mmol, 91% yield). The identity and purity of the final product was confirmed by ^1H , ^{13}C NMR, HRMS & rotational analysis.

^1H -NMR (400 MHz, d_6 -DMSO at 2.5 ppm) δ 11.28 (s, 1H), 8.56 (s, 3H), 7.96 (s, 1H), 7.67-7.77 (m, 3H), 7.55 (m, 2H), 7.29 (dd, $J = 14.9_{\Sigma}$, 7.44 Hz, 1H), 4.31 (s, 1H), 3.01 (m, $J = 47.8$ Hz, 2H);

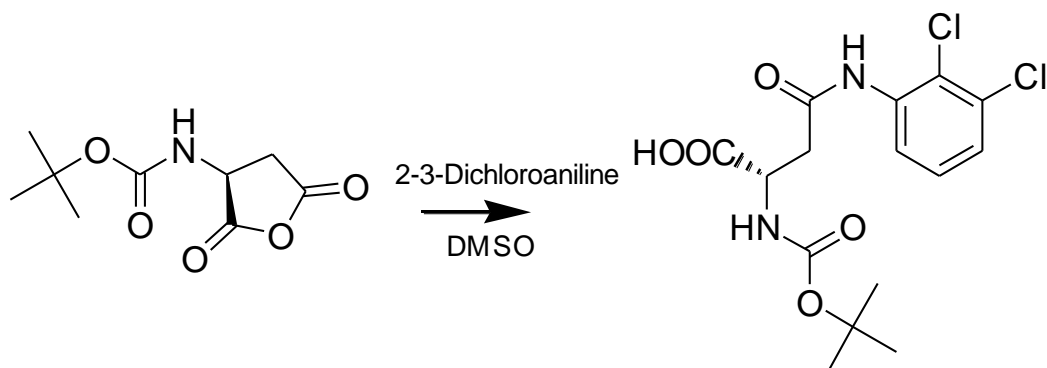
^{13}C -NMR (400 MHz, d_6 -DMSO at 39.5 ppm) δ 192.9, 170.8, 166.6, 144.0, 139.5, 139.2, 135.6, 134.1, 133.4, 128.9, 125.2, 124.0, 121.8, 120.8, 115.0, 49.8, 35.2;

CHN analysis for $\text{C}_{17}\text{H}_{16}\text{ClN}_2\text{O}_4 \cdot \text{H}_2\text{O}$ calc. C, 56.13; H, 4.43; N, 7.70; O, 21.99; Cl, 9.75

Found: C, 56.67; H, 4.23; N, 7.14;

HRMS m/e calcd. For $\text{C}_{17}\text{H}_{15}\text{N}_2\text{O}_4 = 311.1032$, found 311.1011;

$[\alpha]_{\text{D}}^{22} = +9^\circ$ ($c = 0.27$, DMSO)

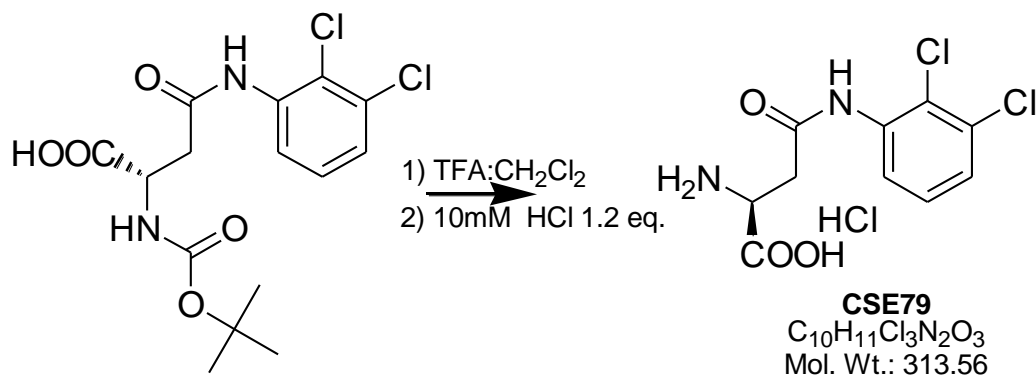


N-tBoc-2,3-dichloro-phenyl-aspartamide: BRL:32

Protected aspartate anhydride (1.61 g, 7.48 mmol) was stirred in DMSO (150 mL, to make the concentration 0.05 M) and to this 2-3-dichloroaniline (1.04 g, 6.42 mmol, 0.85 eq.-assuming 85% yield from previous anhydride formation) was added. The solution was allowed to stir at 55° C for 58 h until it was observed that the reaction had completed (determined TLC). The product in DMSO was then diluted with CHCl₃ (400 mL) and washed with 6 x 250 mL aliquots of pH = 2 brine (adjusted by 2M HCl) to remove the DMSO. Extracted products, observed by TLC, contained primarily the β-amide addition product; N-tBoc-protected-2-3-dichlorophenyl-L-aspartamide, but also included a significant quantity of α-amide addition product and starting material N-tBoc protected aspartate, approx. 20% each. The extracted products were then subsequently concentrated by rotovap to a dry solid and separated by silica gel (mobile phase = 94% CH₂Cl₂ / 5% MeOH / 1% acetic acid). The β addition product (R_f = 0.2) was collected and concentrated by rotovap to afford N-tBoc-2-3-dichloro-phenyl-aspartamide- (0.486g, 1.29 mmol, 17 % yield) as a yellow/white residue and used in the next synthetic step without further purification.

$^1\text{H-NMR}$ (500 MHz, $\text{d}_6\text{-DMSO}$ at 2.5 ppm) δ 9.72 (s, 1H), 7.68 (d, $J = 7.83\text{z}$, 1H), 7.42 (d, $J = 8.1\text{Hz}$, 1H), 7.32 (dd, $J = 16.1\text{z}$, 8.1 Hz, 1H), 7.06 (d, $J = 7.8$ Hz, 1H), 4.34 (d, $J = 5.6$ Hz, 1H), 2.85 (dd, $J = 16.6\text{z}$, 13.7, 10.8 Hz, 1Ha), 2.72 (dd, $J = 22.0\text{z}$, 14.2, 6.8 Hz, 1Hb), 1.35 (s, 9H);

$^{13}\text{C-NMR}$ (500 MHz, $\text{d}_6\text{-DMSO}$ at 39.5 ppm) δ 173.5, 169.3, 155.6, 137.3, 132.2, 128.36, 127.0, 125.2, 124.9, 78.6, 50.7, 38.3, 28.6.



2,3-Dichloro-phenyl-aspartamide: CSE79 / BRL:33

CH_2Cl_2 (3 mL) and trifluoroacetic-acid (TFA, 3 mL, 17.74 mmol, 13.75 eq) were added to a round bottom flask followed by N-tBoc protected aspartamide-phenyl (0.486 g, 1.29 mmol) which dissolved immediately and turned a dark yellow/brown color. The solution was allowed to stir for 60 min, whereby it was observed that the reaction had completed as determined by TLC. The solution was then air dried with compressed air to remove the remaining TFA and CH_2Cl_2 and washed 3 x 30 mL CH_2Cl_2 . The remaining residue (deprotected product and TFA salt) was then mixed thoroughly with 0.01M HCl (141 mL water, 1.1 eq. HCl) and sonicated. The solution was then frozen to $-80^\circ C$ and placed on the lyophilizer to freeze dry / remove all the water and remaining TFA leaving an off white powder (0.3127 g, 0.997 mmol, 77% yield). The identity and purity of the final product was confirmed by 1H , ^{13}C NMR, HRMS & rotational analysis.

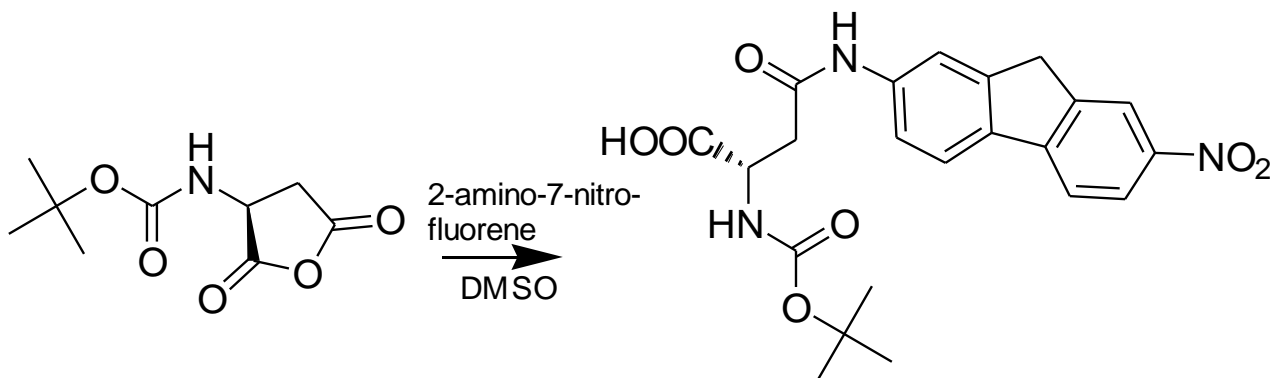
1H -NMR (500 MHz, d_6 -DMSO at 2.5 ppm) δ 10.10 (s, 1H), 8.26 (s, 2.5H), 7.66 (d, J = 8.1Hz, 1H), 7.46 (d, J = 7.8 Hz, 1H), 7.35 (dd, J = 16.1 Σ , 8.1 Hz, 1H), 4.23 (dd, J = 10.3 Σ ,

5.1 Hz, 1H), 3.07 (dd, $J = 21.5_{\Sigma}, 17.5, 13.0$ Hz, 1H), 3.00 (dd, $J = 22.8_{\Sigma}, 16.6, 11.7$ Hz, 1H);

^{13}C -NMR (500 MHz, d_6 -DMSO at 39.5 ppm) δ 170.6, 168.8, 137.1, 132.3, 128.3, 127.21, 125.6, 125.3, 49.5, 36.4;

HRMS m/e calcd. For $\text{C}_{10}\text{H}_{11}\text{N}_2\text{O}_3\text{Cl}_2 = 277.0147$, found 277.0153;

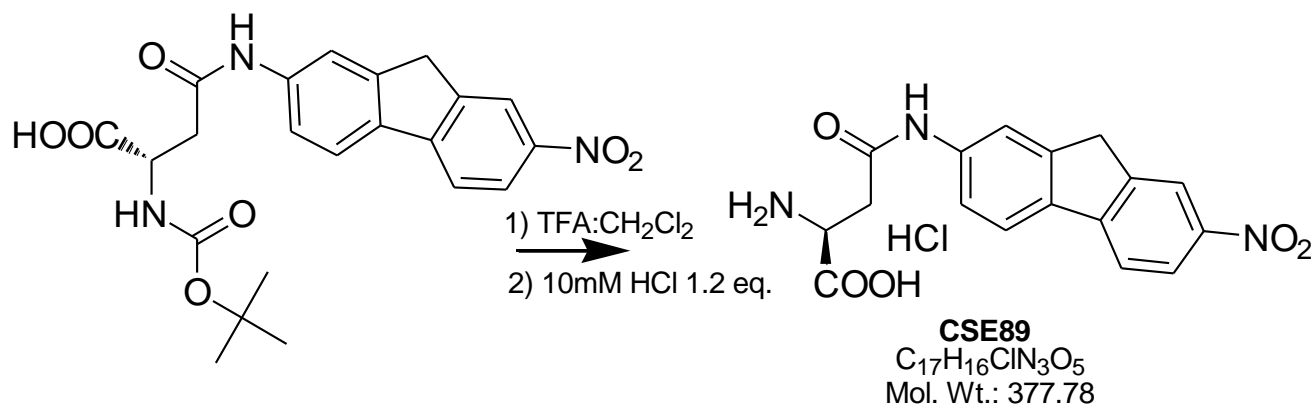
$[\alpha]_{\text{D}}^{22} = +20^\circ$ ($c = 0.26$, DMSO)



N-tBoc-2-fluorenyl-7-nitro-aspartamide: BRL:75

N-tBoc protected aspartate anhydride (0.923 g, 4.29 mmol) was stirred in DMSO (~44 mL, to make 0.1 M final conc.). To this was added 0.824mg of 2-amino-7-nitro-fluorene (0.85 eq, 3.64mmol) synthesized from 2-nitrofluorene (Saroja G., et al. 2004). The

solution was allowed to stir for 24 h at 40° C in which the reaction had reached completion (determined by absence of 2-amino-7-nitro-fluorene on TLC). The product in DMSO was then diluted with 100 mL water (pH adjusted to ~2, by phosphoric acid) and extracted with CHCl₃ (3 x 400 mL). The separated organic solutions were combined and then washed with brine adjusted to pH = 2 by addition of conc. H₃PO₄ (6 x 250 mL aliquots) to remove the DMSO. Extracted products, observed by TLC, contained primarily the β amide addition product; N-tBoc protected aspartamide-7-nitro-fluorene, but also included small amounts of α amide addition product. The extracted products, in chloroform, were then subsequently concentrated by rotovap to a dry solid and separated by silica gel (mobile phase = 95% CH₂Cl₂ / 4% MeOH / 1% acetic acid). The β addition product (R_f = 0.25) was collected from several combined fractions and then concentrated by rotovap to afford N-tBoc-7-nitrofluorne-aspartamide (0.260 g, 3.556 mmol) as a yellow/orange residue, which was used in the next synthetic step without further purification.



2-Fluorenyl-7-nitro-L-aspartamide: BRL:76

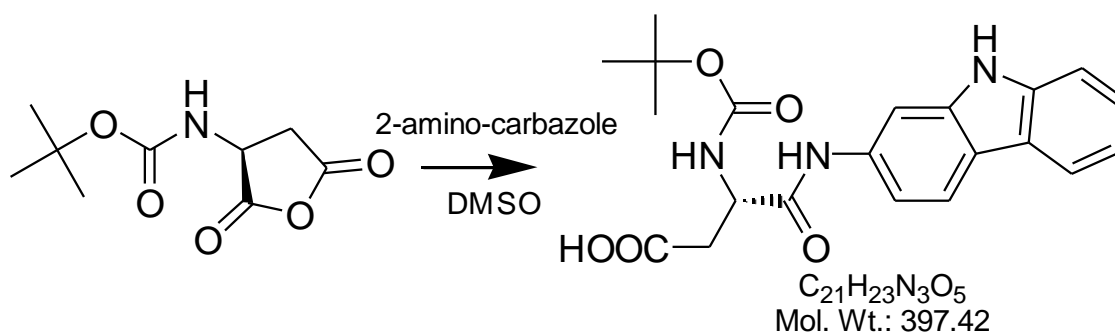
CH_2Cl_2 (3 mL) and trifluoroacetic-acid (TFA, 3 mL) 1:1 solution was added to a round bottom flask containing N-tBoc protected 7-nitro-2-fluorenyl-aspartamide (0.463 g, 1.05 mmol) which dissolved immediately and turned a yellow/orange color in solution. The solution was allowed to stir for 1 h where it was observed that the reaction had completed as determined by TLC. The solution was then air dried with compressed air to remove the remaining TFA and CH_2Cl_2 . The residue was washed with 3 x 30 ml CH_2Cl_2 and aspirated until dry. The remaining solid (deprotected product and TFA salt) was then mixed thoroughly with 0.01M HCl (115 mL water, 1.1 eq. HCl) and sonicated. The solution was then frozen to $-80^\circ C$ and placed on the lyophilizer to freeze dry / remove all the water and remaining TFA leaving an orange colored residue (0.372 g, 0.984 mmol, 94% yield). The purity and identity of the final product was confirmed by 1H , ^{13}C NMR, HRMS, and rotational analysis.

$^1\text{H-NMR}$ (400 MHz, $\text{d}_6\text{-DMSO}$ at 2.5 ppm) δ 10.63 (s, 1H), 8.39 (s, 1H), 8.27 (d, $J = 7.8$ Hz, 1H), 8.05 (s, 1H), 8.03 (d, $J = 3.2$ Hz, 1H), 8.00 (d, $J = 2.6$ Hz, 1H), 7.63 (d, $J = 8.4$ Hz, 1H), 4.21 (dd, $J = 9.0_{\Sigma}, 4.5$ Hz, 1H), 4.05 (s, 2H), 3.07 (dd, $J = 21.4_{\Sigma}, 17.5, 5.2$ Hz, 1H), 2.97 (dd, $J = 22.6_{\Sigma}, 17.5, 5.2$ Hz, 1H);

$^{13}\text{C-NMR}$ (400 MHz, $\text{d}_6\text{-DMSO}$ at 39.5 ppm) δ 170.3, 167.7, 147.7, 146.2, 145.7, 144.07, 139.7, 134.3, 123.1, 122.3, 120.3, 119.9, 118.4, 115.6, 48.8, 36.8, 36.2;

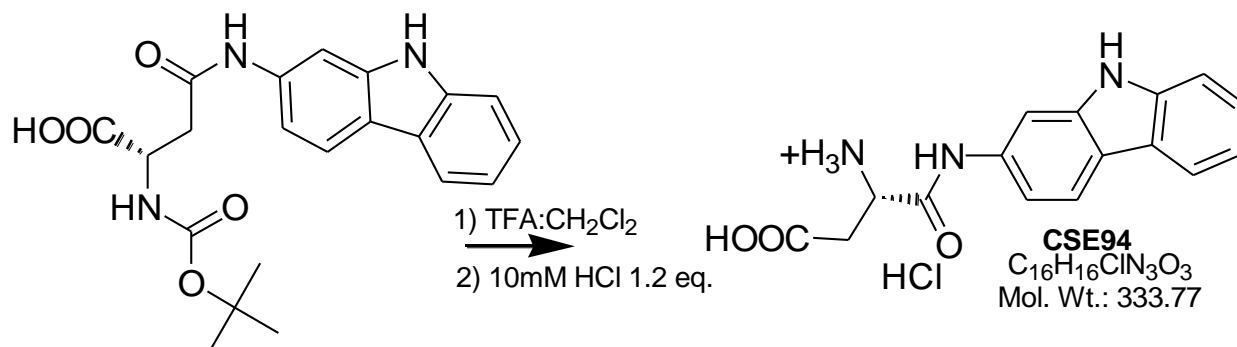
HRMS m/e calcd. For $\text{C}_{17}\text{H}_{16}\text{N}_3\text{O}_5 = 342.1090$, found 342.1099;

$[\alpha]_{\text{D}}^{22} = +4.5^\circ$ ($c = 0.067$, methanol, Na^+ D lamp)



N-tBoc-2-carbazole- α -amide-L-aspartate: BRL: 102

Protected aspartate anhydride (0.978 g, 4.55 mmol) dissolved in 90 mL DMSO. To this was added 0.710 g of 2-amino-carbazole (0.855 eq, 3.90 mmol) synthesized from carbazole (Kyziol J.B., Lyżniak A. 1980). The solution was allowed to stir for 24 h at 60° C in which the reaction had reached completion (determined by absence of 2-amino-carbazole on TLC). The product in DMSO was then diluted with 100 mL water and pH adjusted to ~2 by addition of phosphoric acid. The aqueous solution was extracted with CHCl₃ (400 mL x 3 times). The CHCl₃ washes were combined and then washed with brine adjusted to pH = 2 by addition of H₃PO₄ conc. in 6 x 250 mL aliquots to remove the DMSO. The CHCl₃ layer was then concentrated to an off light-brown residue by reduced pressure. TLC revealed the crude residue to be primarily the β-amide addition product N-tBoc protected 2-carbazole-β-aspartamide, but also includes a small amount of α-amide addition product. The crude products were then subsequently separated by silica gel (mobile phase = 95% CH₂Cl₂ / 4% MeOH / 1% acetic acid). The α addition product (R_f = 0.3) was collected from several fractions, combined and then concentrated by rotovap to afford N-tBoc-2-carbazole-α-aspartamide (0.106 g, 0.267 mmol)(note: not all was isolated) as an off white residue, which was used in the next synthetic step without further purification.



2-Carbazole- α -amide-L-aspartate: BRL: 104

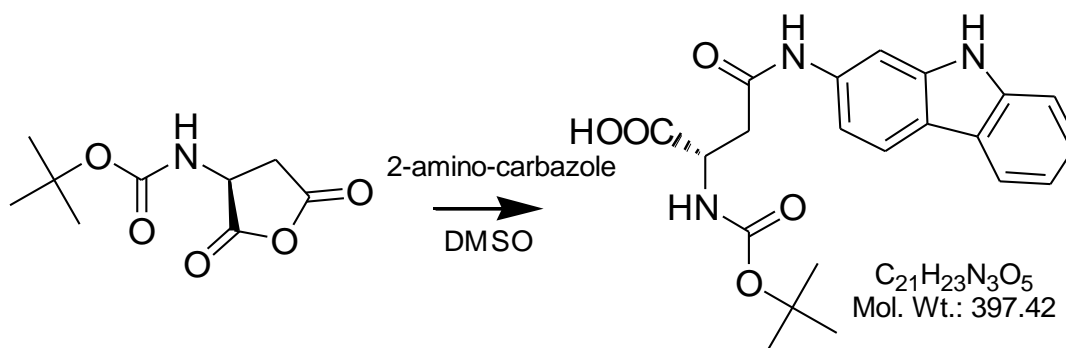
2 mL of a 1:1 CH₂Cl₂ and trifluoroacetic-acid solution added to a round bottom containing 30.0 mg of N-tBoc-2-carbazole- α -amide-aspartate. The residue dissolves immediately making a dark brown solution and was allowed to stir for 1 h. The solution was aspirated with compressed air until only a dry residue remained. The light brown residue was then washed 3 x 25 mL CH₂Cl₂ and dried again. The residue was then resuspended by addition of 3 mL 0.01M HCl (1.2 eq.) and brief sonication. The mixture was then frozen to -80° C and lyophilized until dry leaving 20.0 mg of pure 2-carbazole- α -amide-L-aspartate an 88% yield. The identity of the final product was confirmed by ¹H, ¹³C NMR, HRMS and analyzed by rotational analysis.

¹H-NMR (400 MHz, d₆-DMSO at 2.5 ppm) ppm 11.32 (s, 1H), 10.83 (s, 1H), 8.48 (s, 3H), 8.04 (d, J = 1.9 Hz, 1H), 8.02 (s, 1H), 7.99 (s, 1H), 7.43 (d, J = 7.8 Hz, 1H), 7.28-7.35 (m, 2H), 7.12 (dd, J = 14.9_Σ, 7.8, 7.1 Hz, 1H), 4.31(s, 1H), 3.03 (dd, J = 22.0_Σ, 16.8, 5.2 Hz, 1H), 2.92 (dd, J = 24.6_Σ, 17.5, 7.1 Hz, 1H);

^{13}C -NMR (400 MHz, d_6 -DMSO at 39.5 ppm) ppm 170.9, 166.0, 140.0, 140.0, 136.1, 125.2, 122.3, 120.4, 119.8, 118.9, 118.7, 111.3, 110.8, 101.7, 49.9, 35.4;

HRMS m/e calcd. For $\text{C}_{16}\text{H}_{16}\text{N}_3\text{O}_3 = 298.1192$, found 298.1207;

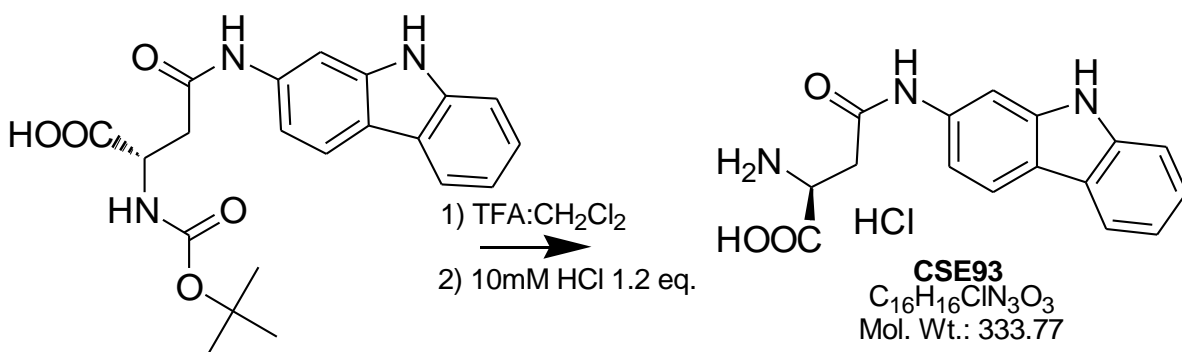
$[\alpha]_{\text{D}}^{22} = +19^\circ$ ($c = 0.10$, methanol, Na^+ D lamp)



N-tBoc-2-carbazole-L-aspartamide: BRL: 102

Protected aspartate anhydride (0.978 g, 4.55 mmol) dissolved in 90 mL DMSO. To this was added 0.710 g of 2-amino-carbazole (0.855 eq, 3.90 mmol) synthesized from carbazole (Kyziol J.B., Lyżniak A. 1980). The solution was allowed to stir for 24 h at 60°C . The reaction had reached completion (determined by absence of 2-amino-carbazole on TLC). The product in DMSO was then diluted with 100 mL water and pH adjusted to ~ 2 by addition of phosphoric acid. The aqueous solution was extracted with CHCl_3 (400 mL x 3 times). The CHCl_3 washes were combined and then rinsed with brine adjusted to $\text{pH} = 2$ by addition of conc. H_3PO_4 in 6 x 250 mL aliquots to remove the

DMSO. The CHCl_3 layer was then concentrated to an off light-brown residue by reduced pressure. TLC revealed the crude residue to be primarily the β -amide addition product N-tBoc protected 2-carbazole- β -aspartamide, but also includes a small amount of α -amide addition product. The crude products were then subsequently separated by silica gel column (mobile phase = 95% CH_2Cl_2 / 4% MeOH / 1% acetic acid). The β addition product ($R_f = 0.2$) was collected from several fractions, combined and then concentrated by rotovap to afford N-tBoc-2-carbazole- β -aspartamide (0.300 g, 0.755 mmol) (note: only a portion was isolated) as an off light brown residue, which was used for the next synthetic step without further purification.



2-Carbazole-L-aspartamide: BRL: 103

To a round bottom flask containing 28.0 mg of N-tBoc protected 2-carbazole- β -aspartamide (0.0705 mmol) was added 2 mL of a 1:1 CH_2Cl_2 and TFA solution. The

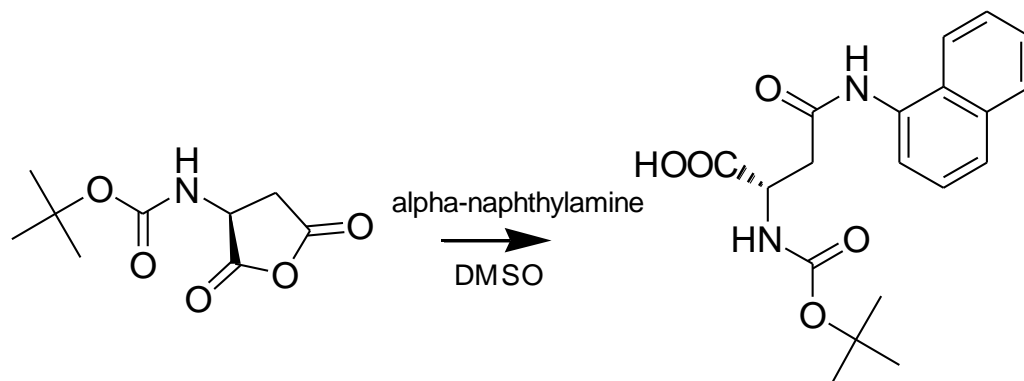
protected aspartamide dissolved immediately creating a vibrant green colored solution which was allowed to stir for 1 hour. The solution was then aspirated with compressed air until only a residue remained. The residue was then washed 3 x 20 mL of CH₂Cl₂ and resuspended in 3 mL of a 0.01 M HCl (1.2 eq) and briefly sonicated to dissolve. This mixture was then frozen to -80° C and lyophilized until dry leaving 20.0 mg of 2-carbazole-β-aspartamide (.0600 mmol) at 85% yield a light brown residue. The final product was analyzed by ¹H, ¹³C NMR, HRMS and rotational analysis to confirm identity and purity.

¹H-NMR (400 MHz, d₆-DMSO at 2.5 ppm) δ 11.30 (s, 1H), 10.55 (s, 1H), 8.44 (s, 2.5H), 7.98-8.01(m, 3H), 7.42 (d, J = 8.4 Hz, 1H), 7.24-7.35 (m, 2H), 7.11 (dd, J = 14.9_Σ, 7.8, 7.1 Hz, 1H), 4.26(s, 1H), 3.13 (dd, J = 22.0_Σ, 17.5, 16.8, 5.2 Hz, 1H), 3.04 (dd, J = 22.6_Σ, 17.5,16.8, 5.8 Hz, 1H);

¹³C-NMR (400 MHz, d₆-DMSO at 39.5 ppm) δ 170.3, 167.1, 140.1, 140.0, 136.8, 124.8, 122.4, 120.3, 119.6, 118.6, 118.4, 111.1, 110.7, 101.4, 48.7, 35.9;

HRMS *m/e* calcd. for C₁₆H₁₆N₃O₃ = 298.1192, found 298.1180;

[α]_D²² = -3° (c = 1.27, methanol, Na⁺ D Lamp)



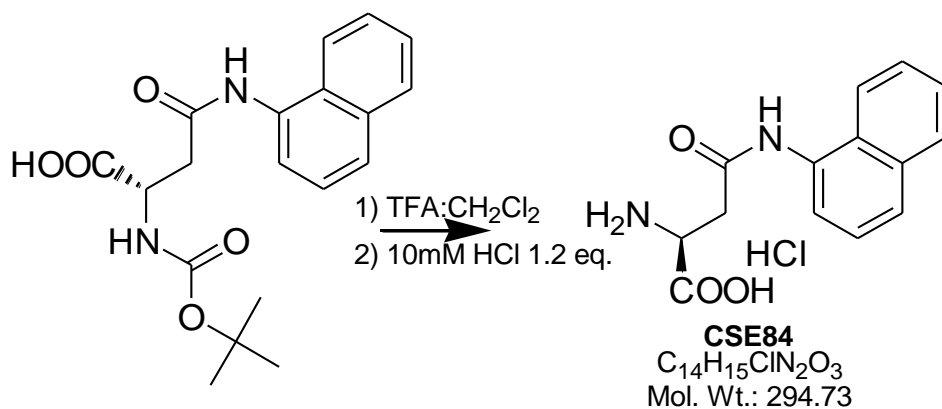
N-tBoc- α -naphthyl-aspartamide: BRL: 228

Protected aspartate anhydride (1.98 g, 9.2 mmol) was dissolved in DMSO (80 mL). To this was added α -naphthylamine (2.37 g, 0.9 eq., 88% aryl amine). The solution was allowed to stir for 48 hours at $\sim 40^\circ\text{C}$ or until the reaction had completed (determined by TLC in the absence of α -naphthylamine with mobile phase 95% CH_2Cl_2 / 4% MeOH / 1% acetic acid). The solution was then diluted with CHCl_3 (450 mL) and washed with brine adjusted to $\text{pH} = 2$ by addition of H_3PO_4 conc. (4 x 200 mL aliquots) to remove the DMSO. The organic phase was then concentrated, leaving a dark red/purple residue. The product were then isolated by silica gel (mobile phase = 95% CH_2Cl_2 / 4% MeOH / 1% acetic acid). The α addition bi-product was collected at $R_f = 0.3$, concentrated and stored. The β addition product was isolated at $R_f = 0.2$, concentrated by rotovap to a

white (slight purple) residue (1.90 g. recovered, 5.31 mmol) and used in the next synthetic step without further purification.

$^1\text{H-NMR}$ (500 MHz, d_6 -DMSO at 2.5 ppm) δ 12.68 (s, 1H), 9.93 (s, 1H), 8.09 (d, $J = 9.0$ Hz, 1H), 7.92 (dd, $J = 8.8_{\Sigma}, 5.4$ Hz, 1H), 7.74 (d, $J = 8.1$ Hz, 1H), 7.64 (d, $J = 7.3$ Hz, 1H), 7.52 (dd, $J = 7.6_{\Sigma}, 3.9, 3.7$ Hz, 2H), 7.47 (dd, $J = 15.6_{\Sigma}, 7.8$ Hz, 1H), 7.16 (d, $J = 8.3$ Hz, 1H), 4.42 (dd, $21.3_{\Sigma}, 13.7, 6.1$ Hz, 2H), 2.95 (dd, $J = 20.3_{\Sigma}, 14.9, 9.5$ Hz, 1H), 2.84 (dd, $J = 23.0_{\Sigma}, 14.9, 6.8$ Hz, 1H), 1.39 (s, 9H)

$^{13}\text{C-NMR}$ (500 MHz, d_6 -DMSO at 39.5 ppm) δ 173.8, 169.4, 155.7, 128.5, 128.2, 126.45, 126.1, 126.0, 125.7, 123.4, 122.1, 78.6, 50.9, 38.3, 28.6



1-Naphthyl-aspartamide: BRL: 229

CH₂Cl₂ (4 mL) and trifluoroacetic-acid (TFA, 4 mL) solution 1:1 were added to a round bottom flask containing N-tBoc- β -naphthyl-aspartamide (1.14 g, 3.18 mmol) which

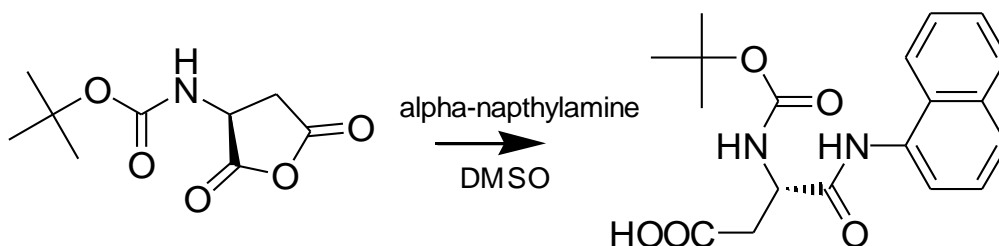
dissolved immediately and turned a dark red/purple color. The solution was allowed to stir for an additional 45 min. at rt (~22° C) whereby it was observed that the reaction had completed as determined by TLC (mobile phase 90% CH₂Cl₂ / 9% MeOH / 1% AcOH; R_f = 0.01). The solution was then aspirated until dry by compressed air to remove TFA and CH₂Cl₂. The remaining solid (deprotected product and TFA salt) was washed with 3 x 80mL CH₂Cl₂ and then mixed with 193 mL 0.01M HCl (1.1 eq.) followed by light sonication to suspend the solid residue. The solution was then frozen to -80° C and placed on the lyophilizer to freeze dry / remove all the water and remaining TFA leaving a slight purple/white powder (1-naphthyl-aspartamide 0.870 g, 2.95 mmol, 93% yield). The final product was analyzed by ¹H, ¹³C NMR, HRMS and rotational analysis to confirm identity and purity.

¹H-NMR (500 MHz, d₆-DMSO at 2.5 ppm) δ 10.33 (s, 1H), 8.38 (s, 2.5H), 8.09 (dd, J = 9.0_Σ, 3.7 Hz, 1H), 7.92 (dd, J = 9.3_Σ, 5.9 Hz, 1H), 7.77 (d, J = 8.1 Hz, 1H), 7.65 (d, J = 7.3 Hz, 1H), 7.53 (dd, J = 9.3_Σ, 4.4, 3.2 Hz, 2H), 7.48 (dd, J = 15.6_Σ, 7.8 Hz, 1H), 4.28 (dd, 9.8_Σ, 4.9 Hz, 1H), 3.19 (dd, J = 21.8_Σ, 16.9, 5.1 Hz, 1H), 3.13 (dd, J = 22.5_Σ, 16.9, 5.6 Hz, 1H);

¹³C-NMR (500 MHz, d₆-DMSO at 39.5 ppm) δ 170.7, 168.6, 134.1, 133.5, 128.5, 128.22, 126.5, 126.3, 126.0, 125.9, 123.4, 122.3, 49.2, 35.9;

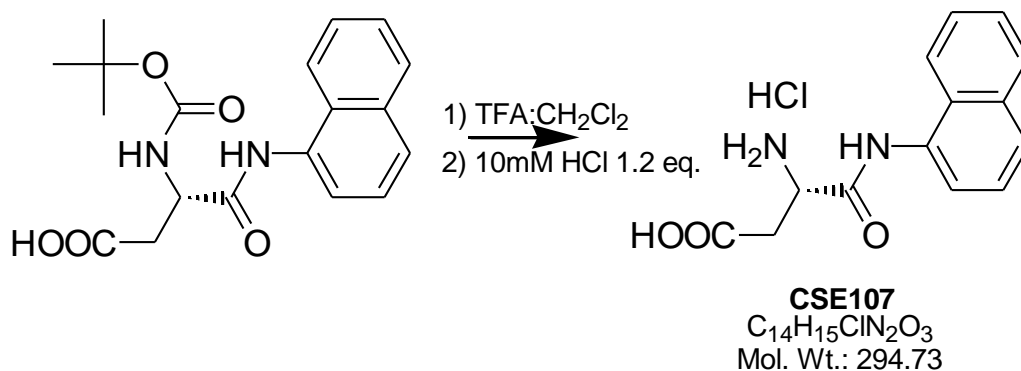
HRMS m/e calcd. for $C_{14}H_{15}N_2O_3$ = 259.1083, found 259.1088;

$[\alpha]_D^{22} = +24^\circ$ ($c = 0.22$, methanol, Na^+ D lamp)



N-tBoc-1-naphthyl - α -amide-L-aspartate: BRL: 228

Protected aspartate anhydride (1.98 g, 9.22 mmol) was dissolved in DMSO (80 mL). To this was added α -naphthylamine (2.37 g, 0.9 eq., 88% aryl amine). The solution was allowed to stir for 48 h at $\sim 40^\circ$ C or until the reaction had completed as determined by TLC (mobile phase 95% CH_2Cl_2 / 4% MeOH / 1% acetic acid). The solution was then diluted with $CHCl_3$ (450 mL) and washed with brine adjusted to pH = 2 by addition of H_3PO_4 conc. (4 x 200 mL aliquots) to remove the DMSO. The organic phase was then concentrated by rotovap leaving a dark red/purple residue. The products were then isolated by silica gel (mobile phase = 95% CH_2Cl_2 / 4% MeOH / 1% acetic acid). The β -addition bi-product was collected at $R_f = 0.2$, concentrated and stored. A portion of the α -addition product was isolated at $R_f = 0.3$ and subsequently concentrated by rotovap to a red/brown residue (0.230 g, 0.642 mmol.) which was used within the next synthetic step without further characterization or purification.



1-Naphthyl - α -amide-L-aspartate: BRL: 250

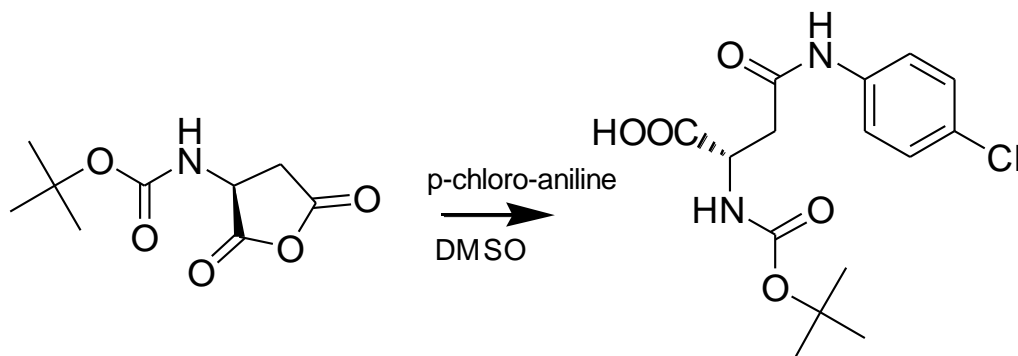
CH₂Cl₂ (1.5 mL) and trifluoroacetic-acid (TFA, 1.5 mL) solution 1:1 were added to a round bottom flask containing N-tBoc- α -amide-L-aspartate (0.230 g, 0.642 mmol) which dissolved immediately and turned a dark red/brown color. The solution was allowed to stir for 1 hour at rt (~21° C) whereby it was observed that the reaction had completed as determined by TLC (mobile phase 90% CH₂Cl₂ / 9% MeOH / 1% AcOH; R_f = 0.01). The solution was then aspirated until dry by compressed air to remove the TFA and CH₂Cl₂. The remaining residue (deprotected product and TFA salt) was taken up into 30 mL deionized water using light sonication to suspend residue and washed with 3 x 10 mL CH₂Cl₂. To the aqueous solution containing the final product 0.385 mL 2 M HCl (1.2 eq.) was added and was then frozen to -80° C and placed on the lyophilizer until dry leaving a off white solid residue (α -naphthyl-amide-L-aspartate 0.179 g, 0.610 mmol, 95% yield). The final product was analyzed by ¹H, ¹³C NMR, HRMS and rotational analysis to confirm identity and purity.

$^1\text{H-NMR}$ (500 MHz, d_6 -DMSO at 2.5 ppm) δ 10.70 (s, 1H), 8.13 (dd, $J= 8.8_\Sigma, 5.4, 3.4$ Hz, 1H), 7.94 (dd, $J= 9.0_\Sigma, 5.6, 3.4$ Hz, 1H), 7.805 (d, $J = 8.1$ Hz, 1H), 7.64 (d, $J = 7.3$ Hz, 1H), 7.53 (m, 26.2 Hz, 3H), 4.47 (dd, $12.0_\Sigma, 6.1, 5.9$ Hz, 1H), 3.04 (dd, $J = 23.7_\Sigma, 17.4, 5.9$ Hz, 1H), 3.01 (dd, $J = 24.9_\Sigma, 18.1, 7.6$ Hz, 1H);

$^{13}\text{C-NMR}$ (500 MHz, d_6 -DMSO at 39.5 ppm) δ 171.5, 167.8, 134.1, 133.0, 128.5, 128.31, 126.7, 126.5, 126.4, 126.0, 123.4, 122.4, 50.0, 36.0;

HRMS m/e calcd. For $\text{C}_{14}\text{H}_{15}\text{N}_2\text{O}_3 = 259.1083$, found 259.1063;

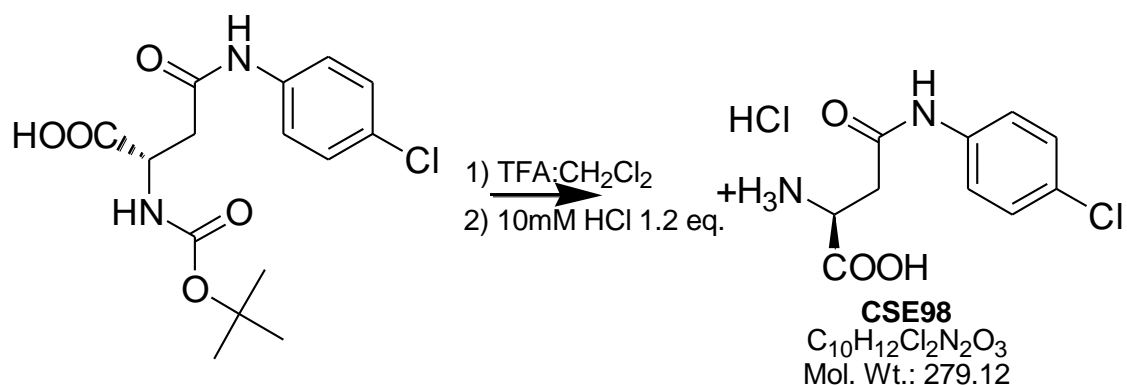
$[\alpha]_D^{22} = +5^\circ$ ($c = 0.12$, methanol, Na^+ D lamp)



N-tBoc-p-chloro-phenyl-L-aspartamide: BRL: 132

N-tBoc protected aspartate anhydride (0.932 g, 4.33 mmol) was dissolved in DMSO (90 mL). To this was added p-chloroaniline (.522 g, .85 eq., 3.68 mmol). The solution was allowed to stir for 48 h at $\sim 70^\circ$ C or until the reaction had completed as determined by TLC (mobile phase 95% CH_2Cl_2 / 4% MeOH / 1% acetic acid). The solution was then diluted with CHCl_3 (200 mL) and washed with brine adjusted to pH = 2 by addition of H_3PO_4 conc. (4 x 250 mL aliquots) to remove DMSO. The organic phase was then concentrated, leaving a light brown residue. The products were isolated by silica gel (mobile phase = 95% CH_2Cl_2 / 4% MeOH / 1% acetic acid). The α -addition bi-product was collected at $R_f = 0.2$, concentrated and stored for later use. The β addition product was isolated at $R_f = 0.15$ and subsequently concentrated by rotovap to an off white residue (0.663 g. recovered, 1.93 mmol) which was used in the next synthetic step without further purification.

$^1\text{H-NMR}$ (500 MHz, d_6 -DMSO at 2.5 ppm) δ 12.34 (s, 5H), 10.12 (s, 1H), 7.60 (d, J = 8.4 Hz, 2H), 7.34 (d, J = 8.4 Hz, 2H), 7.08 (d, J = 8.4 Hz, 1H), 4.34 (dd, 20.7 Σ , 13.6, 7.1 Hz, 1H), 2.80 (dd, J = 20.7 Σ , 15.5, 5.8 Hz, 1H), 2.63 (dd, J = 22.6 Σ , 15.5, 7.8 Hz, 1H), 1.36 (s, 9H)



p-Chloro-phenyl-L-aspartamide: BRL: 144

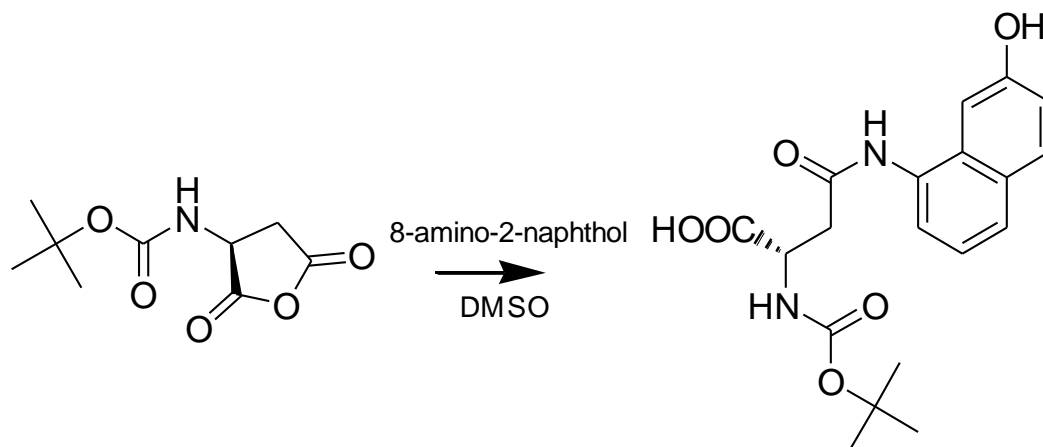
A solution of 50% trifluoroacetic-acid in CH₂Cl₂ (4 mL) was added to a round bottom flask containing N-tBoc-p-chloro-phenyl-aspartamide (0.114 g, 0.333 mmol) which dissolved immediately and turned a dark brown color. The solution was allowed to stir for 1 h at rt (~22° C) whereby it was observed that the reaction had completed as determined by TLC (mobile phase 90% CH₂Cl₂ / 9% MeOH / 1% AcOH; R_f = 0.01). The solution was then aspirated until dry with compressed air to remove TFA and CH₂Cl₂. The remaining residue (deprotected product and TFA salt) was washed with 4 x 10 mL CH₂Cl₂ and taken up into 20 mL 0.01 M HCl using light sonication to resuspend the residue. The solution was then frozen to -80° C and placed on the lyophilizer until dry, leaving a white solid residue (p-chloro-phenyl-aspartamide 0.087 g, .312 mmol, 94% yield). The final product was analyzed by ¹H, ¹³C NMR, HRMS and rotational analysis to confirm identity and purity.

$^1\text{H-NMR}$ (500 MHz, d_6 -DMSO at 2.5 ppm) δ 10.69 (s, 1H), 8.39 (s, 2.5H), 7.64 (d, J=9.1 Hz, 2H), 7.36 (d, J = 9.1 Hz, 2H), 4.15 (dd, 10.4_{Σ} , 5.2 Hz, 1H), 3.05 (dd, J = 21.4_{Σ} , 16.8, 4.5 Hz, 1H), 2.95 (dd, J = 22.6_{Σ} , 16.8, 5.2 Hz, 1H);

$^{13}\text{C-NMR}$ (500 MHz, d_6 -DMSO at 39.5 ppm) δ 170.2, 167.7, 137.9, 128.7, 126.9, 120.74, 48.8, 36.1;

HRMS m/e calcd. For $\text{C}_{10}\text{H}_{12}\text{N}_2\text{ClO}_3 = 243.0536$, found 243.0565;

$[\alpha]_{\text{D}}^{22} = -5^\circ$ (c = 0.080, methanol, Na^+ D lamp)

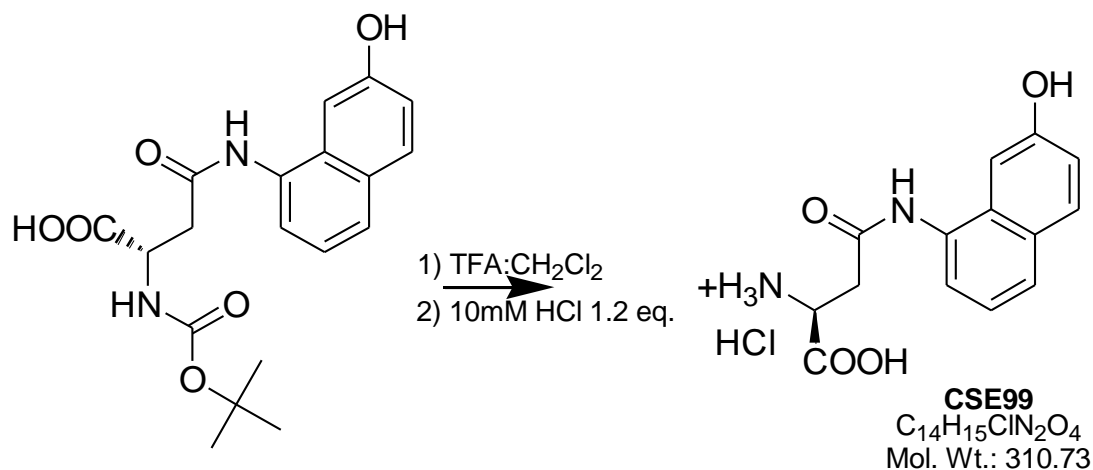


N-tBoc-1-naphth-7-ol-aspartamide: BRL: 137

Protected aspartate anhydride (0.561 g, 2.41 mmol) was dissolved in DMSO (80 mL). To this was added 8-amino-2-naphthol (0.373 g, 0.85eq, 96%). The solution was allowed to stir for 48 h at $\sim 40^\circ\text{C}$ or until the reaction had completed as determined by TLC (mobile phase 90% CH_2Cl_2 / 9% MeOH / 1% acetic acid). The solution was then diluted with CHCl_3 (450 mL) and washed with brine adjusted to pH = 2 by conc. H_3PO_4 (4 x 200 mL aliquots) to remove DMSO. The organic phase was then concentrated, leaving a dark red/brown residue. The crude product was then separated by silica gel (mobile phase = 95% CH_2Cl_2 / 4% MeOH / 1% acetic acid). The α -addition bi-product was collected at $R_f = 0.3$, concentrated and stored. Some of the β -addition product was isolated at $R_f = 0.2$ and concentrated by rotovap to a light brown residue (0.422 g., 1.13 mmol), which was used in the next synthetic step without further purification.

$^1\text{H-NMR}$ (500 MHz, d_6 -DMSO at 2.5 ppm) δ 10.59 (s, 1H), 7.74 (d, $J = 9.1$ Hz 1H), 7.65 (d, $J = 7.1$ Hz, 1H), 7.57 (d, $J = 7.8$ Hz, 1H), 7.45 (s, 1H), 7.19 (dd, 15.5_Σ , 7.8 Hz, 1H),

7.10 (dd, $J = 10.4_{\Sigma}, 9.1, 7.1\text{Hz}$, 1H), 6.58 (d, $J = 5.8$, 1H), 4.195 (d, $J = 5.2\text{ Hz}$, 1H), 2.87 (dd, $20.7_{\Sigma}, 14.9, 5.8\text{ Hz}$, 1H), 2.70 (dd, $J = 20.1_{\Sigma}, 14.9, 5.2\text{ Hz}$, 1H), 1.37 (s, 9H)



1-Naphth-7-ol-L-aspartamide: BRL: 232

A 1:1 solution of CH_2Cl_2 (2 mL) and trifluoro-acetic-acid (TFA, 2 mL) was added to a round bottom flask containing N-tBoc-2-naphthol-8- β -aspartamide (0.10 g, 0.267mmol) in 2 mL CH_2Cl_2 , which dissolved immediately and turned a dark red/brown color. The solution was allowed to stir for 1 hour at rt ($\sim 21^\circ\text{C}$) whereby it was observed that the reaction had completed as determined by TLC (mobile phase 85% CH_2Cl_2 / 14% MeOH / 1% AcOH; $R_f = 0.01$). The solution was then aspirated until dry with compressed air to remove the remaining TFA and CH_2Cl_2 . The remaining solid (deprotected product and TFA salt) was washed with 2 x 50 mL CH_2Cl_2 and then taken up into 29.4 mL of 0.01M HCl (diluted from 160 μL 2M HCl, 1.1 eq.) followed by light sonication to

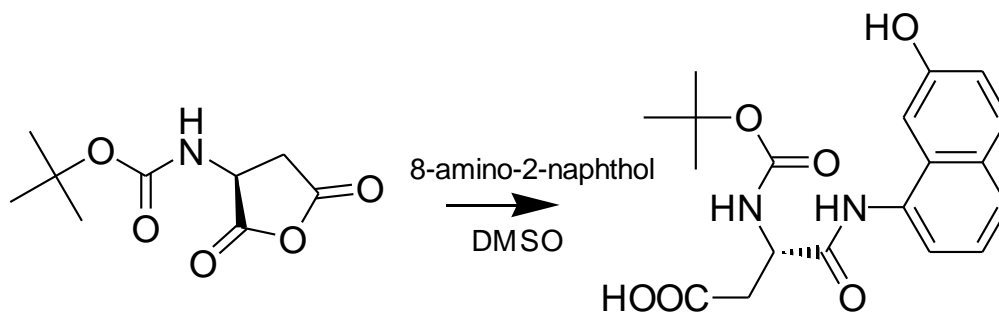
dissolve/suspend remaining solid residue. The solution was then frozen to -80°C and placed on the lyophilizer to freeze dry / remove all the water and remaining TFA leaving a dark red/brown solid (1-naphth-7-ol-L-aspartamide, 0.075 g, 90% yield). The final product was analyzed by ^1H , ^{13}C NMR, HRMS and rotational analysis to confirm identity and purity.

^1H -NMR (500 MHz, d_6 -DMSO at 2.5 ppm) δ 10.17 (s, 1H), 9.92 (s, 1H), 8.44 (s, 2.5H), 7.77 (d, $J = 8.4$ Hz, 1H), 7.64 (d, $J = 7.8$ Hz, 1H), 7.52 (d, $J = 7.8$ Hz, 1H), 7.31 (s, 1H), 7.23 (dd, $J = 15.5_{\Sigma}$, 7.76, 1H), 7.15 (dd, $J = 10.4_{\Sigma}$, 8.4, 6.5 Hz, 1H), 4.26 (dd, 9.1_{Σ} , 4.5 Hz, 1H), 3.195 (dd, $J = 22.0_{\Sigma}$, 17.5, 12.3 Hz, 1H), 3.15 (dd, $J = 22.6_{\Sigma}$, 16.8, 11.0 Hz, 1H);

^{13}C -NMR (500 MHz, d_6 -DMSO at 39.5 ppm) δ 170.3, 168.1, 155.6, 131.4, 129.7, 128.42, 125.5, 122.4, 121.9, 118.7, 104.5, 48.9, 35.4;

HRMS m/e calcd. For $\text{C}_{14}\text{H}_{15}\text{N}_2\text{O}_4 = 275.1032$, found 275.1030;

$[\alpha]_{\text{D}}^{22} = +18^{\circ}$ ($c = 0.29$, methanol, Na^+ D lamp)

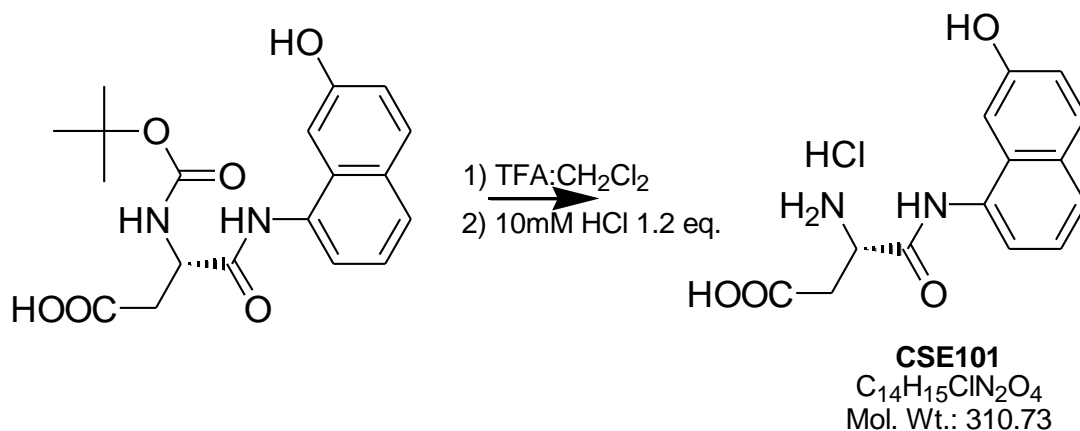


N-tBoc-1-naphth-7-ol- α -amide-aspartate: BRL: 137

Protected aspartate anhydride (0.561 g, 2.41 mmol) was dissolved in DMSO (80 mL). To this was added 8-amino-2-naphthol (0.373 g, 0.85eq, 96%). The solution was allowed to stir for 48 h at $\sim 40^\circ\text{C}$ or until the reaction had completed as determined by TLC (mobile phase 90% CH_2Cl_2 / 9% MeOH / 1% acetic acid). The solution was then diluted with CHCl_3 (450 mL) and washed with brine adjusted to pH = 2 by conc. H_3PO_4 (4 x 200 mL aliquots) to remove DMSO. The organic phase was then concentrated, leaving a dark red/brown residue. The crude product was then separated by silica gel (mobile phase = 95% CH_2Cl_2 / 4% MeOH / 1% acetic acid). The β -addition bi-product was collected at $R_f = 0.2$, concentrated and stored. The α -addition product was isolated at $R_f = 0.3$ and concentrated by rotovap to a light brown residue (0.040 g., 0.107 mmol). The isolated product was used in the next synthetic step without further purification or characterization.

$^1\text{H-NMR}$ (500 MHz, d_6 -DMSO at 2.5 ppm) δ 9.75 (s, 1H), 7.76 (d, $J = 9.1$ Hz 1H), 7.63 (d, $J = 7.8$ Hz, 1H), 7.50 (d, $J = 7.8$ Hz, 1H), 7.24 (m, 3H), 7.11 (d, $J = 8.4$ Hz, 1H), 4.59

(d, J = 5.2 Hz, 1H), 2.80 (dd, 19.4_Σ, 15.5, 3.9 Hz, 1H), 2.65 (dd, J = 24.6_Σ, 15.5, 6.5 Hz, 1H), 1.41 (s, 9H)



1-Naphth-7-ol- α -amide-aspartate: BRL: 147

A 50 % solution of trifluoro-acetic-acid in CH₂Cl₂ (3 mL) was added to a round bottom flask containing N-tBoc-1-naphth-7-ol- α -amide-aspartate (0.040 g, 0.107 mmol), which dissolved immediately and turned a dark red/brown color. The solution was allowed to stir for 1 h at rt (~21° C) whereby it was observed that the reaction had completed as determined by TLC (mobile phase 85% CH₂Cl₂ / 14% MeOH / 1% AcOH; R_f = 0.01). The solution was then aspirated with compressed air until dry to remove TFA and CH₂Cl₂. The remaining solid (deprotected product and TFA salt) was washed with 2 x 60 mL CH₂Cl₂ and then taken up into 20 mL deionized water followed by the addition of 64 μ L 2 M HCl (1.2 eq.) and light sonication to dissolve / resuspend the solid residue. The solution was then frozen to -80° C and placed on the lyophilizer to freeze dry leaving a

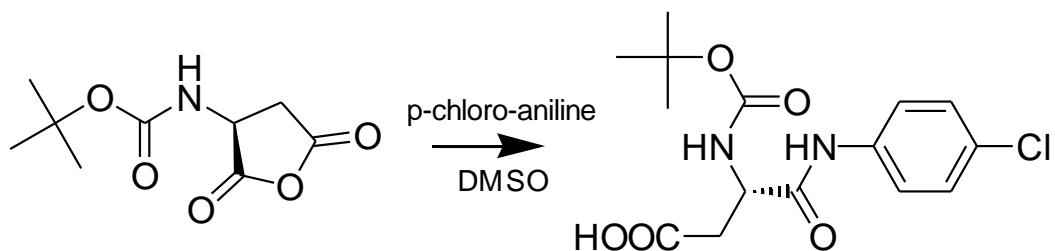
dark red/brown solid (1-naphth-7-ol- α -amide-aspartate, 0.031 g, 92% yield). The final product was analyzed by ^1H , ^{13}C NMR, HRMS and rotational analysis to confirm identity and purity.

^1H -NMR (500 MHz, d_6 -DMSO at 2.5 ppm) δ 10.33 (s, 1H), 9.88 (s, 1H), 8.41 (s, 2.5H), 7.79 (d, $J = 8.8\text{Hz}$, 1H), 7.68 (d, $J = 7.8\text{ Hz}$, 1H), 7.51 (d, $J = 7.1\text{ Hz}$, 1H), 7.28 (s, 2H), 7.24 (d, 7.6, 1H), 7.14 (d, 8.3 Hz, 1H), 4.44 (s, 1H), 3.07 (dd, $J = 20.8_{\Sigma}$, 17.4, 3.4 Hz, 1H), 2.96 (dd, $J = 24.9_{\Sigma}$, 17.1, 7.8 Hz, 1H);

^{13}C -NMR (500 MHz, d_6 -DMSO at 39.5 ppm) δ 171.4, 167.5, 156.1, 131.2, 130.2, 130.2, 128.8, 126.4, 122.9, 122.4, 119.2, 104.8, 49.9, 36.1;

HRMS m/e calcd. $\text{C}_{14}\text{H}_{15}\text{N}_2\text{O}_4 = 275.1032$, found 275.1018;

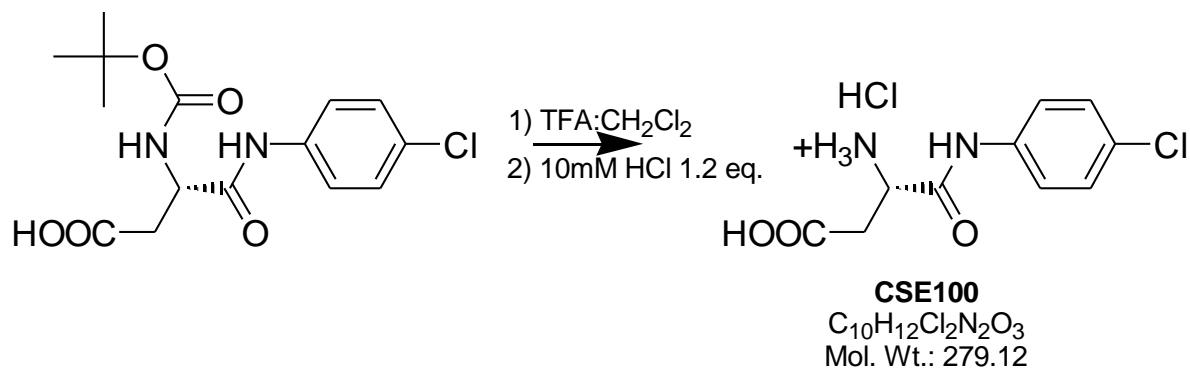
$[\alpha]_{\text{D}}^{22} = -5^\circ$ ($c = 0.11$, methanol, Na^+ D lamp)



N-tBoc-p-chloro-phenyl- α -amide-aspartate: BRL: 132

Protected aspartate anhydride (0.932 g, 4.33 mmol) was dissolved in DMSO (90 mL). To this was added p-chloroaniline (0.522 g, 0.85 eq., 3.68 mmol). The solution was allowed to stir for 48 h at $\sim 70^\circ$ C or until the reaction had completed as determined by TLC. The solution was then diluted with CHCl_3 (200 mL) and washed with brine adjusted to pH 2 by conc. H_3PO_4 (4 x 250 mL aliquots) to remove DMSO. The organic phase was then concentrated, leaving a light brown residue. The products were then isolated by silica gel (mobile phase = 95% CH_2Cl_2 / 4% MeOH / 1% acetic acid). The β -addition bi-product was collected at $R_f = 0.15$, concentrated and stored for later use. The α -addition product was isolated at $R_f = 0.2$ and subsequently concentrated by rotovap to a white residue (0.120 g recovered, 0.350 mmol), which was used in the next synthetic step without further purification.

$^1\text{H-NMR}$ (500 MHz, d_6 -DMSO at 2.5 ppm) δ 10.15 (s, 1H), 7.62 (d, $J = 9.1$ Hz, 2H), 7.35 (d, $J = 9.1$ Hz, 2H), 7.21 (d, $J = 7.8$ Hz, 1H), 4.40 (dd, 20.1 Σ , 12.9, 7.1 Hz, 1H), 2.66 (dd, $J = 21.4\text{\Sigma}$, 16.2, 5.8 Hz, 1H), 2.51 (dd, overlap with DMSO, 1H), 1.37 (s, 9H)



p-Chloro-phenyl- α -amide-aspartate: BRL: 146

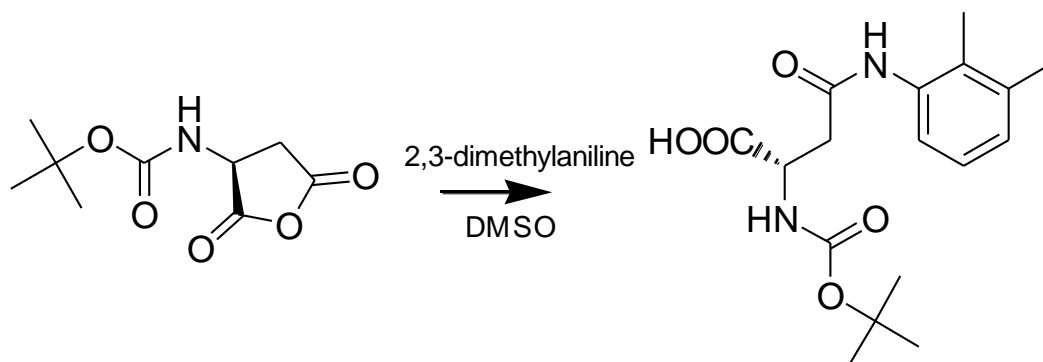
A solution of 50% trifluoroacetic-acid in CH_2Cl_2 (4 mL) was added to a round bottom flask containing N-tBoc-p-chloro-phenyl- α -amide-aspartate (0.120 g, 0.333 mmol), which dissolved immediately and turned a dark brown color. The solution was allowed to stir for 1 h at rt ($\sim 21^\circ C$) whereby it was observed that the reaction had completed as determined by TLC (mobile phase 90% CH_2Cl_2 / 9% MeOH / 1% AcOH; $R_f = 0.01$). The solution was then aspirated with compressed air until dry to remove the TFA and CH_2Cl_2 . The remaining residue (deprotected product and TFA salt) was washed with CH_2Cl_2 (3 x 10 mL) and then taken up into 20 mL deionized water using light sonication to suspend the residue where 0.210 mL 2 M HCl (1.2 eq.) was added. The solution was then frozen to $-80^\circ C$ and placed on the lyophilizer until dry, leaving a white solid (p-chloro-phenyl- α -amide-aspartate 0.094 g, 0.336 mmol, 96% yield). The final product was analyzed by 1H , ^{13}C NMR, HRMS and rotational analysis to confirm identity and purity.

$^1\text{H-NMR}$ (500 MHz, $\text{d}_6\text{-DMSO}$ at 2.5 ppm) δ 10.95 (s, 1H), 8.62 (s, 2.0H), 7.64 (d, J = 8.8 Hz, 2H), 7.40 (d, J = 8.6 Hz, 2H), 4.24 (dd, 12.7 $_{\Sigma}$, 6.6 Hz, 1H), 2.96 (dd, J = 22.7 $_{\Sigma}$, 17.6, 5.4 Hz, 1H), 2.88 (dd, J = 24.9 $_{\Sigma}$, 17.4, 7.3 Hz, 1H);

$^{13}\text{C-NMR}$ (500 MHz, $\text{d}_6\text{-DMSO}$ at 39.5 ppm) δ 175.9, 171.6, 142.4, 134.0, 132.8, 126.2, 55.0, 40.4;

HRMS m/e calcd. For $\text{C}_{10}\text{H}_{12}\text{ClN}_2\text{O}_3 = 243.0536$, found 243.0548;

$[\alpha]_{\text{D}}^{22} = +16^\circ$ (c = 0.12, methanol, Na^+ D lamp)

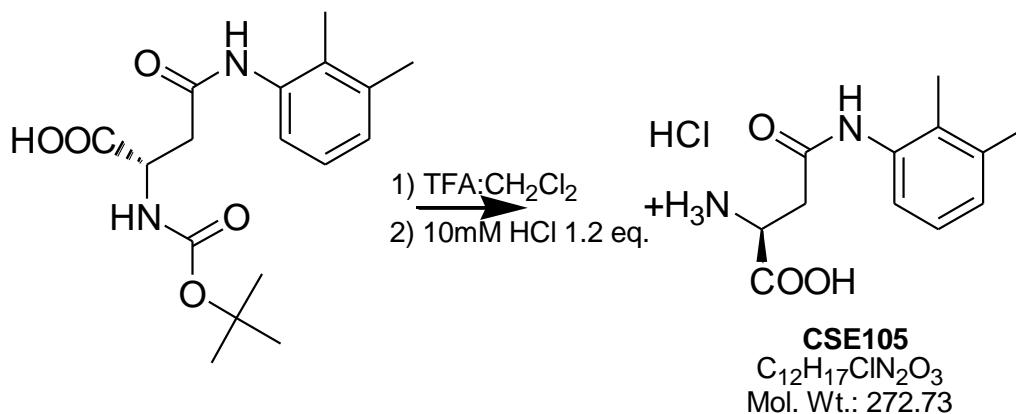


N-tBoc-2,3-dimethyl-phenyl-aspartamide: BRL: 236

Protected aspartate anhydride (1.846 g, 8.58 mmol) was dissolved in DMSO (120 mL). To this was added 2,3-dimethylaniline (0.954 mL, 0.9 eq., 7.72 mmol). The solution was allowed to stir for 48 h at $\sim 40^\circ\text{C}$ or until the reaction had completed as determined by TLC. The solution was then diluted with CHCl_3 (200 mL) and washed with brine adjusted to $\text{pH} = 2$ by addition of conc. H_3PO_4 (6 x 200 mL aliquots) to remove DMSO. The organic phase was then concentrated, leaving a light yellow residue. The products were then isolated by silica gel (mobile phase = 95% CH_2Cl_2 / 4% MeOH / 1% acetic acid). The α -addition bi-product was collected at $R_f = 0.3$, concentrated and stored for later use. The β -addition product was isolated at $R_f = 0.2$ and subsequently concentrated by rotovap to a white solid (0.450 g. recovered, 1.34 mmol), N-tBoc-2,3-dimethyl-phenyl-aspartamide. The product was used without further purification in the next synthetic step.

$^1\text{H-NMR}$ (500 MHz, $\text{d}_6\text{-DMSO}$ at 2.5 ppm) δ 12.62 (b, 2.5H), 9.35 (s, 1H), 7.03 (m, $J = 64.6$ Hz, 3 H), 4.34 (dd, 21.5 Σ , 13.9, 7.8 Hz, 1H), 2.76 (dd, $J = 20.5\Sigma$, 14.9, 5.6 Hz, 1H), 2.64 (dd, $J = 22.7\Sigma$, 14.7, 7.8 Hz, 1H), 2.22 (s, 3H), 2.03 (s, 3H), 1.36 (s, 9H);

$^{13}\text{C-NMR}$ (500 MHz, $\text{d}_6\text{-DMSO}$ at 39.5 ppm) δ 173.8, 168.6, 155.6, 137.3, 136.4, 131.6, 127.3, 125.5, 123.9, 78.6, 50.9, 38.1, 28.6, 20.6, 14.4



2,3-Dimethyl-phenyl-aspartamide: BRL: 237

A solution of 50% trifluoroacetic-acid in CH_2Cl_2 (6 mL) was added to a round bottom flask containing N-tBoc-2,3-dimethyl-phenyl- β -aspartamide (0.450 g, 1.34 mmol) which dissolved immediately and turned a dark yellow color. The solution was allowed to stir for 1 h at rt ($\sim 21^\circ\text{C}$) whereby it was observed that the reaction had completed as determined by TLC (mobile phase 90% CH_2Cl_2 / 9% MeOH / 1% AcOH; $R_f = 0.01$). The solution was then aspirated with compressed air until dry to remove all TFA and

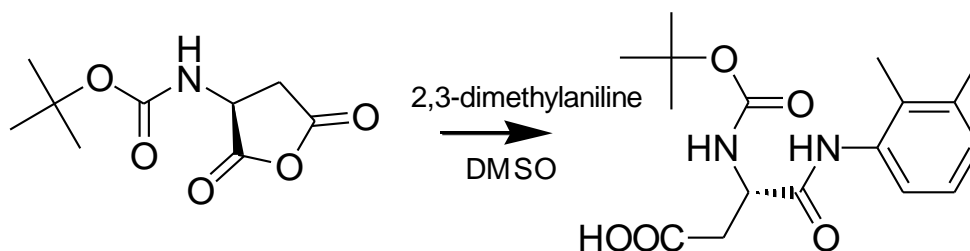
CH₂Cl₂. The remaining residue (deprotected product and TFA salt) was washed with 3 x 60 mL CH₂Cl₂ and then taken up into 80 mL deionized water using light sonication to suspend the residue followed by addition of 0.803 mL 2.0 M HCl (1.2 eq.). The solution was then frozen to -80° C and placed on the lyophilizer until dry, leaving a white residue (2,3-dimethyl-phenyl-β-aspartamide 0.347 g, 1.27 mmol, 95% yield). The final product was analyzed by ¹H, ¹³C NMR, HRMS and rotational analysis to confirm identity and purity.

¹H-NMR (500 MHz, d₆-DMSO at 2.5 ppm) δ 9.87 (s, 1H), 8.49 (s, 2.5H), 7.10 (d, J = 7.6 Hz, 1H), 7.00 (m, J = 28.1 Hz, 2H), 4.20 (d, 4.2 Hz, 1H), 3.08 (dd, J = 22.0_Σ, 16.6, 5.4 Hz, 1H), 3.02 (dd, J = 22.0_Σ, 16.6, 5.4 Hz, 1H), 2.21 (s, 3H), 2.05 (s, 3H);

¹³C-NMR (500 MHz, d₆-DMSO at 39.5 ppm) δ 170.7, 167.9, 137.4, 136.1, 131.7, 127.5, 125.5, 124.1, 49.2, 35.5, 20.6, 14.6;

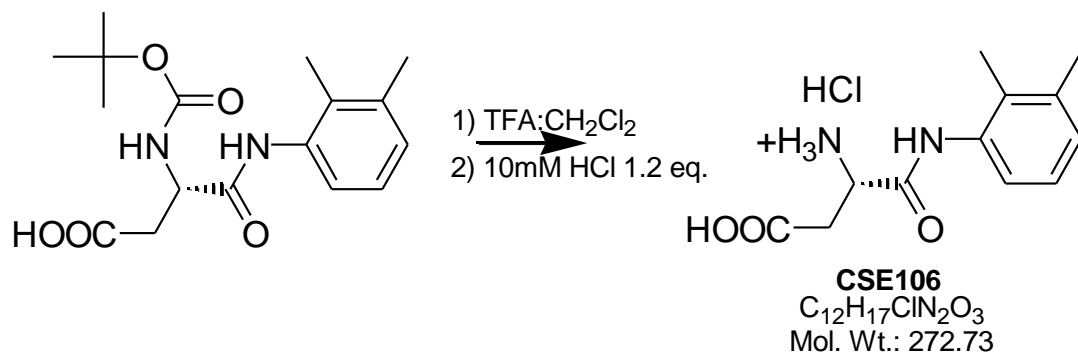
HRMS *m/e* calcd. For C₁₂H₁₇N₂O₃ = 237.1239, found 237.1252

[α]_D²² = -2° (c = 0.17, methanol, Na⁺ D lamp)



N-tBoc-2,3-dimethyl-phenyl- α -amide-aspartate: BRL: 236

Protected aspartate anhydride (1.846g, 8.58 mmol) was dissolved in DMSO (120 mL). To this was added 2,3-dimethylaniline (0.954 mL, 0.9 eq., 7.72 mmol). The solution was allowed to stir for 48 h at $\sim 40^{\circ}$ C or until the reaction had reached completion as determined by TLC. The solution was then diluted with CHCl_3 (200 mL) and washed with brine adjusted to pH ~ 2 by addition of conc. H_3PO_4 (6 x 200 mL aliquots) to remove DMSO. The organic phase was then concentrated leaving a light yellow residue. The products were then isolated by silica gel (mobile phase = 95% CH_2Cl_2 / 4% MeOH / 1% acetic acid). The β -addition bi-product was collected at $R_f = 0.2$, concentrated and stored for later use. The α -addition product was isolated at $R_f = 0.3$ and subsequently concentrated by rotovap to a white residue (0.300 g. recovered, 0.892 mmol), which was used in the next synthetic step without further purification.



2,3-Dimethyl-phenyl- α -amide-aspartate: BRL: 248

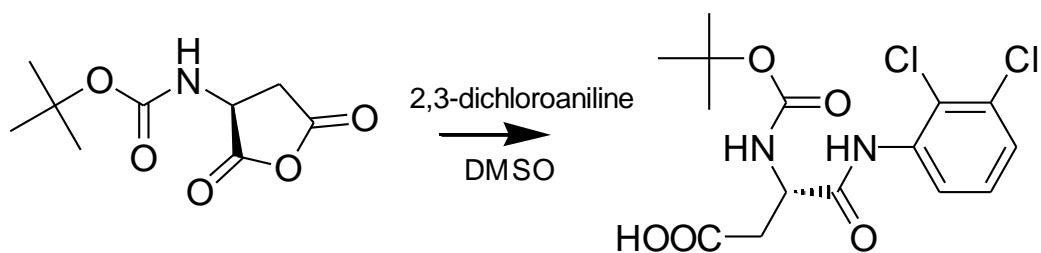
A solution of 50% trifluoroacetic-acid in CH_2Cl_2 (6 mL) was added to a round bottom flask containing N-tBoc-2,3-dimethyl-phenyl- α -amide-aspartate (0.300 g, 0.892 mmol) which dissolved immediately and turned a dark yellow color. The solution was allowed to stir for 1 h at rt ($\sim 21^\circ C$) whereby it was observed that the reaction had completed as determined by TLC (mobile phase 90% CH_2Cl_2 / 9% MeOH / 1% AcOH; $R_f = 0.01$). The solution was then aspirated with compressed air until dry to remove the TFA and CH_2Cl_2 . The remaining residue (deprotected product and TFA salt) was washed with 3 x 20 mL CH_2Cl_2 and then taken up into 40 mL deionized water using light sonication to suspend the residue followed by addition of 0.535 mL 2.0 M HCl (1.2 eq.). The solution was then frozen to $-80^\circ C$ and placed on the lyophilizer until dry, leaving a white solid (2,3-dimethyl-phenyl- α -amide-aspartate, 0.234 g, 0.856 mmol, 96% yield). The final product was analyzed by 1H , ^{13}C NMR, HRMS and rotational analysis to confirm identity and purity.

$^1\text{H-NMR}$ (500 MHz, $\text{d}_6\text{-DMSO}$ at 2.5 ppm) δ 10.07 (s, 1H), 8.45 (s, 2.5H), 7.11 (d, $J = 7.3$ Hz, 1H), 7.05 (m, $J = 24.4$ Hz, 2H), 4.30 (dd, $J = 11.2_{\Sigma}, 5.6$ Hz, 1H), 2.98 (dd, $J = 22.2_{\Sigma}, 16.6, 5.6$ Hz, 1H), 2.93 (dd, $J = 23.7_{\Sigma}, 16.6, 5.9$ Hz, 1H), 2.23 (s, 3H), 2.06 (s, 3H);

$^{13}\text{C-NMR}$ (500 MHz, d-DMSO at 39.5 ppm) ppm 171.31, 166.93, 137.62, 135.43, 131.93, 127.96, 125.73, 123.89, 49.72, 35.88, 20.56, 14.42;

HRMS m/e calcd. For $\text{C}_{12}\text{H}_{17}\text{N}_2\text{O}_3 = 237.1239$, found 237.1222;

$[\alpha]_{\text{D}}^{22} = -2^\circ$ ($c = 0.14$, methanol, Na^+ D lamp)

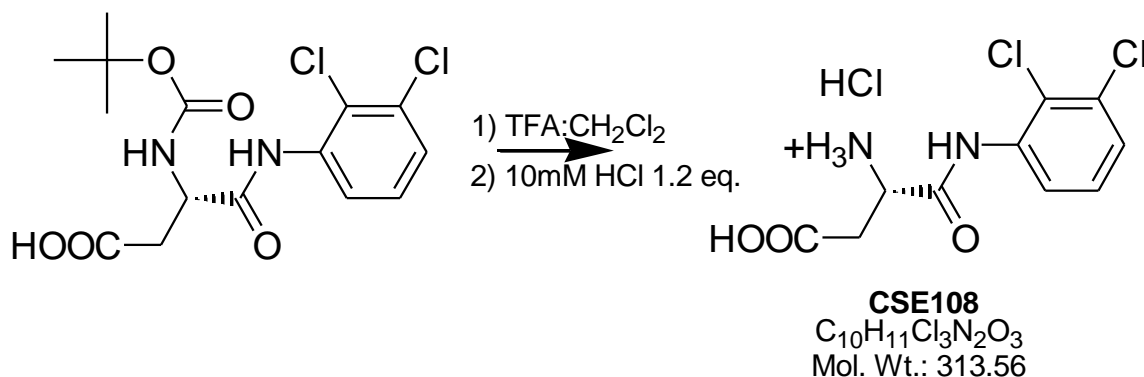


N-tBoc-2,3-dichloro-phenyl- α -amide-aspartate: BRL: 227

N-tBoc protected aspartate anhydride (1.855g, 8.618 mmol) was dissolved in DMSO (120 mL). To this was added 2,3-dichloroaniline (1.268 g, 0.9 eq., 7.75 mmol). The solution was allowed to stir for 48 h at $\sim 65^\circ\text{C}$ or until the reaction had completed as determined by TLC. The solution was then diluted with CHCl_3 (200 mL) and washed

with brine acidified to pH = 2 by addition of conc. H₃PO₄ (6 x 200 mL aliquots) to take up the DMSO. The organic phase was then concentrated leaving a light yellow residue. The products were then isolated by silica gel (mobile phase = 95% CH₂Cl₂ / 4% MeOH / 1% acetic acid). The β-addition bi-product was collected at R_f = 0.2, concentrated and stored for later use. The α-addition product was isolated at R_f = 0.3 and subsequently concentrated by rotovap to a white residue (0.200 g. recovered, 0.530 mmol), N-tBoc-2,3-dichloro-phenyl-α-amide-aspartate. The product was used in the next synthetic step without further purification.

¹H-NMR (500 MHz, d₆-DMSO at 2.5 ppm) δ 12.39 (b, 0.5H), 9.52 (s, 1H), 7.84 (d, J = 8.1 Hz, 1H), 7.44 (dd, J = 18.1_Σ, 9.1 Hz, 1H), 7.35 (dd, J = 16.1_Σ, 8.1 Hz, 1H), 4.48 (dd, 20.5_Σ, 13.4, 7.1 Hz, 1H), 2.76 (dd, J = 22.2_Σ, 16.6, 5.6 Hz, 1H), 2.58 (dd, J = 24.7_Σ, 16.8, 8.1 Hz, 1H), 1.39 (s, 9H).



2,3-Dichloro-phenyl- α -amide-aspartate: BRL: 252

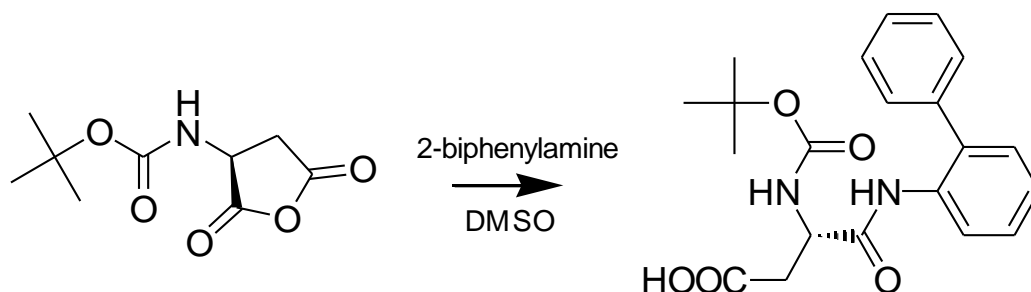
A solution of 50% trifluoroacetic-acid in CH_2Cl_2 (6 mL) was added to a round bottom flask containing N-tBoc-2,3-dichloroaniline- α -aspartamide (0.200 g, 0.530 mmol) which dissolved immediately and turned a dark brown color. The solution was allowed to stir for 1 h at rt ($\sim 21^\circ C$) whereby it was observed that the reaction had completed as determined by TLC (mobile phase 90% CH_2Cl_2 / 9% MeOH / 1% AcOH; $R_f = 0.01$). The solution was then aspirated with compressed air until dry to remove the remaining TFA and CH_2Cl_2 . The remaining residue (deprotected product and TFA salt) was washed with 3 x 10 mL CH_2Cl_2 and then taken up into 20 mL deionized water using light sonication to suspend the residue followed by addition of 0.318 mL 2.0 M HCl (1.2 eq.). The solution was then frozen to $-80^\circ C$ and placed on the lyophilizer until dry, leaving a white residue (2,3-dichloro-phenyl- α -amide-aspartate 0.153 g, 0.488 mmol, 92% yield). The final product was analyzed by 1H , ^{13}C NMR, HRMS and rotational analysis to confirm identity and purity.

$^1\text{H-NMR}$ (500 MHz, d_6 -DMSO at 2.5 ppm) δ 10.49 (s, 1H), 8.52 (s, 2.5H), 7.61 (d, $J = 8.1$ Hz, 1H), 7.51 (d, $J = 7.8$ Hz, 1H), 7.38 (dd, $J = 16.4_{\Sigma}, 8.3$ Hz, 1H), 4.39 (d, $J = 2.7$ Hz, 1H), 2.98 (m, $J = 44.5$ Hz, 2H);

$^{13}\text{C-NMR}$ (500 MHz, d_6 -DMSO at 39.5 ppm) δ 171.2, 167.5, 136.3, 132.5, 128.6, 128.0, 126.3, 125.5, 49.8, 35.8;

HRMS m/e calcd. For $\text{C}_{10}\text{H}_{11}\text{Cl}_2\text{N}_2\text{O}_3 = 277.0147$, found 277.0118;

$[\alpha]_D^{22} = -3^\circ$ ($c = 0.11$, methanol, Na^+ D lamp)

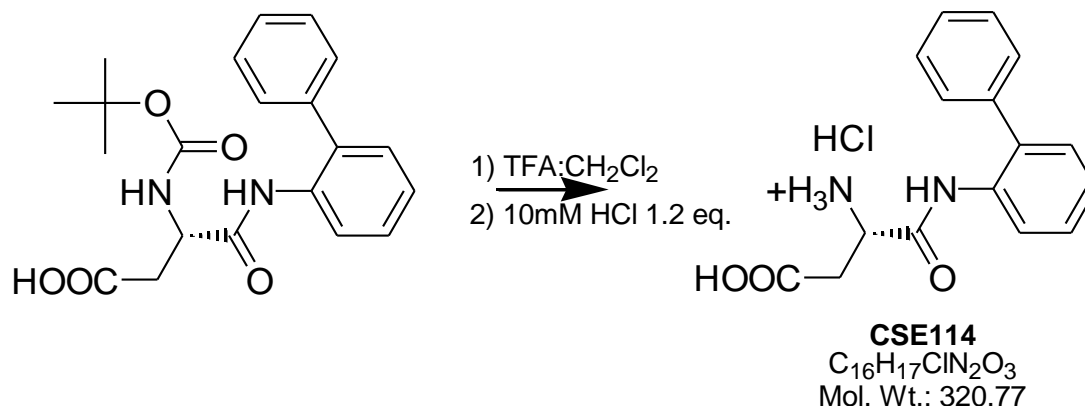


N-tBoc-1-biphenyl- α -amide-aspartate: BRL: 27

Protected aspartate anhydride (1.41g, 6.56 mmol) was dissolved into DMSO (120 mL). To this was added 2-aminobiphenyl (0.963 g, 0.85 eq., 5.58 mmol). The solution was allowed to stir for 24 h at $\sim 40^\circ\text{C}$ or until the reaction had completed as determined by TLC (95% CH_2Cl_2 / 4% MeOH / 1% acetic acid). The solution was then diluted with CHCl_3 (200 mL) and washed with brine adjusted to pH = 2 by addition of conc. H_3PO_4 ,

(4 x 250 mL aliquots) to remove DMSO. The organic phase was then concentrated, leaving a light brown residue. The products were then isolated by silica gel (mobile phase = 94% CH₂Cl₂ / 5% MeOH / 1% acetic acid). The β -addition bi-product was collected at R_f = 0.2, concentrated and stored for later use. The α -addition product was isolated at R_f = 0.3 and concentrated *in-vacuo* to a light/brown residue (0.270 g. recovered, 0.702 mmol) N-tBoc-1-biphenyl- α -amide-aspartate, which was used in the next synthetic step without further purification.

¹H-NMR (400 MHz, d₆-DMSO at 2.5 ppm) δ 9.10 (s, 1H), 7.75 (d, J= 7.8 Hz, 1H), 7.43 (d, J = 6.8 Hz, 2H), 7.35 (m, J = 77.5 Σ Hz, 4H), 7.26 (m, 35.5 Σ Hz, 2H), 7.10 (d, 7.6 Hz, 1H), 4.28 (dd, 20.0 Σ , 12.7, 7.3 Hz, 1H), 2.58 (dd, J = 21.0 Σ , 16.6, 4.6 Hz, 1H), 2.44 (dd, J = 25.4 Σ , 17.1, 9.0 Hz, 1H), 1.32(s,9H).



1-Biphenyl- α -amide-aspartate: BRL: 276

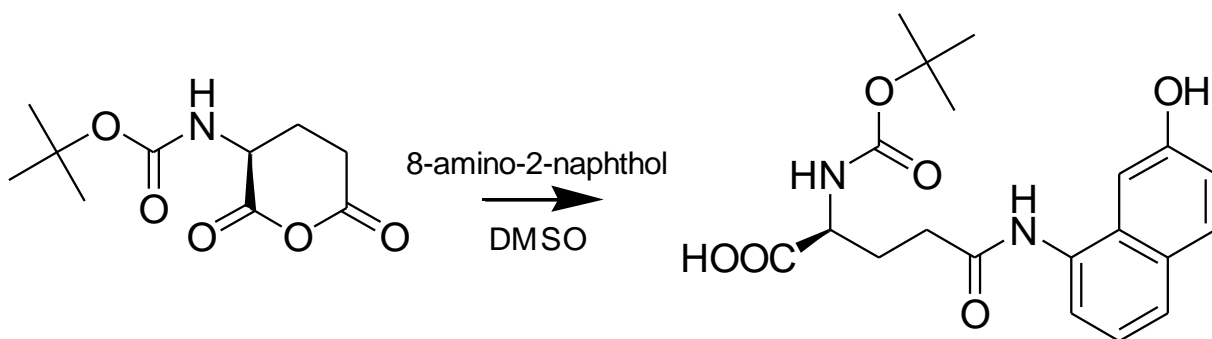
To 0.270 g (0.702 mmol) of N-tBoc-1-biphenyl- α -amide-aspartate in a round bottom flask was added 6 mL of 50% TFA in CH_2Cl_2 , which dissolved immediately and turned a dark yellow color. The solution was allowed to stir for 1 h at rt ($\sim 21^\circ C$) whereby it was observed that the reaction had completed as determined by TLC (90% CH_2Cl_2 / 9% MeOH / 1% AcOH; $R_f = 0.01$). The solution was then aspirated with compressed air until dry to remove TFA and CH_2Cl_2 . The remaining residue (deprotected product and TFA salt) was washed with 3 x 20 mL CH_2Cl_2 and then taken up into 20 mL dionized water using light sonication to suspend the residue and 0.421 mL (1.2 eq.) of 2 M HCl was added. The mixture was then frozen to $-80^\circ C$ and lyophilized until dry, leaving a white residue (1-biphenyl- α -amide-aspartate 0.203 g, 0.632 mmol, 90% yield). The final product was analyzed by 1H , ^{13}C NMR, HRMS and rotational analysis to confirm identity and determine purity.

$^1\text{H-NMR}$ (500 MHz, d_6 -DMSO at 2.5 ppm) δ 9.94 (s, 1H), 8.33 (s, 2.5H), 7.41 (m, $J = 80.7_{\Sigma}$ Hz, 9H), 4.10 (dd, $J = 11.5_{\Sigma}, 7.1, 4.4$ Hz, 1H), 2.74 (dd, $J = 21.8_{\Sigma}, 17.8, 4.2$ Hz, 1H), 2.67 (dd, $J = 25.4_{\Sigma}, 17.6, 7.8$ Hz, 1H);

$^{13}\text{C-NMR}$ (500 MHz, d_6 -DMSO at 39.5 ppm) δ 171.3, 167.2, 138.9, 137.1, 133.9, 130.89, 129.3, 128.9, 128.3, 127.9, 127.2, 127.1, 49.6, 35.4;

HRMS m/e calcd. For $\text{C}_{16}\text{H}_{17}\text{N}_2\text{O}_3 = 285.1239$, found 285.1263;

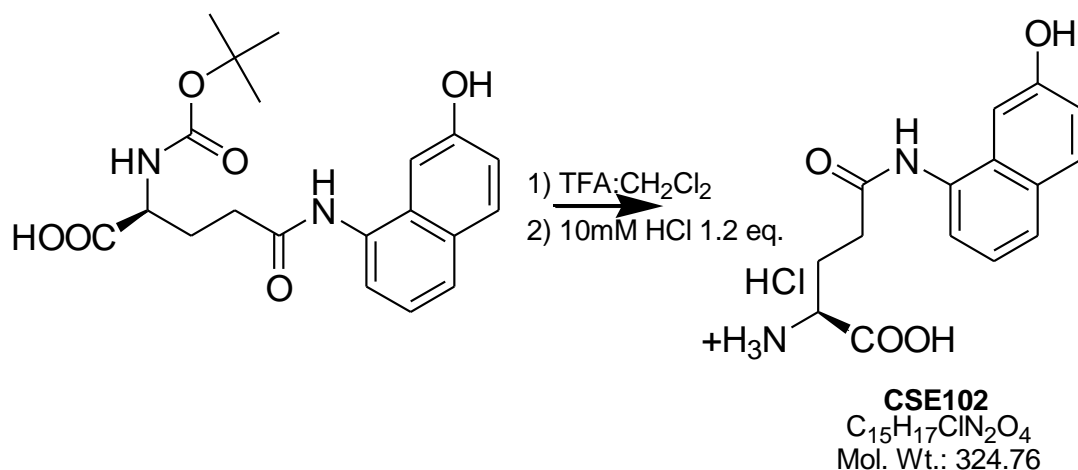
$[\alpha]_D^{22} = -11^\circ$ ($c = 0.12$, methanol, Na^+ D lamp);



N-tBoc-1-naphth-7-ol-glutamide: BRL: 153

Protected glutamate anhydride (2.02 g, 8.17mmol) derived from N-tBoc-L-glutamate by reflux in acetic anhydride [Huang *et al.* 1997] was dissolved into 100 mL DMSO. To

this was added 8-amino-2-naphthol (1.300 g, 1 eq., 96%). The mixture was allowed to stir for 48 h at $\sim 40^{\circ}$ C or until the reaction had completed as determined by TLC (95% CH_2Cl_2 / 4% MeOH / 1% acetic acid; $R_f = 0.25$). The solution was then diluted with CHCl_3 (200 mL) and washed with brine adjusted to pH = 2 by addition of conc H_3PO_4 , (4 x 250 mL aliquots) to remove DMSO. The organic phase was concentrated, leaving a dark red/brown crude residue and separated by silica gel (95% CH_2Cl_2 / 4% MeOH / 1% acetic acid). The product, N-tBoc-1-naphth-7-ol-glutamide, was isolated at $R_f = 0.25$ and subsequently concentrated by rotovap to a dark red brown oil and used without further purification.



1-Naphth-7-ol-glutamide: BRL: 234

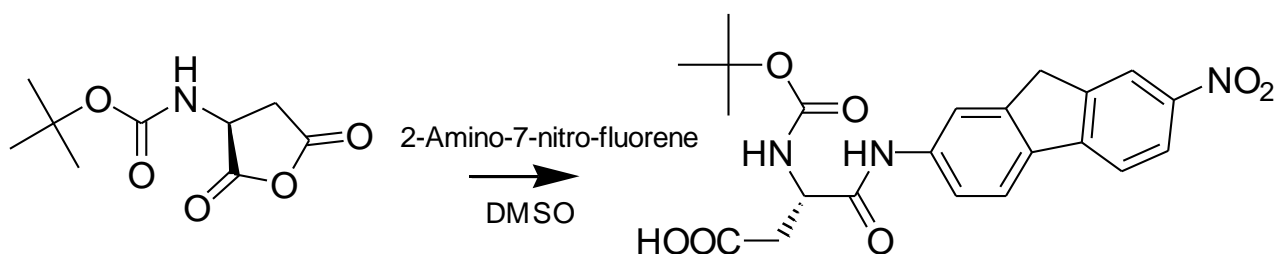
A 50 % solution of TFA in CH_2Cl_2 (6 mL) was added to a round bottom flask containing 0.520 g (1.34 mmol) of N-tBoc-8-naphthol-2-glutamide which dissolved immediately and turned a dark red/brown color. The mixture was allowed to stir for an additional 45 min. at room temp ($\sim 21^\circ C$) whereby it was observed that the reaction had completed as determined by TLC (90% CH_2Cl_2 / 9% MeOH / 1% AcOH; $R_f = 0.01$). The solution was then aspirated with compressed air until dry to remove TFA and CH_2Cl_2 . The remaining solid (deprotected product and TFA salt) was washed with 3 x 80 mL CH_2Cl_2 and then mixed with 147 mL 0.01 M HCl (737 μL of 2.0 M HCl, 1.1 eq.) followed by light sonication to suspend the residue. The solution was then frozen to $-80^\circ C$ and placed on the lyophilizer to dry / remove all the water and remaining TFA leaving a dark red residue (8-naphthol-2-glutamide). The final product was analyzed by 1H , ^{13}C NMR, and rotational analysis to confirm identity and determine purity.

$^1\text{H-NMR}$ (500 MHz, $\text{d}_6\text{-DMSO}$ at 2.5 ppm) δ 9.95 (s, 1H), 8.58 (s, 2.5H), 7.74 (d, $J = 8.8$ Hz, 1H), 7.61 (d, $J = 8.1$ Hz, 1H), 7.44 (d, $J = 7.1$ Hz, 1H), 7.24 (s, 1H), 7.20 (dd, $J = 15.2_{\Sigma}$, 7.6, 1H), 7.12 (d, $J = 8.3$ Hz, 1H), 3.96 (dd, $J = 15.4_{\Sigma}$, 5.2 Hz, 1H), 2.73 (m, 30.8 $_{\Sigma}$, 7.8, 7.6 Hz, 1H), 2.62 (m, $J = 30.3_{\Sigma}$, 7.8, 7.6, 7.1, Hz, 1H), 2.16 (m, $J = 6.6$ Hz, 2H);

$^{13}\text{C-NMR}$ (500 MHz, $\text{d}_6\text{-DMSO}$ at 39.5 ppm) δ 171.2, 170.9, 155.9, 132.2, 130.5, 130.1, 128.8, 125.9, 123.2, 122.4, 119.0, 104.9, 52.0, 31.6, 26.5;

CHN analysis for $\text{C}_{15}\text{H}_{17}\text{ClN}_2\text{O}_4 \cdot 5\text{H}_2\text{O}$ calc. C, 43.43; H, 6.56; N, 6.75; O, 34.71; Cl, 8.55 Found: C, 41.83; H, 6.17; N, 5.29;

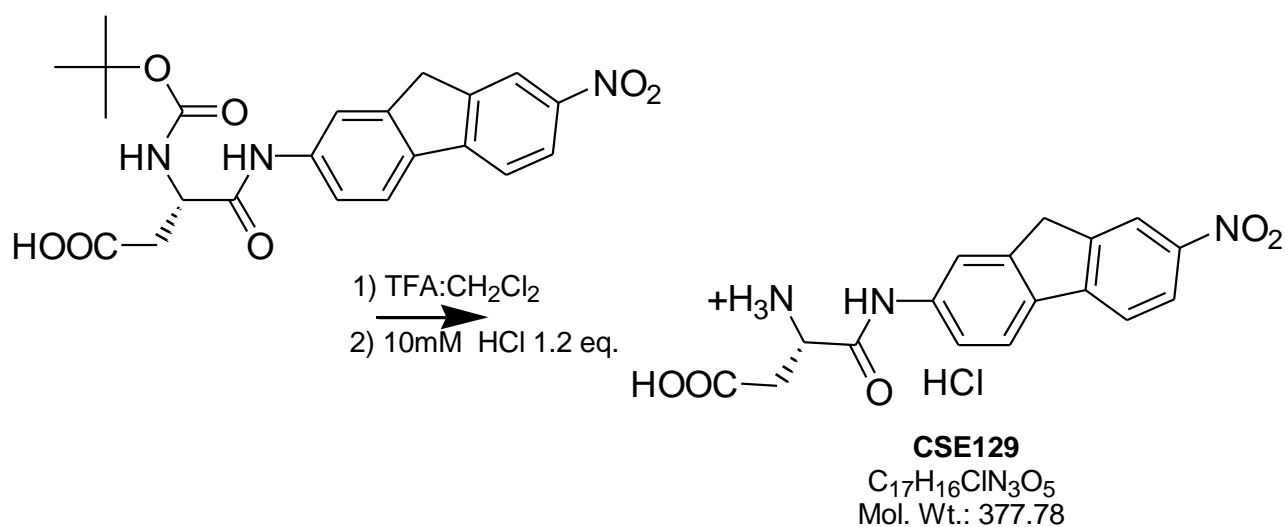
$[\alpha]_{\text{D}}^{22} = +10^\circ$ ($c = 0.50$, methanol, Na^+ D lamp).



N-tBoc-7-nitro-fluorenyl-1- α -amide-aspartate: BRL: 75

Aspartate anhydride, 0.923 g (4.29 mmol), was dissolved into 44 mL DMSO (0.1 M final conc.). To this was added 0.824mg of 2-amino-7-nitrofluorene (0.85 eq, 3.64mmol)

synthesized from 2-nitrofluorene (Saroja G., et al. 2004). The solution was allowed to stir for 24 h at 40° C in which the reaction had reached completion as determined by TLC. The reaction crude in DMSO was then diluted with 100 mL water (pH = 2, adjusted by addition of conc. H₃PO₄) and extracted with CHCl₃ (3 x 400 mL). The separated organic layers were combined and washed with brine at pH = 2 adjusted by H₃PO₄ 6 x 250 mL aliquots to remove DMSO. The organic phase was dried over Na₂SO₄ and concentrated to an oil. The product was then isolated by silica gel (mobile phase = 95% CH₂Cl₂ / 4% MeOH / 1% acetic acid). The α -addition product (R_f = 0.5) was collected from several combined fractions and concentrated to a yellow solid residue, 0.100 g (0.226 mmol) of N-tBoc-7-nitro-fluorenyl-1- α -amide-aspartate, which was used in the next synthetic step without further purification.



7-Nitro-fluorenyl-2- α -amide-aspartate: BRL: 299

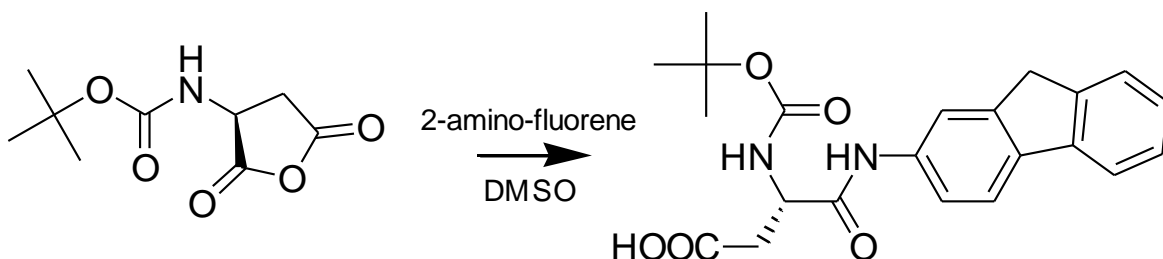
To 0.100 g of N-tBoc-7-nitro-fluorenyl-2- α -amide-aspartate was added 6 mL of 50% TFA in CH₂Cl₂ (% vol) which dissolved immediately and turned a dark orange color. The solution was allowed to stir for 60 min whereby it was observed that the reaction had completed as determined by TLC. The solution was then aspirated until dry with compressed air to remove the TFA and CH₂Cl₂. The remaining solid (deprotected product and TFA salt) was then suspended by addition of 1.2 eq. 0.01M HCl and light sonication and frozen to -80°C. Once frozen the sample was placed on the lyophilizer until dry, removing all remaining TFA and leaving an orange solid residue. The residue was then washed 3 x 30 mL of CH₂Cl₂, leaving 0.075 g of 7-nitro-fluorenyl-2- α -amide-aspartate (an 88% yield). The final product was confirmed by ¹H, ¹³C NMR, HRMS and rotational analysis.

¹H-NMR (500 MHz, d₆-DMSO at 2.5 ppm) δ 11.01 (s, 1H), 8.41 (s, 1H), 8.27 (dd, J = 10.0 Σ , 8.7, 1.5 Hz, 1H), 8.06 (dd, J = 16.9 Σ , 8.6 Hz, 1H), 8.02 (s, 1H), 7.69 (d, J = 8.3 Hz, 1H), 4.29 (dd, J = 12.7 Σ , 6.8 Hz, 1H), 4.08 (s, 2H), 3.00 (dd, J = 22.5 Σ , 17.4, 5.1 Hz, 1H), 2.97 (dd, J = 24.7 Σ , 17.1, 7.6 Hz, 1H);

¹³C-NMR (500 MHz, d₆-DMSO at 39.5 ppm) δ 171.2, 166.9, 147.9, 146.7, 146.2, 144.6, 139.6, 135.3, 123.5, 122.8, 120.8, 120.5, 119.1, 116.6, 50.3, 37.2, 35.8;

HRMS *m/e* calcd. For C₁₇H₁₆N₃O₅ = 342.1090, found 342.1087;

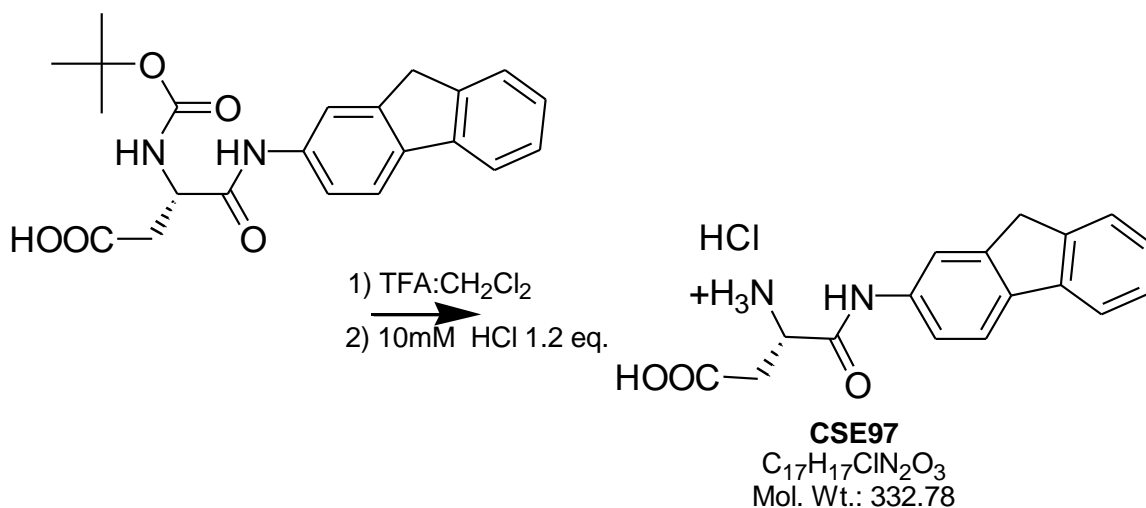
[α]_D²² = + 29° (c = 0.12, methanol, Na⁺ D lamp).



N-tBoc-2-fluorenyl- α -amide-aspartate: BRL: 25

Aspartate anhydride, 0.936 g (4.35 mmol) was dissolved into 87 mL DMSO (0.05 M final conc). To this was added 0.684 g of 2-amino-fluorene (0.85 eq., 98%, 3.77mmol). The solution was allowed to stir for 24 h at rt in which the reaction had reached completion as determined TLC. The product in DMSO was then diluted with 100 mL water pH = 2 adjusted by H₃PO₄ conc and extracted with 3 x 400 mL CHCl₃. The organic layers were combined and washed with 6 x 250 mL aliquots brine, adjusted to pH = 2 by addition of H₃PO₄ conc, to remove DMSO. The organic layer was then dried over Na₂SO₄ and concentrated by rotovap to a crude residue and subsequently separated by silica gel (95% CH₂Cl₂ / 4% MeOH / 1% acetic acid). The α -addition product (R_f = 0.3) was collected from several combined fractions and concentrated *in-vacuo* leaving N-

tBoc-2-fluorenyl- α -amide-aspartate as an off white solid which was used in the next synthetic step without further purification.



2-fluorenyl- α -amide-aspartate: BRL: 130

To 0.305 g of N-tBoc-2-fluorenyl- α -amide-aspartate was added 6 mL of a 50% TFA in CH₂Cl₂ (%vol) solution which turned dark brown and dissolved immediately. The solution was allowed to stir for 60 min where it was observed that the reaction had completed (determined by absence of starting material on TLC). The solution was then aspirated until dry to remove TFA and CH₂Cl₂. To the remaining solid (deprotected product and TFA salt) was added 1.2 eq. of a 0.01M HCl solution followed by resuspension of the residue via sonication. The solution was then frozen to -80°C and placed on the lyophilizer until dry, removing all remaining TFA and leaving an orange solid residue. The residue was washed with CH₂Cl₂ (3 x 30mL), leaving 0.241 g of 2-

fluorenyl- α -amide-aspartate (a 94% yield). The final product was confirmed by ^1H , ^{13}C NMR, HRMS and rotational analysis.

^1H -NMR (500 MHz, d_6 -DMSO at 2.5 ppm) δ 10.67 (s, 1H), 7.90 (s, 1H), 7.86 (d, $J = 8.4$ Hz, 1H), 7.83 (d, $J = 7.1$ Hz, 1H), 7.56 (dd, $J = 15.5_\Sigma$, 7.1 Hz, 1H), 7.36 (dd, $J = 14.2_\Sigma$, 7.1 Hz, 1H), 7.28 (dd, $J = 14.9_\Sigma$, 7.1 Hz, 1H), 4.26 (dd, $J = 12.3_\Sigma$, 5.2 Hz, 1H), 3.92 (s, 2H), 2.99 (dd, $J = 22.0_\Sigma$, 17.5, 4.5 Hz, 1H), 2.87 (dd, $J = 25.2_\Sigma$, 17.5, 7.8 Hz, 1H);

^{13}C -NMR (500 MHz, d_6 -DMSO at 39.5 ppm) δ 170.9, 166.2, 143.9, 142.9, 140.8, 137.23, 137.1, 126.8, 126.4, 125.1, 120.3, 119.7, 118.3, 116.4, 49.9, 36.6, 35.5;

HRMS m/e calcd. For $\text{C}_{17}\text{H}_{17}\text{N}_2\text{O}_3 = 297.1239$, found 297.1226;

$[\alpha]_D^{22} = +21^\circ$ (c = 0.13, methanol, Na^+ D lamp).

Chapter 3.

Derivatives of *trans*-hydroxy-L-proline: Inhibitors of the neutral amino acid transporters
ASCT1 and ASCT2.

Brent R. Lyda, Greg Leary, Michael Kavanaugh, Nicholas Natale, C. Sean Esslinger

Department of Biomedical and Pharmaceutical Sciences, The University of Montana, 32
Campus Dr., Missoula, Montana 59801-1552

***Corresponding authors**

Brent R. Lyda
Dept. Biomedical and Pharmaceutical Sciences
University of Montana
Missoula MT 59801
Tel: 406-855-7401
Brent.Lyda@gmail.com

Nicholas Natale
Dept. Biomedical and Pharmaceutical Sciences
University of Montana
Missoula, MT 59801
Tel: 406-243-4132
nicholas.natale@umontana.edu

Abstract

Hydroxy-L-proline represents an excellent molecular scaffold for the synthesis of diverse multifunctionalized unnatural amino acids with distinctive three dimensional configurations for probing the structure of a biological target. The conformationally restricted proline ring makes it ideal to construct high potency inhibitors of amino acid transport and for computational modeling of the synthetic products. We have synthesized a series of hydroxy-L-proline derivatives for activity screening at the ASCT neutral amino acid transporters. A number of these synthetic prolinols were identified as non substrate inhibitors of low micro molar, and nano molar affinity towards the neutral amino acid transporters ASCT1 and ASCT2 by electrophysiological recordings. The synthetic compounds (active and inactive) were computationally docked into an ASCT2 seeded crystal homology model and analyzed with respect to structure / activity. In a ligand binding domain where there exists multiple hydrophobic pockets and a multitude of plausible polar interactions, starting with a conformationally restricted molecular scaffold has helped to focus our attention along a clear path to finding an inhibitor of high potency for our target. This biologically oriented synthetic approach has proved invaluable for the development of this project and will continue to provide insight and generate new ideas geared towards designing next generation inhibitors for our target amino acid transporters.

1. INTRODUCTION

The neutral amino-acid transporter ASCT2 (alanine serine cysteine transporter subtype 2; gene SLC1A5) is known to transport amino acids alanine, serine, cysteine, threonine, asparagine, and glutamine in or out of a cell in a sodium dependent obligate exchange process [Utsunomiya-Tate *et al.* 1996; Broer *et al.* 1999]. Similarly, the sister transporter ASCT1 (gene SLC1A4) transports serine, cysteine, alanine and to a lesser extent threonine [Arriza *et al.* 1993; Zerangue *et al.* 1996]. Both transporters are understood to exist within the same family of solute carrier 1, Na⁺ dependant, membrane spanning, amino acid transporters as does the excitatory amino acid transporters subtypes 1-5 (EAATs 1-5)); substantially differing between the amino acids transported (neutral verses acidic) and net ion flux during transport. The ASC transporters are included within a superfamily of solute transporters for which there is a homolog crystal structure, Glt_{ph}, a sodium dependant L-aspartate transporter isolated from *Pyrococcus horikoshii* [Yernool *et al.* 2004]. The homology between the ASC and the EAAT transporters can be exemplified by an alignment of their primary sequence, suggesting approximately 40-44% homology [Y. Kanai *et al.* 1995]. Site-directed mutagenesis of a highly conserved arginine Arg479 in GLAST-1 (rat equivalent to human EAAT-1) or of Arg447 in EAAC-1 (rabbit homologue of human EAAT-3) to a threonine and cysteine, respectively, have

shown that this arginine residue is necessary for transport of acidic amino acids aspartate or glutamate [Conradt *et al.* 1995; Bendahan *et al.* 2000]. Interestingly, the mutation of arginine 447 for a cysteine in EAAC-1 increased the affinity and transport of the neutral amino acids serine, alanine and cysteine. The equivalent residue in hASCT1 and mASCT2 by position and sequence alignment contains a threonine at residue 459 and cysteine at residue 479, respectively [Arriza *et al.* 1993; Utsunomiya-Tate *et al.* 1996]. This suggested that this residue at 447 in GLAST-1, 479 in EAAC-1 and equivalent in the ASC transporters is solely responsible for discriminating in-between neutral and acidic amino acids transported by this family. Conceptually, this presents a unique opportunity to construct inhibitors of the ASC transporters based off of similar structural and functional pharmacophore models developed from the numerous and well characterized EAAT inhibitors.

There are a number of well known classes of synthetic EAAT inhibitors including, in particular, the pyrrolidine dicarboxylates and N_β-aryl-aspartamides. The synthetic compound L-trans-2,4-PDC (pyrrolidine-dicarboxylate) **I** was identified as a potent substrate inhibitor of the EAAT transporters by a group investigating radiolabeled glutamate uptake in synaptosomes [R. J. Bridges; *et al.* 1990].

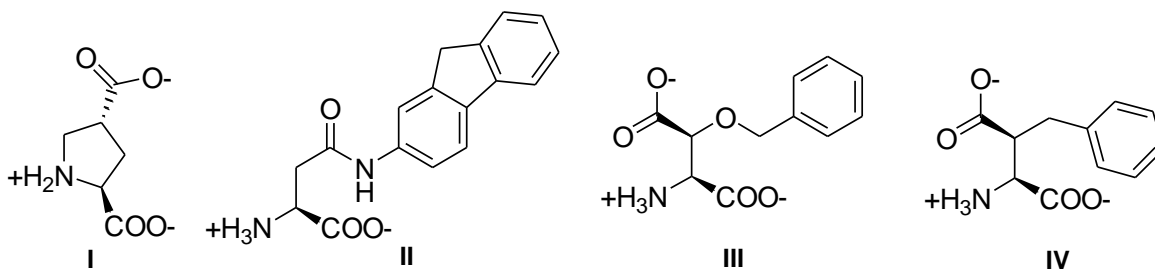


Figure 1. EAAT inhibitors: 2,4-PDC **I**, β-fluorenyl-L-aspartamide **II**, β-threo-benzyloxy-L-aspartate (TBOA) **III**, L-β-*threo*-benzylaspartate **IV**.

Importantly, it was observed that addition of a methyl group to the ring of L-*trans*-2,4-PDC to make 2,4-methyl-PDC changed the transport properties of this compound from a substrate to a non-substrate inhibitor of the EAATs, and similarly an isopropyl derivative of kainite, dihydrokainate [Koch *et al.* 1999]. This observation has been consistent with the next generation EAAT inhibitors, namely the high potency ($IC_{50} \approx 0.020, 0.200 \mu\text{M}$; EAAT-3 & EAAT-1) 2-fluorenyl-L-aspartamide **II** [Dunlop *et al.* 2007] and other derivatives of N_β-aryl-aspartamides [Greenfield *et al.* 2005], which have led to the identification of a relatively large hydrophobic pocket. Additionally, there has been considerable effort to create selective inhibitors of the EAATs through discovery of analogs of TBOA (L-*threo*-beta-benzyloxyaspartate) **III** and threo-benzyl-L-aspartate **IV** by extension of the benzyloxy and benzyl groups [Shimamoto *et al.* 1998; Esslinger *et al.* 2005]. Similarly, a hydrophobic pocket near the ligand binding domain of the ASC transporters may also exist that could be exploited to develop high potency and/or selective inhibitors. Lending support to this credence is the activity of benzyl-L-serine, and benzyl-L-cysteine, of which resemble TBOA minus the beta carboxylic acid. Both

of these compounds act as non-substrate inhibitors of ASCT2, although with a considerably low affinity, $K_i \approx 780 \mu\text{M}$ for benzyl-L-cysteine and $900 \mu\text{M}$ for benzyl-L-serine [Grewer *et al.* 2004]. Furthermore, our lab has observed that N γ -aryl-glutamine analogs are capable of inhibiting ASCT2 mediated uptake of L-glutamine and thus also supporting the existence of a large hydrophobic pocket [Esslinger *et al.* 2005].

ASCT2, particularly, has been suggested to play an important physiologic role by the shuttling of glutamine which itself may facilitate or regulate various physiological processes such as cell growth, proliferation, and possibly even glutamatergic neurotransmission via the glutamate / glutamine cycle. Recently ASCT2 transport has garnered attention because of its link to the, though somewhat unclear, regulation of the mammalian-target-of-rapamycin (mTOR), a serine/threonine protein kinase that is implicated in the regulation of cell growth and survival [Fuchs *et al.* 2007, Nicklin, *et al.* 2009]. Although the involvement of ASCT2 in growth and proliferation of certain tumor cell lines has been initially investigated [Fuchs *et al.* 2005]; the physiological significance, the contribution to the glutamate / glutamine cycle and function of both ASC transporters in mammalian tissues, like those in the central nervous system, is poorly understood. This may be owing to the absence of potent and/or selective inhibitors to act as pharmacologic tools for probing of ASC transporter function. Thus far, there has been little progress in developing inhibitors to study the ASC transport system. This might be explained by the lower affinity the ASC transporters have for their

endogenous substrates; 24-400 μM for preferred substrates of ASCT(1 & 2) [Utsunomiya-Tate *et al.* 1996; Broer *et al.* 1999] relative to transporters such as the serotonin transporters. Additionally, the activity of the first ASCT2 inhibitors, benzyl cysteine and L- γ -glutamyl-p-nitroanilide ($K_i > 800$; data not shown), as leads have a discouragingly low affinity. Recently, it was reported that trans-4-hydroxy-L-proline is a high affinity, or preferred substrate transported by ASCT1 [Pinilla-Tenas *et al.* 2003]. The proline ring itself is particularly useful as a scaffold for creating molecules with multiple stereocenters with unique spatial arrangement. We were also drawn to the idea that the conformationally restrained ring of hydroxy-proline derivatives when combined with computational modeling would help to establish the fundamental molecular interactions that take place between ligand and ASCT transporter. Here we report the synthesis, activity and computational docking of a unique series of hydroxy-L-proline derivatives, or prolinols, as inhibitors of the neutral amino acid transporters hASCT1 and mASCT2 measured by electrophysiological recordings of blocking a Na^+ -dependant anion leak.

2. Methods

2.1. Chemicals and Reagents

L- ^3H -alanine and L- ^3H -glutamine was purchased from Dupont NEN (Boston, MA). *Trans*-4-hydroxy-L-proline, *trans*-3-hydroxy-L-proline, and benzyl alcohols were obtained from Acros Organics (Morris Plains, NJ). LC-MS grade acetonitrile for HPLC

was obtained from EMD Chemicals USA. The synthesis of all hydroxy-L-proline derivatives were synthesized by Brent R. Lyda under the mentorship of Dr. Sean Esslinger. Separation of regioisomers and isolation of final products were performed on a HPLC C18, 250mm x 21.2mm, 10 μ column using a Waters 486 Tunable Detector, and a Milton Roy pump. Full experimental details are reported in the experimental section. All other chemical reagents were purchased from Acros Organics (Morris Plains, NJ). All solvents were purchases from VWR International (Radnor, PA).

2.3. Radiolabeled Uptake in *Xenopus laevis* oocytes

Briefly, uptake in oocytes was performed in 12 well plates, 3-5 oocytes / well x 3 wells, with 10 minute incubations at 2 minute intervals / row, and 50 μ l of L-glutamine in each well. Oocytes were injected with 50.6 ng of mASCT2 RNA. L-Glutamine 10 μ M with 3 μ l/ml L-[³H]-glutamine in Nd96 buffer at pH 7.4 \pm 0.05 was used for each experiment. After 10 minutes, eggs were vortexed and lysed by addition of 2 M NaOH (1 mL) and placed in scintillation vials for quantification by a radiosciintillation counter.

Oocytes were preloaded for 20 minutes with 100 μ M L-alanine (4 μ L/mL L-[³H]-alanine) in Nd96 buffer at pH 7.4 \pm 0.05. The experiment was done in 12 well plates, with 3-5 oocytes / well and totaling with 3 wells. Radiolabeled L-[³H]-alanine exchange was performed over a course of 20 minutes with 1 mM of substrates (L-glutamine, or L-alanine) or 1 mM *trans*-3-hydroxy-L-proline in 2 mL Nd96 buffer. 10

μ L samples were taken at 1 min intervals and placed into scintillation vial for quantification.

2.4. ASCT Expression and Electrophysiological Recordings in *Xenopus laevis* oocytes.

Human ASCT1 and murine ASCT2 cRNA were microinjected in stage V-VI oocytes. Uncoupled anion currents associated with the transport of substrate were recorded 3-5 days later as previously described (Zerangue & Kavanaugh, 1996). Recording solution contained 50 mM NaCl, 50 mM NaSCN, 2 mM KCl, 1 mM MgCl₂, 1.8 mM CaCl₂, and 5 mM HEPES (pH7.4). Using two-electrode voltage clamp (TEVC), oocytes were held at -20 mV. Under these recording conditions, transport of substrates results in an outward anion current carried by SCN⁻, or nontransported inhibitors block an anion leak conductance (inward current) (Grewer & Grabsch, 2004). These currents also exist in the related excitatory amino acid transporters (EAATs 1-5; Wadiche et al., 1995). Microelectrodes were filled with 3M KCl and had resistances from 1 to 3 M Ω . Recordings were performed at 22 °C with a Geneclamp 500 amplifier connected to a PowerLab 2/26 (AD instruments). The digital output was interfaced to a MacBook Pro (Macintosh) using Chart v7.1.2 software. The currents were low-pass filtered at 10 Hz and acquired at 20 Hz. Data was analyzed offline and modeling and fitting of substrate concentration-dependence of the currents was performed with Kaleidagraph software (v 4.04). The concentration dependent percent block of the anion leak or substrate activation of the anion current were fit with the Michaelis-Menten equation ($I_{\text{anion}} = I_{\text{max}}$

$x \text{ [Drug]/(K}_m \text{ +[Drug])}$) to define the K_i of inhibition or the apparent affinity (K_m) of transport, respectively.

2.5. Computational Docking

Mouse ASCT2 primary sequence obtained from GenBank, <http://www.ncbi.nlm.nih.gov> was aligned with the Protein Data Bank (PDB) sequences for an archaeal homologue GltPh, 2NWW.pdb; [Boudker et al., 2007]. The ASCT2 homology model was constructed by threading the aligned sequence along 2NWW coordinates using the T-Coffee – Fasta alignment, SCWRL – server (<http://www1.jcsg.org/scripts/prod/scwrl/serve.cgi>). The resulting model was optimized through local energy minimizations of regions with high steric and electrostatic interference using the AMBER7 force field in the SYBYL. Energy minimized prolinols using SYBYL were docked using GOLD into the ASCT2 model. Each of the top ten poses for each of three separate docking experiments was evaluated for their capacity to dock with ASCT2 residues C479 and D476 or ASCT1 residues T459 and D456. The top GOLDScore poses and lowest predicted $-\Delta G$ molecules were incorporated into the homology model and visualized by The PyMOL Molecular Graphics System, Version 1.3, Schrödinger, LLC.

3. Results

3.1. *Trans*-3-hydroxy-L-Proline and *trans*-4-hydroxy-L-Proline are high affinity substrates of ASCT-1 and ASCT-2 transport.

We first set out to identify a synthetically useful molecular scaffold that was commercially available and itself binds to the ASC transporters as a substrate or nonsubstrate (transported or not transported). The hydroxy-L-prolines, *trans*-3-hydroxy-L-proline (3-HP), *trans*-4-hydroxy-L-proline (4-HP) and *cis*-4-hydroxy-L-proline were screened as potential inhibitors by radio labeled L-[³H]-glutamine uptake in *Xenopus laevis* oocytes expressing mouse ASCT2. Consistently, *trans*-3-hydroxy-L-proline, and *trans*-4-hydroxy-L-proline dose dependently inhibited 10 μM L-glutamine uptake ($IC_{50} \approx 49 \pm 23 \mu\text{M}$, n(6); $IC_{50} \approx 85 \pm 35$, n(4); 3-HP and 4-HP, respectively, fit by non-linear regression) whereas *cis*-4-hydroxy-L-proline and L-proline did not (data not shown). Knowing that ASCT2 is an obligate exchanger of one neutral amino acid substrate for another, we conducted an experiment to determine if exchange was taking place in the presence of the *trans*-3-hydroxy-proline. ASCT2 expressing oocytes preloaded for 20 minutes in Nd96 buffer containing L-alanine (100 μM; 4 μL/mL L-[³H]-alanine) was used to determine over a course of 20 minutes whether *trans*-3-hydroxy-L-proline is a substrate or a non-substrate inhibitor of ASCT2. The uninjected oocytes served as a control for nonspecific efflux or radiolabeled alanine “leak”. It was observed that 3-HP induces efflux of radio labeled L-alanine comparatively with the efflux observed by known preferred substrates, L-glutamine and L-alanine, thus suggesting that 3-HP is a substrate of ASCT2 (**Figure 2**).

mASCT2 efflux of L-³H-Alanine, 100 μM L-alanine preloaded for 20 minutes; 1mM Substrate treatment induces efflux over 20 minutes

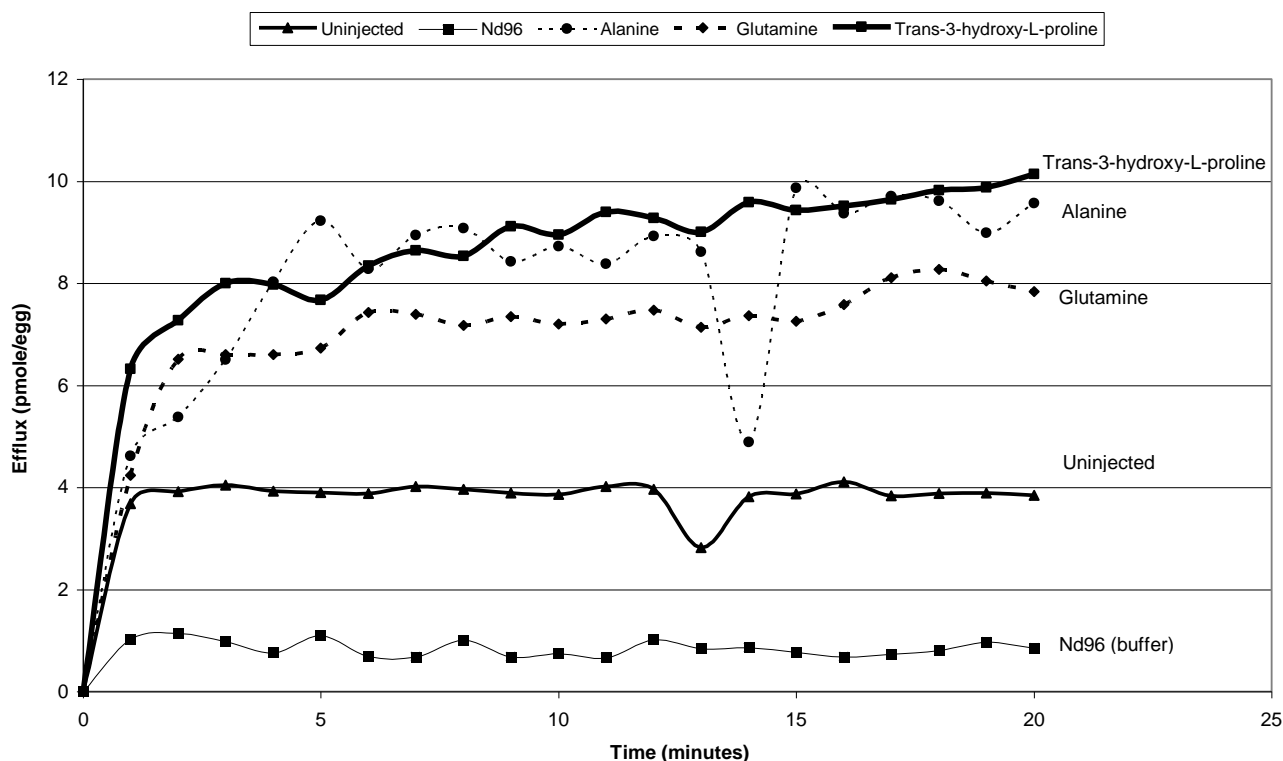


Figure 2. L-³H]-alanine efflux over 20 minute time course in presence of *trans*-3-hydroxy-L-proline (square), L-alanine (circle), or L-glutamine (diamond) and water injected oocytes (triangle). Uninjected preloaded oocyte controls exhibit no discernable radioligand leak or nonspecific efflux.

Trans-3-hydroxy-L-proline and *trans*-4-hydroxy-L-proline were evaluated as substrates of ASCT1 and ASCT2 by two-electrode voltage clamp recordings of a substrate induced ⁻SCN anion current, a technique we have found to be most reliable in screening for inhibitors and for characterizing the transport kinetics of the ASC transporters [Bröer *et al.* 2000; Grewer and Grabsch 2004]. A dose response with 3-HP or 4-HP in oocytes expressing in both ASC transporters reveals a standard and saturable

dose response curve (**Figure 3**). Using non-linear regression best fit to Michaelis-Menten equation we calculated the K_m of both substrates, 3-HP $K_m = 14 \pm 1.8 \mu\text{M}$, and 4-HP $K_m = 17.1 \pm 0.8 \mu\text{M}$ compared to the ASCT1 substrate L-alanine $K_m = 40 \pm 1.8 \mu\text{M}$ (**Figure 3, A**). The K_m found for 4-HP has been reported previously and our finding is in close agreement $33.2 \pm 4.3 \mu\text{M}$ [Pinilla-Tenas *et al.* 2003]. The K_m of 3-HP, 4-HP and endogenous substrate L-glutamine transported by ASCT2 were calculated in the same manner 3-HP $K_m = 28.6 \pm 6.4 \mu\text{M}$; 4-HP $K_m = 76.3 \pm 11.0 \mu\text{M}$, Gln $K_m = 47.4 \pm 4.6 \mu\text{M}$ (**Figure 3, B**). These calculated K_m values for both 3-HP and 4-HP at ASCT-2 are also in close agreement with the IC_{50} values we found by radio-labeled uptake. Additionally, our calculated K_m of $47.4 \mu\text{M}$ for glutamine is also in very good agreement with that found in previous publications, $24 \mu\text{M}$ and $70 \mu\text{M}$ [Utsunomiya-Tate *et al.* 1996; Bröer *et al.* 1999].

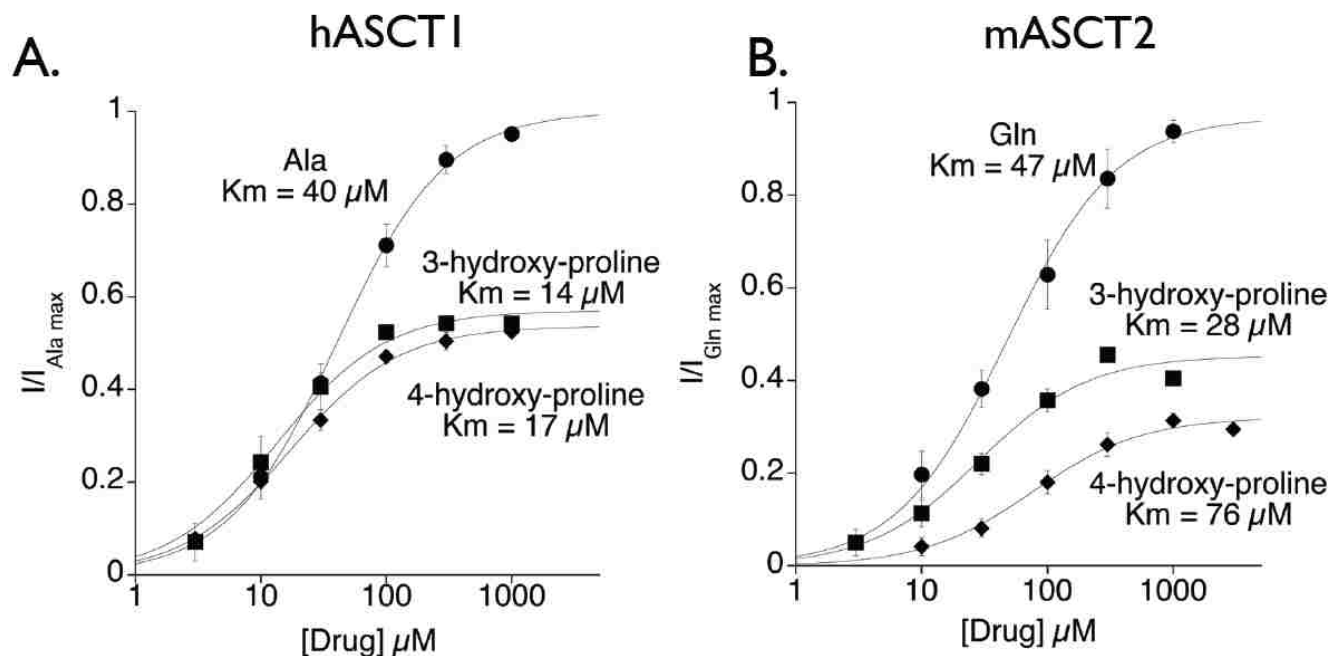


Figure 3. **A.** hASCT1 dose response curve for substrate activated anion currents using two-electrode voltage clamp of *Xenopus laevis* oocytes (-20mV). Currents are normalized to the maximum current estimated for Alanine **B.** mASCT2 dose response curve for substrate activated anion currents using two-electrode voltage clamp of *Xenopus laevis* oocytes (-20mV). Currents are normalized to the maximum current estimated for glutamine. Extracellular solutions contained 50 mM NaSCN, a highly permeable ion to the transporters anion channel. Dose response curves were fit to Michaelis-Menton equation to find K_m .

Although the represented graphs show a difference in substrate elicited currents, it is important to understand that the I_{max} , maximum current, recorded by 3-HP or 4-HP are normalized to maximal current recorded for alanine or glutamine (ASCT1 and ASCT2) within our setup and is not representative of V_{max} , the maximal rate at which the substrates are transported. This can be explained by an amino acid exchange process that is stoichiometrically uncoupled to the anion current, which has been observed in both ASCT1 and ASCT2 [Zerangue and Kavanaugh 1996; Bröer *et al* 2000]. Therefore, in

considering both the current recordings and radiolabeled uptake data it can be concluded that both 3-HP and 4-HP are substrates of the ASC transporters. With the exception of *trans*-4-hydroxy-L-proline acting at ASCT1; this is, to the best of our knowledge, the first time these naturally occurring amino acids as substrates of ASCT1 and ASCT2 have been reported. Importantly, L-proline induces little substrate like current when applied to ASCT1 or ASCT2 at 300 μ M (data not shown). This is consistent with previous radiolabeled uptake studies showing L-proline to have a K_m of 704 \pm 86 μ M at ASCT1 [Pinilla-Tenas *et al.* 2003] and minimal inhibition of ASCT2 mediated radio-labeled L-alanine uptake [Utsunomiya-Tate *et al.* 2006; Kekuda *et al.* 1996], and no inhibition of radio-labeled glutamine uptake detected within our uptake experiments. This indicates that the ASC transporters may have a preference for binding amino acids with a beta or gamma positioned alcohol group, likely as a hydrogen bond acceptor and / or donor.

3.2. Synthetic hydroxy-proline derivatives.

A series of stereochemically distinct substituted hydroxy-L-proline derivatives (**Figure 4**) was synthesized and isolated to be evaluated as non-substrate inhibitors of ASCT1 and ASCT2. Amongst the prolinols produced and isolated included regioisomers of phenyl, methyl or phenol-ether substituted hydroxy-L-prolines (compounds CSE -103, 104, 109, 110, 117, 118) derived from protected 3,4-epoxy-proline under basic conditions. Also included in the series was *cis*-4-methyl-*trans*-4-hydroxy-L-proline (CSE95) and *cis*-4-hydroxy-*trans*-4-methyl-L-proline (CSE96) synthesized from

protected-4-keto-proline under basic condition. Lastly, various benzyl or alkyl ether substituted L-prolinols of both first (CSE-113, 115, 121, 122, 124, 127) and third generation (CSE-130, 131, 132) were produced under acidic conditions from protected *cis* or *trans* 3,4-epoxy-prolines. This stereochemically diverse series was then tested for inhibitor activity against ASCT1 and ASCT2 to probe for activity and thereby guide the discovery of novel pharmacologic lead inhibitors. Refer to the experimental procedures section for full experimental details, procedures and synthetic schemes.

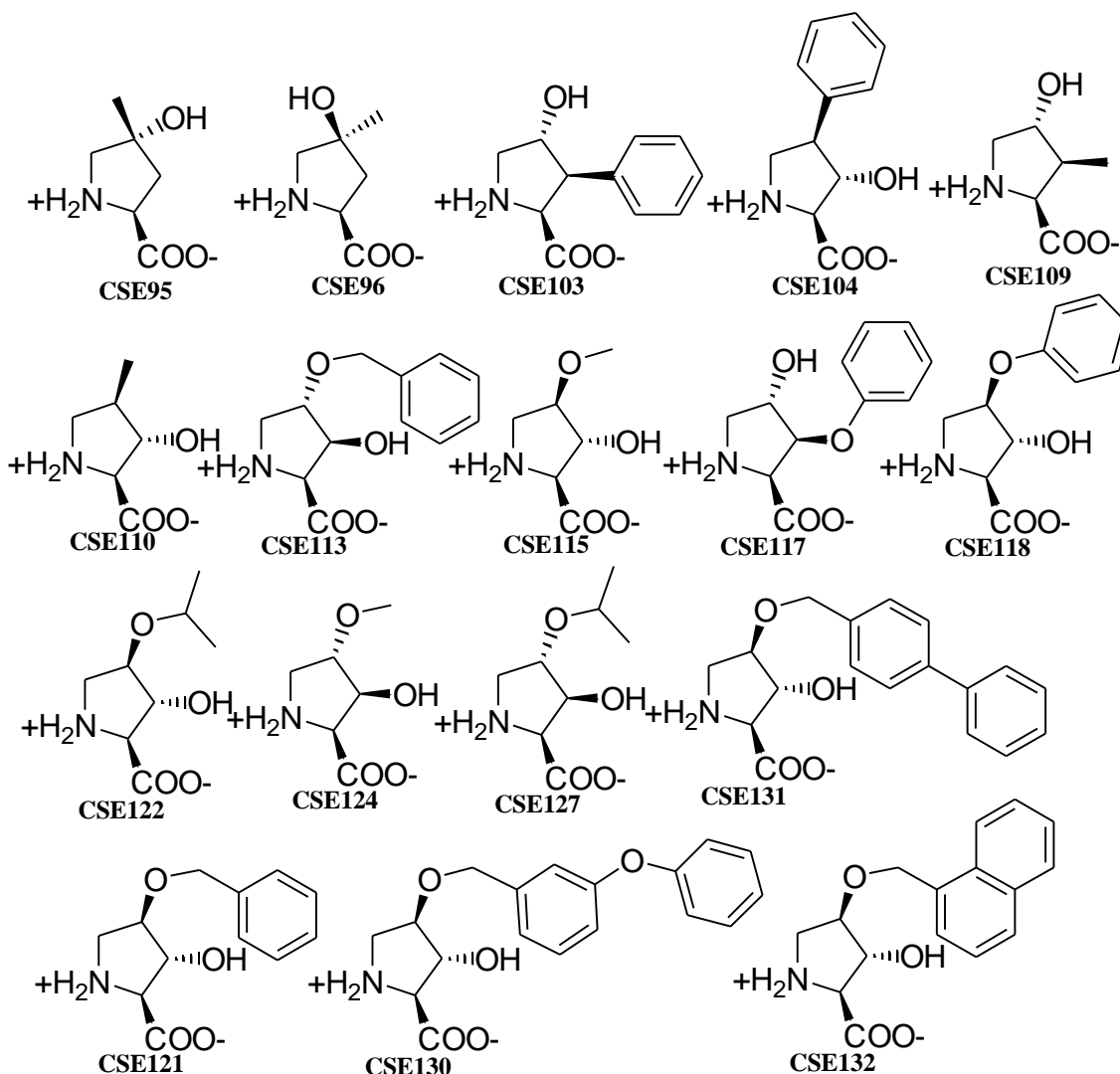


Figure 4: Synthesized substituted prolinols for biological testing as inhibitors of the ASC transporters.

3.3. Non-substrate inhibitors of ASC transporters block leak current.

In screening the synthesized prolinols at ASCT1 and ASCT2 by electrophysiological methods it was critical to determine whether this class of compounds in particular displayed substrate or non-substrate like activity. It has been shown that

non-substrate inhibitors of ASCT2 when applied alone will produce what appears as an inward current that is opposite of a substrate induced current, the effect of inhibiting a tonic anion conductance [Grewer *et al.* 2004]. Our results confirm this in ASCT2 showing block of a tonic anion conductance by synthetic prolinol CSE121 at 300 μ M relative to 300 μ M of glutamine, a substrate, when individually applied (**Figure 5, B**). The anion leak is also present in ASCT1 as seen when applying synthetic prolinol CSE122 relative to the substrate alanine (**Figure 5, A**). Interestingly, we observed a very robust inward current at ASCT2 when applying inhibitors such as CSE 121 at 300 μ M, which is much less pronounced in ASCT1. These results suggest that the synthesized prolinols act as non-substrate inhibitors.

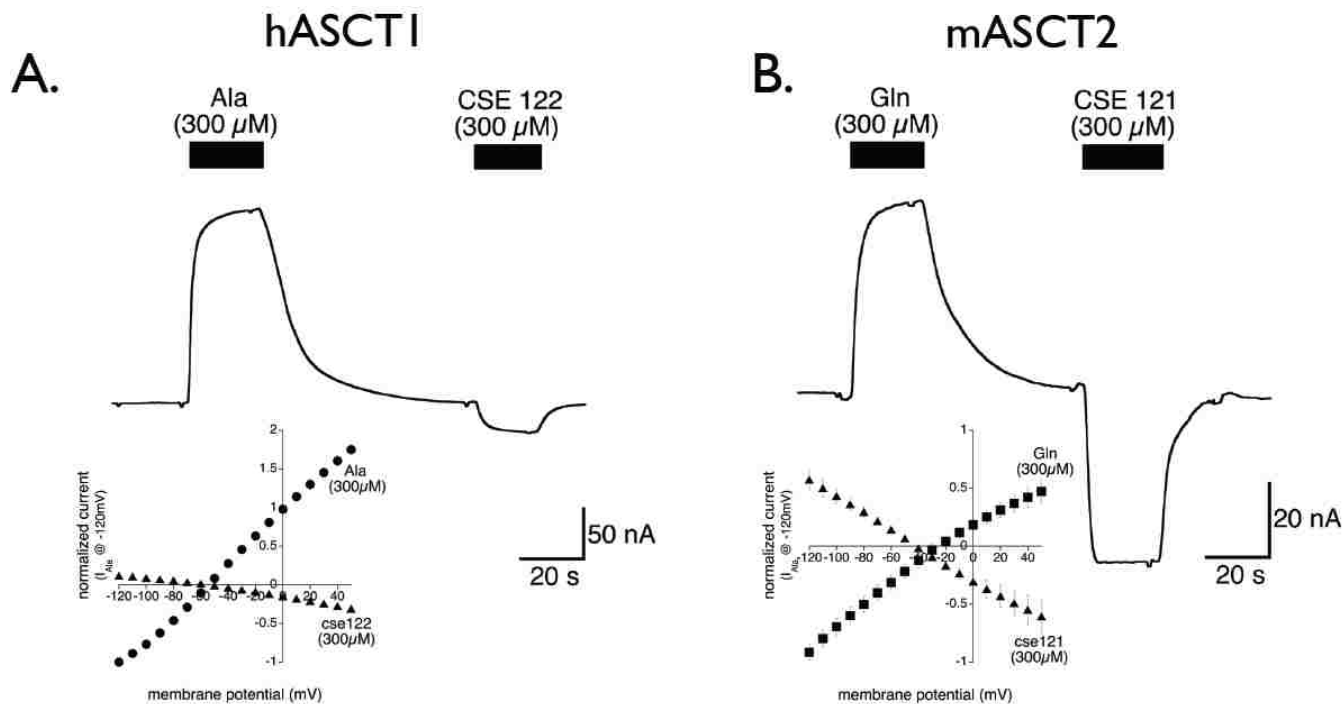


Figure 5. Hydroxy proline derivative CSE 121 (300 μ M) and CSE 122 (300 μ M) block a leak current in mASCT2 and hASCT1, opposite the current induced by substrate (-20mV). **A. Inset:** The current and voltage relationship for hASCT1 currents activated by Ala or blocked by CSE 122 resolved by subtracting away voltage jumps in Ringer solution. **B. Inset:** The current and voltage relationship for mASCT2 currents activated by Gln or blocked by CSE 121 resolved by subtracting away voltage jumps in Ringer solution.

3.4. System ASC Transporters are inhibited by 4-cis-ether substituted-*trans*-3-hydroxy-L-prolines.

Next we wanted to determine the affinity of what seemed to be the more robust prolinol inhibitors identified in our screening. Application of selected prolinol non-substrate inhibitors to oocytes expressing ASCT2 or ASCT1 showed block of the inward anion current that was concentration dependant and saturable (**Figure 6, B Inset**).

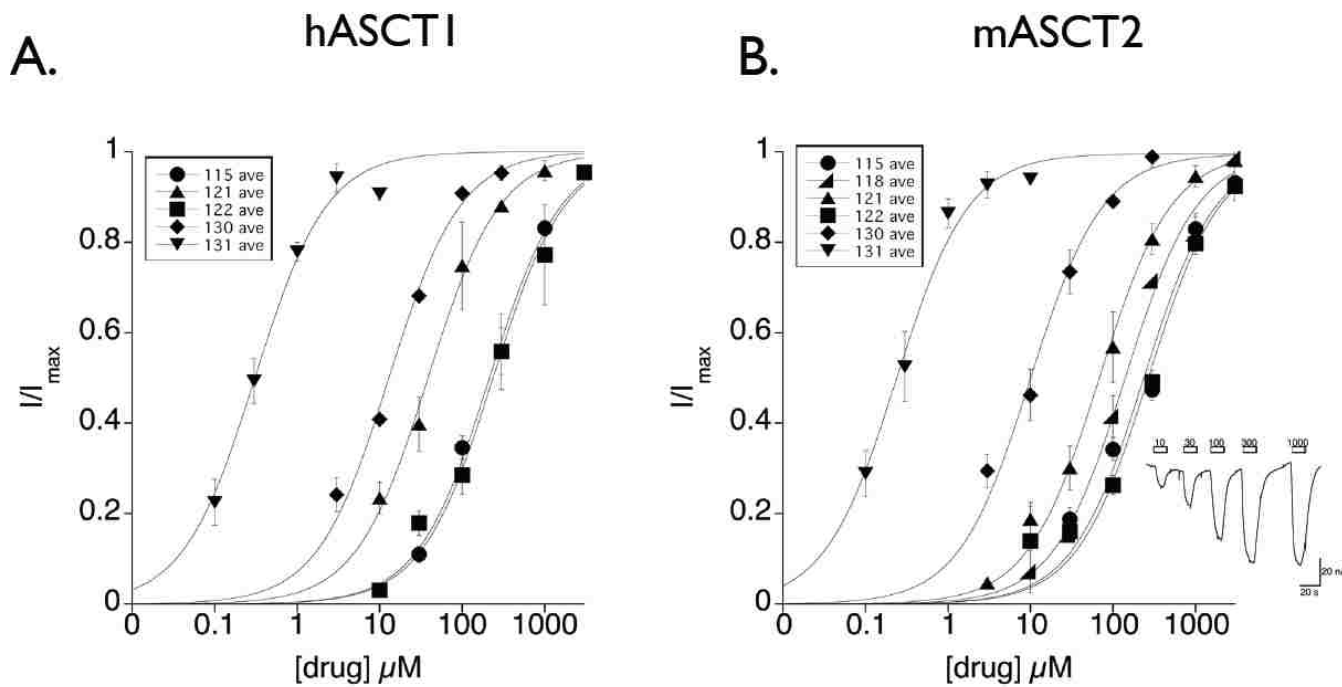
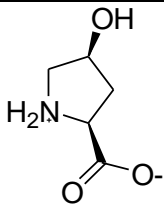
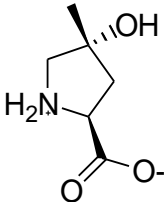
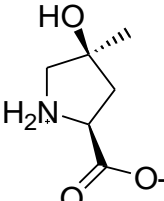
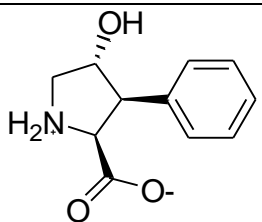
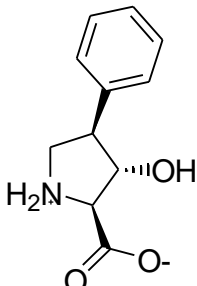
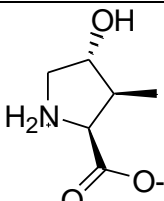
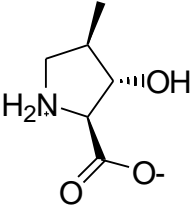
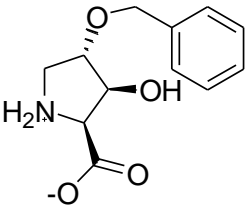
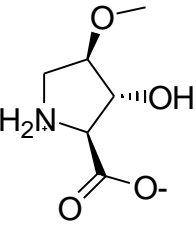
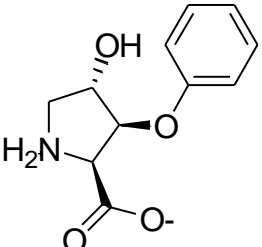
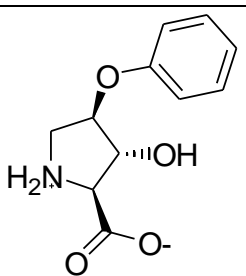
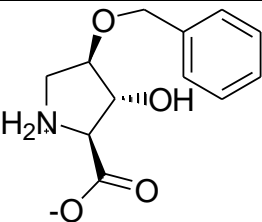


Figure 6. The leak current in hASCT1 and mASCT2 has a saturable block revealed by increasing concentrations of CSE 131 (down triangle), CSE 130 (diamond), CSE 122 (square), CSE 121 (up triangle), CSE 118 (wedge), and CSE 115 (circles). The 50% block is considered to be the K_i for binding of a non-transportable substrate. B. Inset: A representative trace showing the dose relationship for the mASCT2 leak current blocked by CSE 121.

The resulting dose response (**Figure 6, A and B**) recorded at ASCT1 and ASCT2 when applying a particular synthetic prolinol was fitted to Michaelis-Menten by non-linear regression to determine the apparent K_m or actual $K_i \approx K_d$. Actual and estimated K_i 's are reported in **Table 1**.

| CSE # | | Ki(μM) ACST1 | Ki (μM) ASCT2 |
|-----------------------|---|--|------------------|
| cis-hydroxy-L-proline |  | 805 +/- 148 | 872 +/- 201 |
| CSE95 |  | no detectable block of anion conductance | 926 +/- 252 |
| CSE96 |  | no detectable block of anion conductance | 1077 +/- 322 |
| CSE103 |  | 332 +/- 74 | 1128 +/- 318 |
| CSE104 |  | ≈600 | ≈600 |
| CSE109 |  | 564 +/- 149 | 922 +/- 316 |

| | | | |
|--------|---|-----------------|-----------------|
| CSE110 |  | 1050 +/- 110 | 1149 +/- 283 |
| CSE113 |  | 493 +/- 61 | 828 +/- 248 |
| CSE115 |  | 214* +/- 32 | 235* +/- 69 |
| CSE117 |  | 594 +/- 191 | 502 +/- 110 |
| CSE118 |  | 150 +/- 43 | 141* +/- 20 |
| CSE121 |  | 39* +/- 5 | 69* +/- 7 |

| | | | |
|--------|--|----------------|----------------|
| CSE122 | | 237* +/-40 | 268* +/- 70 |
| CSE124 | | 481 +/- 77 | 600 +/- 176 |
| CSE127 | | 505 +/- 105 | ≈400 |
| CSE128 | | ≈150 | ≈150 |

Table 1: Actual * or estimated K_i in μM derived from inhibition of tonic anion leak by first and second generation prolinols in *Xenopus* oocytes expressing human ASCT1 or mouse ASCT2.

The first generation of these synthesized substituted hydroxy-proline derivatives showed modest activity. One prolinol (CSE115) stood out amongst the various phenyl and methyl substituted *trans*-hydroxy-L-prolines (CSE-95, 96, 103, 104, 109, 110) and the substituted *cis*-hydroxy-L-prolines (CSE-113, 124, and *cis*-hydroxy-L-proline) in our

screening. A dose response using *cis*-4-methoxy-*trans*-3-hydroxy-L-proline (CSE115) at both transporters gave the corresponding K_i of 214 +/-32 at ASCT1 and K_i of 235 +/-69 at ASCT2. After assessment of this first series we decided to pursue a second series of ether substituted *trans*-hydroxy-L-prolines more focused on prolinols with a 3 positioned alcohol, this included CSE-117, 118, 121, 122, and 128. The isopropoxy-*cis*-hydroxy-L-proline CSE127 was also made in this series because we felt it was prudent to expand just beyond the addition of a methoxy group before ruling out this class of prolinols as potential leads.

Measuring the blocked anion leak with the second generation of prolinols revealed that addition of a phenoxy or benzyloxy at the four carbon of the proline ring, CSE118 and CSE121, increases potency relative to the 4-methoxy substituent CSE115. However, no real improvement in affinity was gained by the isopropoxy extension from the methoxy group for *cis*- or *trans*-hydroxy-L-prolines. Most encouraging was the benzyloxy product, *trans*-3-hydroxy-*cis*-4-benzyloxy-L-proline CSE121, which provided a 5 and 3 fold increase in potency at ASCT1 and ASCT2 respectively. This is well within the affinity these transporters exhibit for their preferred substrates, an affinity that has not yet been achieved by any non-substrate inhibitor of the ASC transporters to date.

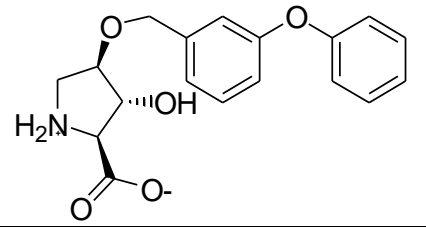
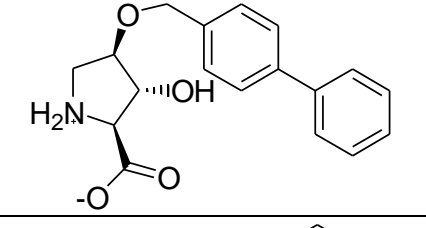
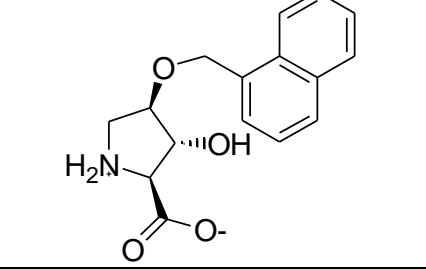
| | | | |
|--------|--|-------------------|-------------------|
| CSE130 |  | 13* +/- 2 | 10* +/- 2 |
| CSE131 |  | 0.31* +/- 0.04 | 0.24* +/- 0.04 |
| CSE132 |  | ≈10 | ≈10 |

Table 2: Actual K_i 's * of third generation prolinols as lead inhibitors of ASCT1 and ASCT2, calculated from measured dose response of blocked anion conductance.

The next step in developing this class of inhibitors was clearly to expand upon the benzyl-ether of 4-*cis*-benzyloxy-*trans*-3-hydroxy-L-proline (CSE121). The third generation of prolinols that were synthesized included the addition of a biphenyl, naphthyl, and diphenyl ether group, **Table 2** CSE-130, 131, and 132. These additions markedly improved the potency of these prolinols at the ASC transporters. Like the other prolinols derivatives, the new inhibitors obeyed Michaelis-Menten kinetics displaying block of the anion leak conductance that was dose dependent and saturable. The corresponding K_i values obtained are a leap from that of the second and first generation prolinols. Strikingly, the addition of a phenyl group para to the methoxybenzyl of CSE 121

afforded a 290-fold improvement in potency at ASCT2. This is also a significant leap, 40-fold, in potency over that of the naphthyl and 3-diphenyl ether prolinols (CSE 132, and 130). This result may indicate that the hydrophobic pocket of these transporters, of which we are probing, is somewhat narrow. The new lead inhibitor (2S, 3R, 4R)-3-hydroxy-4-O-methyl-p-biphenyl-proline (CSE131) was found to have a K_i of 0.24 μM at ASCT2 and 0.31 μM at ASCT1. Unfortunately, this last series did not pull out any selectivity between ASCT1 and ASCT2 as we were hoping.

3.5 Computational docking predicts ligand transporter interaction and hydrophobic pockets.

In addition to the biological screening of the prolinol series we obtained a crystal homology model (Glt_{Ph}) of human ASCT2 from the Protein Data Bank. The synthesized prolinols CSE 113, 121, 128, 130, 131, and 132 (**Figure 4**) were docked using GOLD into the ASCT2 homology model based upon the open, ligand accessible, form of Glt_{Ph} with bound TBOA [Boudker *et al.* 2007]. The top computer generated poses, scored via ChemScore, of three separate docking experiments were evaluated by the presentation of reasonable intermolecular interactions between the docked hydroxy-proline derivatives and residues C479 and D476 of ASCT2. Importantly, both of these residues are the equivalent residues in the putative ligand binding site of EAAT 1 and 3 that were identified by site directed mutagenesis as functionally critical residues for binding and transport of endogenous substrates [Conradt *et al.* 1995; Bendahan *et al.* 2000; Teichman

and Kanner 2007]. The docking experiments were run with one constraint (ChemScore constraint weight = 5.0) to favor an interaction with aspartate residue D476 of ASCT2. Without the constraint the docked poses would otherwise interact entirely with the carbon- peptide backbone and hydrophobic regions of the transporter which would suggest that binding is purely allosteric, which is inaccurate. Essentially, with the constraint the GOLD will avoid this improper docking which coincidentally also favors docked poses of inactive prolinols over active.

Prolinol CSE121 docked into the ASCT2 homology model by aligning with its secondary amine to the β carboxylic acid of Asp476 at 2.2Å and to the nearby Thr480. (**Figure 7**). Additionally, the *trans*-3-hydroxyl group of the prolinol (CSE121) aligned at 2.7 Å to the sulfhydryl group of Cys479; and finally, the α -carboxylic acid of the prolinol aligned with the nearby Asn483 and serine peptide amide from the HP1 loop. Consequently, the orientation that the prolinol CSE121 adopts in order to interact with these critical residues places the benzyloether group down towards the intracellular spanning side of helix transmembrane seven (TM7a; teal) or slightly under the HP2 loop (red).

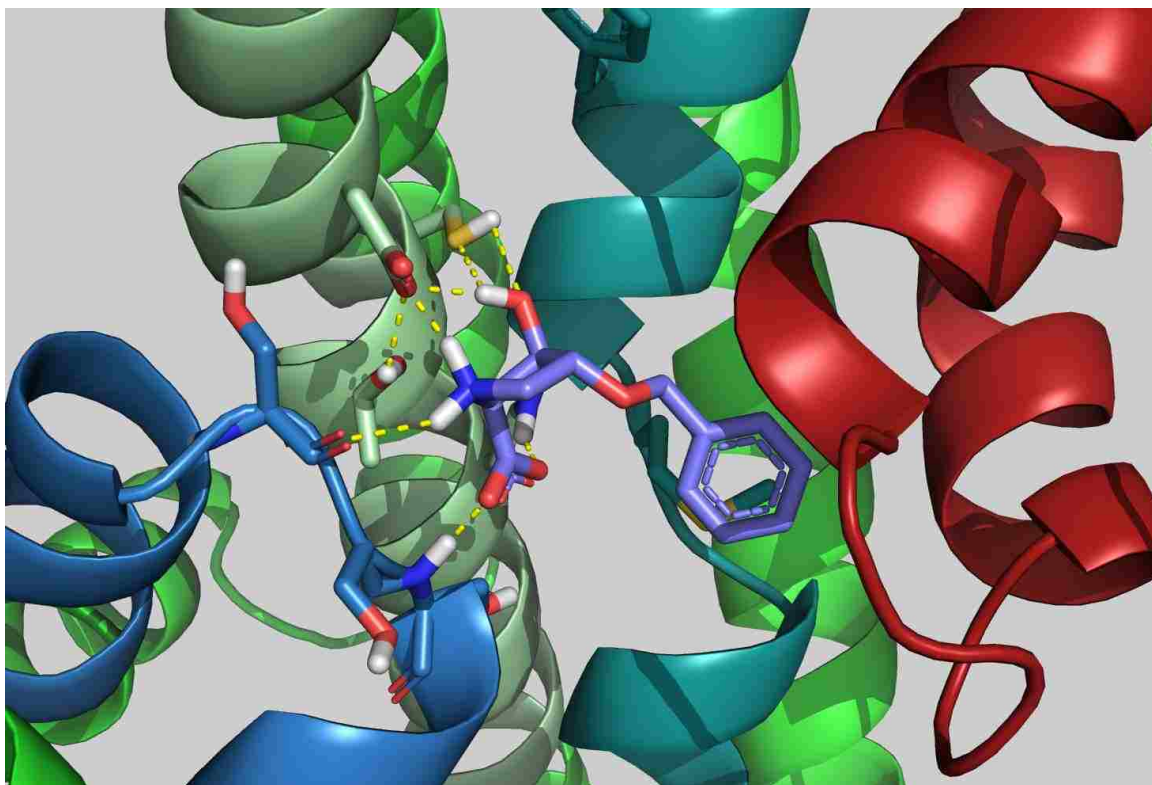


Figure 7: CSE121 (purple) docked into a mouse ASCT2 homology model. Shows intermolecular interactions between the prolinol's functional groups (alcohol, secondary amine (blue), and carboxylic acid) and key residues of ASCT2, Asp476, Cys479 (sulfhydryl in yellow), Asn483 (behind CSE121), and Thr480. The benzyl ether of CSE121 rests over a methionine residue (M399) of TM7 (transmembrane 7, teal) (sulfhydryl in yellow). Image visualized by PyMOL Molecular Graphics System, Version 1.3, Schrödinger, LLC.

Interestingly, the benzyloxy of CSE121 is positioned over a methionine residue, M399, which is equivalent to methionine M311 of Glt_{Ph} that the benzyloxy of TBOA interacts with in the published crystal structure. Upon examining the conformation of CSE121 docked into ASCT2, it was encouraging to see the generated poses resembling the conformation of TBOA bound into Glt_{Ph} (**Figure 8**).

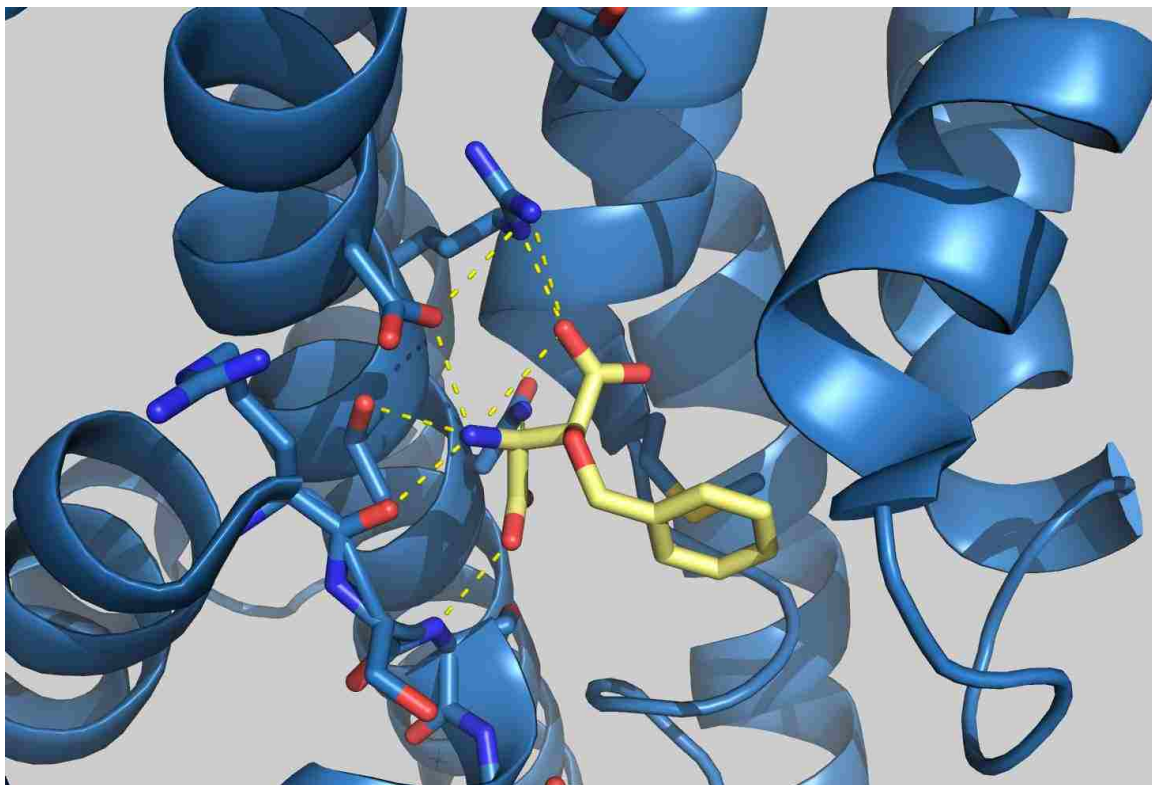


Figure 8: Crystal structure of GltPH with TBOA bound and intermolecular interactions in yellow dotted lines [Boudker *et al.* 2007]. Image visualized by The PyMOL Molecular Graphics System, Version 1.3, Schrödinger, LLC.

Computational docking of an inactive stereo isomer of CSE121, CSE113 (*cis*-3-hydroxy-*trans*-4-benzyloxy-L-proline), revealed a plausible hydrophobic pocket through interaction with a phenyl alanine F405 (**Figure 9**). Both prolinols rings of CSE121 and CSE113 overlay well with each forming an electrostatic interaction with Asp476 and hydrogen bonding interactions with residues Thr480, Asn483. CSE113 consistently and significantly scores higher by both ChemScore (~18-23 vs ~11-13) and GoldScore than does CSE121 suggesting that the hydrophobic pocket of which the benzyl ether group of

CSE113 docks into confers higher potency. Docking of CSE128 into ASCT2 (not shown) positions the phenoxy-ether near the phenyl alanine F405, the amine to Asp476 and the α -carboxylic acid with an amide from the HP1 primary chain. The orientation in this alignment leaves the *trans*-3-hydroxyl interaction with Cys479 intact while maintaining the interaction with phenyl alanine F405. Although CSE128 does not score as high as CSE113 it does score comparably with CSE121.

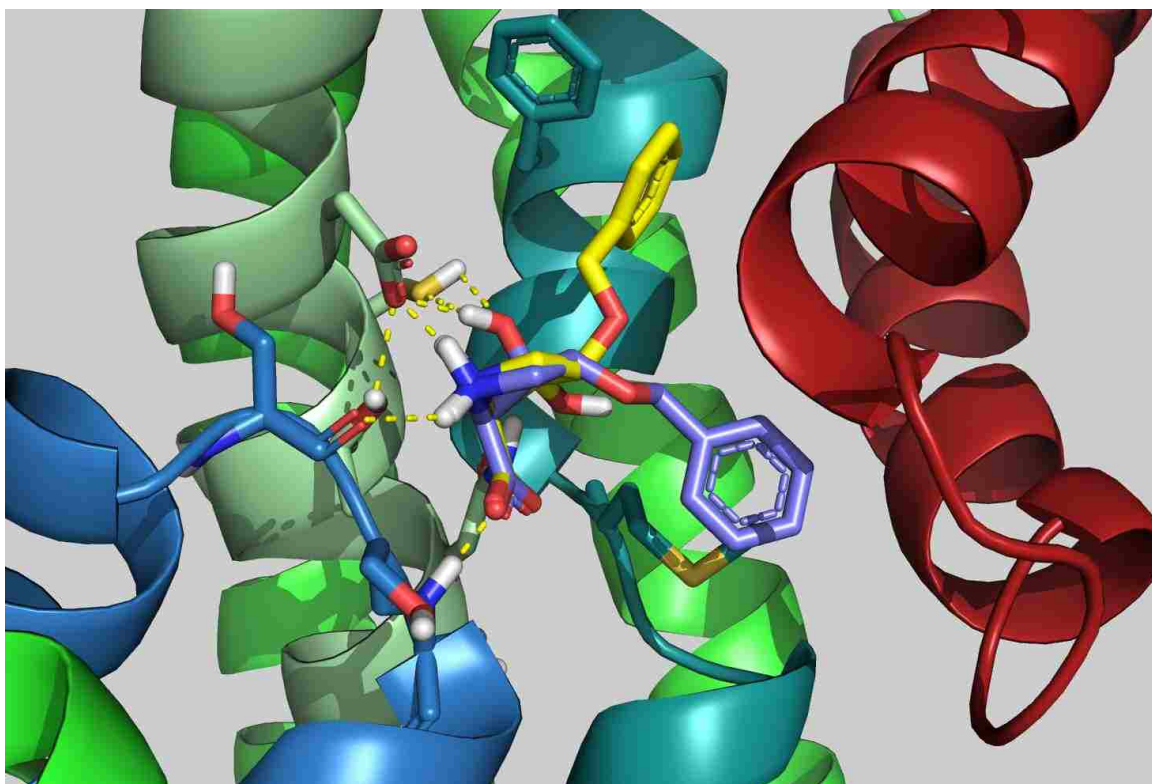
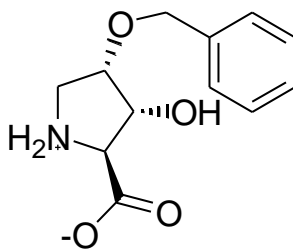


Figure 9: CSE113 (yellow) and CSE121 (purple) overlay in mouse ASCT2 homology model. Shows two hydrophobic pockets, one near phenylalanine F405 on TM7 β (teal); the other on top of a methionine residue (M399) on TM7 α (teal) and under HP2 loop (red).

The only other underlying structural difference between CSE121 and CSE113 is the stereo configuration of the 3 positioned hydroxyl. The two poses of CSE121 and CSE113 in **Figure 9** show the 3-hydroxyl of CSE121 to be above the proline plane and aligning with Cys479; however with CSE113 the 3-hydroxyl is below the proline ring plane with no interaction. This supports our hypothesis that a hydrogen bond (donating) or strong dipole interaction is taking place with Cys479, and therefore only the *trans*-hydroxy-prolines are tolerated. Docking experiments where we have substituted Cys479 in the ASCT-2 homology model for a threonine score in favor of the *trans*-3-hydroxy-proline CSE121 over the *cis*-hydroxy-proline CSE113 (data not shown). This may indicate that equally in ASCT1 there is a preference for ligands (substrate or nonsubstrate) that interact with the equivalent threonine residue T459. A theoretical analog of CSE113 and CSE121 where both the hydroxyl and benzyl ether are *trans* to the L-carboxylate (3,4-*trans*-hydroxy-benzyloxy-L-proline) was created and docked into the homology model (**Structure A**).



Structure A

This analog aligns in the model just as CSE113 does, although now with the hydroxyl functionality aligning with Cys479. One would have predicted that this theoretical

analog would score higher than CSE113, however it scores relatively the same ($\approx 18-23$). Altogether this would suggest that interactions with the sulfhydryl group in this model are not properly weighted or defined in GOLD. We were unable to resolve this issue without resorting to placing a constraint in favor of an interaction with Cys479 into the experiment.

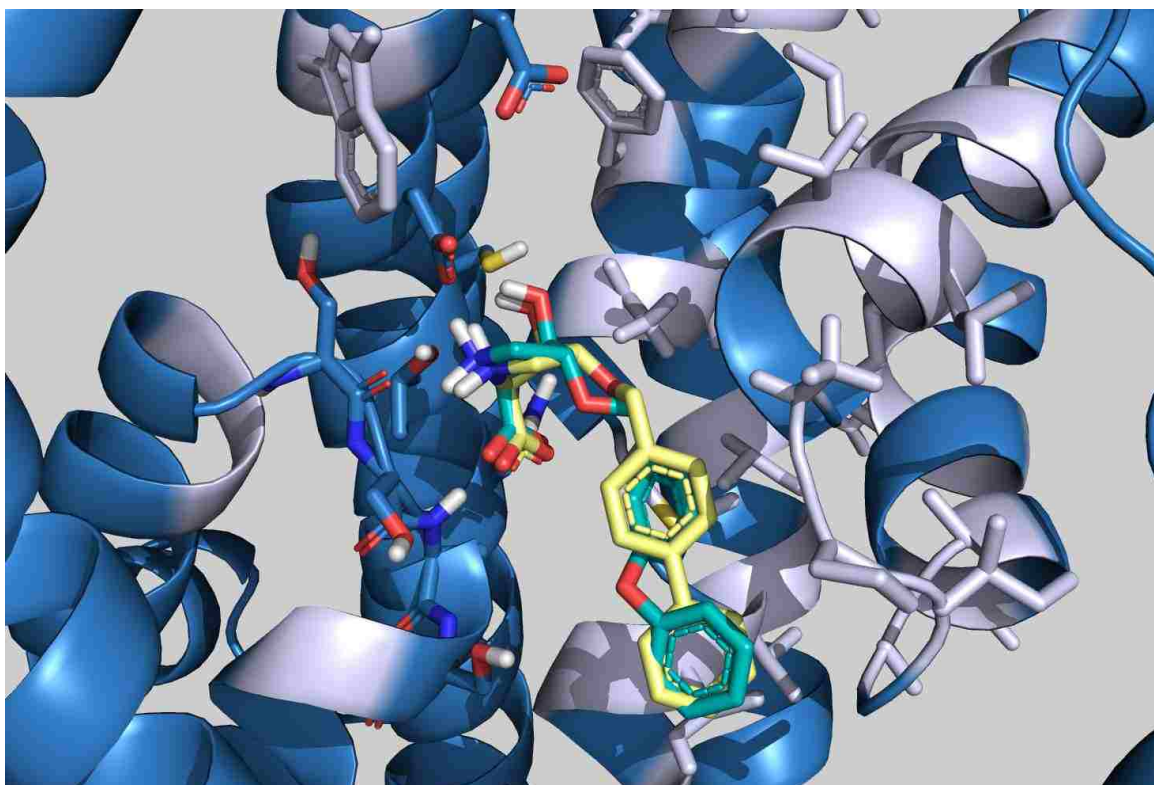


Figure 10: CSE130 (teal) and CSE131 (gold) overlay docked into ASCT2 homology model. Residues with hydrophobic side chains are labeled in white; polar residues are labeled in blue. Docking depicts interactions with Cys479, Asp476, Thr480, Asn483 and amide/carbonyl of HP1 loop backbone.

Docking of our most potent inhibitors CSE131 and 130 identifies a hydrophobic pocket that extends from Met399 and along the beginning TM7 α (**Figure 10**). The orientation and alignment of these prolinols in the binding domain is consistent with that found for CSE121 where again the *trans*-3-hydroxyl aligns with Cys479, the secondary amine aligns with Asp476 and Thr480, and finally the α -carboxylic acid aligns with Asn483. These more highly conjugated prolinols also score quite high by ChemScore, between 23-27. **Figure 11** illustrates the plausible hydrophobic pocket (shown in white) identified by docking of CSE131 into the ASCT2 homology model.

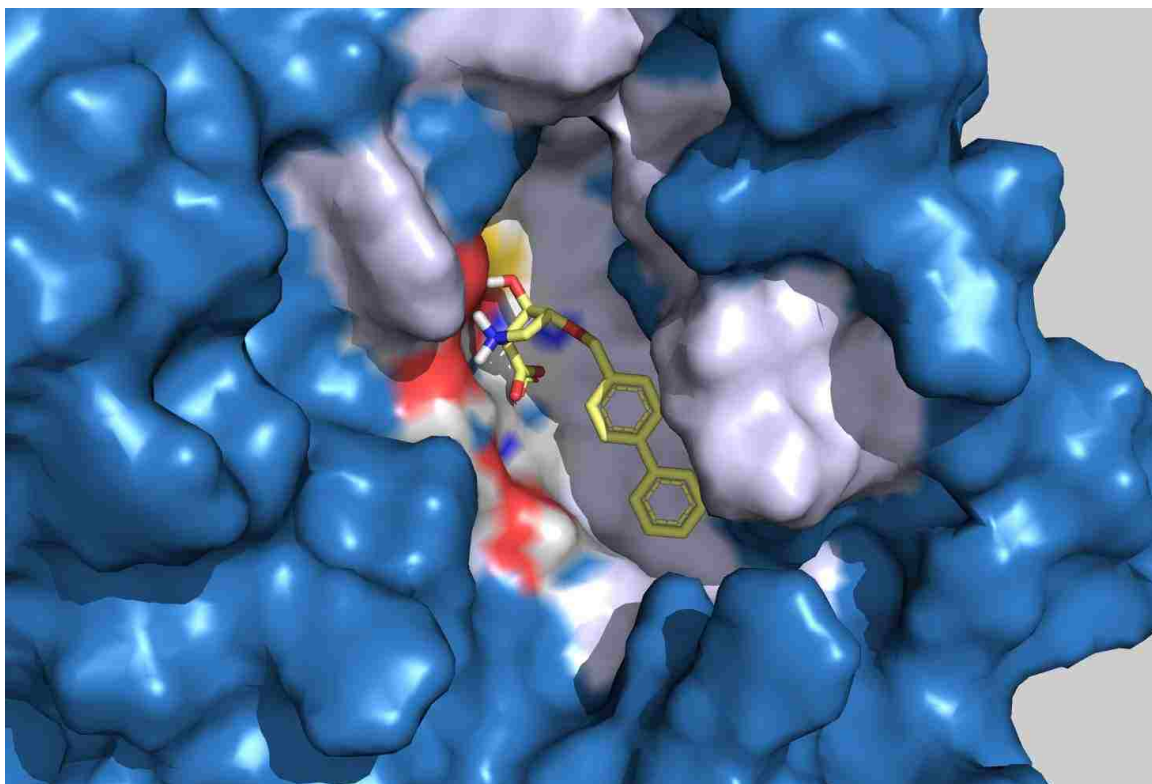


Figure 11. CSE 131 docked in ASCT2 homology model depicting surface density. Residues with hydrophobic side chains are labeled in white, polar residues are labeled in

blue. Shows alignment of CSE131 to polar side chains Asp476 and Thr480 (red), Cys479 (yellow), Asn483 (dark blue).

3. DISCUSSION

The ability to make use of a crystal homology model to analyze structure activity of a series of compounds provides an incredible advantage to understanding the molecular interactions that may be taking place between ligand and receptor, or in this case a transporter. Site directed mutagenesis of specific residues in the ligand binding domain can then further strengthen our understanding of the important interactions taking place by narrowing down which amino acids are critical for binding. Another strategy is to employ a conformationally restricted molecular scaffold when developing a series of potential inhibitors for screening. Indeed, the unique conformations that such a scaffold forces will efficiently guide a developing pharmacophore model. Collectively these strategies make a very compelling argument for the necessary polar molecular interactions taking place between high affinity ligands and ligand binding site, the interactions often necessary to produce potent lead inhibitors.

In this study we have identified *trans*-3 and *trans*-4-hydroxy-L-proline as high affinity substrates of ASCT1 and ASCT2 mediated transport by radiolabeled uptake and electrophysiological recordings of substrate transport induced anion current. These two natural amino acid transporters noticeably prefer the *trans*-3-hydroxy-L-prolines analogs

over the *cis*-diastereomer equivalent. This indicated that the hydroxyl group may be involved in hydrogen bonding or a strong dipole-dipole interaction with the ASC transporters through a key polar residue responsible in ligand recognition. This is not surprising considering ASCT2's selective transport of amino acids Ser, Cys, Gln, and Asn, or preferred substrates of ASCT1, all of which contain a capable hydrogen bonding functional group on their side chain, excluding alanine. Furthermore, ASCT2 mediated transport of glutamate is pH sensitive. In a more acidic environment the glutamate γ -carboxylate becomes protonated and now binds ASCT2 by interaction with a fundamental residue responsible for ligand recognition. This molecular interaction likely occurs through a hydrogen bond in ASCT transporters versus an electrostatic interaction as seen in the EAATs via an arginine residue [Utsunomiya-Tate *et al.* 1998]. The pH sensitivity of ASCT2 has also been demonstrated through inhibition or radiolabeled uptake by N γ -aryl-glutamine analogs (Esslinger *et al.* BOMC 2005). The prevalent view is that cysteine 479 in ASCT2 or threonine 459 in ASCT1 are responsible for discriminating between acidic and neutral amino acids. Unfortunately, the modeling software GOLD does not recognize all the necessary interactions and often docks *trans*-3- or 4-hydroxy-proline nonspecifically with the carbon peptide backbone or by improper alignment of the α -carboxylate with Asp476 of the ASCT2 homology model. However, it is visually apparent that the energy minimized structures of the *trans*-hydroxy-prolines are capable of aligning with Cys479 and Asp476 through the secondary amine and hydroxyl group where *cis*-hydroxy-prolines are not.

We have been successful in using *trans*-4-hydroxy-L-proline as a molecular scaffold to synthesize inhibitors of the ASCT neutral amino acid transporters. Our first lead in this series, although not all that potent, was CSE115 a *trans*-3-hydroxy-*cis*-4-methoxy-L-proline. Surprisingly, the methyl analog of this CSE110, *trans*-3-hydroxy-*cis*-4-methyl-L-proline, showed no activity when tested at the ASCT transporters. A rational explanation for the observed loss in activity from substitution of a methoxy for a methyl prolinol may be that the two compounds adopt different boat conformations. The substituted methyl prolinol positions the amine away from the hydroxyl group. In comparison, the methoxy substituent positions the amine close to the hydroxyl group in prolinol CSE115. The resulting energy minimized structures and docking of CSE110 and CSE115 using SYBYL supports this idea. The conformation CSE110 adopts essentially would not allow for interaction of the prolinol functional groups with Cys479 and Asp476 to occur simultaneously, whereas the conformation of CSE115 does.

The extension of CSE115 to produce the isopropoxy-prolinol CSE122 provided no additional benefit in activity. Introduction of a phenoxy to produce CSE118 did add a measurable increase in affinity. However, the greatest increase in potency came from the extension of CSE115 to produce CSE121, a benzyloxy substituent. Although it is not exactly clear as to why this substitution provides greater activity than the phenol ether CSE118, it may stem from the added flexibility of the benzyl group. This may help to position the aromatic ring slightly underneath the HP2 loop where it can fully interact with Met399.

Although incomplete, this prolinol series has already begun to describe a pharmacophore model for designing inhibitors of the ASCT transporters and may have also provided some leads to achieving an ASCT subtype selective inhibitor. One interesting avenue to pursue ASCT1 selective inhibitors could include analogs of *cis*-3-phenyl-4-*trans*-hydroxy-L-proline, CSE103. The 3-positioned *cis*-methyl prolinol CSE109 from our screening showed slight selectivity for ASCT1 over ASCT2. This selectivity is further improved by substitution for a phenyl, CSE103, observed by an increase in activity at ASCT1 and no detectable change in activity at ASCT2 relative to the CSE109. This may also have important implications for designing selective inhibitors of the EAATs. Another possibility may be to create analogs of CSE128, *trans*-3-hydroxy-*trans*-4-phenyl-L-proline, by extension of the phenol ring to exploit the hydrophobic pocket near phenyl alanine F405 or equivalent in ASCT1. Docking experiments of this prolinol derivative suggested that analogs of this configuration would be a valid approach to probing this hydrophobic pocket and still maintain the key interactions with Cys479 and Asp476 or equivalent in ASCT1.

In investigating the structure activity of the various EAAT's inhibitors it is revealed that extension of the benzyloxy group of TBOA to create a diphenyl amide analog (TFB-TBOA) [Shimamoto *et al.* 2004] produced an inhibitor with over a 250-fold improved potency. Another class of EAAT inhibitors in which this improvement in potency has also been observed is the various analogs of aryl-aspartamides where the substitution of a phenyl amide group for a fluorene or a biphenyl substituent dramatically

increased potency. Thus, when confronted whether or not to optimize activity of the benzyl-ether derivative CSE121 by addition of a methyl, fluorine, methoxy, or isopropyl groups to the benzyloxy ring we instead choose to pursue more conjugated substituent's such as a biphenyl, naphthyl or diphenylether analogs. Of the three tested, addition of a biphenyl to generate (2S, 3R, 4R)-3-hydroxy-4-O-methyl-p-biphenyl-proline (CSE131) was the most potent inhibitor at both ASCT transporters. To the best of our knowledge, this compound is also the most potent ASCT transport inhibitor yet to be reported.

The prolinol scaffold and biphenyl group of CSE131 has granted unparalleled inhibitory activity at the ASCT transporters. Although this is the first time a compound of this potency has been reported at system ASC, inhibitors of even greater potency are common at the EAATs. Already, the developing pharmacophore at the ASCT transporters very much resembles that of the EAATs. With respect to the key amino acid binding residues and the hydrophobic pocket, pharmacologic evaluation would suggest that the ASC/EAAT family of transporters is well conserved. It remains to be seen whether these prolinol inhibitors of ASC transport also act at the EAATs or for that matter any of the other neutral amino acid transporters such as system A or system N.

The computational docking of these prolinols into a homology model has allowed for a unique perspective to help explain trends and activity observed with the presented series of prolinols we have created. Notably, the homology model combined with the known activities of our prolinols has helped confirm the relevance of Cys479 in ASCT2 or Thr459 in ASCT1 as a crucial interaction for binding of ligand for either translocation

or as an inhibitor. Though, computational modeling does have its limitations, as observed by the insistence of the software to score CSE113 as high as it does even though this diastereomer is inactive. Our strategy was to use the conformationally restricted prolinol scaffold to support the homology model. Thus far both strategies have supported one another and this has proved useful in elucidating structure activity.

4. Conclusion.

We have described a novel series of prolinols that act as potent inhibitors of the neutral amino acid transport mediated by ASCT1 and ASCT2. Significant gains in potency were achieved by incorporation and extension of a benzylic ether substituent to a hydroxy-L-proline scaffold in a specific stereo and regio configuration. As a result of the conformationally constrained proline ring, the activity of this series of prolinols has important implications concerning the structure and function of the ligand binding domain at the ASCT / EAAT family of transporters. This work itself has also been beneficial in establishing a synthetic method for developing prolinol analogs and will likely facilitate the synthesis of next generation neutral amino acid transport inhibitors. Ultimately it is hoped that the identified inhibitors from this study will provide as useful pharmacologic tools to evaluate the physiological significance of the ASCT1 and ASCT2 transporters.

Prolinols as selective ASCT inhibitors

In searching for a practical scaffold to synthesize selective ASC transport inhibitors our group identified both *trans*-4-hydroxy-L-proline and *trans*-3-hydroxy-L-proline as high affinity selective substrates of ASC (1 and 2) mediated transport via radio-labeled uptake and substrate induced current electrophysiological techniques. Particularly, hydroxy-proline analogs (**Figure 12**) were an attractive target that was pursued because of the conformationally restricted ring which would allow us to effectively delineate transporter structure and activity relationship (Bridges, R. *et al.* 1990). Additionally, these analogs resemble the high affinity endogenous ASC transporter substrates L-serine, L-threonine (For characterization of ASC transport see, Arriza J., *et al.* 1993; Utsunomiya-Tate, N. *et al.* 1996; or review Broer, A. 1999) as well as the unnatural amino acid L-homoserine (data not yet published). In short, a series of diverse, substituted hydroxy-L-proline analogs with an array of different stereo- and regiochemistry was synthesized to be evaluated as inhibitors of amino acid transport, specifically ASC transport. From this series we identified a number of potent ASCT selective inhibitors that may be used to further elucidate the role and function of this transporter. This work has been beneficial in establishing a synthetic method for developing prolinol analogs and will likely facilitate the synthesis of next generation inhibitors of the system ASC transporters.

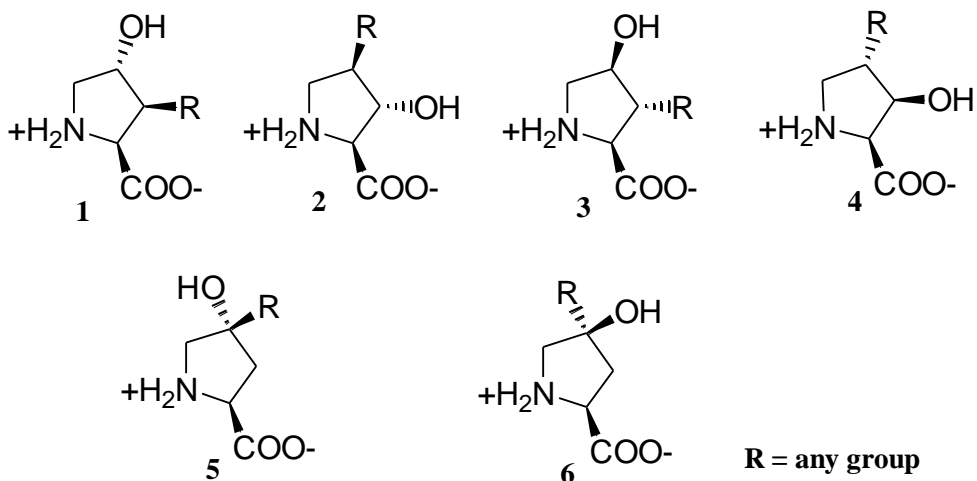


Figure 12: Substituted prolinol targets.

A key point to be resolved during the development and synthesis of these prolinols was the elucidation of their stereo and regiochemistry. The stereochemistry of the synthesized prolinol compounds was established from the fully protected (N-Cbz & benzyl ester) 3,4-epoxy-prolines from which they are derived. The two stereoisomers are easily separable which allowed their stereochemistry to be easily determined by two dimensional nuclear overhauser effect spectroscopy (NOESY) on a 500 MHz NMR (mixing time of 0.7 seconds). One NOE that was readily observable by these epoxides (*trans* and *cis*) was between the α carbon proton H-1 (refer to **Figure 13**) and H-4 of the methylene that is adjacent to the amine. When comparing the *trans*-epoxide to the *cis*-epoxide, the H-3 & H-2 proton display a strong NOE to the H-4 proton of the *cis*-3,4-epoxide compared to a very weak or nonexistent NOE correlation between the H-3 or H-2 protons and the H-4 proton of the *trans*-3,4-epoxide. This suggests that the stereo

chemistry of both isomers was properly assigned and is also consistent to that previously reported by (Robinson, J.K.; *et al.* 1998).

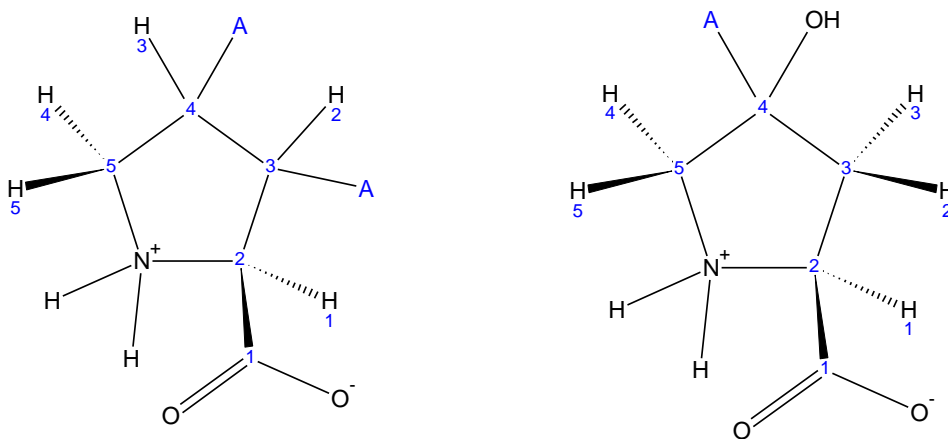


Figure 13: Proton and carbon numbering scheme used in $^1\text{H-NMR}$ & $^{13}\text{C-NMR}$ assignments. “A” represents any atom or group.

The regiochemistry of the final product hydroxy-proline derivatives was determined by 2D correlation spectroscopy or COSY. **Figure 14** illustrates an example of how the proton assignments and regiochemistry were made from a COSY experiment of prolinol product CSE122. The numerical labels such as 0.09 (2,2) indicate intensity (first number) and protons correlated in parentheses. The methylene protons H-4 & H-5 are easily spotted at ppm 3.4-3.56 by their strong J_2 coupling and chemical shift. It is clear that the methylene protons are coupled to a proton at ppm 4.1.

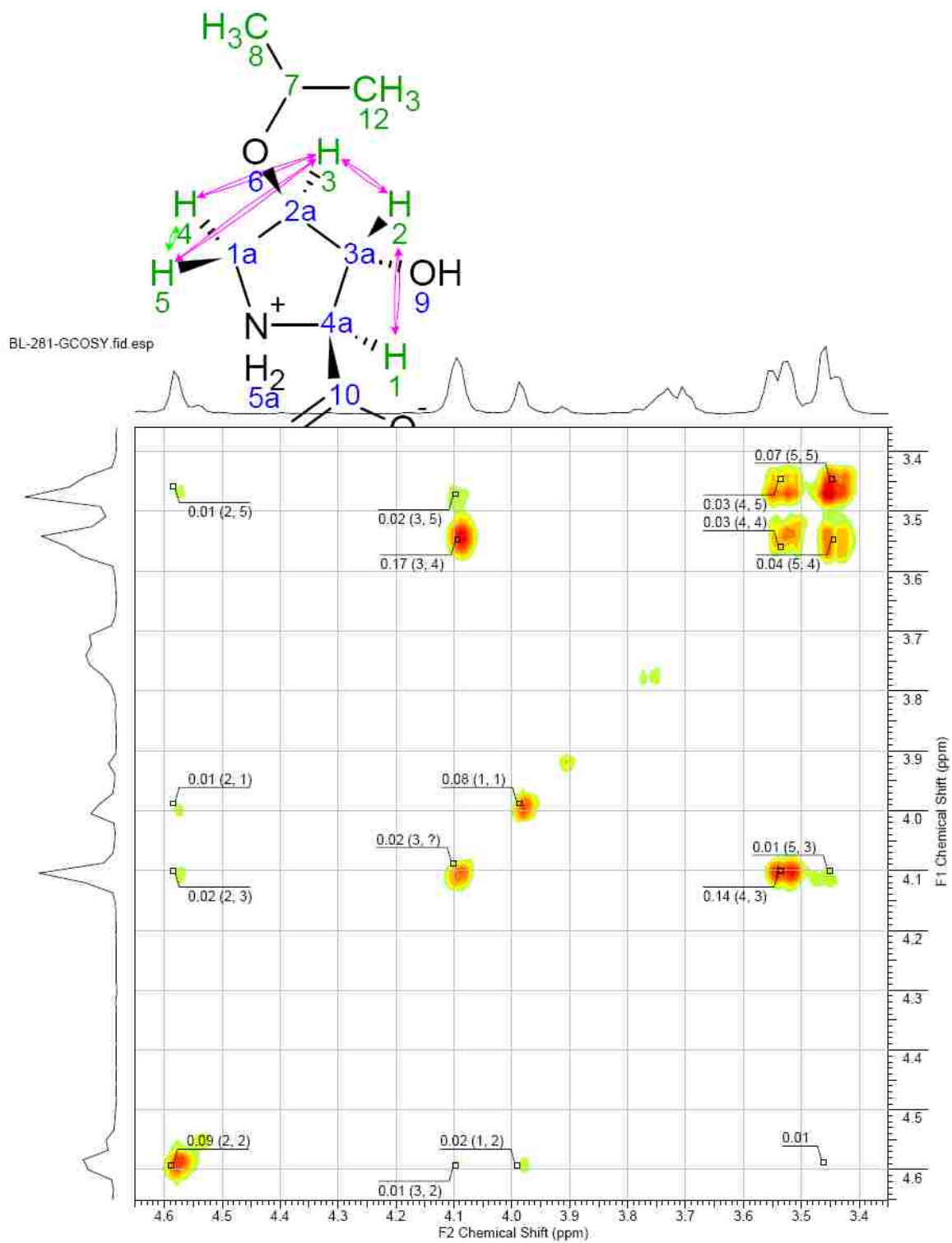


Figure 14: gCOSY of CSE 122, shows correlation intensity in 0.0x and proton # in (x,x).

Importantly, one of these methylene protons is more strongly coupled to this proton, a result of a small dihedral angle between these two protons suggesting they reside on the same plane of the proline ring. The alpha proton H-1, seen at ppm 3.98, is weakly coupled to only one other proton at ppm 4.58. This proton has small couplings with two other protons at ppm 3.42 and 4.1 (a methylene proton). The weak J3 couplings (opposite plane of the proline ring) and its chemical shift suggest this proton is H-2 and therefore the proton at ppm 4.1 is H-3. The methylene protons were then assigned according to coupling intensity with the H-3 proton, with H-4 at ppm 3.56 and H-5 at ppm 3.42. This assignment is also consistent with the small J4 coupling observed between H-2 and H-5.

Experimental section:

Proton ^1H and carbon ^{13}C nuclear magnetic resonance (NMR) spectra were obtained from Varian 500 MHz spectrometers as specified. Both ^1H and ^{13}C spectra are reported in parts per million (ppm or δ) downfield from tetramethylsilane as an internal standard. All chemical shifts reported were referenced to residual protonated D_2O or DMSO solvent peaks at 4.75 or 2.5 ppm, respectively, for ^1H proton spectra and 39.5 ppm for ^{13}C carbon spectra unless specified otherwise. Multiplicity is reported as doublets (d), doublet of doublets (dd) etc. where Σ represents the sum of all couplings, b = broad. N.O.e. experiments were performed on a Varian 500 MHz using 2D NOESY parameters with

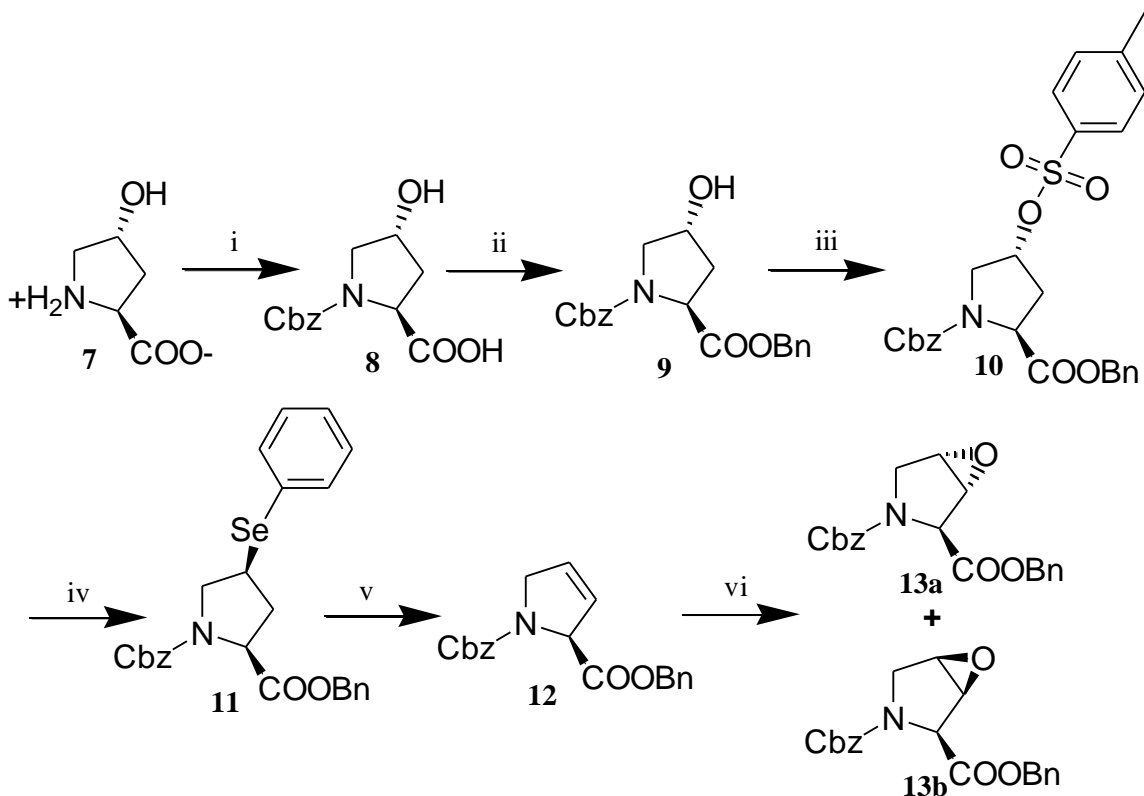
zero-quantum suppression and mixing times of 0.7 s to determine the stereochemistry of diastereomers. Gradient correlation spectroscopy (gCOSY) to determine regiochemistry was also performed using a Varian 500 MHz. Optical rotations of final compounds dissolved in methanol or DMSO, as specified, with concentrations given in g/100 mL were determined via a Perkin-Elmer Model 241 polarimeter in a 1.0 dm glass cell sodium D line. High resolution mass spectra (HRMS) were determined on a Waters LC-MS spectrometer using caffeine or trimethoprim as a mass standard at m/z 195.0882 or 291.1457 respectively for HRMS. All reagents were purchased from Acros Organics and used without further purification. Solvents as well as 40-60 μ M silica gel for flash chromatography were obtained from EMD chemicals (Gibbstown, NJ). Intermediates were isolated by silica gel used without further purification, unless specified otherwise. A mobile phase consisting of 95% CH_2Cl_2 / 4% MeOH / 1% AcOH or hexanes / ethyl acetate was used for TLC and flash chromatography, as specified. Ion exchange chromatography was carried out using Bio-rad AG[®] 50W cation exchange resin which was pre-equilibrated in 1M HCl followed by deionized water. Semi-prep reverse phase HPLC was carried out using a C18, 250 mm x 21.2 mm, 10 μ , Chromegabond WR 120A column from ES Industries using acetonitrile / water 0.5% ammonium acetate.

Synthesis section 1

General procedure for synthesis of *cis*-4-hydroxy-L-proline:

Cis-4-Hydroxy-L-proline was synthesized from *trans*-4-hydroxy-L-proline as previously reported [Papaloannou; *et al.* 1990]. Explained briefly, *trans*-4-hydroxy-L-proline was protected using Boc anhydride under standard conditions and workup, 1:1 MeOH / triethylamine and 1.2 equivalents of Boc anhydride reflux overnight. The isolated N-tBoc-*trans*-4-hydroxy-L-proline was then converted to the N-tBoc-*cis*-proline lactone by standard Mitsunobu esterification by adding PPH₃, diethyl azodicarboxylate (DEAD) in THF at 0°C and then stirring overnight at rt. Standard workup including dilution with Et₂O and multiple washes with water. The N-tBoc-proline lactone can then be converted to *cis*-4-hydroxy-proline in a one pot reaction in 2.0 M HCl, (2.2 eq) which is then diluted with water and lyophilized to concentrate leaving *cis*-4-hydroxy-L-proline. Analysis of product by ¹H and ¹³C NMR is in agreement with NMR spectra reported in literature.

Synthesis section 2



Scheme 1: Synthesis of N-Cbz-*trans*- and *cis*-3,4-epoxy-proline-benzyl ester **13a** & **13b**. (i) benzylchloroformate, H₂O, NaOH, rt; (ii) benzylbromide, Na₂CO₃, NaI, rt; (iii) p-toluenesulfonyl-Cl, pyridine, 0°C; (iv) tBuOH, phenylselenide, reflux; (v) CH₂Cl₂, H₂O₂, 0°C-RT; (vi) mCPBA, CH₂Cl₂, reflux.

General procedure for synthesis of N-Cbz-(*cis*- or *trans*)-3,4-epoxy-L-proline benzyl ester:

To arrive at prolinol targets **1-4**, *trans*-4-hydroxy-L-proline was converted to the protected *trans*- and *cis*-3,4-epoxides **13a** & **13b** as outlined in **Scheme 1** with only slight modifications in conditions to that previously reported [Robinson; *et al.* 1998]. Briefly,

the amine of *trans*-4-hydroxy-L-proline was protected using benzylchloroformate in water at a pH ~10. The acid functionality of N-Cbz-*trans*-4-hydroxy-L-proline was then protected using benzylbromide, Na₂CO₃, NaI, in DMF at room temperature (~22°C) and isolated by flash chromatography. Compound **9** (Scheme 1) was then converted to the 4-tosylate using p-toluenesulphonyl chloride in pyridine at 0°C for 1 week. It was important to allow this reaction to proceed under cool conditions as to avoid possible racemization of the chiral alpha center. The resulting N-Cbz-4-tosyl-L-proline benzyl ester was then separated by silica gel. The tosyl group was then displaced via nucleophilic substitution with reduced phenyl selenide, prepared by reduction of diphenyldiselenide using NaBH₄ (sodium borohydride) in tert-butanol at reflux. The isolated phenylseleno proline was then oxidized in an elimination reaction using H₂O₂ in CH₂Cl₂ at 0°C to produce the fully protected 3,4-dehydro-L-proline **12**. It was extremely important to perform this reaction in cold, dilute conditions to avoid overheating and a possible H₂O₂ driven explosion. The protected 3,4-dehydro-L-proline **12**, once isolated, was then treated with mCPBA (meta-chloro-peroxybenzoic acid) in CH₂Cl₂ at reflux to give the protected *trans*- and *cis*-3,4-epoxy-prolines at ratios of 6:4 respectively. The *trans*- and *cis*-epoxides were efficiently isolated by silica gel with overall modest yield of 53% for the entire synthetic scheme. The epoxide intermediates **13a** or **13b** were then used directly in an acid catalyzed ring opening addition step (**Scheme 3**) or converted to the free acid prior to an addition under basic conditions (**Scheme 4**).

N-Cbz-4-hydroxyproline 8: BRL: 247

trans-4-Hydroxyproline (27.5 g, 209.7 mmol) **7** was dissolved into 200mL of 50% MeOH in water. This was then chilled on ice bath to 0°C. To this mixture was added 85.9 mL of benzyl chloroformate (0.252 mmol; 1.2 eq; 50% vol. in toluene) dropwise. Pellets of NaOH were added to maintain the pH at ~9-10 (monitored by litmus paper). The mixture was then allowed to warm to rt (22°C). The mixture was allowed to stir over night at rt and the pH closely monitored and maintained at pH = 10 by addition of NaOH pellets. The mixture was then diluted by addition of 200 mL water and then extracted with 3 x 200 mL toluene (to remove remaining benzyl chloroformate). The aqueous layer was then salted with NaCl until saturated and the pH was adjusted to ~2 by addition of HCl conc. This was then extracted with 4 x 200 mL of ethyl acetate. The ethyl acetate washes were then combined and concentrated via rotovap, leaving an oil residue. Dichloromethane (50 mL) was added 4 times to remaining oil and then removed by vacuum. Hexanes (50 mL) was then added to the oil and again removed by vacuum, leaving a sticky foam N-Cbz-4-hydroxyproline crude (quantitative yield) which was then used w/o any further purification. This residue can also be recrystallized in 10:1, hexanes:CH₂Cl₂. ¹H and ¹³C NMR spectra were in agreement with ¹H and ¹³C NMR spectra previously reported [Robinson; *et al.* 1998].

N-Cbz-4-hydroxyproline benzyl ester 9: BRL: 151

N-Cbz-4-hydroxyproline (40.00 g, 150.8 mmol) **8** was dissolved into 110 mL DMF. To this mixture was added 45.85 g of K_2CO_3 (2.2 eq; 331.7 mmol) and 2.30 g of NaI (0.1 eq). The reaction flask was purged with argon and 55.4 mL of benzylbromide (3 eq; 452 mmol) was added dropwise. This mixture was then stirred over night at rt. The reaction was then diluted with 300 mL ethyl acetate and washed with water (8 x 200 mL) to remove DMF, followed by washing with 100 mL brine. The organic layer was dried over Na_2SO_4 and concentrated to a yellow oil. The oil was then washed several times with 100 mL hexanes to remove any remaining benzyl bromide and then separated by silica gel in hexanes : ethyl acetate, 3:2, isolating N-Cbz-4-hydroxyproline benzyl ester at $R_f = 0.25$ in nearly quantitative yield. 1H and ^{13}C NMR spectra were in agreement with 1H and ^{13}C NMR spectra previously reported [Robinson; *et al.* 1998].

N-Cbz-4-p-toluenesulphonyl-ether-proline-benzyl ester 10: BRL: 205

N-Cbz-4-hydroxyproline benzyl ester (21.77 g, 61.3 mmol) **9** was dissolved into 150 mL cold pyridine $0^\circ C$. Immediately, 12.976 g of p-toluenesulfonyl chloride (1.1 eq.; 67.4 mmol) was added. The flask containing this mixture was then purged with argon and placed into a refrigerator at $\sim 0^\circ C$ for one full week with occasional vortex. After one week it was observed that a significant amount of pyridine-HCl had formed and all the starting material appeared to have been consumed (determined by TLC). The mixture was then taken up into 100 mL Et_2O and 50 mL ethyl acetate and washed 2 x 100 mL cold 5% HCl and then 3 x 200 mL water. The organic layers were combined and dried

over Na₂SO₄, filtered and concentrated to an oil. The product N-Cbz-4-p-toluenesulphonyl-ether-proline-benzyl ester **10** was isolated by silica gel in hexanes / ethyl acetate, 7:3; R_f = 0.25 to recover 28.05 g, (90% yield). ¹H and ¹³C NMR spectra were in agreement with ¹H and ¹³C NMR spectra previously reported [Robinson; *et al.* 1998].

N-Cbz-4-phenylseleno-L-proline-benzyl ester 11: BRL: 211

Diphenyldiselenide (9.504 g, 0.6 eq.; 30.2 mmol) was dissolved into 60 mL of tBuOH and purged of air by vacuum and replaced with argon. The solution was brought to a reflux where of NaBH₄ (2.293 g, 1.2 eq, 60.3 mmol) was added slowly over 15 min. This mixture was refluxed for 30 min until the mixture had turned completely white. To this was added N-Cbz-4-p-toluenesulphonyl-ether-proline-benzyl ester **10** (25.6 g, 50.2 mmol) in 40mL tBuOH. The reflux was continued under argon for ~3 h then allowed to cool to rt. The mixture was then diluted with 200 mL ethyl acetate and washed 3 x 250 mL water followed by 100 mL brine then treated with MgSO₄ to dry, filtered and concentrated to a crude oil. The product N-Cbz-4-phenylseleno-L-proline-benzyl ester **11** was isolated by silica gel 3:1 hexanes : ethyl acetate at R_f = 0.3, recovering 22.21 g, (89% yield). ¹H and ¹³C NMR spectra were in agreement with ¹H and ¹³C NMR spectra previously reported [Robinson; *et al.* 1998].

N-Cbz-3,4-dehydro-L-proline-benzyl ester 12: BRL: 212

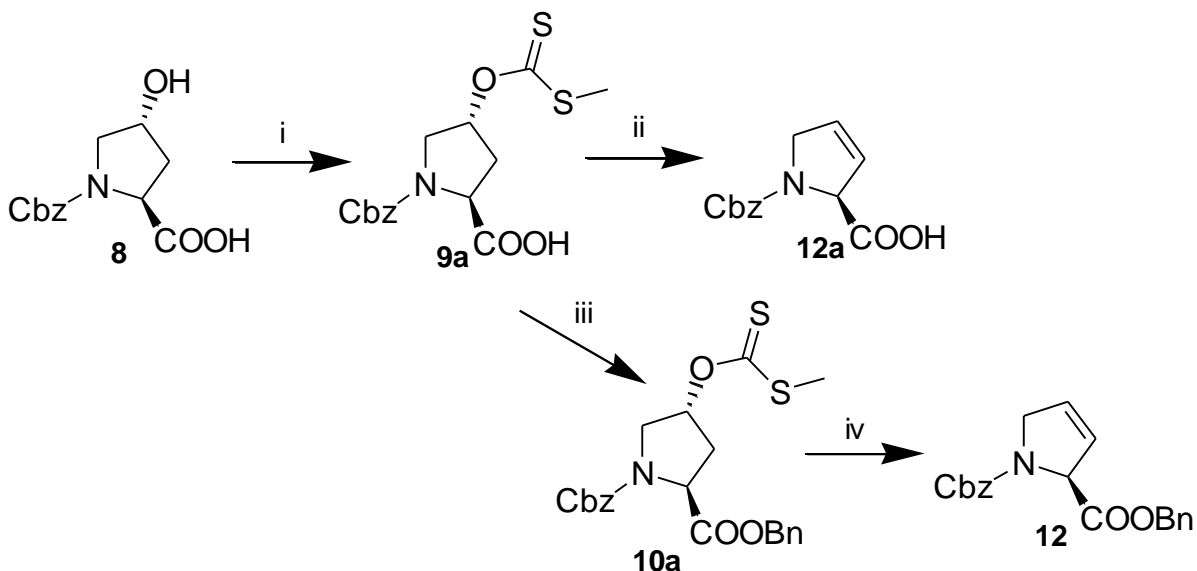
N-Cbz-4-phenylseleno-L-proline-benzyl ester **11** (22.11 g, 44.7 mmol) was dissolved in 80 mL CH₂Cl₂ (warning! explosive conditions: needs to be performed in more dilute conditions than in this example or ~200 mL per 10 g of starting material). The solution was chilled on ice bath over argon and 4.9 mL pyridine (1.34 eq.; 60 mmol) was added followed by addition of 11.50 mL 30% H₂O₂ (2.5 eq.; 112.0 mmol) drop wise. The solution was gradually allowed to return to room temp over the course of one hour where it was stirred for 2.5 h. The solution, now brown in color, was diluted with 100 mL CH₂Cl₂ and washed with 100 mL of 5% NaHSO₄, 2 x 50 mL NaHCO₃, and 3 x 150 mL water. The organic layer was dried over Na₂SO₄ and filtered. A total of 12.02 g of N-Cbz-3,4-dehydro-L-proline-benzyl ester **12** was isolated by silica gel in mobile phase of 4:1 hexanes / ethyl acetate; R_f = 0.15; (80% yield). ¹H and ¹³C NMR spectra were in agreement with ¹H and ¹³C NMR spectra previously reported [Robinson; *et al.* 1998].

N-Cbz-*trans*-3,4-epoxy-L-proline-benzyl ester 13a and N-Cbz-*cis*-3,4-epoxy-L-proline-benzyl ester 13b: BRL: 287

N-Cbz-3,4-dehydro-L-proline-benzyl ester (9.80 g, 29.0 mmol) **12** was dissolved into 12 mL CH₂Cl₂. To this was added mCPBA (14.3 g, 70% weight; 58.1 mmol; 2 eq.) and 2,8-di-*tert*-butyl-4-methylphenol (30 mg, radical inhibitor). The solution was heated to reflux and allowed to stir overnight under argon balloon. An additional 1 eq. of mCPBA

(7.15 g) was added and the solution was allowed to reflux again overnight. The flask was then placed on an ice bath where a white precipitate formed and was subsequently filtered using cold dichloromethane to wash. The CH₂Cl₂ was removed by rotovap leaving a white solid residue. The residue was taken up into 150 mL Et₂O and washed 8 times with 100 mL (aq) NaHCO₃, 2 x 100 mL water, and 100 mL brine then dried over Na₂SO₄ and filtered. The remaining oil was then separated by silica gel in 4:1 hexanes / ethyl acetate. The *trans* isomer 5.228 g, N-Cbz-3,4-*trans*-epoxy-L-proline-benzyl ester **13a**, was isolated at R_f = 0.2 and the *cis* isomer 4.100 g, N-Cbz-3,4-*cis*-epoxy-L-proline-benzyl ester **13b** being isolated at R_f = 0.1, a total yield of 91% and ratio of 5:4 *trans* / *cis*. ¹H and ¹³C NMR spectra for both diastereomers were in agreement with ¹H and ¹³C NMR spectra previously reported [Robinson; *et al.* 1998].

Synthesis section 3



Scheme 2: Synthesis of 3,4-dehydroprolines. (i) NaH, THF, CS₂, iodomethane, 22°C; (ii) H₂O, NaHCO₃, microwave 100°C; (iii) benzylbromide, Na₂CO₃, NaI, rt; (iv). H₂O, Na₂CO₃, microwave 100°C.

Procedure for alternative synthesis of N-Cbz-3,4-dehydro-L-proline-benzyl ester **12** or N-Cbz-3,4-dehydro-L-proline **12a**

In searching for a synthetic route to produce 3,4-dehydro-L-prolines with fewer synthetic steps than through tosyl and selenide intermediates (scheme 1), we designed an alternative route by using a xanthate intermediate **9a** or **10a**. We reasoned that the free acid 3,4-dehydro-proline **12a** or benzyl ester protected 3,4-dehydro-proline **12** could be generated via microwave elimination of a methyl xanthate **9a** or **10a** as seen in Scheme 2. Briefly, N-Cbz-*trans*-4-hydroxy-L-proline **8** was used in an esterification with CS₂ and iodomethane using NaH as a base in THF to produce N-Cbz-*trans*-4-methylxanthate-L-

proline **9a**. From this the benzyl-ester derivative **10a** (N-Cbz-*trans*-4-methylxanthate-L-proline benzyl ester) were synthesized under standard conditions as shown in Scheme 1 (ii). Both methyl xanthate conjugated prolines **9a** and **10a** were successfully eliminated under open container pyrolysis like conditions using microwave radiation, sodium carbonate as a base, and water as a semi-solvent to produce 3,4-dehydroprolines **12a** and **12**.

N-Cbz-*trans*-4-methylxanthate-L-proline 9a: BRL: 131

To 3.635 g (13.7 mmol) of N-Cbz-*trans*-4-hydroxy-L-proline **8** was added 35 mL of dry THF and slow addition of 1.73 g of NaH (95%; 5 eq.; 68.5 mmol). The solution was then purged with argon and allowed to stir for 10 min. To this was added 4.14 mL of CS₂ (68.5 mmol; 5 eq.) and allowed to stir for 2 h at rt, forming the xanthate salt. To the flask was then added 2.87 mL of iodomethane (48.0 mmol; 3.5 eq) and allowed to stir overnight at rt and under argon balloon. The reaction mixture was then chilled on ice bath where ~10 mL of glacial acetic acid was added to quench the excess NaH (heavy white precipitate forms). The quenched reaction mixture was then diluted with 100 mL of Et₂O, filtered using excess ether, and then concentrated by rotovap, leaving a yellow / brown oil. The final product, 4.19 g, N-Cbz-*trans*-4-methylxanthate-L-proline **9a** was isolated by silica gel at R_f = 0.15 in 97% CH₂Cl₂, 2% MeOH 1% AcOH, 70% yield as a crude mixture which was used in the next step without further purification.

N-Cbz-*trans*-4-methylxanthate-L-proline benzyl ester 10a: BRL: 133

To 3.40 g (9.57 mmol) of N-Cbz-*trans*-4-methylxanthate-L-proline **9a** was added 30 mL DMF, 2.64 g (19.1 mmol; 2 eq.) of K₂CO₃, and 143 mg of NaI (0.957 mmol; 0.1 eq.). The reaction flask was purged with argon, and 3.58 mL of benzyl bromide (98 %; 29.3 mmol; 3 eq.). The mixture was allowed to stir at rt for 24 h under argon balloon. The solution was taken up into 100 mL ethyl acetate and then washed with H₂O (4 x 300 mL). The organic layer was separated and dried with MgSO₄, filtered and concentrated to a yellow oil. The final product N-Cbz-*trans*-4-methylxanthate-L-proline benzyl ester **10a** was isolated by silica gel in 4: 1 hexanes / ethyl acetate, R_f = 0.25, with a quantitative yield.

¹H-NMR (400 MHz, CDCl₃) δ 7.40-7.20 (m, 10H), 5.95 (d, J = 2.2 Hz, 1H), 5.25-5.16 (m, 1H), 5.17 (s, 1H), 5.07 (s, 1H), 5.00 (s, 1H), 4.62-4.52 (ddd, J = 44.0, 28.6, 8.1 Hz, 1H), 3.99 (d, J = 12.4 Hz, 1H), 3.88 (s, 1H), 2.67-2.59 (m, J = 8.1, 2.2 Hz, 1H), 2.53 (s, 3H), 2.36 (m, J = 8.1, 2.1 Hz, 1H).

N-Cbz-3,4-dehydro-L-proline 12a: BRL:177

A pressure flask containing a mixture of 0.240 g of N-Cbz-*trans*-4-methylxanthate-L-proline (0.675 mmol) **9a**, 1 mL ethanol, 10 mL water, and 42 mg Na₂CO₃ (anhydrous; 0.5 eq) was placed into a microwave on medium (100 watt noncontinuous radiation; retail

purchased Sunbeam microwave) for ~3-4 min. The contents were allowed to cool to rt (keep in hood; xanthate elimination creates a very undesirable smell). The reaction mixture was diluted with 20 mL water and the pH was adjusted to ~2-3 by addition of H₃PO₄. The aqueous mixture was salted with NaCl until saturated, then extracted with 3 x 50 mL ethyl acetate, dried with Na₂SO₄, and concentrated to a crude orange colored oil. The product N-Cbz-3,4-dehydro-L-proline **12a** was isolated by silica gel (96% CH₂Cl₂, 3% MeOH, 1% AcOH, R_f = 0.25) for 0.120 g of total recovered product, a 72% yield.

¹H-NMR (400 MHz, CDCl₃) δ 9.91 (b, 1H [COOH]), 7.37-7.27 (m, 5H), 5.98-5.93 (ddd, J = 21.3_Σ, 14.9, 6.11, 2.0 Hz 1H), 5.82-5.75 (ddd, J = 35.7_Σ, 29.6, 6.1, 2.2 Hz, 1H), 5.25-5.13 (m, J = 1.7 Hz, 2H), 5.06 (dd, J = 4.0_Σ, 2.2 Hz, 1H), 4.32-4.27 (m, J = 2.2, 2.0, 1.7 Hz, 2H).

N-Cbz-3,4-dehydro-L-proline benzyl ester 12: BRL: 195

A pressure flask containing a mixture of 0.551 g (1.28 mmol) of N-Cbz-*trans*-4-methylxanthate-L-proline benzyl ester **10a**, 1 mL ethanol, 10 mL water, and 68 mg Na₂CO₃ (anhydrous; 0.5 eq; 0.64 mmol) was placed into a microwave on medium low (100 watt noncontinuous radiation, retail purchased Sunbeam microwave) for ~7 min. The contents were allowed to cool to rt (keep in hood). The reaction mixture was diluted with 20 mL water and then extracted with 3 x 50 mL Et₂O, washed 2 x 50 mL water, dried over Na₂SO₄, and concentrated to a crude orange oil. The product N-Cbz-3,4-dehydro-L-

proline benzyl ester **12** was isolated by a silica gel (70% hexanes, 30% ethyl acetate, $R_f = 0.25$) for 0.362 g of total recovered product, an 84% yield.

$^1\text{H-NMR}$ (400 MHz, CDCl_3) δ 7.40-7.25 (m, 10H), 6.01-5.94 (ddd, $J = 19.0_\Sigma$, 5.9, 1.5 Hz, 1H), 5.80-5.74 (ddd, $J = 16.8_\Sigma$, 5.9, 2.2 Hz, 1H), 5.26-5.04 (m, 5H), 4.40-4.26 (m, $J = 5.9_\Sigma$, 2.2, 1.5 Hz, 2H).

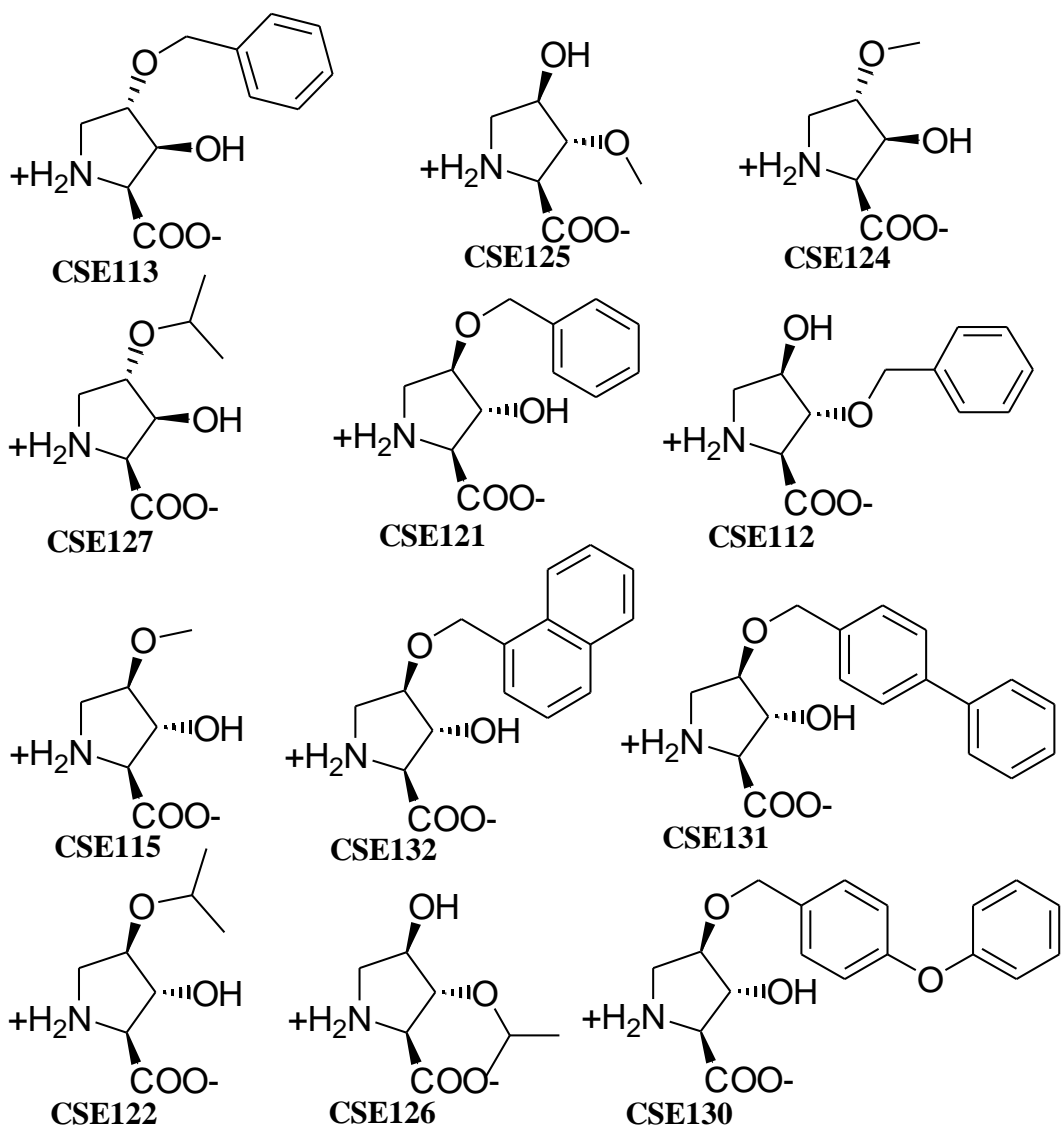
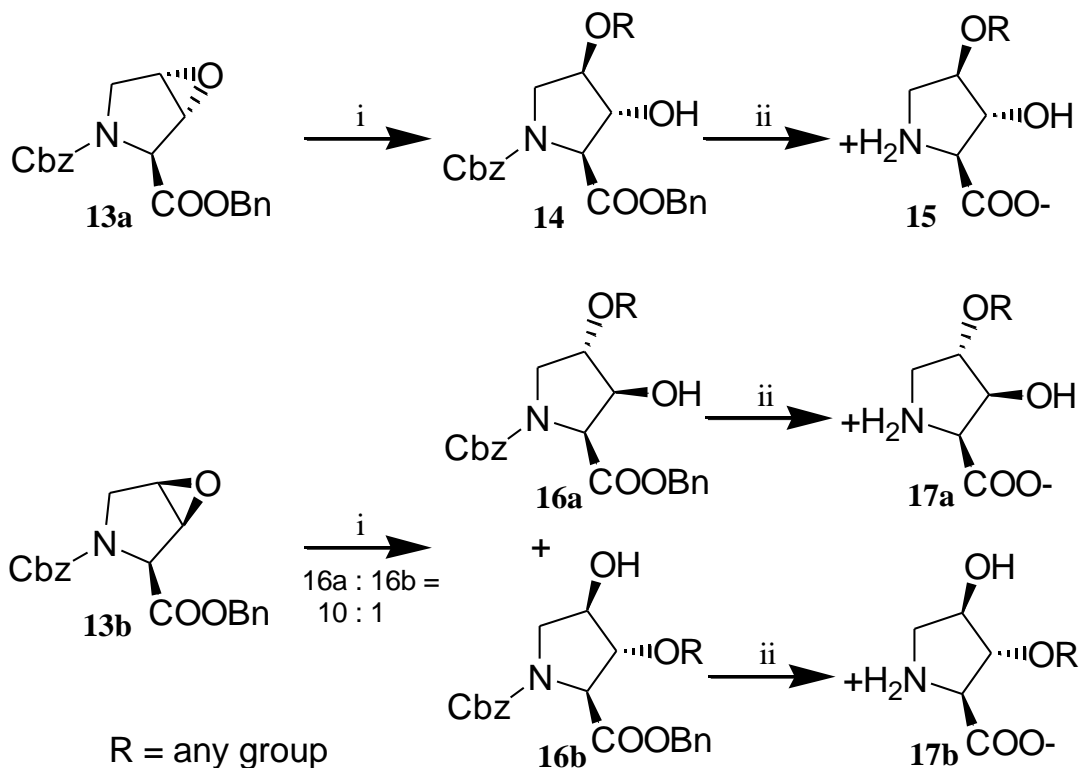


Figure 15: Synthesized ether substituted prolinols.

Synthesis section 4



Scheme 3: Synthesis of ether substituted prolinols. (i) $\text{BF}_3 \cdot \text{Et}_2\text{O}$, CH_2Cl_2 , desired alcohol, 22°C ; (ii) 10% Pd/C (.10% weight. eq.), H_2 , MeOH, H_2O , NH_4OAc .

Procedure for synthesis of ether substituted prolinols:

A series of ether substituted prolinols (**Figure 15**) were synthesized to act as selective inhibitors of the ASC transporters. This was accomplished by a $\text{BF}_3 \cdot \text{Et}_2\text{O}$ catalyzed nucleophilic ring opening of the epoxide **13a** or **13b** by an alcohol and subsequent deprotection via a 10% Pd/C catalyzed hydrogenation to produce *trans*-hydroxy derivative **15** or *cis*-hydroxy derivatives **17a** & **17b** (**Scheme 3**). Under optimized conditions, $\text{BF}_3 \cdot \text{Et}_2\text{O}$ as a catalyst provided far superior product yields (quantitative) as

opposed to using toluene sulfonic acid which produced multiple undesired products, including nucleophilic addition of the tosyl (tosic acid) group itself as a major product. It was also observed that ring opening of *trans*-epoxide **13a** under these conditions produced exclusively one regioisomer, the N-Cbz-*trans*-3-hydroxy-*cis*-4-ether-L-proline benzyl ester **14** (Figure 16). Whereas the ring opening of the *cis*-epoxide **13b** produced both regioisomers **16a** & **16b** in ratios, 10:1, that strongly favored the 3- positioned alcohol **16a**, consistent with azide or HCl ring opening of these epoxides (Herdeis; *et al.* 2007; Robinson; *et al.* 1998). Separation of these two regioisomers was carried out by reverse phase HPLC after the addition step following hydrolysis of the benzyl ester with KOH or just after hydrogenation depending upon the ether R group present. Of importance, however, but not fully explored, the *cis*-3-ether-*trans*-4-hydroxy-proline regioisomer of **15** can be obtained with reasonable yield if the free acid *trans*-3,4-epoxy-proline derivative **13c** (shown in Scheme 4) is used as the starting reagent instead of fully protected *trans*-3,4-epoxy-proline **13a** in the BF₃•Et₂O catalyzed addition step under similar conditions and following separation by HPLC. This was observed when using MeOH or isopropanol as the nucleophilic agent. The resulting ether substituted prolinol **14**, **16a** or **16b** could then be deprotected under standard palladium (Pd / carbon) catalyzed hydrogenation to afford the final products **15**, **17a**, or **17b** in good yield. Surprisingly, hydrogenation under these conditions was selective in removal of the benzyl carbamate and the benzyl ester while leaving the benzyl ether group intact. For

additional precaution, ammonium acetate (NH₄OAc) was added to the reaction mixture as an inhibitor of debenzylation during the hydrogenation step [Sajiki 1995].

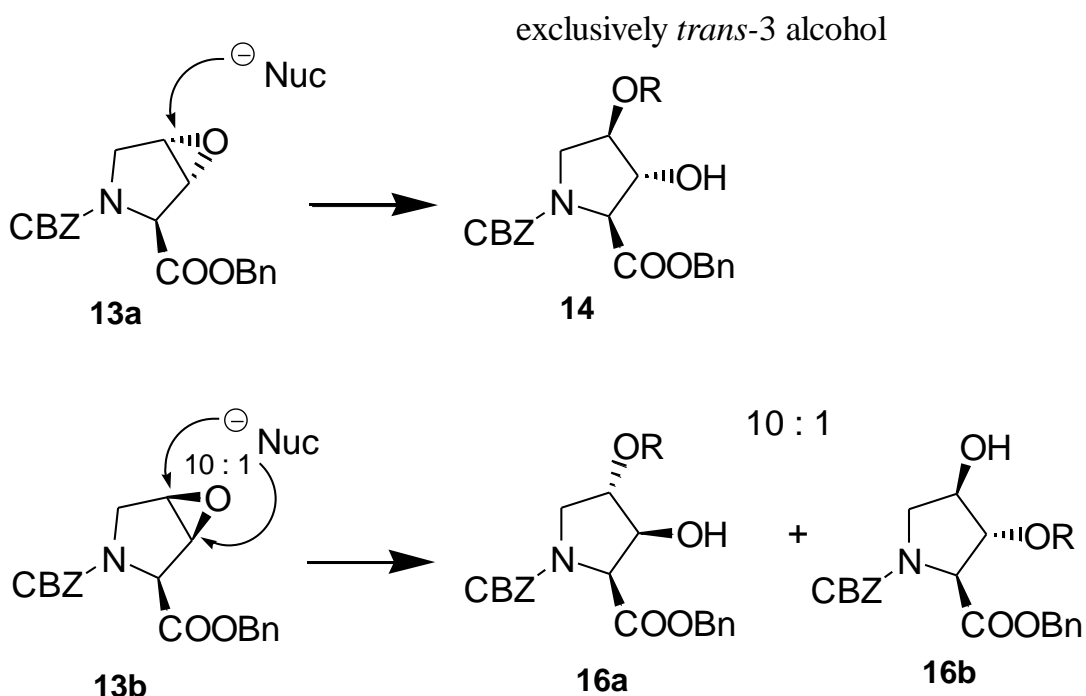


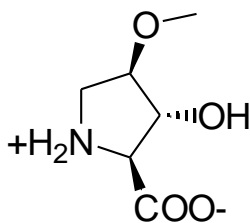
Figure 16: Regioselective addition and ring opening of protected *trans*- and *cis*-3,4-epoxy-L-prolines.

N-Cbz-*trans*-3-hydroxy-*cis*-4-methoxy-L-proline benzyl ester: BRL: 294

To 0.514 g (1.45 mmol) of N-Cbz-*trans*-3,4-epoxy-L-proline benzyl ester **13a** was added 5 mL of dry (MgSO₄ treated) CH₂Cl₂ and 2.0 mL (~34 eq.; 50 mmol) absolute MeOH.

The flask was capped, purged with argon and chilled on an ice bath with argon balloon. Once cooled, 1.15 mL (48%; 3.0 eq.; 4.36 mmol) of $\text{BF}_3 \cdot \text{Et}_2\text{O}$ was added to the mixture. The mixture was allowed to return to rt and stir over night. The reaction mixture was quenched by the addition of 20 mL saturated NaHCO_3 solution which was allowed to stir for ~30 min. The mixture was then diluted with 100 mL CH_2Cl_2 , washed with 3 x 100 mL water, 50 mL brine, dried over Na_2SO_4 and concentrated by rotovap to a foam. The final product N-Cbz-*trans*-3-hydroxy-*cis*-4-methoxy-L-proline benzyl ester, 467 mg, and unreacted epoxide starting material, 115 mg, were isolated by silica gel (75% hexanes, 25% ethyl acetate, R_f product = 0.1 ; R_f epoxide = 0.3) for a total yield of 83% product and complete recovery in molecular equivalents of unreacted starting material. The material was used in the next step without further purification.

$^1\text{H-NMR}$ (500 MHz, CDCl_3) (2 conformational isomers) δ 7.33-7.25 (m, 10H), 5.27-5.01 (m, 4H), 4.50 and 4.40 (s, 1H), 3.85-3.75 (m, $J = 4.89, 4.4$ Hz, 2H), 3.70 (d, $J = 4.9$ Hz, 1H), 3.57 (m, 1H), 3.15 and 3.12 (s, 3H).



CSE115
 Chemical Formula: C₆H₁₁NO₄
 Molecular Weight: 161.16

***trans*-3-hydroxy-*cis*-4-methoxy-L-proline:** BRL: 298 / CSE115

To 0.417 g (1.08 mmol) of Cbz-3-*trans*-hydroxy-4-*cis*-methoxy-L-proline benzyl ester was added 4 mL methanol which was then transferred to a pressure flask containing 42 mg of 10% Pd/carbon (0.1 eq. weight), 1 mL water and 42 mg (~0.5 eq.) NH₄OAc. The pressure flask was connected to a Parr shaker, the air was removed by vacuum and replaced with 40 psi H₂ (g). The assembly was allowed to shake for 3 h. The pressure flask was vented and the solution diluted with 10 mL water and then filtered through CM-cellulose (carboxy-methyl-cellulose), using excess water for consecutive washes. The filtrate was then frozen and placed onto a lyophilizer until dry. The remaining residue was washed 3 x 10 mL ethyl acetate / CH₂Cl₂ (1:1), and dried leaving 0.172 g of a white solid, *trans*-3-hydroxy-*cis*-4-methoxy-L-proline with a yield of 99%.

¹H-NMR (500 MHz, D₂O 4.75) δ 4.65 (s, 1H, H-2), 4.02 (s, 1H, H-1), 3.91 (s, 1H, H-3), 3.53 (s, 2H, H-4 and 5), 3.25 (s, 3H). ¹³C-NMR (500 MHz, D₂O) ppm 170.7, 82.8, 74.8, 67.4, 56.3, 48.9. HRMS *m/e* calcd. For C₆H₁₂NO₄ = 162.0749, found 162.0766. [α]_{Na}²² = -15° (c = 0.14, EtOH).

N-Cbz-*cis*-3-hydroxy-*trans*-4-methoxy-L-proline benzyl ester and N-Cbz-*trans*-3-methoxy-*cis*-4-hydroxy-L-proline benzyl ester: BRL: 295

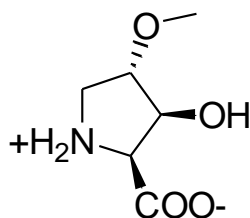
To 0.280 g (0.792 mmol) of N-Cbz-*cis*-3,4-epoxy-L-proline benzyl ester **13b** was added 3 mL (dry MgSO₄ treated) CH₂Cl₂ and 1 mL MeOH (~30 eq.; 25 mmol). The flask was purged with argon and cooled on ice bath for 10 min. Once cooled, 0.625 mL of BF₃•Et₂O (48%; 3.0 eq.; 2.38 mmol) was added dropwise and the solution was allowed to return to rt. After stirring overnight the reaction was quenched by the addition of 20 mL saturated solution of NaCO₃. This was then further diluted with 100 mL CH₂Cl₂ and washed 3 x 100 mL water and 1 x 100 mL brine, dried with Na₂SO₄ and filtered. The two regioisomer products N-Cbz-*cis*-3-hydroxy-*trans*-4-methoxy-L-proline benzyl ester and N-Cbz-*trans*-3-methoxy-*cis*-4-hydroxy-L-proline benzyl ester, 0.288 g, were isolated together by silica gel (70 % hexanes, 30% ethyl acetate, R_f = 0.15) a 94% yield. The material was used in the next step without further purification.

N-CBZ-*cis*-3-hydroxy-4-*trans*-methoxy-L-proline: BRL: 278

To 0.410 g (1.06 mmol) of N-Cbz-*cis*-3-hydroxy-*trans*-4-methoxy-L-proline benzyl ester and N-Cbz-*trans*-3-methoxy-*cis*-4-hydroxy-L-proline benzyl ester was added 10 mL THF, 1 mL water and 72 mg (1.2 eq.; 1.28 mmol) KOH. The mixture was allowed to stir for 2 h at rt where it was observed by TLC (hexanes : EtOAc, 7 : 3) that all starting

material was consumed. The mixture was concentrated to an oil by rotovap and diluted with 20 mL water. The pH of this solution was adjusted to ~2 by addition of H₃PO₄ and NaCl was added until saturated. The mixture was then extracted with 2 x 100 mL ethyl acetate. The separated organic layers were combined, washed 20 mL pH of ~2 brine, dried with NaSO₄, filtered and concentrated. The free acid products, 290 mg (0.979 mmol; 92% yield), were separated from the crude oil by silica gel (94% CH₂Cl₂, 5% MeOH, 1% AcOH, R_f = 0.2) and again concentrated. A portion of this regioisomer mixture was isolated by reverse phase HPLC (C18, 250mm x 21.2mm, 10μ) (88% 0.05 M NH₄OAc, 12% acetonitrile, 9 mL/min) at retention times of 44 min. for N-Cbz-*cis*-3-hydroxy-4-*trans*-methoxy-L-proline or 46 min for the other isomer and concentrated by freezing / lyophilization. The material was used in the next step without further purification.

¹H-NMR (500 MHz, D₂O 4.65) (2 conformational isomers) δ 7.26-7.20 (m, 5H), 5.02-4.95 (dd, J = 25.4, 12.2 Hz, 1H), 4.94 (s, 1H), 4.34 and 4.33 (s, 1H), 4.23 and 4.18 (d, J = 6.4 Hz, 1H), 3.74 and 3.73 (s, 1H), 3.74-3.73 (m, 1H), 3.50 and 3.42 (d, 12.0 Hz, 1H), 3.23 and 3.21 (s, 3H).



CSE124

Chemical Formula: C₆H₁₁NO₄

Molecular Weight: 161.16

***cis*-3-hydroxy-*trans*-4-methoxy-L-proline:** BRL: 292 / CSE124

To 90.0 mg (0.305 mmol) of N-Cbz-*cis*-3-hydroxy-4-*trans*-methoxy-L-proline was added 3 mL MeOH and 1 mL water. This was transferred to a pressure flask containing 10 mg of wet 10% Pd/carbon (0.1 eq. weight) and 12 mg NH₄OAc (0.5 eq.). The reaction flask was placed onto a Parr shaker, the air was removed by vacuum and replaced by 40 psi H₂ (g). The flask was allowed to shake for 8 h where the flask was vented and mixture was diluted with ~ 20 mL water. The contents were then filtered through CM-cellulose using excess water for consecutive washes. The filtrate was frozen and lyophilized to a white residue which was washed 3 x 20 mL ethyl acetate / dichloromethane (1:1) and dried leaving a white solid residue; 44.0 mg of *cis*-3-hydroxy-*trans*-4-methoxy-L-proline a 90% yield.

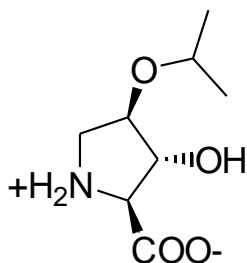
¹H-NMR (500 MHz, D₂O 4.75) δ 4.56 (d, J = 3.8 Hz, 1H, H-2), 4.22 (d, J = 3.8 Hz, 1H, H-1), 4.01 (d, J = 3.5 Hz, 1H, H-3), 3.62-3.59 (dd, J = 13.0, 3.5 Hz, 1H, H-5), 3.41-3.39 (d, J = 13.0 Hz, 1H, H-4), 3.35 (s, 3H). ¹³C-NMR (500 MHz, D₂O) δ 170.3, 83.9, 72.4, 65.2, 56.5, 48.36. HRMS *m/e* calcd. For C₆H₁₁NO₄ = 162.0749, found 162.0753. [α]_{Na}²² = -10° (c = 0.23, EtOH).

N-Cbz-*trans*-3-hydroxy-*cis*-4-isopropoxy-L-proline benzyl ester: BRL: 290

To 0.460 g (1.30 mmol) of N-Cbz-*trans*-3,4-epoxy-L-proline benzyl ester **13a** was added 4 mL of dry (MgSO₄ treated) CH₂Cl₂ and 2.0 mL isopropanol (~20 eq.; 26 mmol). The flask was capped, purged with argon and chilled on an ice bath with argon balloon. Once cooled, 1.03 mL of BF₃•Et₂O (48%; 3 eq.; 3.90 mmol) was added to the mixture. The mixture was allowed to return to rt and stir over night. The reaction mixture was quenched by the addition of 20 mL saturated NaHCO₃ solution which was allowed to stir for ~30 min. The mixture was then diluted with 100 mL CH₂Cl₂, washed with water (3 x 200 mL), washed with 50 mL brine, dried over Na₂SO₄ and concentrated. The final product N-Cbz-*trans*-3-hydroxy-*cis*-4-isopropoxy-L-proline benzyl ester, 430 mg, and unreacted epoxide starting material, were isolated by silica gel (hexanes : ethyl acetate 3 : 1, R_f product = 0.15 ; R_f epoxide = 0.3) for a total yield of 76% product and complete recovery in molecular equivalents of unreacted starting material (epoxide). The material was used in the next step without further purification.

¹H-NMR (500 MHz, CDCl₃) (2 conformational isomers) δ 7.33-7.22 (m, 10H), 5.28-5.03 (m, 4H), 4.49 and 4.44 (s, 1H), 4.43 and 4.37 (s, 1H), 3.91-3.89 (d, J = 2.4 Hz, 1H), 3.86-3.82 and 3.81-3.77 (dd, J = 11.5, 4.9 Hz, 1H), 3.65-3.58 (m, J = 6.1 Hz, 1H), 3.53-3.50 (d, J = 2.4 Hz, 1H), 1.07-1.00 (m, J = 5.9 Hz, 6H). ¹³C-NMR (500 MHz, CDCl₃) (2 conformational isomers) δ 167.2 and 166.8, 152.9 and 152.4, 133.8 and 133.0, 125.9,

125.9, 125.8, 125.6, 125.5, 125.4, 125.4, 125.4, 125.3, 125.2, 76.5, 75.8, 74.8, 74.6, 74.6, 74.3, 67.8 and 67.7, 64.8 and 64.7, 64.4 and 64.3, 63.7 and 63.2, 48.2 and 48.0, 19.7 and 19.6, 19.5 and 19.5.



CSE122

Chemical Formula: $C_8H_{15}NO_4$

Molecular Weight: 189.21

***trans*-3-hydroxy-*cis*-4-isopropoxy-L-proline:** BRL: 297 / CSE122

To 0.190 g (0.460 mmol) of Cbz-3-*trans*-hydroxy-4-*cis*-methoxy-L-proline benzyl ester was added 4 mL methanol which was then transferred to a pressure flask containing 19 mg (0.1 eq. weight) of 10 % Pd / carbon, 1 mL water and 18 mg (0.5 eq.) of NH_4OAc . The pressure flask was connected to a Parr shaker, the air was removed by house vacuum and replaced with 40 psi H_2 (g). The assembly was allowed to shake for 3 h. The pressure flask was vented and the solution diluted with 10 mL water and then filtered through CM-cellulose (carboxy-methyl-cellulose), using excess water for consecutive washes. The filtrate was then frozen and placed onto a lyophilizer until dry. The remaining residue was washed 3 x 20 mL EtOAc / CH_2Cl_2 (1:1), and dried leaving 80.0 mg of a white solid, *trans*-3-hydroxy-*cis*-4-isopropoxy-L-proline with a yield of 92%.

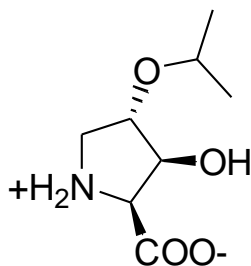
¹H-NMR (500 MHz, D₂O 4.75) δ 4.58 (s, 1H, H-2), 4.10 (d, J = 4.0 Hz, 1H, H-3), 3.99 (s, 1H, H-1), 3.75-3.70 (m, J = 6.1 Hz, 1H), 3.56-3.53 (dd, J = 12.7, 4.0 Hz, 1H, H-4), 3.47-3.44 (d, J = 12.7 Hz, 1H, H-5), 1.06 (d, J = 6.1 Hz, 3H), 1.01 (d, J = 6.1 Hz, 3H). ¹³C-NMR (500 MHz, D₂O) (2 conformational isomers) δ 170.7, 78.4 and 78.2, 75.7 and 75.7, 70.9 and 70.8, 67.6 and 67.4, 49.7, 21.4 and 21.4, 20.6 and 20.5. HRMS *m/e* calcd. For C₈H₁₆NO₄ = 190.1079, found 190.1089. [α]_{Na}²² = -5° (c = 0.24, EtOH).

N-Cbz-*cis*-3-hydroxy-*trans*-4-isopropoxy-L-proline benzyl ester: BRL: 296

To 0.407 g (1.15 mmol) of N-Cbz-*cis*-3,4-epoxy-L-proline benzyl ester **13b** was added 5 mL (dry MgSO₄ treated) CH₂Cl₂ and 2 mL isopropanol (~23 eq.; 26 mmol). The flask was purged with argon and cooled on ice bath for 10 min. Once cooled, 0.910 mL of BF₃•Et₂O (48%; 3 eq.; 3.45 mmol) was added dropwise and the solution was allowed to return to rt. After stirring overnight the reaction was quenched by the addition of 20 mL saturated solution of NaCO₃. This was then further diluted with 20 mL CH₂Cl₂ and washed 3 x 100 mL water and 1 x 100 mL brine, dried with Na₂SO₄ and concentrated by rotovap. The two regioisomer products N-Cbz-*cis*-3-hydroxy-*trans*-4-isopropoxy-L-proline benzyl ester and N-Cbz-*trans*-3-isopropoxy-*cis*-4-hydroxy-L-proline benzyl ester, 0.440 g, were isolated together by silica gel (3:1 hexanes : EtOAc, R_f = 0.20) a 92% yield. The material as a regioisomer mixture was used in the next step without further purification.

N-Cbz-*cis*-3-hydroxy-4-*trans*-isopropoxy-L-proline: BRL: 305

To 0.400 g (0.967 mmol) of N-Cbz-*cis*-3-hydroxy-*trans*-4-isopropoxy-L-proline benzyl ester and N-Cbz-*trans*-3-isopropoxy-*cis*-4-hydroxy-L-proline benzyl ester was added 10 mL THF, 1 mL water and 81 mg KOH (1.5 eq.; 1.45 mmol). The mixture was allowed to stir for 2 h at rt until complete, as determined by TLC (50% hexanes, 49% ethyl acetate, 1% AcOH). The mixture was concentrated to an oil by rotovap and diluted with 20 mL water. The pH of solution was adjusted to ~2 by addition of H₃PO₄ and NaCl was added until saturated. The mixture was then extracted with 3 x 100 mL EtOAc. The separated organic layers were combined, dried with Na₂SO₄, filtered and concentrated to a residue. The free acid products, 280 mg (0.866 mmol; 89% yield), were separated by silica gel (60% hexanes, 39% ethyl acetate, 1% AcOH, R_f = 0.1) and again concentrated. A portion of the regioisomer mixture were isolated by reverse phase HPLC (C18, 250mm x 21.2mm, 10μ) (85% 0.05 M NH₄OAc, 15% acetonitrile, 9 mL/min) at retention times of 48 min for N-Cbz-*cis*-3-hydroxy-4-*trans*-methoxy-L-proline & 52 min. for the other isomer and concentrated by freezing / lyophilization. The material was used in the next step without further purification.



CSE127

Chemical Formula: C₈H₁₅NO₄

Molecular Weight: 189.21

cis-3-hydroxy-trans-4-isopropoxy-L-proline: BRL: 305 / CSE127

To 21.0 mg (0.0650 mmol) of N-Cbz-*cis*-3-hydroxy-4-*trans*-isopropoxy-L-proline was added 3 mL MeOH and 1 mL water. This was transferred to a pressure flask containing 5 mg of wet 10% (0.25 eq. weight) Pd/carbon and 5 mg (0.5 eq) NH₄OAc. The reaction flask was placed onto a Parr shaker, the air was removed by vacuum and replaced by 40 psi H₂ (g). The flask was allowed to shake for 8 h where the flask was vented and mixture was diluted with ~ 20 mL water. The contents were then filtered through CM-cellulose using excess water for consecutive washes. The filtrate was frozen and lyophilized to a white solid and washed with EtOAc / CH₂Cl₂ 1:1 (3 x 20 mL) and dried by rotovap leaving a white solid; 11.6 mg of *cis*-3-hydroxy-*trans*-4-isopropoxy-L-proline a 94% yield.

¹H-NMR (500 MHz, D₂O 4.75) δ 4.48 (d, J = 3.9 Hz, 1H, H-2), 4.24 (d, J = 3.9 Hz, 1H, H-1), 4.21 (d, J = 3.6 Hz, 1H, H-3), 3.82-3.78 (m, J = 5.9 Hz, 1H), 3.65-3.62 (dd, J = 12.7, 3.6 Hz, 1H, H-5), 3.15 (d, J = 12.7 Hz, 1H, H-4), 1.12-1.10 (m, J = 5.9, 3.9 Hz, 6H).

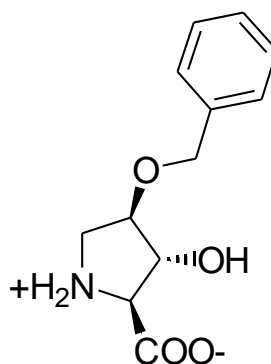
^{13}C -NMR (500 MHz, D_2O) (2 conformational isomers) δ 79.9, 73.5, 71.4, 65.3, 49.3, 21.3, 21.2. HRMS m/e calcd. For $\text{C}_8\text{H}_{16}\text{NO}_4 = 190.1079$, found 190.1092. $[\alpha]_{\text{Na}}^{22} = -7^\circ$ ($c = 0.13$, EtOH).

N-Cbz-*trans*-3-hydroxy-*cis*-4-benzyloxy-L-proline benzyl ester: BRL: 288

To 0.564 g (1.59 mmol) of N-Cbz-*trans*-3,4-epoxy-L-proline benzyl ester **13a** was added 5 mL of dry (MgSO_4 treated) CH_2Cl_2 and 2.5 mL benzyl alcohol (~15 eq; 24 mmol) (treated with molecular sieves). The flask was capped, purged with argon and chilled on an ice bath under argon balloon. Once cooled, 1.26 mL (48%; 3 eq.; 4.78 mmol) of $\text{BF}_3 \cdot \text{Et}_2\text{O}$ was added to the mixture. The mixture was allowed to return to rt and stir for 48 h. The reaction was quenched by the addition of 40 mL saturated NaHCO_3 solution and allowed to stir for 30 min. The mixture was then diluted with 100 mL CH_2Cl_2 , washed water (2 x 200 mL), washed with 50 mL brine, dried over Na_2SO_4 and concentrated to a white residue by rotovap. The final product N-Cbz-*trans*-3-hydroxy-*cis*-4-benzyloxy-L-proline benzyl ester, 0.710 mg (1.54 mmol), was isolated by silica gel (85% hexanes, 15% ethyl acetate, $R_f = 0.10$) for a total yield of 96%. The material was used in the next step without further purification.

^1H -NMR (500 MHz, CDCl_3) (2 conformational isomers) δ 7.33-7.18 (m, 15H), 5.18-5.10 (m, 1H), 5.05 (s, 1H), 5.03-4.92 (m, 1H), 4.55 (s, 1H), 4.50-4.39 (m, 2H), 3.91 (dd, $J =$

10.3, 5.1 Hz, 1H), 3.85-3.77 (m, J = 11.7, 5.1 Hz, 1H), 3.67-3.62 (dd, J = 12.0, 11.7 Hz, 1H), 3.42 (s, 2H).



CSE121

Chemical Formula: C₁₂H₁₅NO₄

Molecular Weight: 237.25

***trans*-3-hydroxy-*cis*-4-benzyloxy-L-proline: BRL: 289 / CSE121**

To 0.710 g (1.56 mmol) of Cbz-3-*trans*-hydroxy-4-*cis*-benzyloxy-L-proline benzyl ester was added 5 mL methanol which was then transferred to a pressure flask containing 71 mg (0.1 eq. weight) of 10% Pd/carbon, 0.3 mL water and 59.3 mg (0.5 eq.; 0.769 mmol) NH₄OAc. The pressure flask was connected to a Parr shaker, the air was removed by vacuum and replaced with 40 psi H₂ (g). The assembly was allowed to shake for 3 h. The pressure flask was vented and the contents were diluted with 30 mL water and filtered through CM-cellulose using excess water for consecutive washes. The filtrate was then frozen and placed onto a lyophilizer until dry. The remaining residue was washed EtOAc / CH₂Cl₂ 1:1 (3 x 20 mL), and dried leaving 0.340 mg of a white crude

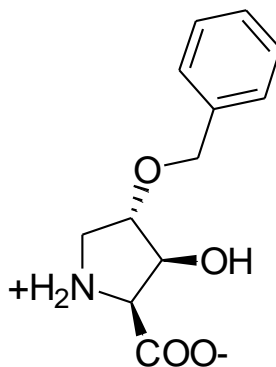
residue *trans*-3-hydroxy-*cis*-4-benzyloxy-L-proline, a yield of 93%. A portion of this crude product was isolated by reverse phase HPLC (C18, 250mm x 21.2mm, 10 μ) (92% 0.05 M NH₄OAc, 8% acetonitrile, 9 mL/min) at a retention time of 42 min. The collected fractions containing the desired product were concentrated by freezing / lyophilization. Once dry ~20 mL of water was added, the solution was again frozen and lyophilized until dry removing any remaining NH₄OAc. This was repeated until NH₄OAc was no longer present, leaving a white residue *trans*-3-hydroxy-*cis*-4-benzyloxy-L-proline, CSE 121.

¹H-NMR (500 MHz, D₂O 4.75) δ 7.37-7.30 (m, 5H), 4.71 (s, 1H, H-2), 4.56-4.47 (dd, J = 31.1, 11.5 Hz, 2H, methylene), 4.09 (s, 1H, H-3), 4.04 (s, 1H, H-1), 3.55-3.54 (d, J = 1.5 Hz, 2H, H-4 and 5). ¹³C-NMR (500 MHz, D₂O) δ 170.5, 136.7, 128.6, 128.2, 128.2, 80.8, 75.1, 71.0, 67.5, 49.4. HRMS *m/e* calcd. For C₁₂H₁₆NO₄ = 238.1079, found 238.1094. $[\alpha]_{\text{Na}}^{22} = -13^\circ$ (c = 0.08, EtOH).

N-Cbz-*cis*-3-hydroxy-*trans*-4-benzyloxy-L-proline benzyl ester and N-Cbz-*trans*-3-benzyloxy-*cis*-4-hydroxy-L-proline benzyl ester: BRL: 264

To 0.484 g (1.37 mmol) of N-Cbz-*cis*-3,4-epoxy-L-proline benzyl ester **13b** was added 5 mL of dry (MgSO₄ treated) CH₂Cl₂, 20 mL benzyl alcohol (treated with molecular sieves), and 13.0 mg (0.10 eq) of p-toluenesulfonic acid monohydrate. The mixture was heated to ~60°C and stirred for several days until the reaction appeared to be complete as

determined by TLC (hexanes : ethyl acetate, 1:1, $R_f = 0.4$). The solution was then allowed to cool to rt, diluted with 100 mL Et₂O and washed with water (3 x 100 mL). After drying with Na₂SO₄, the separated organic solution was filtered and run through a silica plug using 90% hexanes 10% ethyl acetate to remove most of the excess benzyl alcohol. The product was then eluted with 1:1 hexanes / ethyl acetate and concentrated. The final products N-Cbz-*cis*-3-hydroxy-*trans*-4-benzyloxy-L-proline benzyl ester and N-Cbz-*trans*-3-benzyloxy-*cis*-4-hydroxy-L-proline benzyl ester, 0.426 g (0.923 mmol), were isolated by silica gel (7: 3 hexanes : ethyl acetate, R_f product = 0.15) for a total yield of 67% including both regioisomers. Note: this addition was repeated by using 3.0 eq. of BF₃•Et₂O catalyst instead of tosic acid and under similar conditions as in the *trans*-epoxide – benzyl alcohol coupling. Yield improved dramatically, 197 mg of the two regioisomers were isolated starting from 160 mg of starting material, a 95% yield. The resulting products as a regioisomer mixture were used in the next step without further purification.



CSE113

Chemical Formula: C₁₂H₁₅NO₄

Molecular Weight: 237.25

***cis*-3-hydroxy-*trans*-4-benzyloxy-L-proline: BRL: 267 / CSE113**

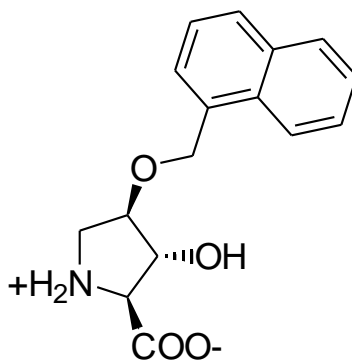
To 0.426 g (0.923 mmol) of Cbz-3-*trans*-hydroxy-4-*cis*-benzyloxy-L-proline benzyl ester was added 5 mL methanol which was then transferred to a pressure flask containing 40 mg (0.1 eq. weight) of 10% Pd/carbon, 2 mL MeOH, 1 mL water and 36 mg (~0.5 eq.; 0.47 mmol) of NH₄OAc. The pressure flask was connected to a Parr shaker, the air was removed by vacuum and replaced with 40 psi H₂ (g). The assembly was allowed to shake for 1.5 h where the reaction was complete as determined by TLC (7 : 3 hexanes/ EtOAc). The pressure flask was vented and the contents were diluted with 30 mL water and filtered through CM-cellulose (carboxy-methyl-cellulose), using excess water for consecutive washes. The filtrate was then frozen and lyophilized until dry. The remaining residue was washed with EtOAc / CH₂Cl₂ 1:1 (3 x 20 mL), and dried leaving an 0.206 mg of an off white solid, a mixture of *cis*-3-hydroxy-*trans*-4-benzyloxy-L-proline and *trans*-3-benzyloxy-*cis*-4-hydroxy-L-proline, and possibly 3,4 dihydroxy proline as a result of debenzylation. A portion of this crude product was isolated by

reverse phase HPLC (C18, 250mm x 21.2mm, 10 μ) (92% 0.05 M NH₄OAc, 8% acetonitrile, 9 mL/min) and concentrated by lyophilization. Once dry ~20 mL of water was added, the solution was again frozen and lyophilized until dry (removes remaining NH₄OAc). This was repeated until NH₄OAc was no longer present, leaving *cis*-3-hydroxy-*trans*-4-benzyloxy-L-proline, CSE113.

¹H-NMR (500 MHz, D₂O 4.75) δ 7.38-7.35 (m, 5H), 4.60 (s, 1H, H-2), 4.59 (s, 2H, methylene), 4.27-4.26 (d, J = 3.9 Hz, 1H, H-1), 4.21-4.20 (d, J = 3.9 Hz, 1H, H-3), 3.66-3.62 (dd, J = 13.2, 3.9 Hz, 1H, H-5), 3.44-3.42 (d, J = 13.2 Hz, 1H, H-4). ¹³C-NMR (500 MHz, D₂O) δ 172.8, 139.2, 131.3, 131.1, 130.9, 84.7, 75.4, 73.8, 67.9, 51.4. HRMS *m/e* calcd. For C₁₂H₁₆NO₄ = 238.1079, found 238.1064. $[\alpha]_{\text{Na}}^{22} = -20^\circ$ (c = 0.22, EtOH).

(2S, 3R, 4R)-N-Cbz-3-hydroxy-4-o-methyl- α -naphthyl-proline benzyl ester: BRL: 300
To 0.285 g (0.806 mmol) of N-Cbz-*trans*-3,4-epoxy-L-proline benzyl ester **13a** was added 2 mL of dry (MgSO₄ treated) CH₂Cl₂ and 0.191 g (98%, 1.5 eq.; 1.20 mmol) of 1-naphthylenemethanol. The flask was capped, purged with argon and chilled on an ice bath with argon balloon. Once cooled, 64 μ L (48%; 0.3 eq.; 0.242 mmol) of BF₃•Et₂O was added to the stirring solution mixture. The mixture was allowed to return to rt and stir over night. The reaction was quenched by the addition of 20 mL saturated NaHCO₃ solution and allowed to stir for ~30 min. The contents of the flask were then diluted with

100 mL CH₂Cl₂, washed with water (3 x 100 mL), 50 mL brine, dried over Na₂SO₄ and concentrated to a white crude. The final product (2S, 3R, 4R)-N-Cbz-3-hydroxy-4-o-methyl- α -naphthyl-proline benzyl ester, 0.220 mg (0.430 mmol), was isolated by silica gel (7 : 3 hexanes, EtOAc, R_f = 0.1) a yield of 53%, only a portion of product was isolated, and recovery of 30 mg epoxide starting material. The product was used in the next step without further purification.



CSE132

Chemical Formula: C₁₆H₁₇NO₄

Molecular Weight: 287.31

(2S, 3R, 4R)-3-hydroxy-4-o-methyl- α -naphthyl-proline: BRL: 307 / CSE132

To 0.120 g (0.235 mmol) of (2S, 3R, 4R)-N-Cbz-3-hydroxy-4-o-methyl- α -naphthyl-proline benzyl ester was added 5 mL methanol which was heated to dissolve and then transferred to a pressure flask containing 20 mg of 10% Pd/carbon (0.167 eq. weight), and 0.5 mL water. The pressure flask was connected to a Parr shaker, the air was removed by vacuum and replaced with 40 psi H₂ (g). The assembly was allowed to shake over night until it was clear by TLC that all the starting material was consumed (50/49/1;

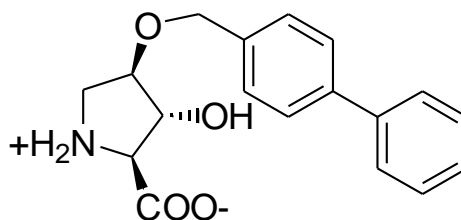
hexanes / EtOAc / AcOH). The pressure flask was vented and the contents were diluted with 30 mL water, followed by filtration through CM-cellulose (carboxy-methyl-cellulose), using excess water for consecutive washes. The filtrate was then frozen and placed onto a lyophilizer until dry. The remaining residue was washed EtOAc / CH₂Cl₂ 1:1 (3 x 20 mL), and dried leaving 58.0 mg of a white solid, primarily consisting of the desired prolinol product, a yield of 86%. A portion of this semi pure prolinol product was isolated by reverse phase HPLC (C18, 250mm x 21.2mm, 10 μ) (75% 0.05 M NH₄OAc, 25% acetonitrile, 9 mL/min) at a retention time of ~44 min. The collected fractions containing the desired prolinol were combined and concentrated by lyophilization. Once dry ~20 mL of water was added, the solution was again frozen and lyophilized until dry (removes remaining NH₄OAc). This was repeated until NH₄OAc was no longer present, leaving a white residue (2S, 3R, 4R)-3-hydroxy-4-o-methyl- α -naphthyl-proline, CSE 132.

¹H-NMR (500 MHz, d₆-DMSO) δ 8.84 (b, 2H (-NH₂⁺), 8.05 (d, J = 7.8 Hz, 1H), 7.93 (d, J = 7.3 Hz, 1 H), 7.87 (d, J = 7.8 Hz, 1H), 7.57-7.51 (m, 3H), 7.46 (dd, J = 7.8, 7.3 Hz, 1H), 5.66 (b, 1H, (-OH)), 4.95-4.88 (dd, J = 19.6, 12.2 Hz, 2H), 4.58 (s, 1H, H-2), 3.94 (d, J = 2.4 Hz, 1H, H-3), 3.50 (s, 1H, H-1), 3.47 (d, J = 12.7 Hz, 1H, H-5), 3.28-3.25 (dd, J = 12.7, 3.4 Hz, 1H, H-4). ¹³C-NMR (500 MHz, d₆-DMSO) δ 166.5, 133.3, 131.0, 128.3, 128.2, 126.3, 125.8, 125.3, 124.0, 119.7, 113.6, 82.1, 75.8, 69.7, 68.2, 48.6.

HRMS *m/e* calcd. For C₁₆H₁₈NO₄ = 288.1236, found 288.1230. [α]²²_{Na} = -18° (c = 0.1, DMSO).

(2S, 3R, 4R)-N-Cbz-3-hydroxy-4-o-methyl-p-biphenyl-proline benzyl ester: BRL:
301

To 0.305 g (0.862 mmol) of N-Cbz-*trans*-3,4-epoxy-L-proline benzyl ester **13a** was added 2 mL of dry (MgSO₄ treated) CH₂Cl₂ and 0.318 g (98%, 2.0 eq.; 1.72 mmol) of 4-biphenylmethanol. The flask was capped, purged with argon and chilled on an ice bath under argon balloon. Once cooled, 91 μ L (48%; 0.4 eq.; 0.345 mmol) of BF₃•Et₂O was added to the stirring solution. The mixture was allowed to return to rt and stir over night. The reaction was quenched by the addition of 20 mL saturated NaHCO₃ solution and allowed to stir for an additional 30 min. The contents of the flask were then diluted with 100 mL CH₂Cl₂, washed with water (3 x 100 mL), washed with 50 mL brine, dried over Na₂SO₄ and concentrated to a white solid by rotovap. The final product (2S, 3R, 4R)-N-Cbz-3-hydroxy-4-o-methyl-p-biphenyl-proline benzyl ester, 0.395 mg (0.735 mmol), was isolated by silica gel (7 : 3 hexanes : EtOAc, R_f = 0.1), a yield of 85%, and some remaining epoxide starting material. The product was used in the next step without further purification.



CSE131

Chemical Formula: C₁₈H₁₉NO₄

Molecular Weight: 313.35

(2S, 3R, 4R)-3-hydroxy-4-o-methyl-p-biphenyl-proline: BRL: 304 / CSE131

To 0.105 g (0.195 mmol) of (2S, 3R, 4R)-N-Cbz-3-hydroxy-4-o-methyl-p-biphenyl-proline benzyl ester was added 5 mL methanol which was heated to dissolve and then transferred to a pressure flask containing 11 mg of 10% Pd/carbon (0.10 eq. weight), 8 mg (0.5 eq) NH₄OAc and 0.5 mL water. The pressure flask was connected to a Parr shaker, the air was removed by vacuum and replaced with 40 psi H₂ (g). The assembly was allowed to shake for 2 h until the reaction had completed as determined by TLC (50/49/1; hexanes/ethyl acetate/AcOH). The pressure flask was vented and the contents were diluted with 30 mL water, followed by filtration through CM-cellulose using excess water for consecutive washes. The filtrate was then frozen and lyophilized until dry. The remaining residue was washed EtOAc / CH₂Cl₂ 1 : 1 (3 x 20 mL), and dried over Na₂SO₄ leaving 51.0 mg of a white solid crude, primarily consisting of the desired prolinol product, a yield of 84%. A portion of this crude product was isolated by reverse phase HPLC (C18, 250mm x 21.2mm, 10μ) (75% 0.05 M NH₄OAc, 25% acetonitrile, 9 mL/min) at a retention time of ~38 min. The collected fractions containing the desired prolinol were combined and concentrated by lyophilization. Once dry, 20 mL of water

was added, the solution was again frozen and lyophilized until dry (removes remaining NH₄OAc). This was repeated until NH₄OAc was no longer present, leaving a white residue (2S, 3R, 4R)-3-hydroxy-4-o-methyl-p-biphenyl-proline, CSE 131.

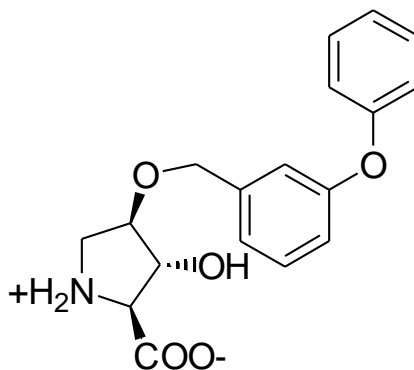
¹H-NMR (500 MHz, d₆-DMSO 2.50) δ 8.82 (b, 1.5H, NH₃⁺), 7.66-7.65 (d, J = 7.6 Hz, 2H), 7.62-7.60 (d, J = 7.8 Hz, 2H), 7.47-7.44 (dd, J = 7.6, 7.3 Hz, 2H), 7.41-7.40 (d, J = 7.6 Hz, 2H), 7.37-7.34 (dd, J = 7.3, 7.1 Hz, 1H), 5.64 (s, 1H, OH), 4.54 (s, 1H, H-2), 4.53-4.46 (dd, J = 21.5, 22.7 Hz, 2H, methylene), 3.86 (s, 1H, H-3), 3.49 (s, 1H, H-1), 3.46-3.43 (d, J = 12.5 Hz, 1H, H-5), 3.33 (H₂O), 3.27-3.25 (d, J = 10.5 Hz, 1H, H-4).
¹³C-NMR (500 MHz, d₆-DMSO) δ 170.2, 140.0, 139.2, 137.1, 128.9, 128.3, 127.4, 126.6, 126.4, 81.8, 75.4, 69.5, 68.2, 46.7. HRMS *m/e* calcd. For C₁₈H₂₀NO₄ = 314.1392, found 314.1378. [α]_{Na}²² = -7° (c = 0.12, DMSO).

(2S, 3R, 4R)-N-Cbz-3-hydroxy-4-o-methyl-3-biphenylether-proline benzyl ester:

BRL: 302

To 0.275 g (0.778 mmol) of N-Cbz-*trans*-3,4-epoxy-L-proline benzyl ester **13a** was added 3 mL of dry (MgSO₄ treated) CH₂Cl₂ and 1 mL (7.34 eq.; 5.74 mmol) of 3-phenoxybenzyl alcohol. The flask was capped, purged with argon and chilled on an ice bath under argon balloon. Once cooled, 0.614 mL (48%; 3 eq.; 2.33 mmol) of BF₃•Et₂O

was added to the mixture. The mixture was allowed to return to rt and stir for 48 h. The reaction was quenched by the addition of 20 mL saturated NaHCO₃ and allowed to stir for 30 min. The mixture was then diluted with 60 mL CH₂Cl₂, washed with water (3 x 200 mL), washed with 50 mL brine, dried over Na₂SO₄ and concentrated via rotovap to a solid residue. The final product (2S, 3R, 4R)-N-Cbz-3-hydroxy-4-o-methyl-3-biphenylether-proline benzyl ester, 0.270 g (0.488 mmol), was isolated by silica gel (7 : 3 hexanes : EtOAc, R_f = 0.10) for a total yield of 63%. The product was used in the next step without further purification.



CSE130

Chemical Formula: C₁₈H₁₉NO₅

Molecular Weight: 329.35

(2S, 3R, 4R)-3-hydroxy-4-o-methyl-3-biphenylether-proline: BRL: 303 / CSE130

To 0.270 g (0.488 mmol) of (2S, 3R, 4R)-N-Cbz-3-hydroxy-4-o-methyl-3-biphenylether-proline benzyl ester was added 5 mL methanol which was then transferred to a pressure flask containing 30 mg of 10% Pd/carbon (0.1 eq. weight), 0.3 mL water and 19.0 mg (0.5 eq.; 0.246 mmol) NH₄OAc. The pressure flask was connected to a Parr shaker, the

air was removed by vacuum and replaced with 40 psi H₂ (g). The assembly was allowed to shake for 2 h. The pressure flask was vented and the contents were diluted with 20 mL water, followed by filtration through CM-cellulose using excess water for consecutive washes. The filtrate was then frozen and placed onto a lyophilizer until dry. The remaining residue was washed with 1:1 EtOAc : CH₂Cl₂ (3 x 20 mL), and dried leaving 0.144 mg of a white solid crude, primarily consisting of the desired prolinol, a yield of 90%. A portion of this crude product was isolated by reverse phase HPLC (C18, 250mm x 21.2mm, 10 μ) (75% 0.05 M NH₄OAc, 25% acetonitrile, 9 mL/min) at a retention time of ~42 min. The collected fractions containing the prolinol product were combined and concentrated by lyophilization. Once dry 20 mL of water was added, the solution was again frozen and lyophilized until dry (removes remaining NH₄OAc). This was repeated until NH₄OAc was no longer present, leaving a white residue (2S, 3R, 4R)-3-hydroxy-4-o-methyl-3-biphenylether-proline, CSE 130.

¹H-NMR (500 MHz, d₆-DMSO 2.50) δ 8.81 (b, 1.5H, NH₃⁺), 7.40-7.37 (dd, J = 14.7 Σ , 7.3 Hz, 2H), 7.34-7.31 (dd, J = 7.8, 7.6 Hz, 1H), 7.15-7.09 (m, J = 18.1, 7.6 Hz, 2H), 6.99 (m, 3H), 6.87 (d, J = 7.6, 1H), 5.62 (s, 1H, OH), 4.51 (s, 1H, H-2), 4.48-4.41 (dd, J = 23.0, 12.0 Hz, 2H, methylene), 3.83 (s, 1H, H-3), 3.47 (s, 1H, H-1), 3.43-3.41 (d, J = 12.2 Hz, 1H, H-5), 3.25-3.23 (d, J = 11.0 Hz, 1H, H-4). ¹³C-NMR (500 MHz, d₆-DMSO) δ 169.1, 156.7, 156.4, 140.3, 130.1, 129.7, 123.4, 122.7, 118.5, 117.8, 117.5, 81.9, 75.4,

69.3, 68.1, 48.7. HRMS *m/e* calcd. For C₁₈H₂₀NO₅ = 330.1328, found 330.1341. $[\alpha]_{\text{Na}}^{22}$
= -29° (c = 0.14, DMSO).

Synthesis section 5

Procedure for synthesis of alkyl, aryl or phenol-ether prolinols:

A considerable amount of time was spent in the discovery and optimization of synthesizing alkyl, aryl and phenol-ether substituted prolinols **figure 17**. Generation of these targets via nucleophilic substitution under basic conditions required the free acid proline epoxide so as to avoid racemization of the chiral α center during the addition step (**Scheme 4**). This was accomplished by hydrolysis of the benzyl ester protection group of the proline olefin **12** to give the free acid olefin **12a**. Epoxidation of the free acid olefin with mCPBA (meta-chloroperoxybenzoic acid) under CH₂Cl₂ reflux w/ 1% radical inhibitor produced the *trans*-epoxide **13c** in excellent yields with no detectable *cis*-epoxide. Epoxidation by dimethyldioxirane or peracetic acid were also met with the same results, however, in lower overall yield.

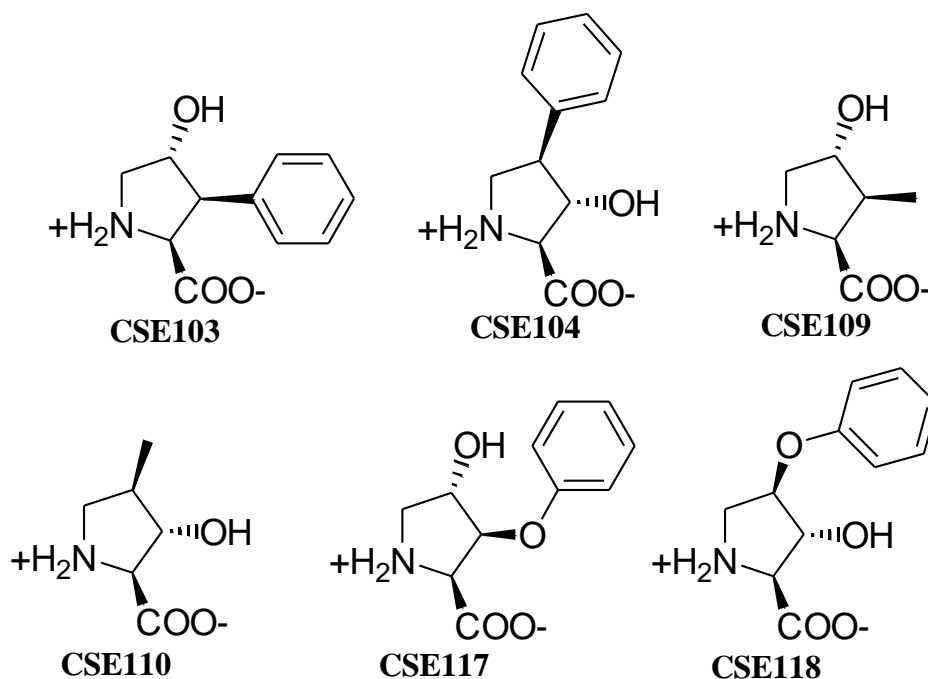
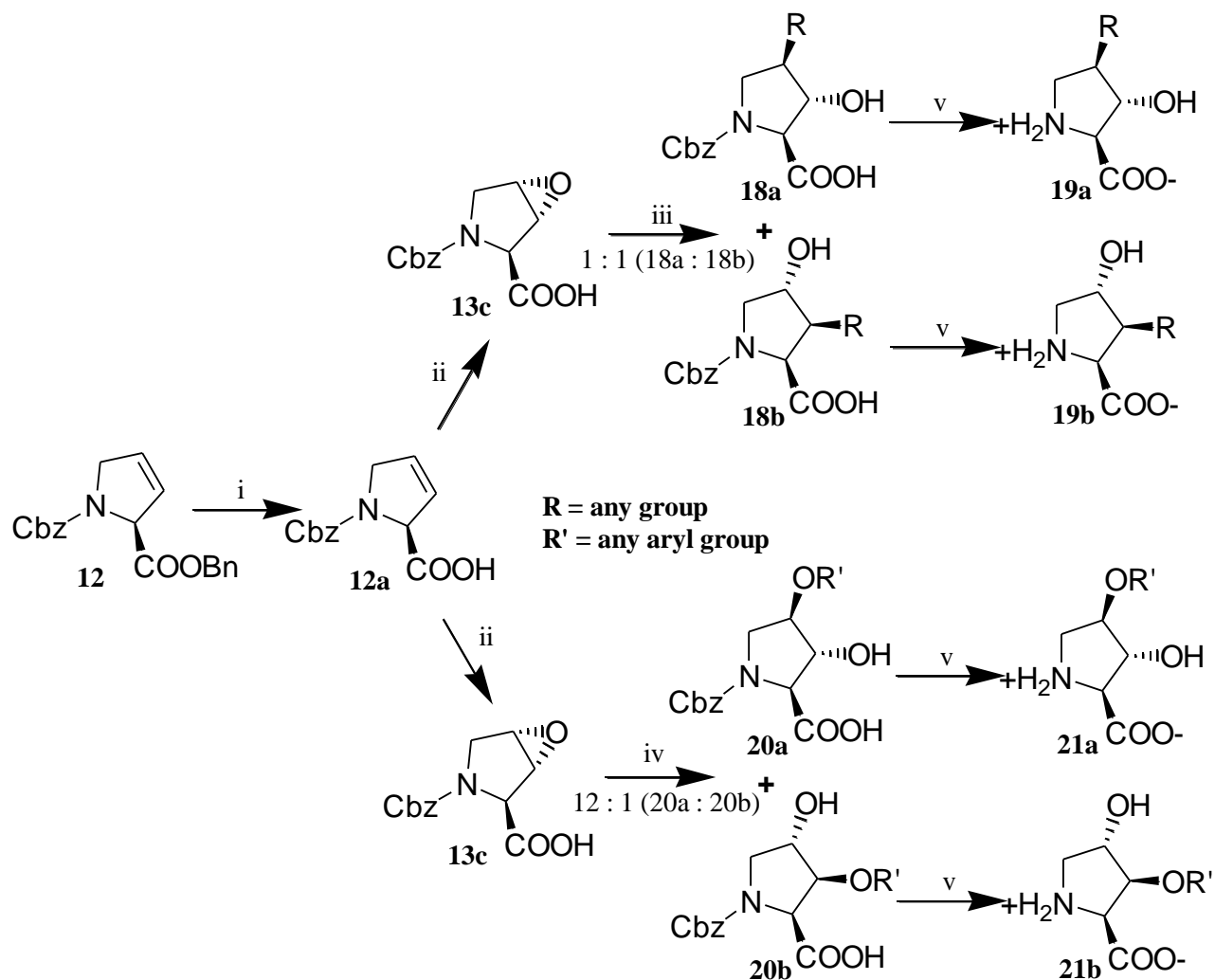


Figure 17: Synthesized alkyl, aryl and phenol-ether prolinols.

Initial attempts to ring open the epoxide of **13c** via nucleophilic addition using Grignard reagents or organolithiums alone or in preparations with soft Lewis acids CeCl_3 , CuBr (catalytic or stoichiometric, (including Gilman reagent (R_2CuMgX or R_2CuLi)), or copper (I) acetate and even SmI_2 catalyzed Barbier addition were all unsuccessful. As a last ditch effort, the N-protected prolinol derivatives **18a** and **18b** were finally obtained from the epoxide by transformation of the organolithium reagent to a higher order cuprate, a rearrangement & complexation between 2 eq organolithium reagent and 1 eq CuCN (Lipshutz *et al* 1982; Lipshutz *et al* 1984) in Et_2O at approximately -40°C

(Scheme 4; iii). The prolinol products were isolated together by silica gel in yields of 90-95% with regioisomer ratio's of nearly 1 : 1.



Scheme 4: Synthesis of alkyl, aryl or phenol-ether prolinols. (i) KOH, THF, H₂O, 22°C; (ii) mCPBA, CH₂Cl₂; (iii) 2 eq. R₂Cu(CN)Li₂, Et₂O, -40°C, Inert atmosphere; (iv) Na⁺ phenoxide in THF, rt; (v) 10% Pd/C (10% weight. eq), 40 psi H₂, MeOH, H₂O, NH₄OAc.

Similarly, the N-protected phenoxy prolinols **20a** & **20b** were synthesized from the free acid *trans*-epoxide **13c** by the addition of a sodium phenoxide in THF at rt in

regioisomeric ratios of 12:1, 3-hydroxy : 4-hydroxy respectively, with overall respectable yields of 80-85%. Hydrogenolysis of the N-benzylcarbamate (Cbz) of protected prolinols **18a**, **18b**, **20a**, or **20b** via 10% Pd / carbon at 40 psi H₂(g) in methanol and subsequent separation of the regioisomers by reverse phase HPLC afforded the substituted prolinol products **19a**, **19b**, **21a** and **21b**.

N-Cbz-3,4-dehydro-L-proline 12a: BRL:256

To 8.26 g (24.5 mmol) of N-Cbz-3,4-dehydro-L-proline benzyl ester **12** was added 50 mL THF, 5 mL H₂O and 1.65 g (1.2 eq.; 29.4 mmol) KOH. The mixture was stirred for 2 h at rt. The mixture was concentrated by rotovap until dry in which 20 mL of water was added to dissolve the remaining residue. The pH of this mixture was adjusted to ~2 by addition of H₃PO₄ and NaCl was added until saturated. The contents were then extracted with EtOAc (3 x 200 mL). The ethyl acetate washes were combined and dried over Na₂SO₄, filtered and concentrated via rotovap to a yellow oil. The product, 6.05 g, N-Cbz-3,4-dehydro-L-proline **12a** was isolated by silica gel (60% hexanes, 39% ethyl acetate, 1% AcOH; R_f = 0.2) a quantitative yield. The material was used in the next step without further purification.

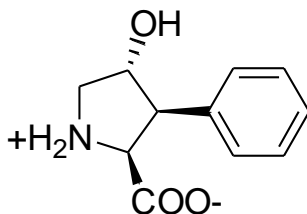
N-Cbz-*trans*-3,4-epoxy-L-proline 13c: BRL:257

To 2.37 g (9.60 mmol) of N-Cbz-3,4-dehydro-L-proline **12a** was added 20 mL CH₂Cl₂, 4.73 g (2 eq; 19.2 mmol) of 70% mCPBA, and 10 mg of (0.4% weight) 2,6-ditertbutyl-4-methyl phenol. The mixture was then refluxed under argon balloon overnight. Another 2.00 g (0.85 eq) of mCPBA was added to the reaction mixture and reflux was continued overnight. The mixture, now with white precipitate, was cooled over ice bath and filtered using 20 mL cold CH₂Cl₂ to wash. The product, 1.68 g of N-Cbz-*trans*-3,4-epoxy-L-proline **13c**, was separated from the crude mixture consisting of excess mCPBA by a series of two silica gel columns; the first using 50% hexanes, 49% ethyl acetate, 1% AcOH as a mobile phase and the second using 96% CH₂Cl₂, 3% MeOH, 1% AcOH. Recovered epoxide product resulted in a yield of 67%, however, this represents only isolated product from two columns; a higher yield was possible with further purification via flash chromatography.

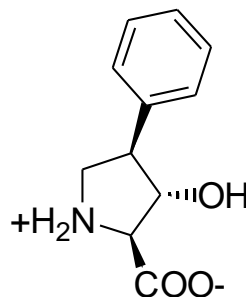
¹H-NMR (500 MHz, CDCl₃) (2 conformational isomers) δ 10.30 (b, 1H [COOH]), 7.35-7.26 (m, 5H), 5.18-5.11 (m, J = 20.8, 12.5 Hz, 1H), 5.12 (s, 1H), 4.75 and 4.68 (s, 1H), 3.97 and 3.92 (d, J = 12.7 Hz, 1H), 3.88 and 3.85 (d, J = 2.7 Hz, 1H), 3.69 (s, 1H), 3.56-3.53 (d, J = 12.7 Hz, 1H).

(2S, 3S, 4R)-N-Cbz-3-hydroxy-4-phenyl-proline and (2S, 3S, 4R)-N-Cbz-3-phenyl-4-hydroxy-proline: BRL: 263

To a flame dried round bottom flask was added 0.143 g (1.60 mmol; 3 eq) of CuCN (dried by high vacuum) and 5 mL dry (MgSO₄ treated) Et₂O. The flask was capped with a septum, purged air vacuum / argon balloon, and chilled to -40°C (acetone bath / cold finger controlled). Once cooled, 1.60 mL (3.19 mmol; 6 eq) of 2.0 M phenyl-lithium in THF was added and the mixture was then allowed to warm to -10°C and kept at this temperature for ~15 min and then returned to -40°C where 0.140 g (0.532 mmol) of N-Cbz-*trans*-3,4-epoxy-L-proline **13c** in 2 mL dry (MgSO₄ treated) Et₂O also at -40°C was added via sterile syringe. The flask was then allowed to warm to -10°C and stir overnight. After stirring overnight, the reaction mixture was allowed to warm to 0°C and was quenched by the addition of 20 mL saturated NH₄Cl. The mixture was then warmed to rt, the pH was adjusted to ~2 by addition of H₃PO₄ and salted with NaCl until saturated. The products were then extracted with EtOAc (3 x 100 mL). The organic washes were combined, dried over Na₂SO₄, and concentrated to a solid residue via rotovap. The products, 0.171 g of (2S, 3S, 4R)-N-Cbz-3-hydroxy-4-phenyl-proline and (2S, 3S, 4R)-N-Cbz-3-phenyl-4-hydroxy-proline were isolated as a regioisomer mixture by silica gel (50% hexanes, 49% ethyl acetate, 1% AcOH) for the first column followed by a second column (96% CH₂Cl₂, 3% MeOH, 1% AcOH), a 94% yield. The material was used in the next step without further purification.



CSE103
 Chemical Formula: C₁₁H₁₃NO₃
 Molecular Weight: 207.23



CSE104
 Chemical Formula: C₁₁H₁₃NO₃
 Molecular Weight: 207.23

(2S, 3S, 4R)-3-hydroxy-4-phenyl-proline and (2S, 3S, 4R)-3-phenyl-4-hydroxy-proline: BRL: 293 / CSE104 and CSE103

To a 0.200 g (0.586 mmol) regioisomer mixture of (2S, 3S, 4R)-N-Cbz-3-hydroxy-4-phenyl-proline and (2S, 3S, 4R)-N-Cbz-3-phenyl-4-hydroxy-proline was added 3 mL MeOH. The mixture was transferred to a pressure flask containing 20.0 mg (0.1 eq weight) 10% Pd / carbon, 0.5 mL H₂O and 23.0 mg (0.5 eq: 0.298 mmol) NH₄OAc. The flask was placed on a Parr shaker, the air was removed by vacuum, and replaced by 40 psi H₂ (g). The apparatus was allowed to shake for 3 h at rt. The pressure flask was vented and the contents were diluted with 30 mL water and filtered through CM-cellulose using excess water for consecutive washes. The filtrate was then frozen and lyophilized until dry. The remaining residue was washed with EtOAc : CH₂Cl₂ 1:1 (3 x 20 mL), and dried leaving 0.108 mg (89% yield) of an off white solid, a crude mixture of (2S, 3S, 4R)-3-hydroxy-4-phenyl-proline and (2S, 3S, 4R)-3-phenyl-4-hydroxy-proline, regioisomeric ratio of 4.4 : 5.6 respectively. A portion of this crude was separated by reverse phase HPLC (C18, 250 mm x 21.2 mm, 10μ) (92% 0.05 M NH₄OAc, 8%

acetonitrile, 9 mL / min). Fractions containing a specific isomer were combined and concentrated by lyophilization. Once dry, 20 mL of water was added to dissolve the remaining residue and the solution was again frozen and lyophilized until dry (removes remaining NH₄OAc). This was repeated until NH₄OAc was no longer present affording (2S, 3S, 4R)-3-hydroxy-4-phenyl-proline (CSE104) or (2S, 3S, 4R)-3-phenyl-4-hydroxy-proline (CSE103) as separate white solids.

(2S, 3S, 4R)-3-phenyl-4-hydroxy-proline : CSE103

¹H-NMR (500 MHz, D₂O 4.75) δ 7.42-7.39 (dd, J = 7.3, 7.1 Hz, 2H), 7.35-7.31 (m, J = 7.6 Hz, 3H), 4.52-4.49 (dd, J = 12.7, 6.4 Hz, 1H, H-3), 4.21 (d, J = 8.8 Hz, 1H, H-1), 3.66-3.62 (dd, J = 11.5, 6.1 Hz, 1H, H-5), 3.38-3.31 (m, J = 8.8, 6.1 Hz, 2H, H-2 & 4). ¹³C-NMR (500 MHz, D₂O) δ 172.6, 136.8, 129.1, 127.9, 127.6, 75.4, 64.7, 55.8, 49.6. HRMS *m/e* calcd. For C₁₁H₁₄NO₃ = 208.0974, found 208.0996. [α]_{Na}²² = -16° (c = 0.23, H₂O), [α]_{Na}²² = -15° (c = 0.24, EtOH).

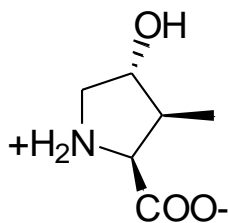
(2S, 3S, 4R)-3-hydroxy-4-phenyl-proline : CSE104

¹H-NMR (500 MHz, D₂O 4.75) δ 7.41-7.38 (dd, J = 7.6, 7.1, 2H), 7.33-7.30 (m, J = 7.6 Hz, 3H), 4.63-4.61 (dd, J = 8.8, 4.4 Hz, 1H, H-2), 4.21-4.20 (d, J = 5.6 Hz, 2H, H-1), 3.91-3.86 (dd, J = 9.8, 5.4 Hz, 1H, H-5), 3.58-3.51 (m, 2H, H-3 & 4). ¹³C-NMR (500 MHz, D₂O) δ 171.0, 137.1, 129.1, 127.8, 127.0, 76.4, 64.6, 50.8, 47.9. HRMS *m/e* calcd. For C₁₁H₁₄NO₃ = 208.0974, found 208.0982. [α]_{Na}²² = -43° (c = 0.08, EtOH).

(2S, 3S, 4R)-N-Cbz-3-hydroxy-4-methyl-proline and (2S, 3S, 4R)-N-Cbz-3-methyl-4-hydroxy-proline: BRL: 259

To a flame dried round bottom flask was added 0.730 g (8.50 mmol; 2.5 eq) of CuCN (dried by high vacuum) and 10 mL dry (MgSO₄ treated) Et₂O. The flask was capped with a septum, purged air with vacuum, filled with argon balloon, and cooled to -60°C (acetone bath / cold finger controlled). Once cooled, 10.0 mL (16.3 mmol; 5 eq) of 1.6 M methyl-lithium in Et₂O was added via sterile syringe and the mixture was allowed to stir for ~15 min until all the CuCN appeared to be dissolved (a clear colorless solution). Once equilibrated, 0.840 g (3.20 mmol) of N-Cbz-*trans*-3,4-epoxy-L-proline **13c** in 10 mL dry (MgSO₄ treated) Et₂O at -60°C was added via sterile syringe. The flask was then allowed to warm to -40°C and stir overnight under argon balloon. After stirring overnight, the reaction mixture was allowed to warm to 0°C and was quenched by the addition of 30 mL saturated NH₄Cl. The mixture was then warmed to rt, the pH was adjusted to ~2 by addition of H₃PO₄ and salted with NaCl until saturated. The products were then extracted with of EtOAc (3 x 100 mL). The organic washes were then combined, dried over NaSO₄, and concentrated to a crude regioisomer mixture, 0.766 g. The products, (2S, 3S, 4R)-N-Cbz-3-hydroxy-4-methyl-proline and (2S, 3S, 4R)-N-Cbz-3-methyl-4-hydroxy-proline (ratio of 1:1) were isolated as a regioisomer mixture by silica gel from two columns (50% hexanes, 49% ethyl acetate, 1% AcOH and 96% CH₂Cl₂, 3% MeOH, 1% AcOH) an 86% yield and recovery of epoxide starting material. A portion of

these regioisomers were separated by reverse phase HPLC (C18, 250 mm x 21.2 mm, 10 μ) (85% 0.05 M NH_4OAc , 15% acetonitrile, 9 mL/min) at a retention time of 22 min for (2S, 3S, 4R)-N-Cbz-3-methyl-4-hydroxy-proline and 24 min for (2S, 3S, 4R)-N-Cbz-3-hydroxy-4-methyl-proline. The fractions containing an individual isomer were combined and concentrated by lyophilization to afford the product as white solid. Each separate isomer was used in the next synthetic step without further purification.



CSE109

Chemical Formula: $\text{C}_6\text{H}_{11}\text{NO}_3$

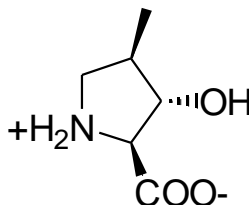
Molecular Weight: 145.16

(2S, 3S, 4R)-3-methyl-4-hydroxy-proline: BRL: 268 / CSE109

To 70.0 mg (0.251 mmol) of (2S, 3S, 4R)-N-Cbz-3-methyl-4-hydroxy-proline was added 2 mL MeOH.. The mixture was transferred to a pressure flask containing 7.0 mg (0.1 eq. weight) 10% Pd/carbon, and 6.3 (0.5 eq) NH_4OAc . The flask was placed on a Parr shaker, the air was removed by vacuum, and replaced by 40 psi H_2 (g). The apparatus was allowed to shake for ~2 h at rt. The pressure flask was vented and the contents were diluted with 30 mL water and filtered through CM-cellulose using excess water for consecutive washes. The filtrate was then frozen and lyophilized until dry. The

remaining residue was washed with 1:1 EtOAc : CH₂Cl₂ (3 x 20 mL), resuspended in 10 mL water and again dried by lyophilization leaving 33.0 mg of (2S, 3S, 4R)-3-methyl-4-hydroxy-proline (CSE109) as a white solid, a 92% yield.

¹H-NMR (500 MHz, D₂O 4.75) δ 4.09 (dd, J = 4.9, 2.4 Hz, 1H, H-3), 3.66 (d, J = 5.9 Hz, 1H, H-1), 3.50-3.46 (dd, J = 12.2, 4.9 Hz, 1H, H-5), 3.29-3.26 (dd, J = 12.2, 2.4 Hz, 1H, H-4), 2.37-2.33 (dd, J = 6.8, 5.9 Hz, 1H, H-2), 1.13 (d, J = 6.8 Hz, 3H, methyl). ¹³C-NMR (500 MHz, D₂O) δ 176.2, 77.4, 68.3, 52.8, 47.6, 18.6. HRMS *m/e* calcd. For C₆H₁₂NO₃ = 146.0817, found 146.0822. [α]_{Na}²² = -4° (c = 0.25, H₂O).



CSE110

Chemical Formula: C₆H₁₁NO₃

Molecular Weight: 145.16

(2S, 3S, 4R)-3-hydroxy-4-methyl-proline: BRL: 254 / CSE110

To 80.0 mg (0.286 mmol) of (2S, 3S, 4R)-N-Cbz-3-hydroxy-4-methyl-proline was added 5 mL MeOH.. The mixture was transferred to a pressure flask containing 20.0 mg (0.25 weight %) 10% Pd/carbon. The flask was placed on a Parr shaker, the air was removed by vacuum, and replaced by 40 psi H₂ (g). The apparatus was allowed to shake for ~24 h

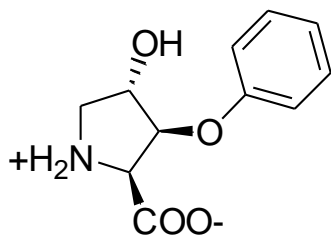
at rt. The pressure flask was vented and the contents were diluted with 30 mL water and filtered through CM-cellulose using excess water for consecutive washes. The filtrate was then frozen and lyophilized until dry. The remaining residue was washed with 1:1 EtOAc / CH₂Cl₂ (3 x 20 mL), resuspended in 10 mL water and again dried by lyophilization leaving 34.0 mg of (2S, 3S, 4R)-3-hydroxy-4-methyl-proline (CSE110) as a white residue, a 82% yield.

¹H-NMR (500 MHz, D₂O 4.75) δ 4.27 (d, J = 4.4 Hz, 1H, H-2), 4.20 (d, J = 4.40 Hz, 1H, H-1), 3.65-3.61 (dd, J = 11.7, 6.60 Hz, 1H, H-4), 3.01-2.99 (dd, J = 11.7, 3.4 Hz, 1H, H-5), 2.42-2.39 (dd, 6.6 Hz, 3.4 Hz, 1H, H-3), 1.00 (d, J = 7.3 Hz, 3H, methyl). ¹³C-NMR (500 MHz, D₂O) ppm 170.7, 76.3, 65.0, 49.8, 40.6, 15.4. HRMS *m/e* calcd. For C₆H₁₂NO₃ = 146.0817, found 146.0829. [α]_{Na}²² = -12° (c = 0.31, H₂O).

(2S, 3S, 4R)-N-Cbz-3-hydroxy-4-phenoxy-proline and (2S, 3S, 4S)-N-Cbz-3-phenoxy-4-hydroxy-proline: BRL: 272

To a round bottom flask containing 1.00 g (7.34 eq; 10.6 mmol) of phenol in 4 mL dry THF (distilled) was added 0.245 g (0.95 eq) of NaH slowly. The flask was then cooled over ice bath and argon balloon. To this mixture was added 0.381 g (1.45 mmol) N-Cbz-*trans*-3,4-epoxy-L-proline **13c** in 2 mL dry THF (distilled) at 0°C. The mixture was then allowed to warm to rt and then heated to reflux under condenser and argon balloon and

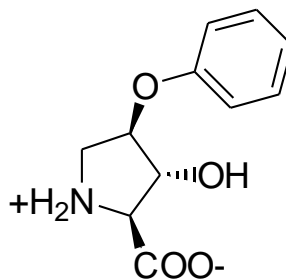
stirred overnight. The reaction was then cooled on ice bath and 20 mL of 10% H₃PO₄ (aq) was added to quench the reaction. The mixture was then salted with NaCl until saturated and extracted with EtOAc (3 x 100 mL). The organic extracts were combined, dried over NaSO₄, and concentrated to a crude solid residue. The products, 0.330 g of (2S, 3S, 4R)-N-Cbz-3-hydroxy-4-phenoxy-proline and (2S, 3S, 4S)-N-Cbz-3-phenoxy-4-hydroxy-proline (12:1 respectively) were isolated as a regioisomer mixture by silica gel (50% hexanes, 49% ethyl acetate, 1% AcOH) and (96% CH₂Cl₂, 3% MeOH, 1% AcOH) from two columns to afford the product, a 64% yield not including recovered starting material. The regioisomer mixture was used in the next step without further purification.



CSE117

Chemical Formula: C₁₁H₁₃NO₄

Molecular Weight: 223.23



CSE118

Chemical Formula: C₁₁H₁₃NO₄

Molecular Weight: 223.23

(2S, 3S, 4R)-3-hydroxy-4-phenoxy-proline and (2S, 3S, 4S)-3-phenoxy-4-hydroxy-proline: BRL: 279 / CSE118 and CSE117

To a 0.550 g (1.54 mmol) regioisomer mixture of (2S, 3S, 4R)-N-Cbz-3-hydroxy-4-phenyl-proline and (2S, 3S, 4R)-N-Cbz-3-phenyl-4-hydroxy-proline was added 10 mL

MeOH. The mixture was transferred to a pressure flask containing 83.0 mg (0.15 eq. weight) 10% Pd/carbon, 0.2 mL H₂O and 60.0 mg (0.5 eq: 0.77 mmol) NH₄OAc. The flask was placed on a Parr shaker, the air was removed by vacuum, and replaced by 50 psi H₂ (g). The apparatus was allowed to shake overnight at rt. The pressure flask was vented and the contents were diluted with 30 mL water and filtered through CM-cellulose using excess water for consecutive washes. The filtrate was then frozen and lyophilized until dry. The remaining residue was washed with 1:1 EtOAc / CH₂Cl₂ (3 x 20 mL), and dried leaving 0.308 mg of an off white solid, a crude mixture of (2S, 3S, 4R)-3-hydroxy-4-phenoxy-proline and (2S, 3S, 4S)-3-phenoxy-4-hydroxy-proline, regioisomeric ratio of 12:1 respectively and a (90% yield). Additionally, there was a large recovery of unreacted starting material from the organic washes. A portion of the product mixture was separated by reverse phase HPLC (C18, 250mm x 21.2mm, 10 μ) (92% 0.05 M NH₄OAc, 8% acetonitrile, 9 mL/min). Collected fractions containing a single isomer were combined and concentrated by lyophilization. Once dry, 20 mL of water was added to redissolve the remaining residue and the solution was again frozen and lyophilized until dry (removes remaining NH₄OAc). This was repeated until NH₄OAc was no longer present leaving (2S, 3S, 4R)-3-hydroxy-4-phenoxy-proline (CSE118) or (2S, 3S, 4S)-3-phenoxy-4-hydroxy-proline (CSE117) as a white solid.

(2S, 3S, 4S)-3-phenoxy-4-hydroxy-proline : CSE117

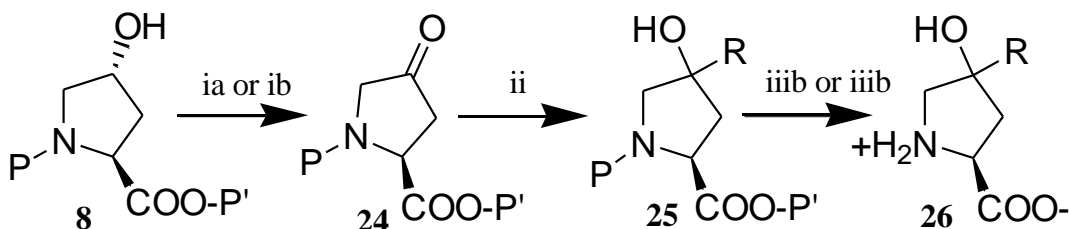
¹H-NMR (500 MHz, D₂O 4.75) δ 7.33-7.30 (dd, J = 7.6, 7.6 Hz, 2H), 7.05-7.02 (dd, J = 8.1, 7.6 Hz, 1H), 7.00-6.98 (d, J = 8.1 Hz, 2H), 5.00 (d, J = 4.3 Hz, 1H, H-2), 4.59 (d, J = 4.3 Hz, 1H, H-1), 4.56 (d, J = 4.0 Hz, 1H, H-3), 3.73-3.69 (dd, J = 13.0, 4.0 Hz, 1H, H-5), 3.36 (d, J = 13.0 Hz, 1H, H-4). ¹³C-NMR (500 MHz, D₂O) δ 169.6, 156.1, 129.8, 122.5, 115.9, 81.2, 71.8, 64.2, 51.0. HRMS *m/e* calcd. For C₁₁H₁₄NO₄ = 224.0923, found 223.0911. [α]_{Na}²² = -15° (c = 0.08, EtOH).

(2S, 3S, 4R)-3-hydroxy-4-phenoxy-proline : CSE118

¹H-NMR (500 MHz, D₂O 4.75) δ 7.33-7.30 (dd, J = 7.3, 7.3 Hz, 2H), 7.04-7.01 (dd, J = 8.3, 7.3 Hz, 1H), 6.93-6.92 (d, J = 8.3 Hz, 2H), 4.92 (d, J = 3.0 Hz, 1H, H-3), 4.67 (s, 1H, H-2), 4.10 (s, 1H, H-1), 3.76-3.73 (dd, J = 13.2, 3.0 Hz, 1H, H-4), 3.72-3.70 (d, J = 13.2 Hz, 1H, H-5). ¹³C-NMR (500 MHz, D₂O) δ 173.0, 157.8, 132.4, 125.0, 118.4, 81.9, 78.1, 70.3, 51.7. HRMS *m/e* calcd. For C₁₁H₁₄NO₄ = 224.0923, found 224.0937. [α]_{Na}²² = -81° (c = 0.1, EtOH).

Synthesis section 6

Procedure for synthesis of 4,4-alkyl-hydroxy-L-prolines



R = any alkyl or aryl group
P = trityl or Cbz protected
P' = H or ethyl ester

Scheme 5: Synthesis of 4-substituted-4-hydroxy-L-prolines. (ia) CrO_3 , H_2SO_4 , Acetone or (ib) Swern oxidation; (ii) organometallic / CuBr or CuCN catalyst (2eq.), Et_2O , -20°C ; (iiiia) 10% Pd/C (.10% weight. eq.), H_2 , MeOH , H_2O , NH_4^+ Acetate or (iiib) 1. KOH , THF ; 2. HCl , THF .

Protected 4-hydroxy-proline **8**, N-trityl and ethyl ester or N-Cbz, was converted to the 4-keto-proline **24** by either Swern oxidation or Jones oxidation respectively, in good yield 80-85% (**Scheme 5**) [Bridges *et al* 1991]. Depending upon the protection group employed, triphenylmethyl (trityl) or Cbz, the stereochemistry of geminal addition via Grignard reagent to the 4-carbonyl was controlled. Geminal addition to a N-trityl protected 4-keto-proline was selective preferring the *trans*-alcohol product, whereas, addition to a N-Cbz protected 4-keto-proline was selective preferring the *cis* product, with no detectable trace of a contaminating diastereomer. The final protect **26** was obtained after deprotection under standard conditions and ion exchange. Briefly, *trans*-4-hydroxy-L-proline was protected under via 1.) thionyl-chloride, EtOH ; 2.) triphenylmethylchloride, triethylamine, CH_2Cl_2 at 22°C to produce N-trityl-*trans*-4-

hydroxy-L-proline ethyl ester or benzylchloroformate, NaOH, H₂O, 22°C to produce N-Cbz-*trans*-4-hydroxy-L-proline. The protected 4-hydroxy proline was then oxidized to the 4-keto-proline via Swern oxidation (1. Oxalyl chloride, DMSO 2. TEA) (if trityl protecting group was present) or by Jones oxidation (CrO₃, H₂SO₄, Acetone) (if Cbz protecting group was present) and isolated by silica gel. The isolated protected 4-keto-proline was then transformed to the 4-alkyl-4-hydroxy proline via Cu(I) catalyzed (R₂CuMgBr) Grignard or organo lithium (R₂CuLi) addition at -20°C in Et₂O. Importantly, it was necessary to isolate the product by silica gel with 1% triethylamine (TEA) immediately after the Grignard or organo lithium addition reaction when N-trityl-4-keto-proline was used as a starting material so as to prevent decomposition. Once isolated, the product was then deprotected under standard conditions using 1.2 eq. KOH in THF at 22°C to hydrolyze the ethyl ester of N-trityl-4,4-alkyl-hydroxy-proline followed by dilute HCl 1.2 eq. in THF at rt and isolated by washing with 1:1 EtOAc, CH₂Cl₂ and ion exchange. Alternatively, N-Cbz-4,4-alkyl-hydroxy-proline was deprotected by hydrogenolysis with 10% Pd/carbon (0.1 eq) at 22°C in MeOH and isolated by washing with 1:1 EtOAc, CH₂Cl₂ and ion exchange. The final product dissolved in water / buffer from the ion exchange, regardless of the protection groups used, was then concentrated by lyophilization to a dry solid.

N-Trityl-4-keto-L-proline ethyl ester: BRL: 41

To a 100 mL round bottom flask containing 20 mL CH₂Cl₂ was added 0.54 mL (6.20 mmol; 1.2 eq) of COCl₂ in 2 mL CH₂Cl₂. The flask was then chilled to -60°C (acetone bath and cold finger) under argon balloon. To this was added 0.88 mL dry (molecular sieve treated) DMSO in 1 mL dry (MgSO₄ treated) CH₂Cl₂ drop wise. The mixture was allowed to stir for 15 min before being brought up to -30°C where 2.02 g (6.17 mmol) of N-trityl-*trans*-4-hydroxy-L-proline ethyl ester in 4 mL CH₂Cl₂ was added dropwise over 10 min. The resulting solution was allowed to stir for 1 h at -30°C under argon balloon. To complete the reaction, 3.6 mL (> 5 eq) of triethylamine was slowly added. The flask was then allowed to warm to rt where 100 mL of water was added. The mixture was then extracted with Et₂O (3 x 100 mL). The organic extracts were combined, dried with Na₂SO₄ and concentrated via rotovap to a solid crude. The remaining crude was then immediately separated by silica gel (90% hexanes, 9% ethylacetate, 1% TEA, R_f = 0.2). The fractions containing the product were combined, concentrated, and placed on a high vacuum pump leaving 1.51 g of N-trityl-4-keto-L-proline ethyl ester, as a white foam, a yield of 75%. This product, once isolated, was then used within 4-6 h in the addition step (trityl group readily decomposes) without further purification.

¹H-NMR (400 MHz, CDCl₃ at 7.27 ppm) δ 7.58-7.56 (d, J = 8.1 Hz, 6H), 7.31-7.19 (m, 9H), 4.30-4.18 (m, 3H), 3.86-3.81 (d, J = 19.8 Hz, 1H), 3.54-3.49 (d, J = 19.8 Hz, 1H), 1.88-1.84 (d, J = 18.3 Hz, 1H), 1.34-1.31 (dd, J = 13.9, 6.6 Hz, 3H), 1.12-1.05 (dd, J =

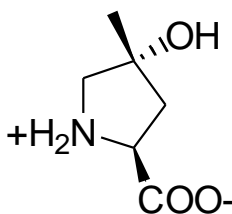
18.3, 10.3, 1.5 Hz, 1H). ^{13}C -NMR (400 MHz, CDCl_3 at 77.00 ppm) δ 215.7, 173.5, 143.6, 128.88, 128.2, 127.9, 126.8, 77.9, 61.1, 60.1, 57.1, 40.2, 14.2.

N-Trityl-*cis*-4-methyl-*trans*-4-hydroxy-L-proline ethyl ester: BRL: 70

To a flame dried / argon purged flask containing 0.123 g (5.00 mmol; 2 eq) of Mg metal in 2 mL diethyl ether was added 0.315 mL (5.00 mmol; 2 eq) of iodomethane over 10 min. The mixture was allowed to stir for ~ 20 min until when it was observed that most or all of the Mg metal was consumed. The flask was cooled to -20°C under argon balloon where it was then transferred to a flask containing 0.359 mg (2.5 mmol; 1 eq) of Cu(I)Br (dried by vacuum) at -20°C . The mixture was allowed to stir for ~15 min. after which 1.00 g (2.50 mmol) of N-trityl-4-keto-L-proline ethyl ester in 6 mL dry Et_2O was added and allowed to stir overnight. The reaction was then quenched by the addition of 15 mL saturated NH_4Cl solution, and diluted with 100 mL Et_2O . The organic phase was washed with water (3 x 100 mL), dried over Na_2SO_4 and concentrated via rotovap to a light brown foam. Immediately following the addition step the product, 0.624 g N-Trityl-*cis*-4-methyl-*trans*-4-hydroxy-L-proline ethyl ester, was isolated by a silica gel (95% hexanes, 4% ethyl acetate, 1% TEA; $R_f = 0.12$), a yield of 60%.

^1H -NMR (400 MHz, CDCl_3 at 7.27 ppm) δ 7.61-7.60 (d, $J = 7.3$ Hz, 6H), 7.32-7.28 (dd, $J = 8.1, 7.3$ Hz, 6H), 7.21-7.18 (dd, $J = 7.3$ Hz, 3H), 4.03-3.90 (m, 3H), 3.63-3.60 (d, $J = 12.4$ Hz, 1H), 2.99-2.96 (d, $J = 12.4$ Hz, 1H), 1.93-1.88 (dd, $J = 13.2, 6.6$ Hz, 1H), 1.71-

1.31 (dd, J = 13.2, 8.1 Hz, 1H), 1.25 (s, 3H), 1.15-1.12 (dd, J = 7.3, 7.3 Hz, 3H). ¹³C-NMR (400 MHz, CDCl₃ at 77.00 ppm) δ 175.9, 144.0, 129.4, 127.8, 126.5, 77.8, 77.3, 63.7, 62.1, 60.4, 46.7, 26.2, 14.0.



CSE95
Chemical Formula: C₆H₁₁NO₃
Molecular Weight: 145.16

***cis*-4-methyl-*trans*-4-hydroxy-L-proline:** BRL: 71 / CSE95

To 0.111 g (0.276 mmol) of N-Triptyl-*cis*-4-methyl-*trans*-4-hydroxy-L-proline ethyl ester was added 2 mL of THF, 0.2 mL H₂O and 20.0 mg (90%, 1.2 eq) KOH. The mixture was allowed to stir for 2 h at rt. The solution was then concentrated to a solid residue by rotovap, and washed with water (2 x 10 mL). The remaining residue was resuspended in 2 mL THF and 0.33 mL (2.5 eq) of 2 M HCl was added. After 1 h of stirring the solution was diluted with 10 mL water. The THF was removed by rotovap leaving mostly water and dissolved product. The sample was frozen and lyophilized to concentrate. The remaining residue was washed 1:1 EtOAc / CH₂Cl₂ (3 x 10 mL). The sample was then diluted with 5 mL water and isolated by cation exchange resin (sulphonic acid resin) using 10% NH₄OAc to elute the final product, *cis*-4-methyl-*trans*-4-hydroxy-L-proline.

The collected fractions were combined and concentrated by lyophilization to afford 32 mg of the product, an 83% yield.

$^1\text{H-NMR}$ (500 MHz, D_2O at 4.75) δ 4.30-4.25 (dd, $J = 10.4, 7.8$ Hz, 1H, H-1), 3.22 (s, 2H, H-4 & 5), 2.40-2.34 (dd, $J = 13.6, 8.4$ Hz, 1H, H-2), 1.98-1.92 (dd, $J = 13.6, 10.4$ Hz, 1H, H-3), 1.38 (s, 3H). $^{13}\text{C-NMR}$ (500 MHz, D_2O) δ 175.1, 78.0, 61.0, 56.8, 42.9, 22.9. HRMS m/e calcd. For $\text{C}_6\text{H}_{12}\text{NO}_3 = 146.0817$, found 146.0803. $[\alpha]_{\text{Na}}^{22} = -60^\circ$ ($c = 0.35$, MeOH).

N-Cbz-4-keto-L-proline ethyl ester: BRL: 47

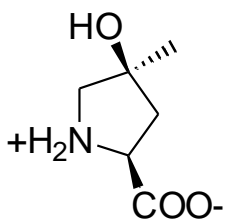
To a round bottom flask containing 14.0 g (52.8 mmol) of N-Cbz-4-hydroxy-L-proline **8** was added 26 mL acetone. The solution was cooled on ice bath where 8.12 mL (0.106 mmol; 2 eq) of Jones reagent (CrO_3 , H_2SO_4 , 1.3 M in water) was added. The mixture was allowed to warm to rt and stir for 3 h where the reaction appeared to be complete, as determined by TLC. The reaction was quenched by the addition of 6 mL isopropanol. After stirring for another 2 h the flask was placed on a glass socket rotovap and the isopropanol/acetone was removed by reduced pressure. The remaining green residue was then diluted into 200 mL water, salted with NaCl and extracted with EtOAc (3 x 200 mL). The organic extracts were combined, dried with MgSO_4 , filtered and concentrated to an oil. The remaining yellow oil was then separated by silica gel (90% CH_2Cl_2 , 9%

MeOH, 1% AcOH, $R_f = 0.3$). The fractions containing the product were combined and concentrated by rotovap to a solid residue and then recrystallized from CH_2Cl_2 leaving 9.86 g (37.5 mmol) of N-Cbz-4-keto-L-proline, a 71% yield. The product material was used in the next synthetic step without further purification.

N-Cbz-*trans*-4-methyl-*cis*-4-hydroxy-L-proline: BRL: 53

To a flame dried / argon purged flask containing 0.231 g (9.40 mmol; 2.5 eq) Mg metal in 2 mL dry diethyl ether was added 0.530 mL (8.40 mmol; 2.2 eq) of iodomethane slowly. The mixture was allowed to stir for ~ 20 min until when it was observed that most or all of the Mg metal was consumed. The mixture was then cooled to -20°C under argon balloon. To this prepared Grignard was added 1.00 g (2.50 mmol) of N-Cbz-4-keto-L-proline in 5 mL cold dry Et_2O . The mixture was allowed to return to rt and then refluxed for 2 h. The reaction was then quenched by the addition of 15 mL saturated NH_4Cl aq and allowed to stir an additional 30 min. The mixture was then acidified with HCl to pH ~2, salted with NaCl and extracted with EtOAc (3 x 100 mL). The organic extracts were then combined, dried with MgSO_4 , filtered, and concentrated to a light brown residue. The product, 0.440 g (1.58 mmol) of N-Cbz-*trans*-4-methyl-*cis*-4-hydroxy-L-proline, was isolated by a silica gl (85% CH_2Cl_2 , 14% MeOH, 1% AcOH; $R_f = 0.25$) with a yield of 41%; not including full recovery of unreacted starting material. The isolated product was then used in the next deprotection step without further purification.

$^1\text{H-NMR}$ (400 MHz, CDCl_3 at 7.27 ppm) δ 8.73 (b, 1H), 7.33-7.27 (m, 5H), 5.18-5.07 (m, 2H), 4.48-4.42 (dd, $J = 15.4, 8.8$ Hz, 1H), 3.70-3.64 (dd, $J = 11.7$ Hz, 1H), 3.37-3.32 (dd, $J = 10.3$ Hz, 1H), 2.25-2.15 (m, 2H), 1.37-1.35 (d, $J = 8.1$ Hz, 3H). $^{13}\text{C-NMR}$ (400 MHz, CDCl_3 at 77.00 ppm) (2 conformational isomers) δ 176.8 and 176.6, 155.4 and 154.8, 135.9, 128.4 and 128.3, 128.0, 127.8 and 127.6, 76.8 and 76.2, 67.5 and 67.4, 59.4 and 59.3, 58.8 and 58.5, 43.4 and 42.4, 24.2 and 20.6.



CSE96

Chemical Formula: $\text{C}_6\text{H}_{11}\text{NO}_3$

Molecular Weight: 145.16

cis-4-hydroxy-trans-4-methyl-L-proline: BRL: 56 / CSE96

To 0.200 g (0.716 mmol) of N-Cbz-*cis-4-hydroxy-trans-4-methyl-L-proline* was added 2 mL MeOH which was transferred to a pressure flask containing 50 mg 10% Pd/carbon and 0.2 mL H_2O . This was then connected to a Parr shaker and the air was removed by vacuum. The container was filled with 50 psi H_2 (g) and the apparatus was allowed to shake overnight. The flask was then vented and the contents were diluted with 20 mL water and filtered through CM-cellulose. The filtrate was then frozen and concentrated by lyophilization to a light brown residue that was then washed with 1:1 EtOAc : CH_2Cl_2

(3 x 10 mL). The sample was then diluted with 5 mL water and isolated by cation exchange resin (sulphonic acid resin) using 10% ammonium acetate to elute the final product. The collected fractions were combined and concentrated by lyophilization to afford 62 mg of *cis*-4-hydroxy-*trans*-4-methyl-L-proline, a 60% yield.

¹H-NMR (400 MHz, D₂O 4.75) δ 4.55-4.52 (dd, J = 9.1, 3.9 Hz, 1H, H-1), 3.37-3.34 (d, J = 11.6 Hz, 1H, H-5), 3.20-3.17 (d, J = 12.3, 1H, H-4), 2.35 (m, H-2 and 3), 1.36 (s, 3H).
¹³C-NMR (500 MHz, D₂O) δ 76.8, 59.4, 57.1, 41.9, 22.4. HRMS *m/e* calcd. For C₆H₁₂NO₃ = 146.0817, found 146.0823. [α]_{Na}²² = -44° (c = 0.39, MeOH).

Albers, A.; Broer, A.; Wagner, C.A.; Setiawan, I.; Lang, P.A.; Kranz E.U.; Lang, F.; Bröer, S. Na⁺ transport by the neural glutamine transporter ATA1. *Pflugers. Arch. Eur J Physiol* **2001**, 443, 92–101.

Albrecht, J.; Sonnewald, U.; Waagepetersen, H.S.; Schousboe, A. Glutamine in the central nervous system: function and dysfunction. *Front Biosci* **2007**, 12, 332-343.

Allen N.J.; Karadottir, R.; Attwell, D.; Reversal or reduction of glutamate and GABA transport in CNS pathology and therapy. *Pflugers Arch. -Eur. J. Physiol.* **2004**, 449, 132-142.

Armano, S.; Matteoli, M.; et al. Localization and functional relevance of system A neutral amino acid transporters in cultured hippocampal neurons. *J. Biol. Chem.* **2002**, 277, 12, 10467-10473.

Arriza, J.L.; Kavanaugh, M.P.; Fairman, W.A.; Wu, Y.; Murdoch, G.H.; North, R.A.; Amara, S.G. Cloning and expression of a human neutral amino acid transporter with structural similarity to the glutamate transporter gene family. *J. Biol. Chem.* **1993**, 268, 15329-15332.

Arriza, J. L., W. A. Fairman, J. I. Wadiche, G. H. Murdoch, M. P. Kavanaugh and S. G. Amara 1994. Functional comparisons of three glutamate transporter subtypes cloned from human motor cortex. *J Neurosci* **14(9)**: 5559-69.

Bak, L.K.; Schousboe, A.; Waagepetersen, H.S. The glutamate/GABA-glutamine cycle: aspects of transport, neurotransmitter homeostasis and ammonia transfer. *J Neurochem* **2006**, 98, 641-653.

Baggetto, L.G. Deviant energetic metabolism of glycolytic cancer cells. *Biochimie* **1992**, 74(11), 959-974.

Barker, G.A.; and Ellory, J.C. The identification of neutral amino acid transport systems. *Exp. Physiol.* **1990**, 75, 3-26.

Bendahan, A.; Armon, A.; Madani, N.; Kavanaugh, M.P.; Kanner, B.I. Arginine 447 plays a pivotal role in substrate interactions in a neuronal glutamate transporter. *J. Biol. Chem.* **2000**, 275, 48, 37436-37442.

Berl, S.; Nicklas, W.J.; Clarke, D.D. Compartmentation of glutamic acid metabolism in brain slices. *J. Neurochem.* **1968**, 15, 131-140.

Bode, B.P.; Fuchs, B.C.; Hurley, B.P.; Conroy, J.L.; Suetterlin, J.E.; Tanabe, K.K.; Rhoads, D.B.; Abcouwer, S.F.; and Souba, W.W. Molecular and functional analysis of glutamine uptake in human hepatoma and liver-derived cells. *Am. J. Physiol. Gastrointest. Liver Physiol.* **2002**; 293: 1062-73.

Bradford, H.F.; Ward, H.K.; Foley, P. Glutaminase inhibition and the release of neurotransmitter glutamate from synaptosomes. *Brain. Res.* **1989**, 476, 29-34

- Bridges, R.J.; Esslinger, C.S. The excitatory amino acid transporters: pharmacological insights on substrate and inhibitor specificity of the EAAT subtypes. *Pharmacol. Ther.*, **2005**; 107 (3), 271-285
- Bode, B.P.; Kaminski, D.L.; Souba, W.W.; Li, A.P. Glutamine transport in isolated human hepatocytes and transformed liver cells. *Hepatology* **1995**, 21, 511-520.
- Boudker, O.; Ryan, R.M.; Yernool, D.; Shimamoto, K.; Gouaux, E. Coupling substrate and ion binding to extracellular gate of a sodium-dependent aspartate transporter. *Nature* **2007**, 445, 387-393.
- Bridges, R.J.; Stanley, M.S.; Anderson, M.W.; Cotman, C.W.; Chamberlin, R.A. Conformationally defined neurotransmitter analogues. Selective inhibition of glutamate uptake by one pyrrolidine-2,4-dicarboxylate diastereomer. *J. Med. Chem.* **1991**, 34, 717-725.
- Bröer, A.; Wagner, C.; Lang, F.; Bröer, S. Neutral amino acid transporter ASCT2 displays substrate-induced Na⁺ exchange and a substrate-gated anion conductance. *J. Biochem.* **2000**, 346, 705-710.
- Bröer, A.; Brookes, N.; Ganapathy, V.; Dimmer, K.S.; Wagner, C.A.; Lang, F.; Bröer, S. The astroglial ASCT2 amino acid transporter as a mediator of glutamine efflux. *J. Neurochem.* **1999**, 73, 2184-2194.
- Bröer, S.; Brookes, N. Transfer of glutamine between astrocytes and neurons. *J. Neurochem.* **2001**, 77, 705-719.
- Bröer, S. Adaptation of plasma membrane amino acid transport mechanisms to physiological demands. *Pflugers Arch. Eur J Physiol* **2002**, 444, 457-466.
- Chaudhry, F.A.; Schmitz, D.; Reimer, R.J.; Larsson, P.; Gray, A.T.; Nicoll, R.; Kavanaugh, M.; Edwards, R.H. Glutamine uptake by neurons: interaction of protons with System A transporters. *J. Neurosci.* **2002**, 22, 62-72.
- Chaudhry F.A.; Reimer, R.J.; Krizaj, D.; Barber, D.; Storm-Mathisen, J.; Copenhagen, D.R.; Edwards, R.H. Molecular analysis of system N suggests novel physiological roles in nitrogen metabolism and synaptic transmission. *Cell* **1999**, 99, 769-780.
- Chaudhry, F.A.; Lehre, K.P.; Lookeren-Campagne, M.; Ottersen, O.P.; Danbolt, N.C.; Storm-Mathisen, J. Glutamate transporters in glial plasma membranes: highly differentiated localizations revealed by quantitative ultrastructural immunocytochemistry. *Neuron*. **1995**, 15, 711-720.
- Cheng Y.; Prusoff, W.H. Relationship between the inhibition constant (K_i) and the concentration of inhibitor, which causes 50 per cent inhibition (I₅₀) of an enzymatic reaction. *Biochem. Pharmacol.* **1973**, 22, 3099-3108.
- Christensen, H.N. Organic ion transport during seven decades: the amino acids. *Biochim. Biophys. Acta* **1984**, 779, 255-269.

- Christensen, H.N.; Liang, M.; Archer, E.G. *J. Biol. Chem.* **1967**, 242, 5237-5246.
- Conradt, M.; Stoffel, W. Functional analysis of the high affinity, Na⁺-dependent glutamate transporter GLAST-1 by site-directed mutagenesis. *J. Biol. Chem.* **1995**, 270 (42), 25207-25212.
- Conti, F.; Minelli, A. Glutamate immunoreactivity in rat cerebral cortex is reversible abolished by 6-diaz-5-oxo-L-norleucine (DON), an inhibitor of phosphate-activated Glutaminase. *J. Histochem. and Cytochem.* **1994**, 42 (6), 717-726
- Cousin, M.A.; Robinson, P.J. Two mechanisms of synaptic vesicle recycling in rat brain nerve terminals. *J. Neurochem.* **2000**, 75, 1645-1653.
- Danbolt, N.C. Glutamate uptake. *Prog. Neurobiol.* **2001**, 65 (1), 1-105
- Dolinska, M.; Albrecht, J.; et al. Glutamine transport in C6 glioma cells: Substrate specificity and modulation in a glutamine deprived culture medium. *J. Neurosci. Res.* **2001** 66, 959-966.
- Dolinska, M.; Zablocka, B.; Sonnewald, U.; Albrecht, J. Glutamine uptake and expression of mRNA's of glutamine transporting proteins in mouse cerebellar and cerebral cortical astrocytes and neurons. *Neurochem Int* **2004**, 44, 75-81.
- Dunlop, J.; Butera, J.A. Ligands targeting the excitatory amino acid transporters (EAATs). *Curr. Topics Med. Chem.* **2006**, 6, 1897-1906.
- Ennis, S.R.; Kawai, X.D.; Ren, G. E.; Abdelkarim and R. F. Keep. Glutamine uptake at the blood-brain barrier is mediated by N-system transport. *J NeuroChem* **1998**: 71 (6), 2565-73
- ErecinÂska, M.; Silver, I.A. Metabolism and the role of glutamate in mammalian brain. *Progr. Neurobiol.* **1990**, 35, 245-296.
- Esslinger, C.S.; Agarwal, S.; Gerdes, J.; Wilson, P.A.; Davis, E.S.; Awes, A.N.; O'Brien, E.; Mavencamp, T.; Koch, H.P.; Poulsen, D.J.; Rhoderick, J.F.; Chamberline, R.; Kavanaugh, M.P.; Bridges, R.J. The substituted aspartate analogue L-β-threo-benzyl-aspartate preferentially inhibits the neuronal excitatory amino acid transporter EAAT3. *NeuroPharm.* **2005**, 49, 850-861
- Esslinger, CS.; Cybulski, KA.; Rhoderick, JF. Nγ-Aryl glutamine analogues as probes of the ASCT2 neutral amino acid transporter binding site. *Bioorg. Med. Chem.* **2005**, 13, 1111-1118.
- Fuchs, B.C.; Bode, BP. Amino acid transporters ASCT2 and LAT1 in cancer: Partners in crime? *Seminars in Cancer Biol.* **2005**, 15, 254-266.
- Fuchs, B.C.; Finger, R.E.; Onan, M.C.; Bode, B.P. ASCT2 silencing regulates mammalian target-of-rapamycin growth and survival signaling in human hepatoma cells. *Am J Physiol Cell Physiol.* **2007**, 293, C55-C63.

Furuta, A.; Martin, L.J.; Lin, C.L.G.; Dykes-Hoberg, M.; Rothstein, J.B. Cellular and synaptic localization of the neuronal glutamate transporters excitatory amino acid transporter 3 and 4. *Neuroscience* **1997**, 81, 1031– 1042.

Gegelashvili, G.; and Schousboe, A. High affinity glutamate transporters: Regulation of expression and activity. *Mol Pharmacol* **1997**, **52**,6-15.

Gilman, H.; Jones, R.G.; Woods, L.A. The preparation of methylcopper and some observations on the decomposition of organocopper compounds. *J. Org. Chem.* **1952**, 17 (12), 1630–1634.

Gliddon, C.M.; Shao, Z.; LeMaistre, J.L.; Anderson, C.M.; Cellular distribution of neutral amino acid transporter subtype ASCT2 in mouse brain. *J. Neuro. Chem.* **2009**, 108, 372-383.

Greenfield, A.; Grosanu, C.; Dunlop, J.; McIlvain, B.; Carrick, T.; Jow, B.; Lu, Q.; Kowal, D.; Williams, J.; Butera, J.; Synthesis and biological activities of aryl-ether-, biaryl-, and fluorene-aspartic acid and diamino propionic acid analogs as potent inhibitors of the high-affinity glutamate transporter EAAT-2. *Bioorg. Med. Chem. Lett.* **2005**, 15, 4985-4988.

Grewer, C.; Grabsch, E.; New inhibitors for the neutral amino acid transporter ASCT2 reveal its Na⁺-dependent anion leak. *J. Physiol.* **2004**, 557.3, 747-759.

Heckel, T.; Bröer, A.; Wiesinger, H.; Lang, F.; Bröer, S. Asymmetry of glutamine transporters in cultured neural cells. *Neurochem. Intern.* **2003**, 43, 289-298.

Herdeis, C.; Aschenbrenner, A.; Kirfel, A.; Schwabenlander, F. Synthesis of trans-epoxy-L-proline and cis-aziridino-L-proline from S-pyroglutamic acid. Regio- and diastereoselective ring opening of its derivatives. *Tetrahedron: Asymm.* **1997**; 8, 2421-2432.

Hertz, L.; Dringen, R.; Schousboe, A.; Robinson, S.R. Astrocytes: glutamate producers for neurons. *J. Neurosci. Res.* **1999**, 57, 417–428.

Hu, W.; Zhang, C.; Wu, R.; Sun, Y.; Levine, A.; Feng, Z. Glutaminase 2, a novel p53 target gene regulating energy metabolism and antioxidant function. *Proc Natl Acad Sci* **2010**, 107 (16), 7455-7460.

Huang, X.; Luo, X.; Roupioz, Y.; Keillor, J.W. Controlled regioselective anilide formation from aspartic and glutamic acid anhydrides. *J. Org. Chem.* **1997**, 62, 8821-8825.

Jacobson, I.; Sandberg, M.; Hamberger, A. Mass transfer in brain dialysis devices ± a new method for the estimation of extracellular amino acids concentration. *J. Neurosci. Methods* **1985**, 15, 263-268.

Jenstad, M.; Chaudhry, F.A.; et al. System A transporter SAT2 mediates replenishment of dendritic glutamate pools controlling retrograde signaling by glutamate. *Cerebral Cortex* **2009**, 19, 1092-1106.

Katsuki, H.; Nonaka, M.; Shirakawa, H.; Kume, T.; Akaike, A. Endogenous D-serine is involved in induction of neuronal death by N-methyl- D-aspartate and simulated ischemia in rat cerebrocortical slices. *J Pharmacol Exp Ther* **2004**, 311, 836-844.

Katsuki H, Watanabe Y, Fujimoto S, Kume T, Akaike A. Contribution of endogenous glycine and d-serine to excitotoxic and ischemic cell death in rat cerebrocortical slice cultures. *Life Sci* **2007**, 81, 740-749.

Kam, K.; Nicoll, R.; Excitatory synaptic transmission persists independently of the glutamate-glutamine cycle. *J. Neurosci.* **2007**, 27, (34), 9192-9200.

Kanai, Y.; and Hediger, M.A. Primary structure and functional characterization of a high-affinity glutamate transporter. *Nature* **1992**, 360, 467-471.

Kanamori, K.; and Ross, B.D. Quantitative determination of extracellular glutamine concentration in rat brain, and its elevation in vivo by system A transport inhibitor, alpha-(methylamino) isobutyrate. *J. Neurochem.* **2004**, 90, 203-210.

Kanner, B.I.; Kavanaugh, M.P.; Bendahan, A. Molecular characterization of substrate-binding sites in the glutamate transporter family. *Biochem. Soc. Trans.* **2001**, 29, 707-710.

Kekuda, R.; Prasad, P.D.; Fei, Y.; Torres-Zamorano, V.; Sinha, S.; Yang-Feng, T.L.; Leibach, F.H.; Ganapathy, V. Cloning of the sodium-dependend, broad-scope, neutral amino acid transporter B from human placental choriocarcinoma cell line. *J. Biol. Chem.* **1996**, 271, 18657-18661.

Kilberg, M.S.; Handlogten, M.E.; Christensen, H.N. Characteristics of an amino acid transport system in rat liver for glutamine, asparagine, histidine, and closely related analogs. *J. Biol. Chem.* **1980**, 255, 4011-4019.

Koch, H.P.; Kavanaugh, M.P.; Esslinger, C.S.; Zerangue, N.; Humphrey, J.M.; Amara, S.G.; Chamberline, A.R.; Bridges, R.J. Differentiation of substrate and nonsubstrate inhibitors of the high-affinity, sodium-dependant glutamate transporters. *Mol. Pharmacol.* **1999**, 56, 1095-1104.

KyzioL, J.B.; LyznIak, A. 2-Aminocarbazole Synthesis. *Tetrahedron* **1980**; 36, 3017-3019.

Lehre, K.P.; Levy, L.M.; Ottersen, O.P.; Storm-Mathisen, J.; Danbolt, N.C. Differential expression of two glial glutamate transporters in the rat brain: quantitative and immunocytochemical observations. *J Neurosci.* **1995**, 15,1835-1853.

Lipshutz, B.H.; Wilhelm, R.S.; Kozlowski, J.A.; Parker, D. Substitution reactions of secondary halides and epoxides with higher order, mixed organocuprates, R₂Cu(CN)Li₂: synthetic, stereochemical, and mechanistic aspects. *J. Org. Chem.* **1984**; 49, 3928-3938.

Lipshutz, B.H.; Kozlowski, J.; Wilhelm, R.S. Chemistry of higher order mixed organocuprates, 2. Reactions of epoxides. *J. Am. Chem. Soc.* **1982**; 104, 2305-2307.

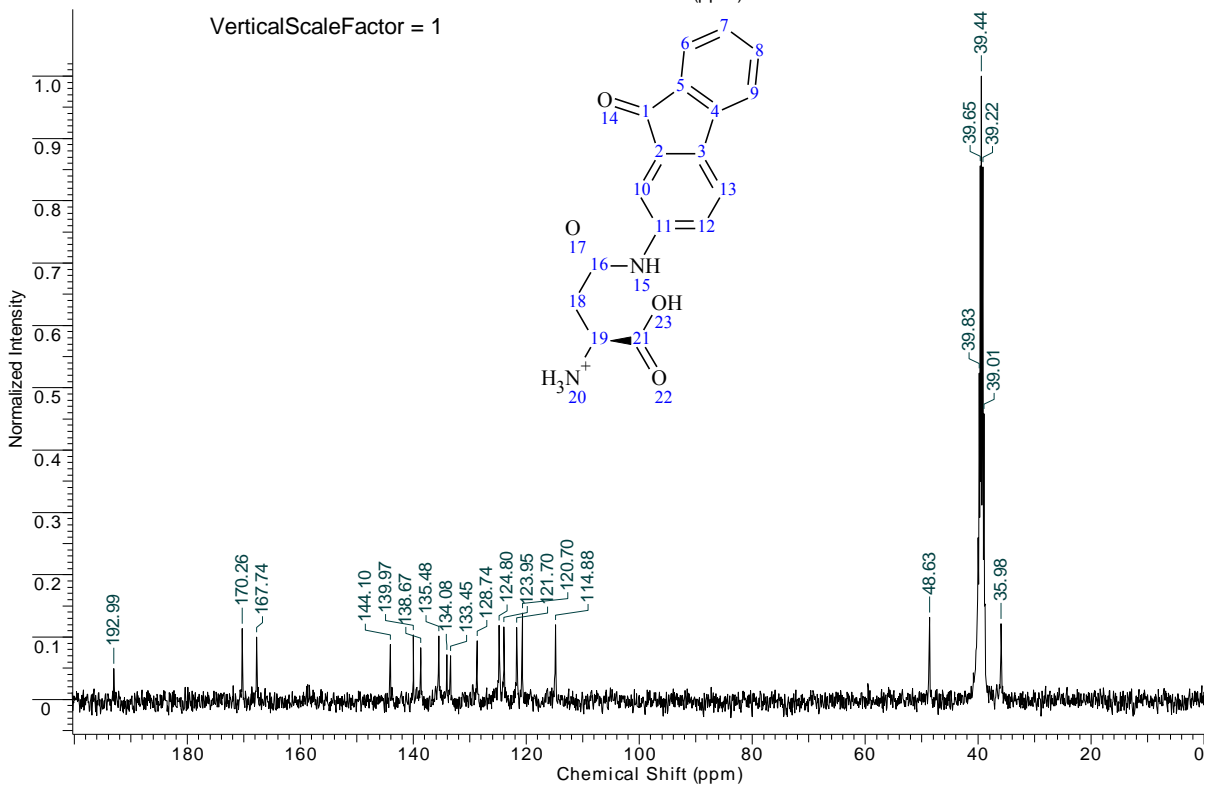
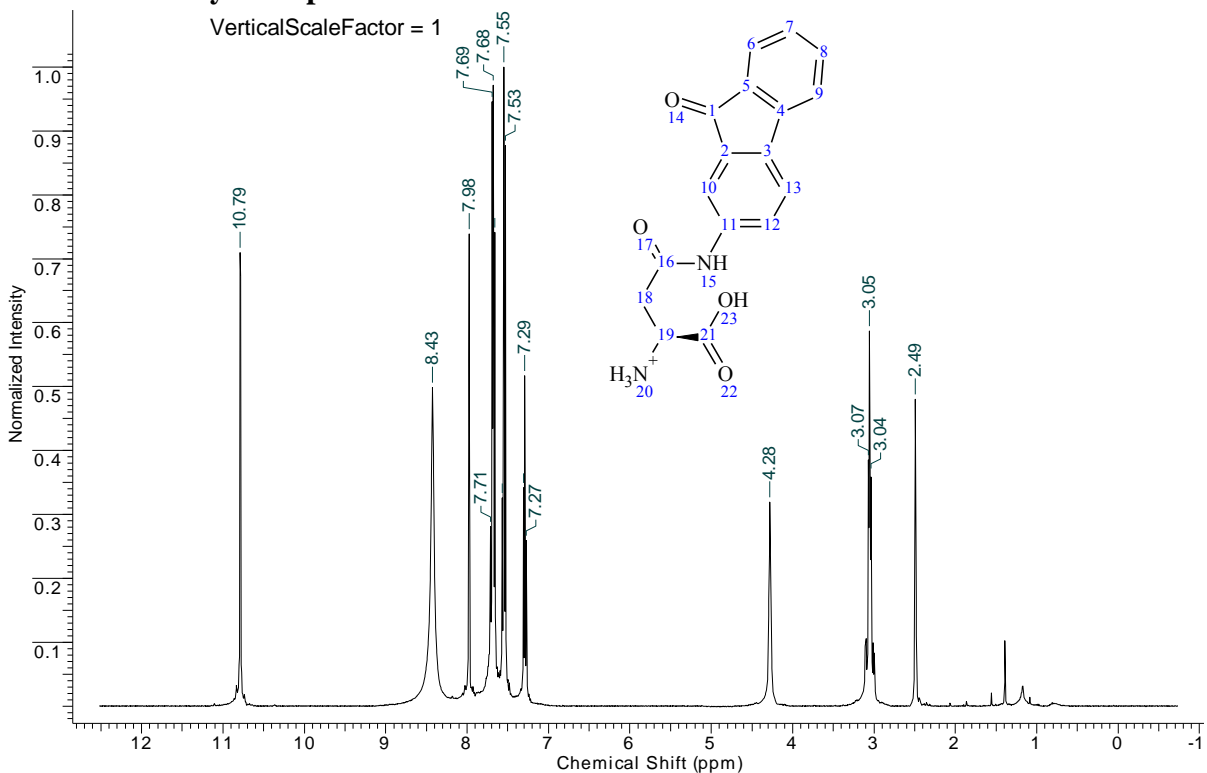
- Mackenzie, B.; Erickson, J.D. Sodium-coupled neutral amino acid (system N/A) transporters of the SLC38 gene family. *Eur. J. Physiol.* **2004**, 447, 784-795.
- Masson, J.; et al. Mice lacking brain/kidney phosphate-activated glutaminase have impaired glutamatergic synaptic transmission, altered breath, disorganized goal-directed behavior and die shortly after birth. *J Neurosci* **2006**, 26(17), 4660-4671.
- Mavencamp, T.L.; Rhoderick, J.F.; Bridges, R.J.; Esslinger, C.S. Synthesis and preliminary pharmacological evaluation of novel derivatives of L-beta-threo-benzylaspartate as inhibitors of the neuronal glutamate transporter EAAT3. *Bioorg. Med. Chem.* **2008**, 16, 7740-7748.
- Medina, M.A. Glutamine and Cancer. *J Nutr* **2001**, 131, 2539s-2542s.
- McGivan, J.D.; Bungard, C.I.; The transport of glutamine into mammalian cells. *Front. Biosci.* **2007**, 12, 874-882.
- Nieoullon, A.B.; Canolle, F.; Masméjean, B.; Guillet, P.; Pisano and S. Lortet. The neuronal excitatory amino acid transporter EAAC1/EAAT3: does it represent a major actor at the brain excitatory synapse? *J Neurochem.* **2006**, 98, 1007-1018.
- Nicklin, P.; Murphy, L.O. Bidirectional transport of amino acids regulates mTOR and autophagy. *Cell* **2009**, 136, 521-534.
- Papaloannou, D.; Stavropoulos, G.; Karagiannis, K.; Francis, G.W.; Brekke, T.; Aksnes, D.W. *Acta Chem. Scand.* **1990**, 44, 243-251.
- Pawlik, T.M.; Souba, W.W.; Sweeney, T.J.; Bode, B.P. Phorbol esters rapidly attenuate glutamine uptake and growth in human colon carcinoma cells. *J Surg Res* **2000**, 90, 149-55.
- Pinilla-Tenas, J.; Barber, A.; Lostao, M.P. Transport of proline and hydroxyproline by the neutral amino-acid exchanger ASCT1. *J. Membrane. Biol.* **2003**, 194, 27-32.
- Rae, C.; Hare, N.; Bubb, W.A.; McEwan, S.R.; Bröer, A.; McQuillan, J.A.; Balcar, V.J. Conigrave, A.D.; Bröer, S. Inhibition of glutamine transport deplete glutamate and GABA neurotransmitter pools: further evidence for metabolic compartmentation. *J Neurochem* **2003**, 85, 503-514.
- Robinson, J.K.; Lee, V.; Claridge, T.; Baldwin, J.E.; Schofield, C.J. Synthesis of (2S, 3R, 4S), (2S,3S, 4R)-Epoxyprolines and Aminohydroxyprolines. *Tetrahedron* **1998**, 54, 981-996.
- Rüeger, H.; Benn, M.H. The preparation of (S)-3,4-dehydroproline from (2S, 4R)-4-hydroxyproline. *Can. J. Chem.* **1982**, 60, 2918-2920.
- Sajiki, H. Selective inhibition of benzyl ether hydrogenolysis with Pd/C due to the presence of ammonia, pyridine or ammonium acetate. *Tet. Lett.* **1995**; 36, 3465-3468.

- Saroja, G.; Pingzhu, Z.; Ernsting, N.P.; Liebscher, J. Synthesis of alkylated aminofluorenes by palladium-catalyzed substitution at halofluorenes. *J. Org. Chem.* **2004**, 69, 987-990.
- Shank, R.P.; Aprison, M.H.; Present status and significance of the glutamine cycle in neural tissues. *Life Sci.* **1981**, 28, 837-842.
- Shao, Z.; Kamboj, A.; Anderson, C.M. Functional and immunocytochemical characterization of D-serine transporters in cortical neuron and astrocyte cultures. *J. Neurosci. Res.* **2009**, 87, 2520-2530.
- Shimamoto, K.; Lebrun, B.; Yasuda-Kamatani, Y.; Sakaitani, M.; Shigeri, Y.; Yumoto, N.; Nakajima, T. DL-threo-beta -benzyloxyaspartate, a potent blocker of excitatory amino acid transporters. *Mol. Pharmacol.* 1998, 53(2), 195-201.
- Shimamoto, K.; Sakai, R.; Takaoka, K.; Yumoto, N.; Nakajima, T.; Amara, S. G.; Shigeri, Y. Characterization of novel L-threo- β - benzyloxyaspartate derivatives, potent blockers of the glutamate transporters. *Mol. Pharmacol.* **2004**, 65(4), 1008-1015.
- Sugawara, M.; Nakanishi, T.; Fei, Y.J.; Huang, H.; Ganapathy, M.; Leibach, F.H.; Ganapathy, V. Cloning of an amino acid transporter with functional characteristics and tissue expression pattern identical to that of system A. *J Biol Chem.* **2000**, 275, 16473-16477.
- Takamori, S. VGLUTs: 'exciting' times for glutamatergic research? *Neuro. Research.* **2006**, 55, 343-51
- Tani, H.; Dulla, C.G.; Huguenard, J.R.; Reimer, R.J. Glutamine is required for persistent epileptiform activity in the disinhibited neocortical brain slice. *J. Neurosci.* **2010**, 30, (4), 1288-1300.
- Taylor, Richard J.K. *Organo Copper Reagents*; Oxford University Press, Oxford, **1994**.
- Teichman, S.; Kanner, B.I. Aspartate-444 is essential for productive substrate interactions in a neuronal glutamate transporter. *J. Gen. Physiol.* **2007**, 129, 527-539.
- Timko, Christopher A., Synthesis of novel N-Aryl asparagine analogues as inhibitors of glutamine transport by the neutral amino acid transporter SN1. *The University of Montana, Masters thesis.* **2005** Dec.
- Utsunomiya-Tate, N.; Endou, H.; Kanai, Y. Cloning and functional characterization of a system ASC-like Na⁺-dependent neutral amino acid transporter. *J. Biol. Chem.* **1996**, 271 (25), 14883-14890.
- Varoqui, H.; Zhu, H.; Yao, D.; Ming, H.; Erickson, J.D. Cloning and functional identification of a neuronal glutamine transporter. *J Biol Chem* **2000**, 275(6), 4049-4054.
- Walton, H.S.; Dodd, P.R. Glutamate-glutamine cyclin in Alzheimer's disease. *Neurochem Int* **2007**, 50, 1052-1066.

- Wasa, M.; Wang, H. S.; Okada, A. Characterization of L-glutamine transport by a human neuroblastoma cell line. *Am. J. Physiol. Cell. Physiol.* **2002**, 282, C1246–C1253.
- Witiak, D.T.; Muhi-Eldeen, Z.; Mashishi, N.; Sethi, O.P.; Gerald, M.C. L(S)- and D(R)-3-Amino-1-phenylpyrrolidines. Stereoselective antagonists for histamine and acetylcholine receptors in Vitro. *J. Med. Chem.* **1971**, 14, 24-30.
- Wu, V.W.; and Schwartz, J.P. Cell culture models for reactive gliosis: new perspectives. *J. Neurosci. Res.* **1998**, 51, 675-681.
- Xu, G.Y.; McAdoo, D.J.; Hughes, M.G.; Robak, G.; de Castro, R.Jr. Considerations in the determination by microdialysis of resting extracellular amino acid concentrations and release upon spinal cord injury. *Neuroscience* **1998**, 86, 1011-1021.
- Yamamoto, T.; Nishizaki, I.; Yamamoto, H.; et al. Characterization of rapid and high-affinity uptake of L-serine in neurons and astrocytes in primary culture. *FEBS Lett.* **2003**, 548, 69-73.
- Yang, C.P.; Su, C.S. Effects of solvents and additives on the reaction of N-benzyloxycarbonyl-L-aspartic anhydride with L-phenylalanine methyl ester (synthesis of aspartame). *J. Org. Chem.* **1986**; 51, 5186-5191.
- Yao, D.; Mackenzie, B.; Ming, H.; Varoqui, H.; Zhu, H.; Hediger, M.A.; Erickson, J.D.; A novel system A isoform mediating Na⁺/neutral amino acid cotransport. *J Biol Chem* **2000**, 275, 22790–22797.
- Yernool, D.; Boudker, O.; Jin, Y.; Gouaux, E. Structure of a glutamate transporter homologue from *Pyrococcus horikoshii*. *Nature* **2004**, 431, 811-818.
- Zerangue, N.; Kavanaugh, M.P. ASCT-1 is a neutral amino acid exchanger with chloride channel activity. *J. Biol. Chem.* **1996**, 271, 45, 27991-27994.
- Zielinska, M.; Stafiej, A.; Law, R.O.; Albrecht, J. Effects of methionine sulfoximine on the glutamine and glutamate content and cell volume in rat cerebral cortical slices: Involvement of mechanisms not related to inhibition of glutamine synthesis. *Neuro. Tox.* **2004**, 25, 443-449.

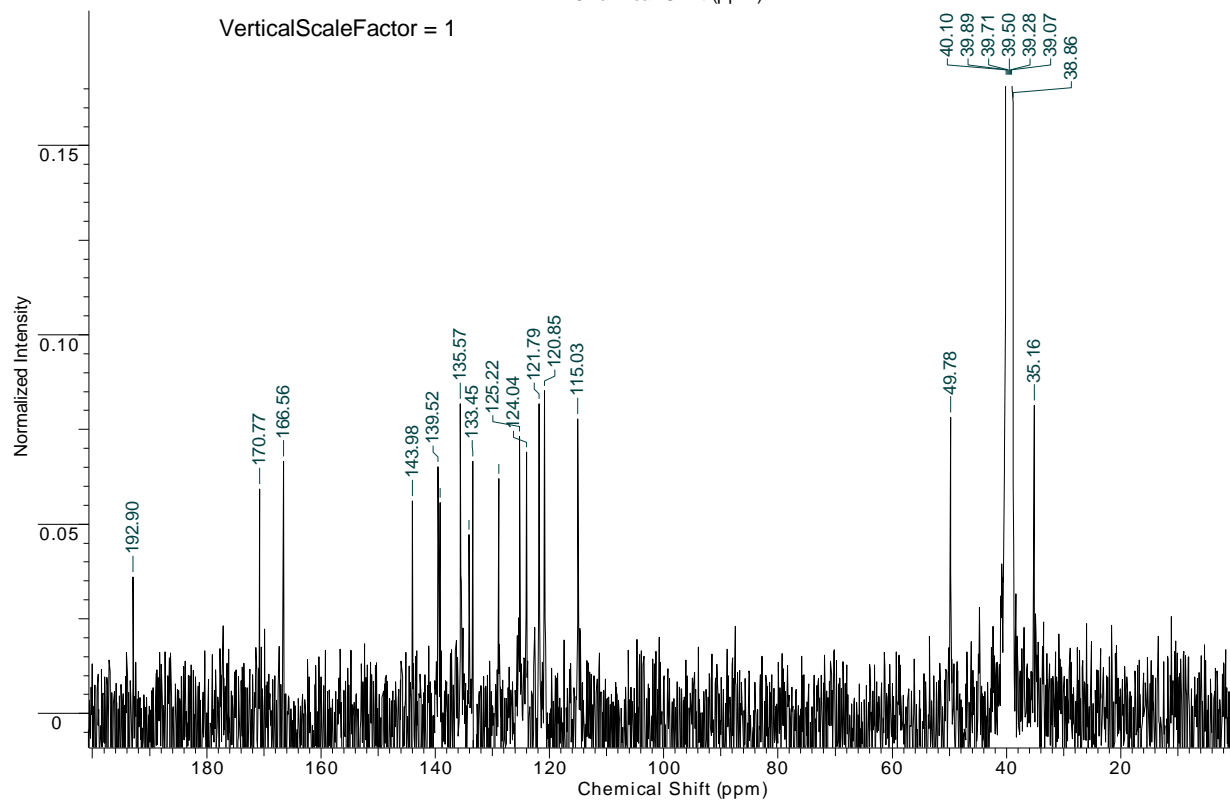
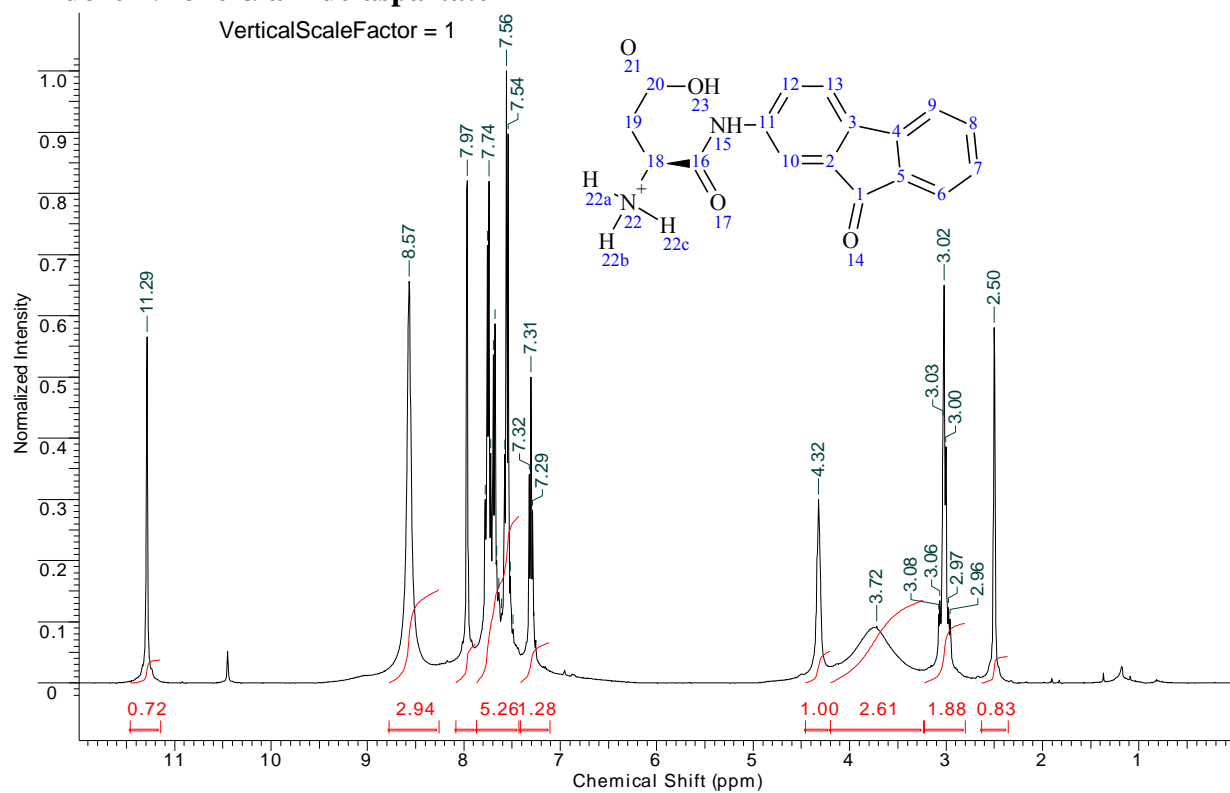
Appendix A: NMR spectra of final product β -aryl-aspartamides & α -aryl-amide aspartates

2-Fluorenon-9-yl-L-aspartamide



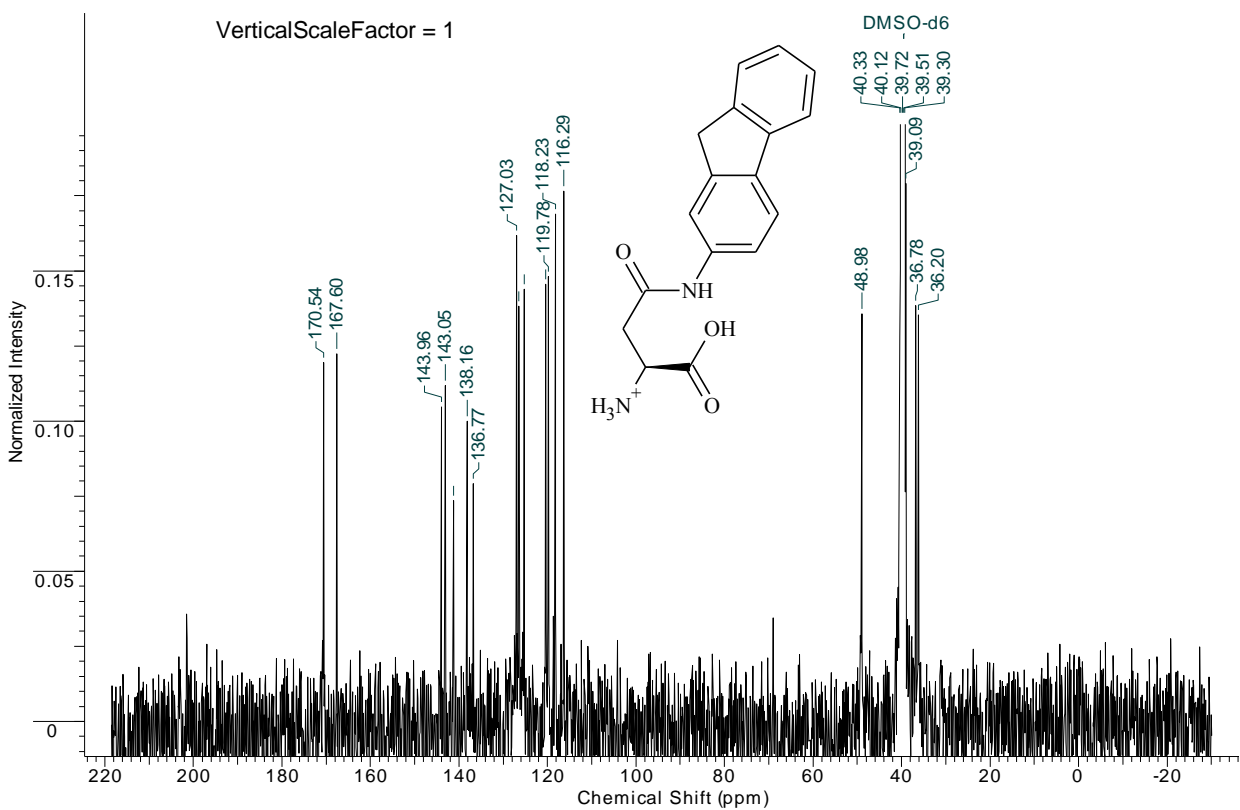
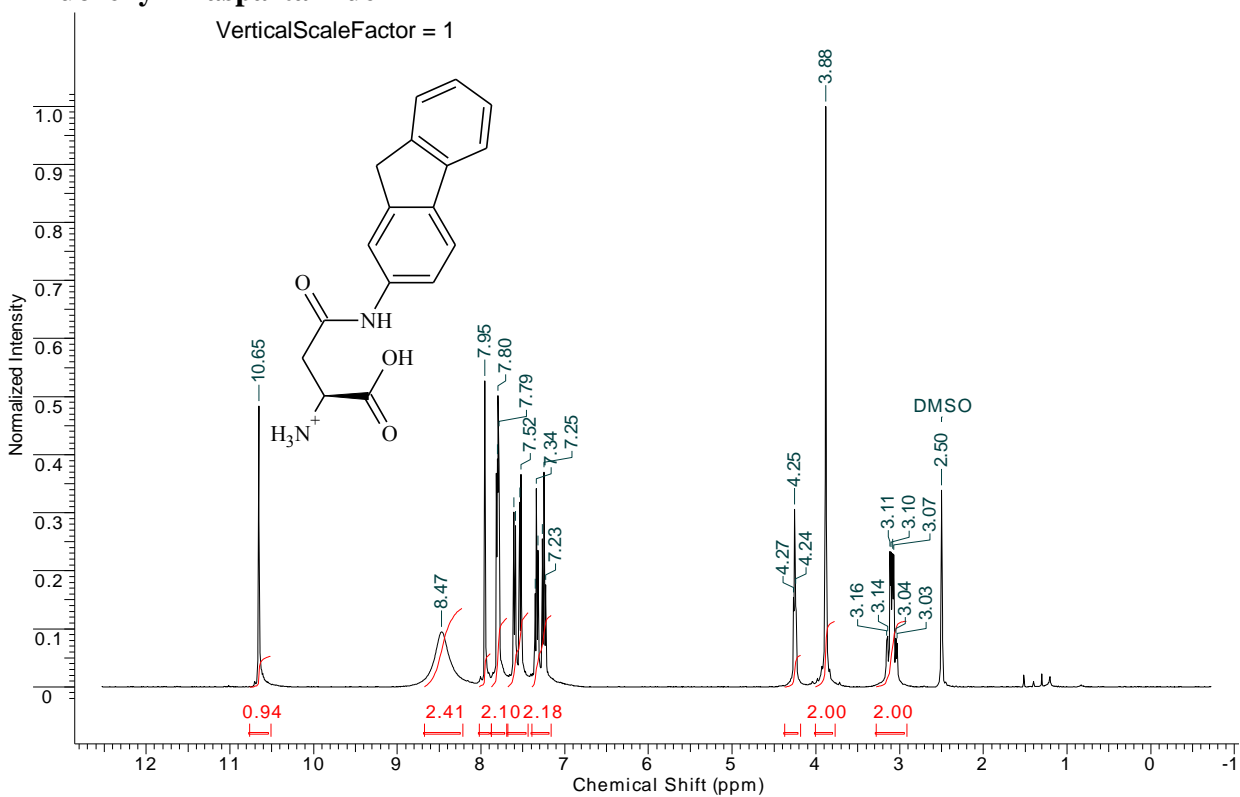
Appendix A: NMR spectra of final product β -aryl-aspartamides & α -aryl-amide aspartates

2-Fluoren-9-one- α -amide-aspartate



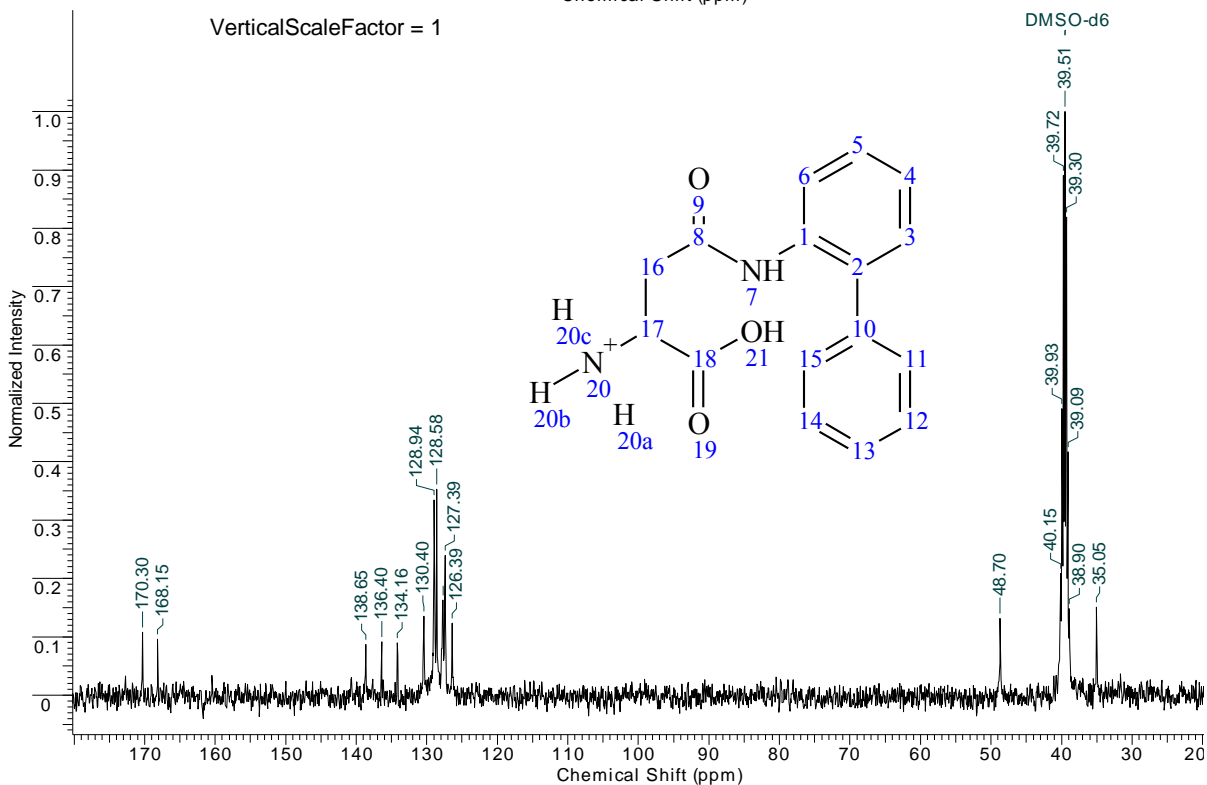
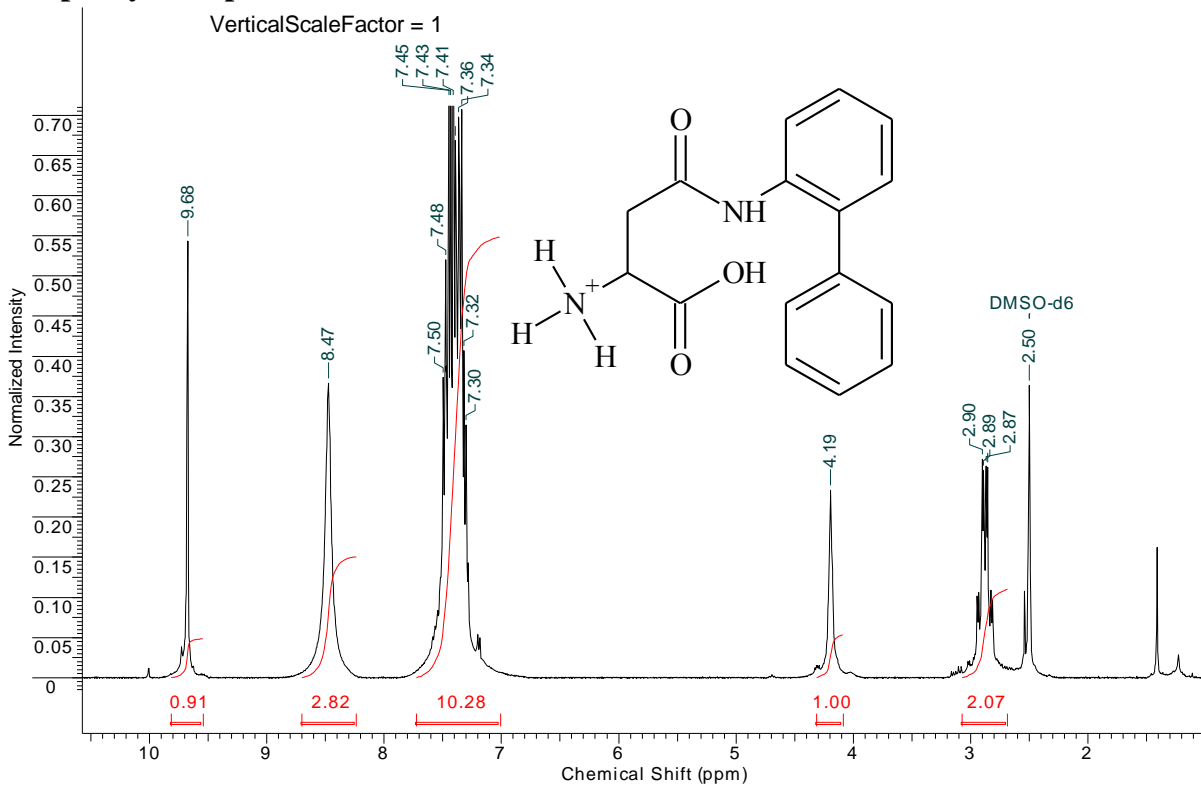
Appendix A: NMR spectra of final product β -aryl-aspartamides & α -aryl-amide aspartates

2-Fluorenyl-L-aspartamide



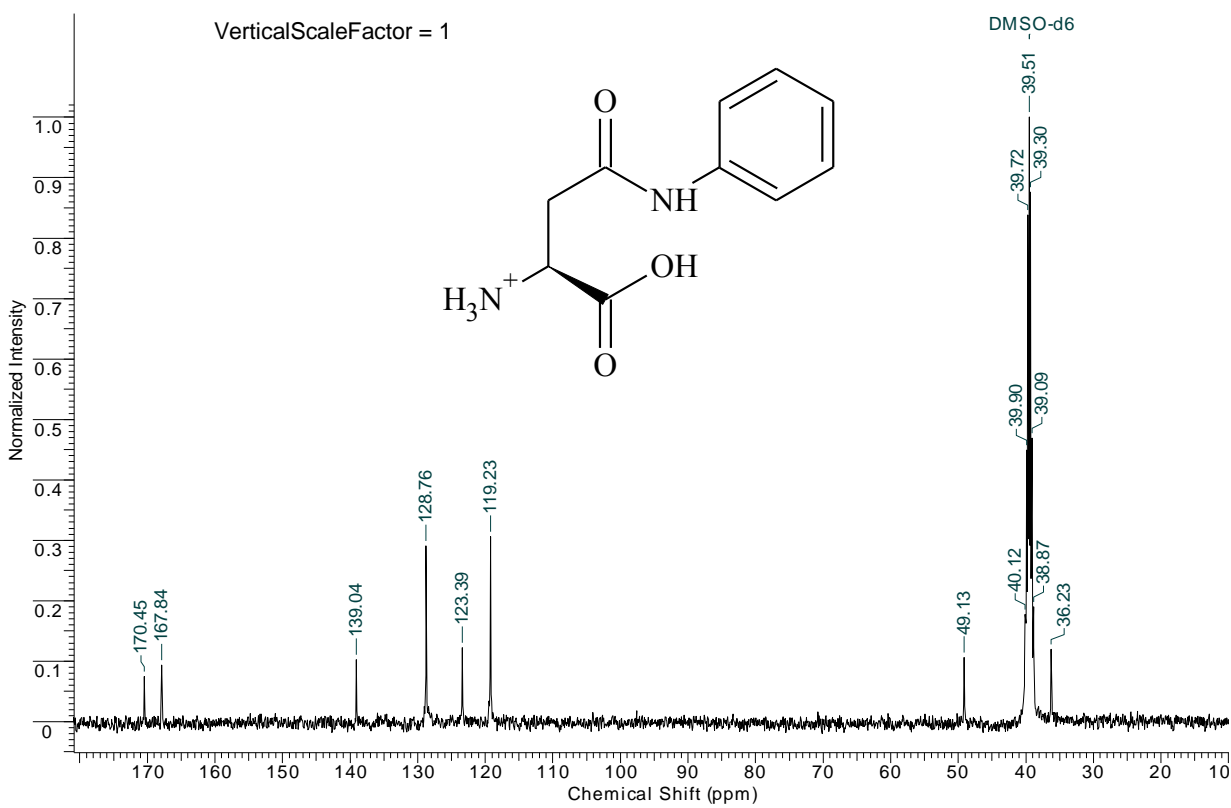
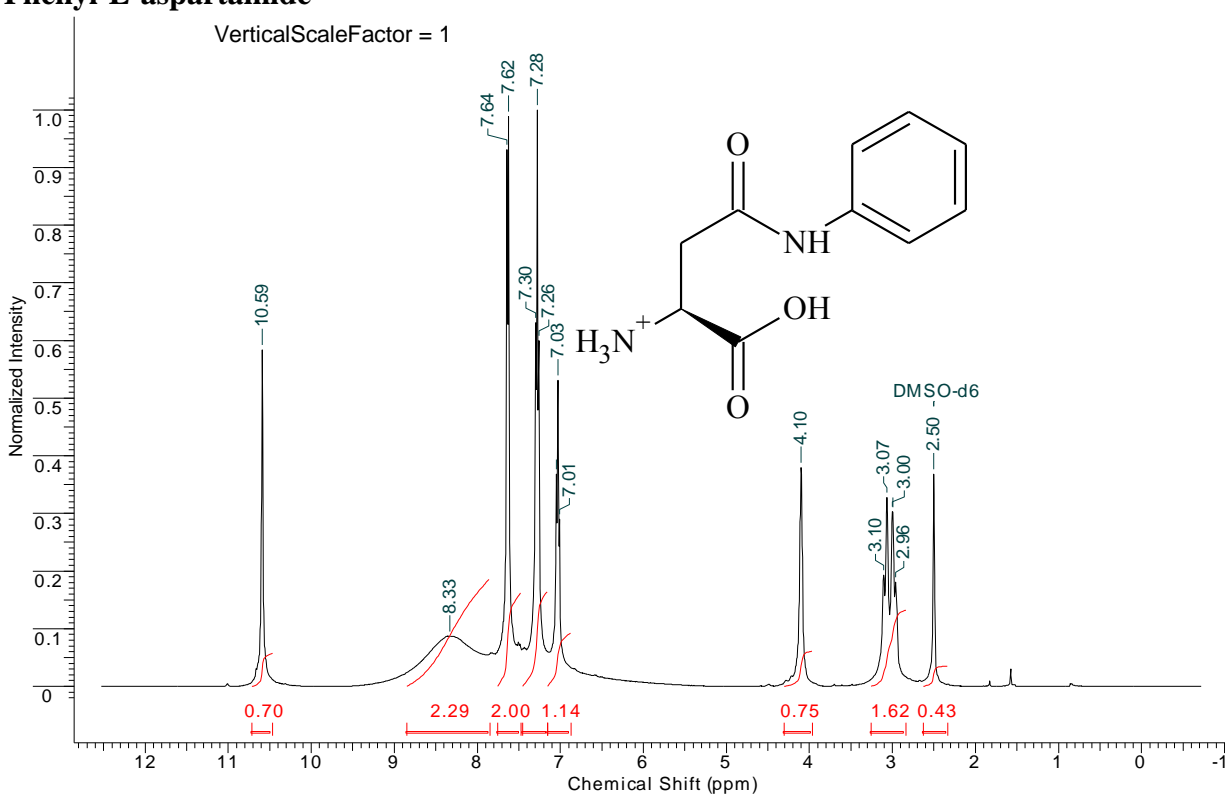
Appendix A: NMR spectra of final product β -aryl-aspartamides & α -aryl-amide aspartates

2-Biphenyl-L-aspartamide



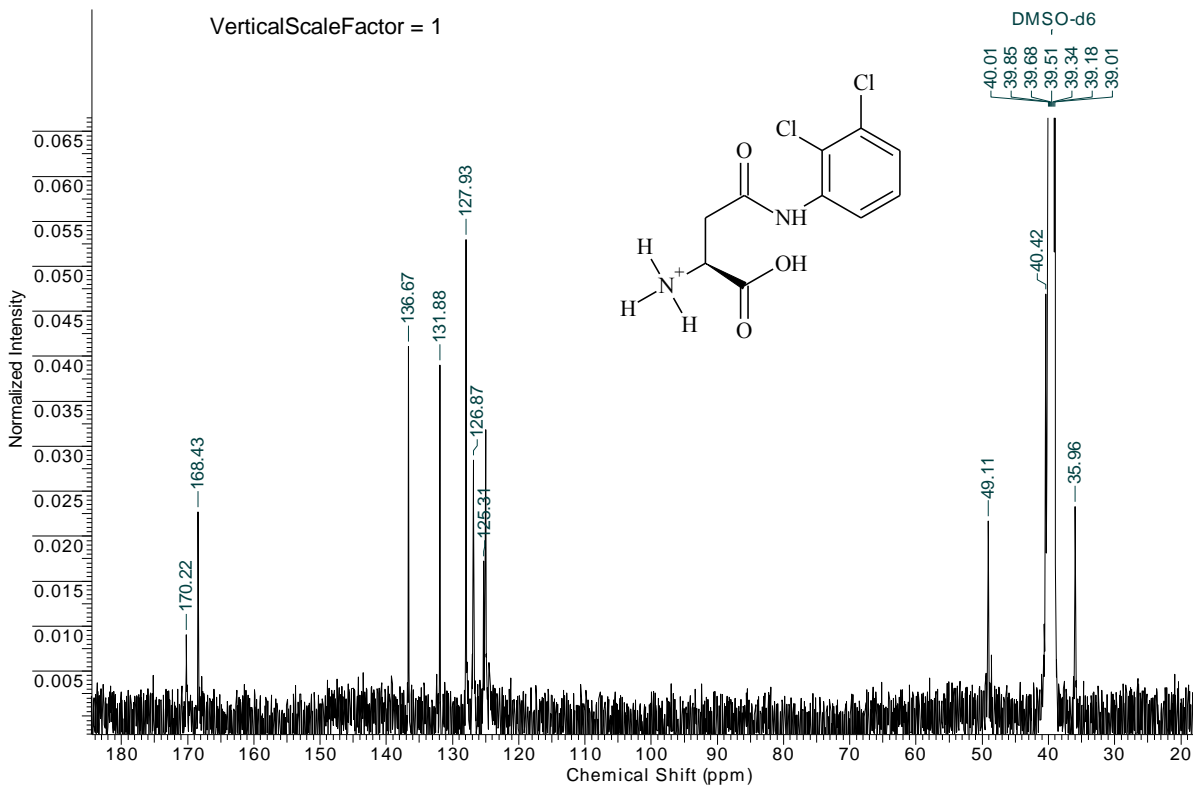
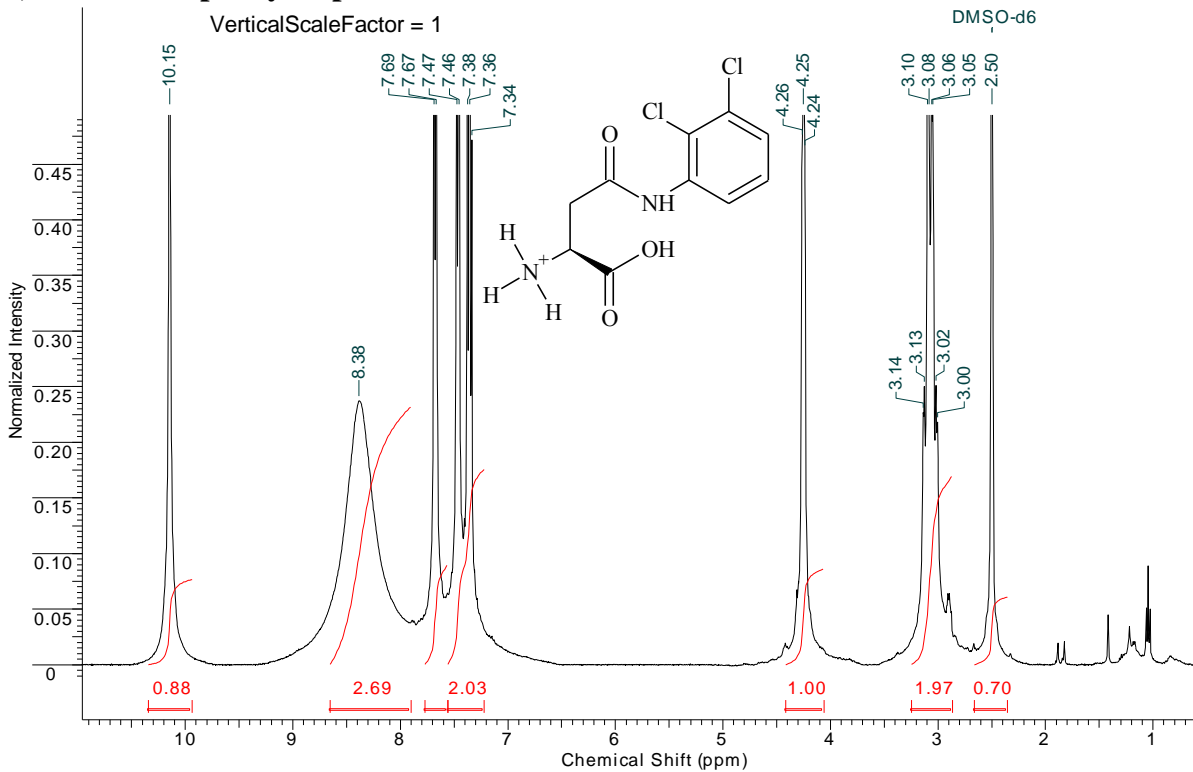
Appendix A: NMR spectra of final product β -aryl-aspartamides & α -aryl-amide aspartates

Phenyl-L-aspartamide



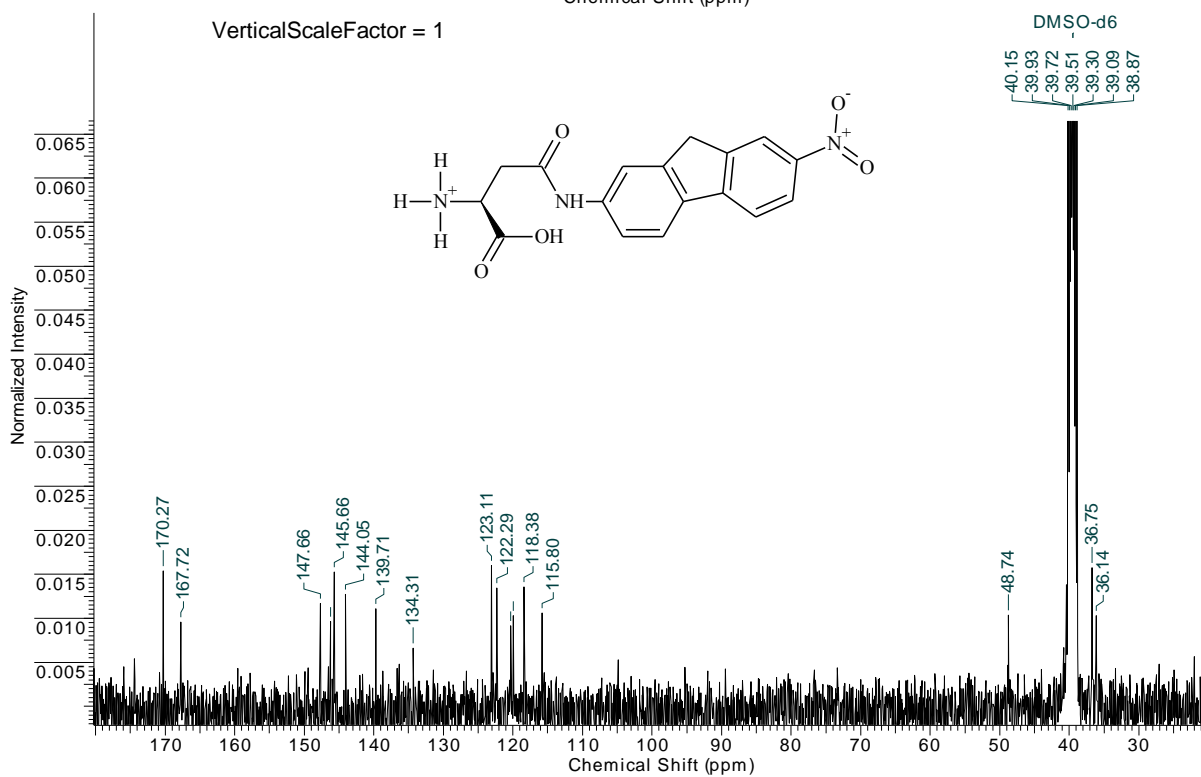
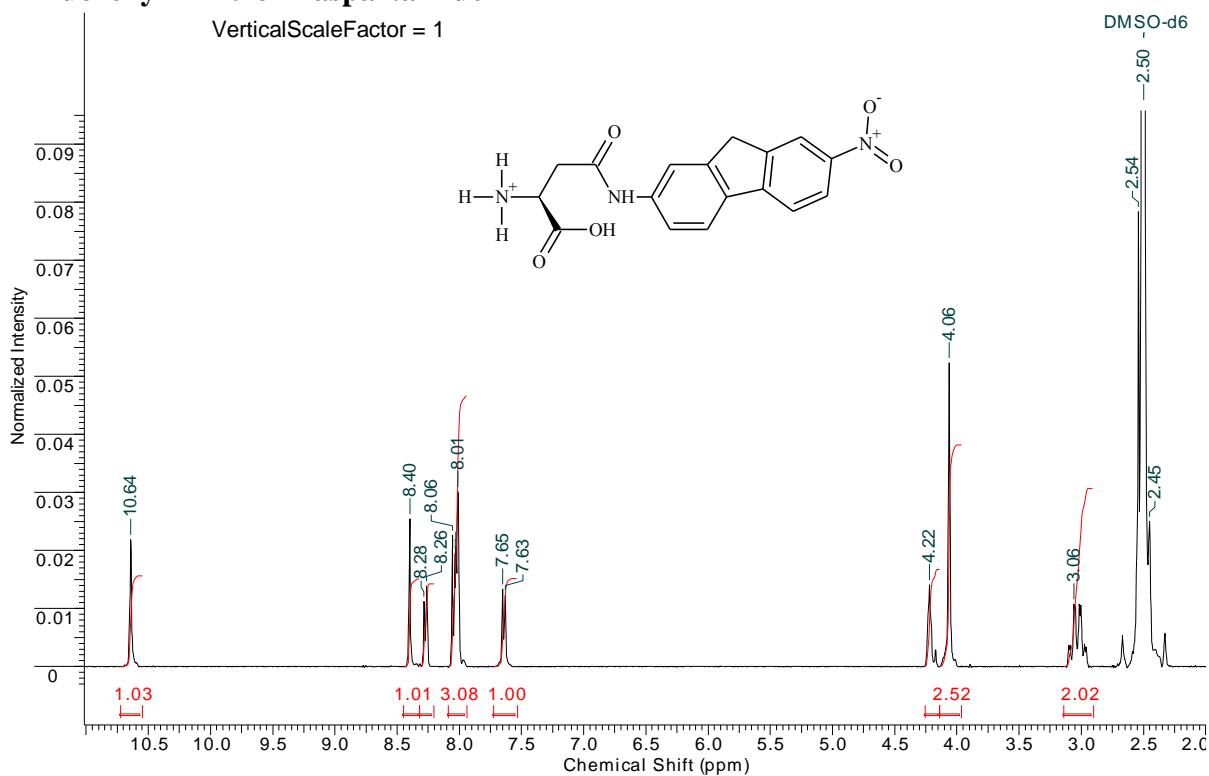
Appendix A: NMR spectra of final product β -aryl-aspartamides & α -aryl-amide aspartates

2,3-Dichloro-phenyl-aspartamide



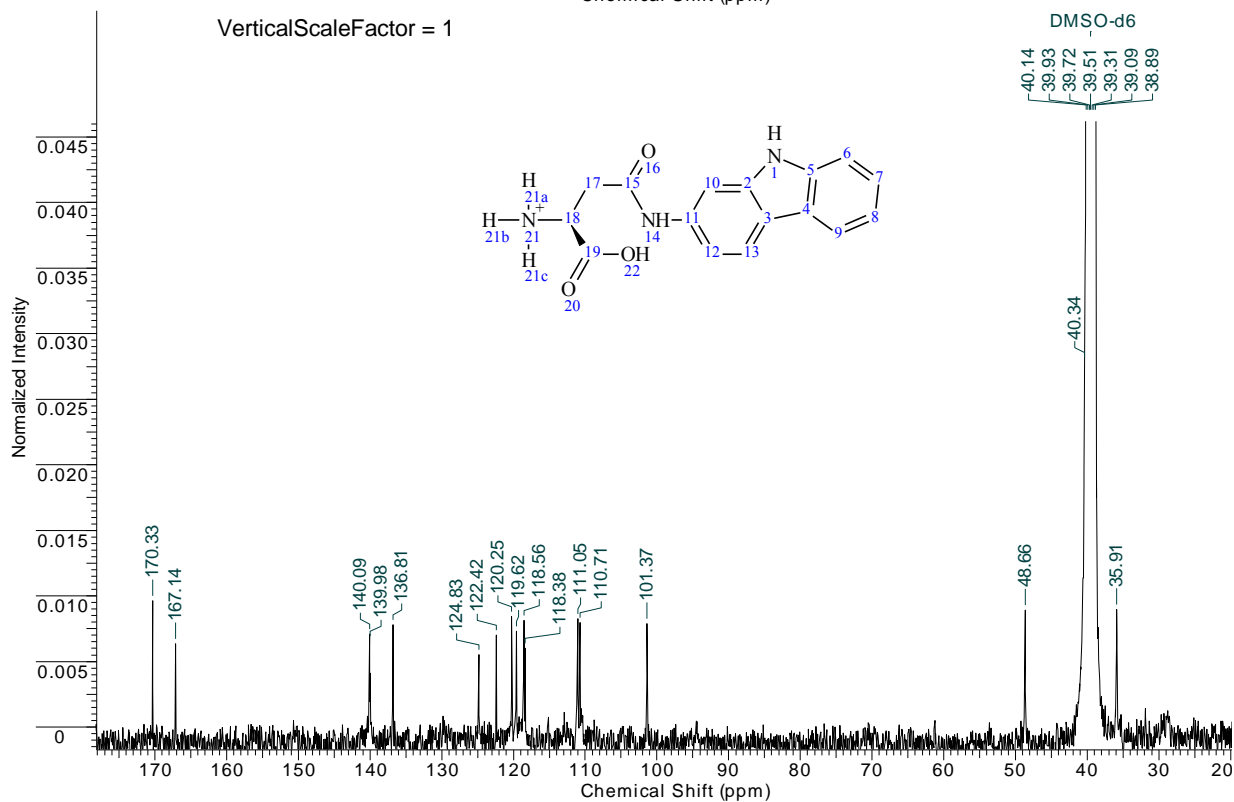
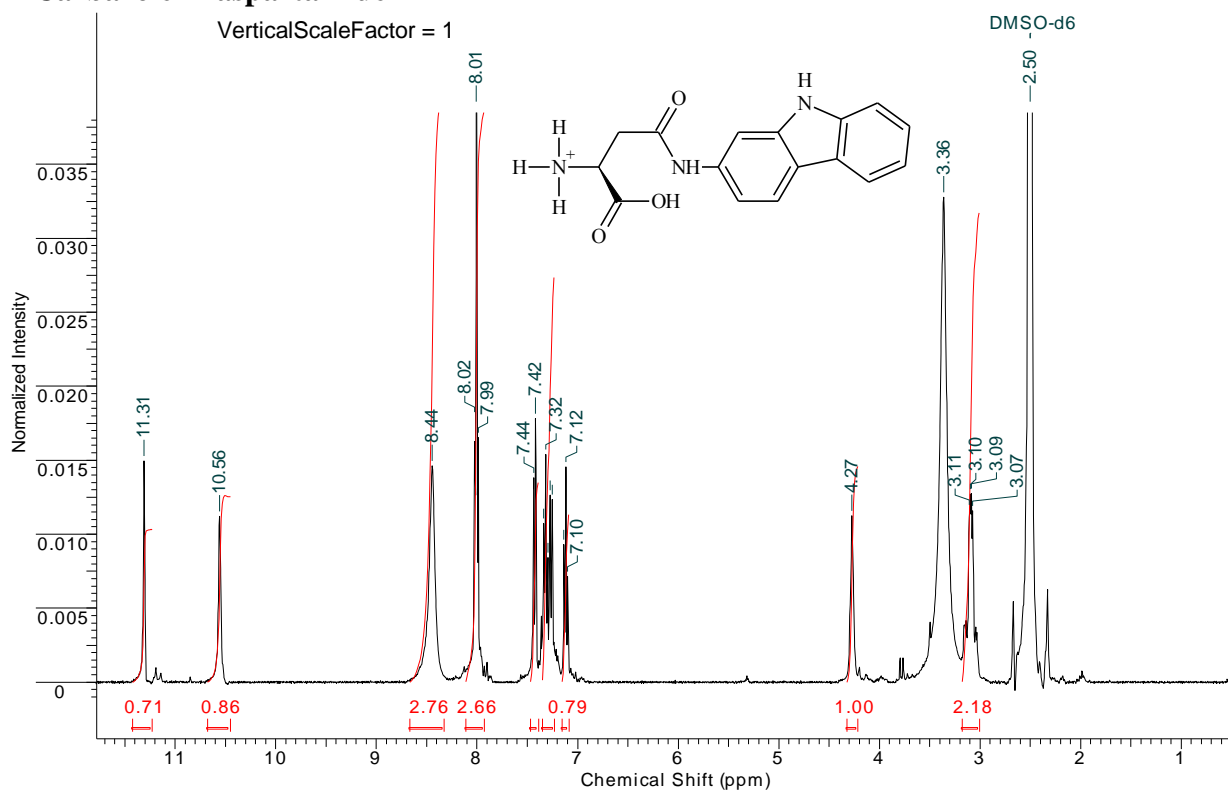
Appendix A: NMR spectra of final product β -aryl-aspartamides & α -aryl-amide aspartates

2-Fluorenyl-7-nitro-L-aspartamide



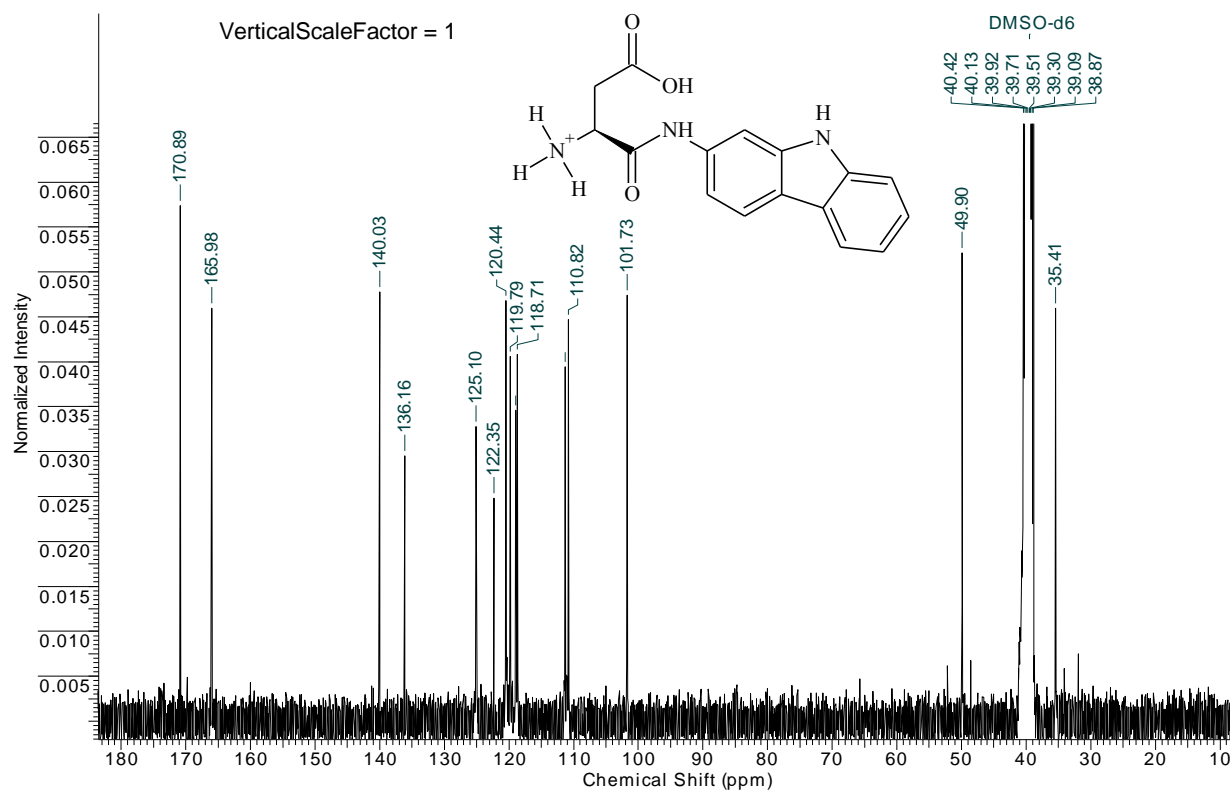
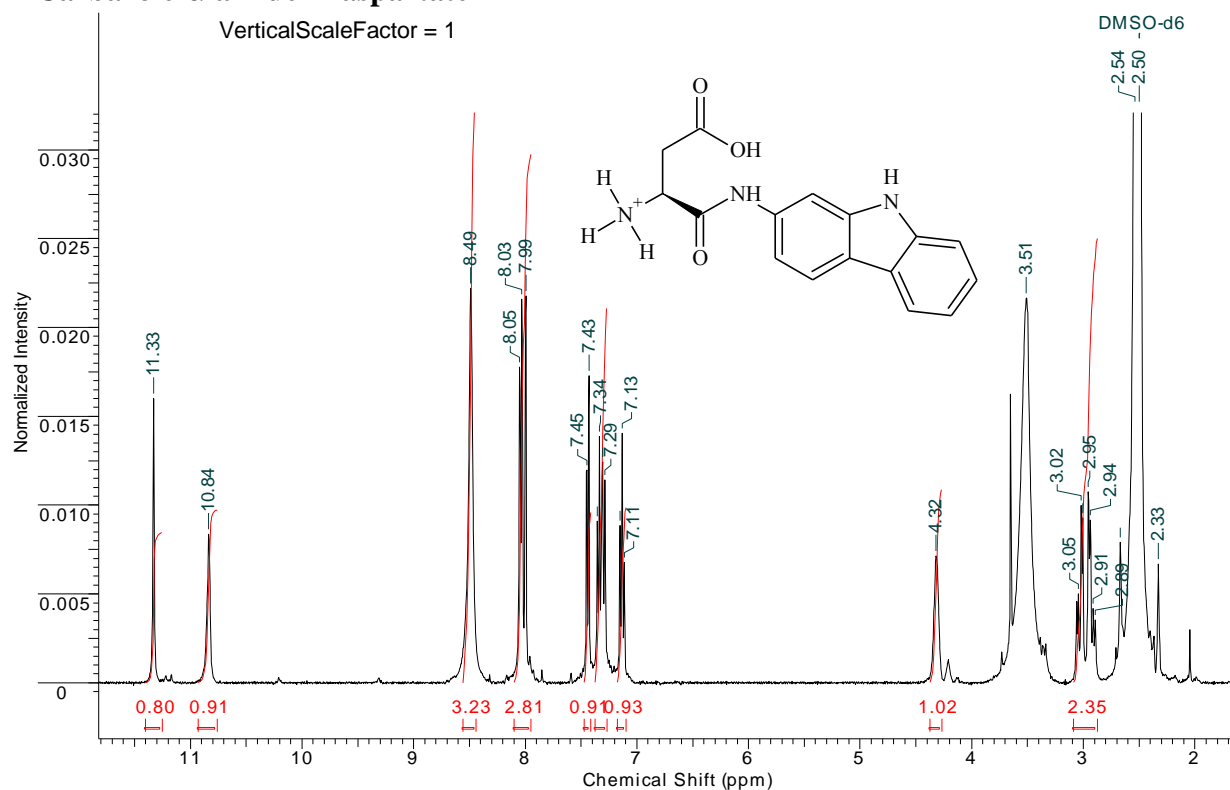
Appendix A: NMR spectra of final product β -aryl-aspartamides & α -aryl-amide aspartates

2-Carbazole-L-aspartamide



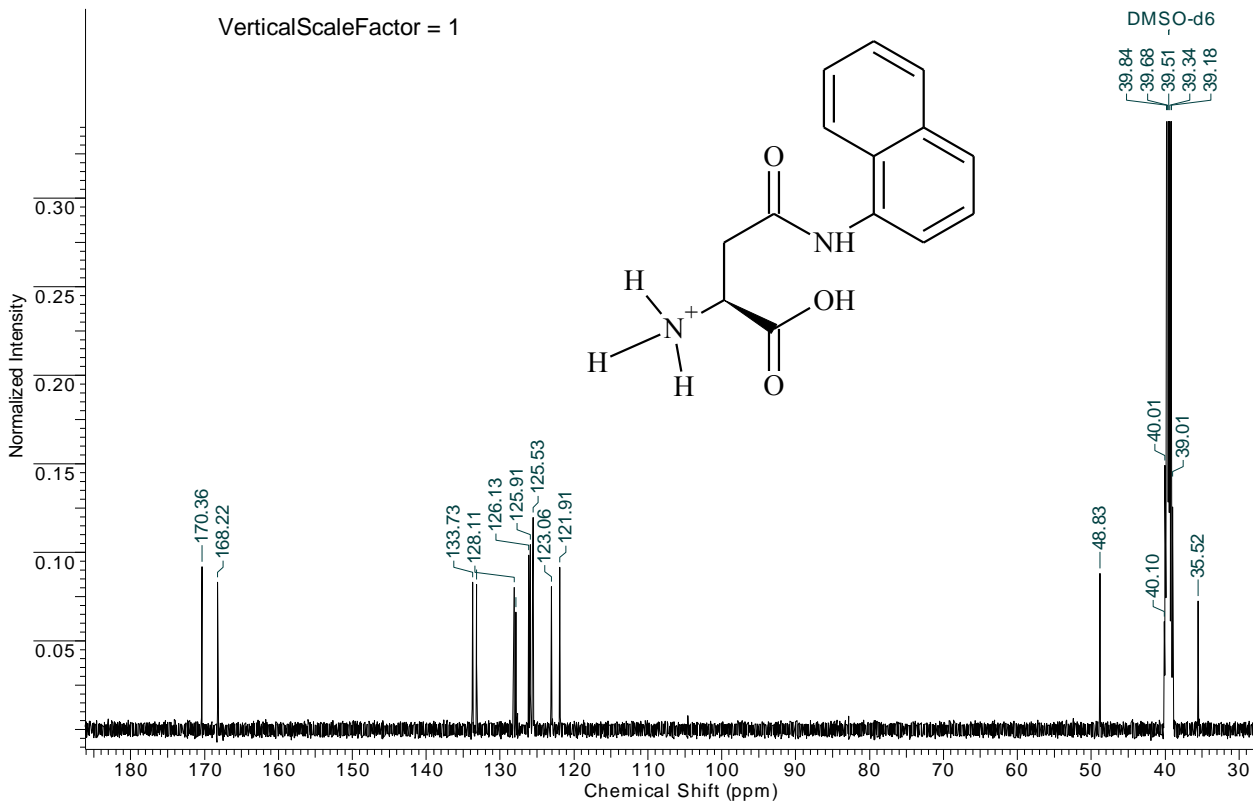
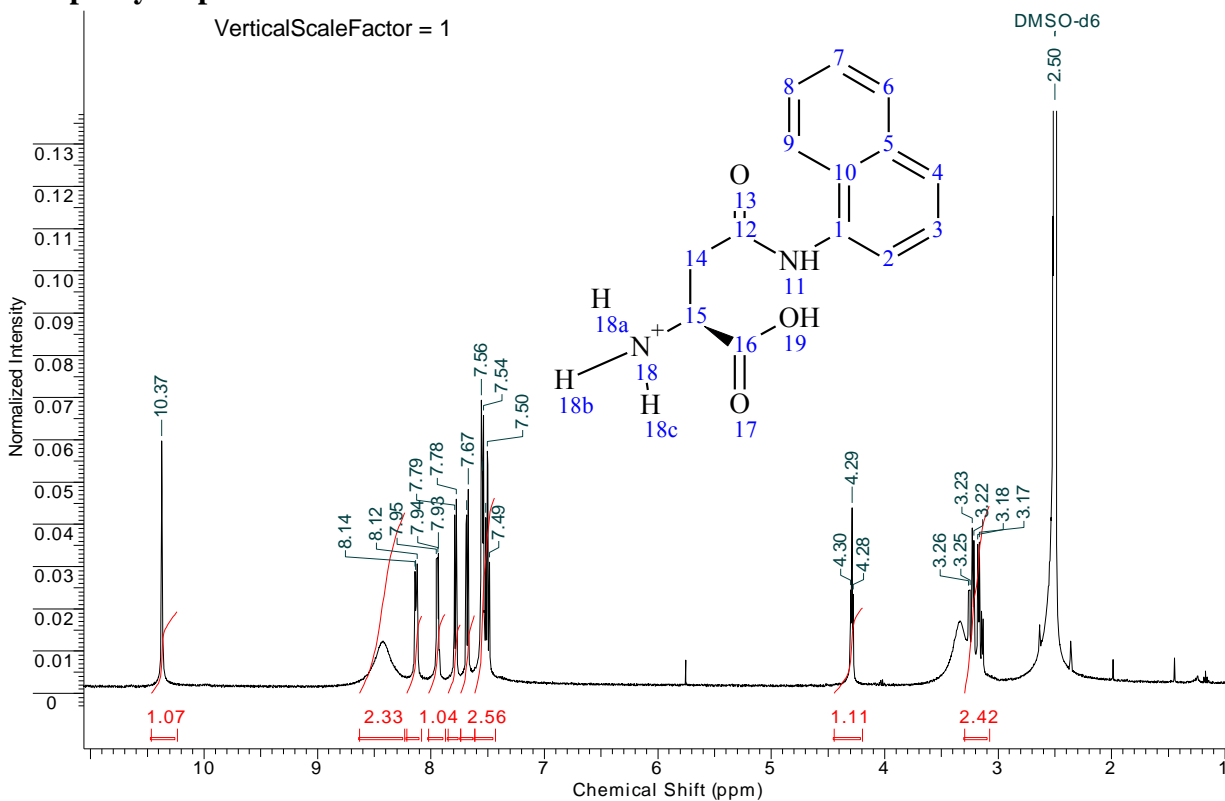
Appendix A: NMR spectra of final product β -aryl-aspartamides & α -aryl-amide aspartates

2-Carbazole- α -amide-L-aspartate



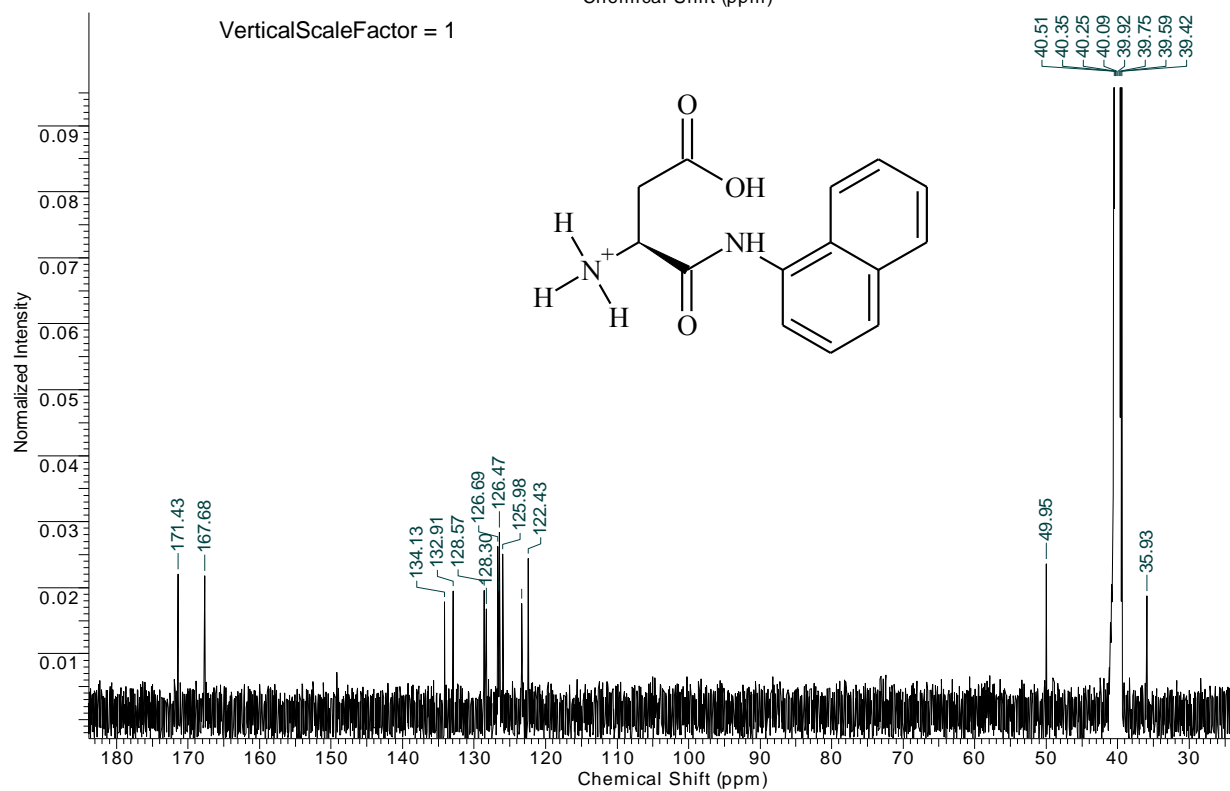
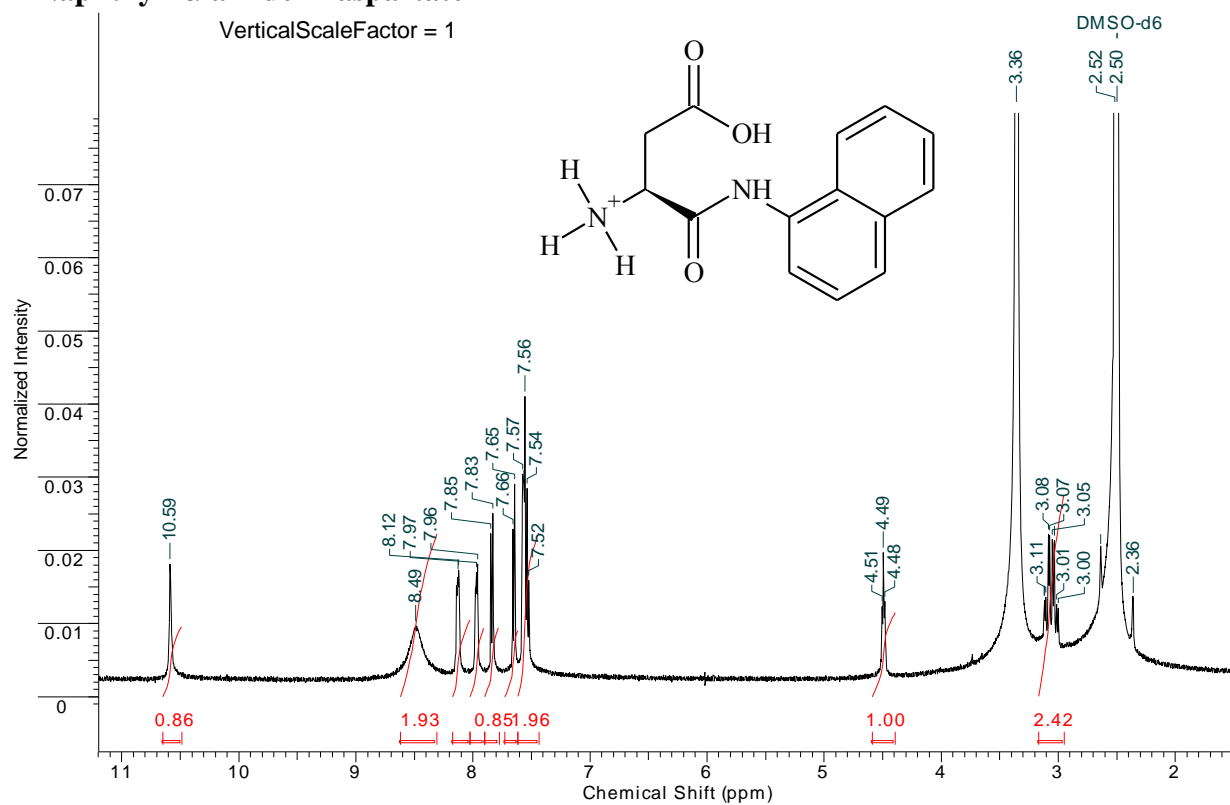
Appendix A: NMR spectra of final product β -aryl-aspartamides & α -aryl-amide aspartates

1-Naphthyl-aspartamide



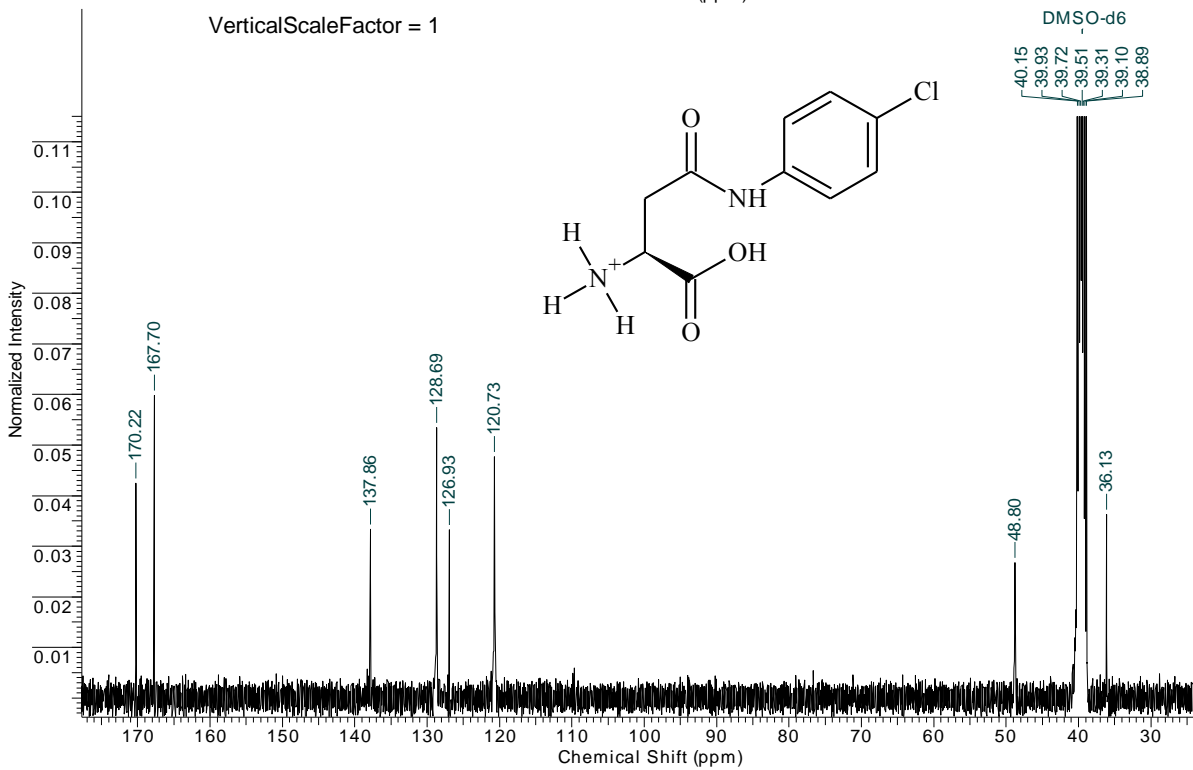
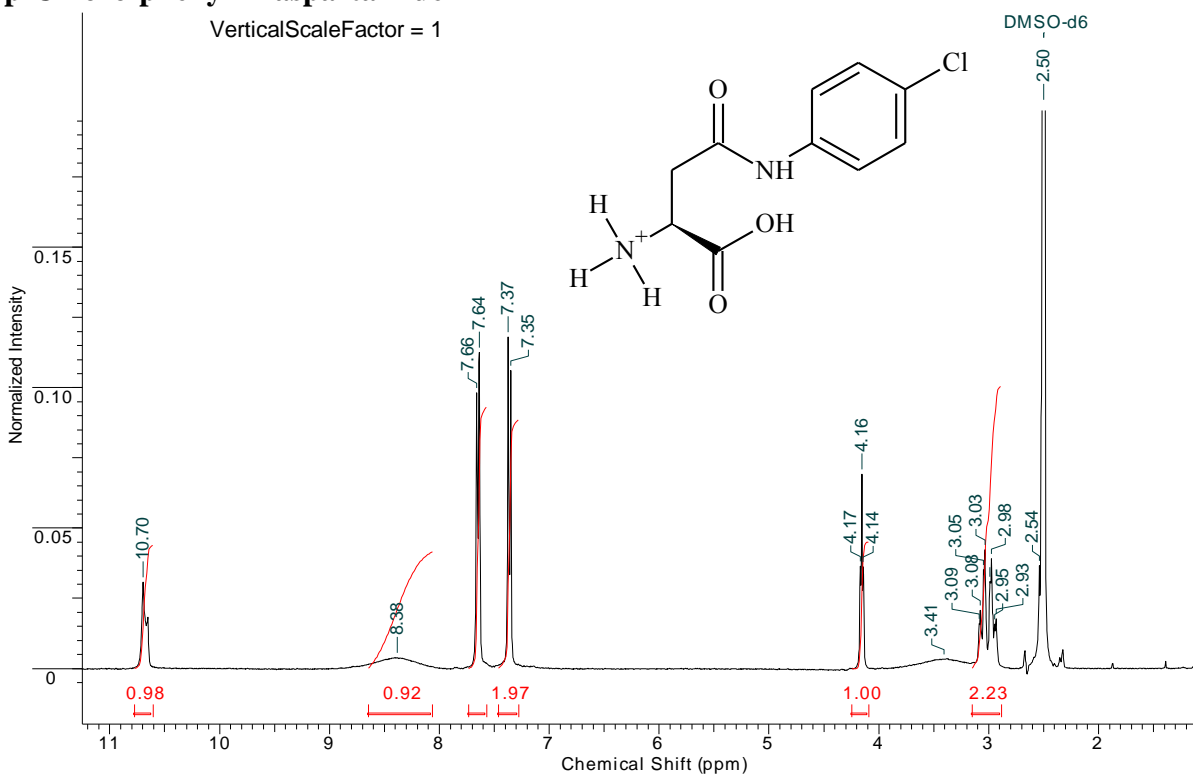
Appendix A: NMR spectra of final product β -aryl-aspartamides & α -aryl-amide aspartates

1-Naphthyl - α -amide-L-aspartate



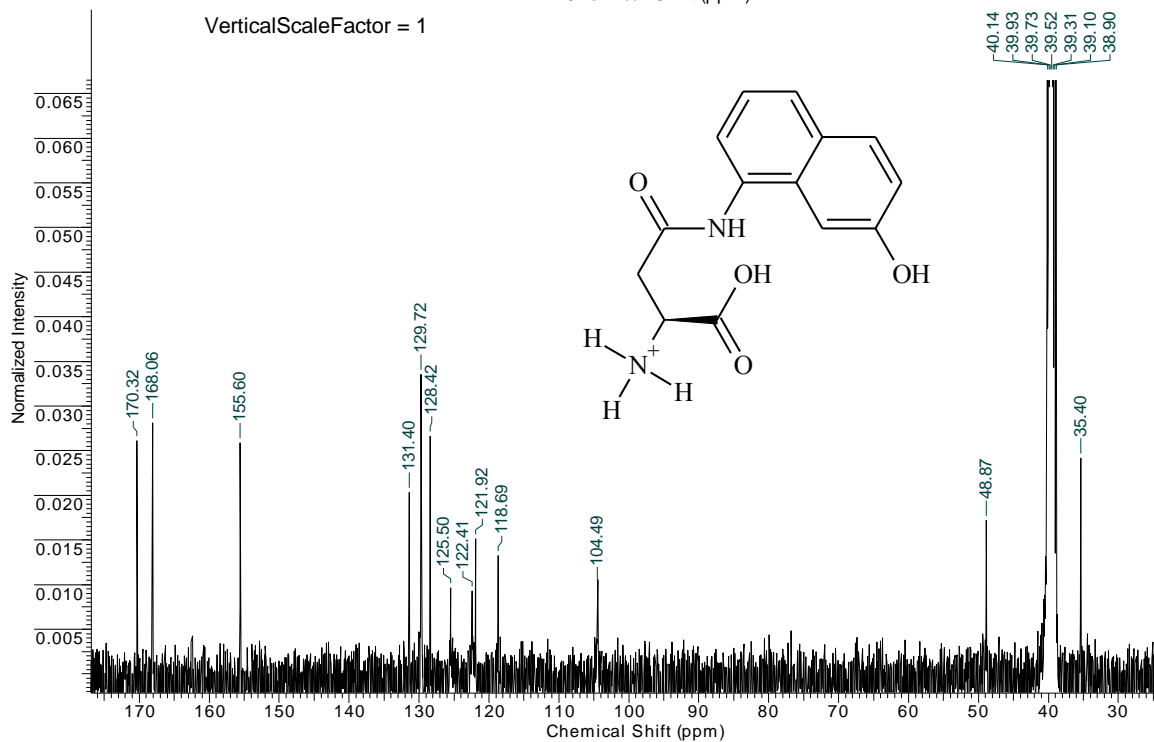
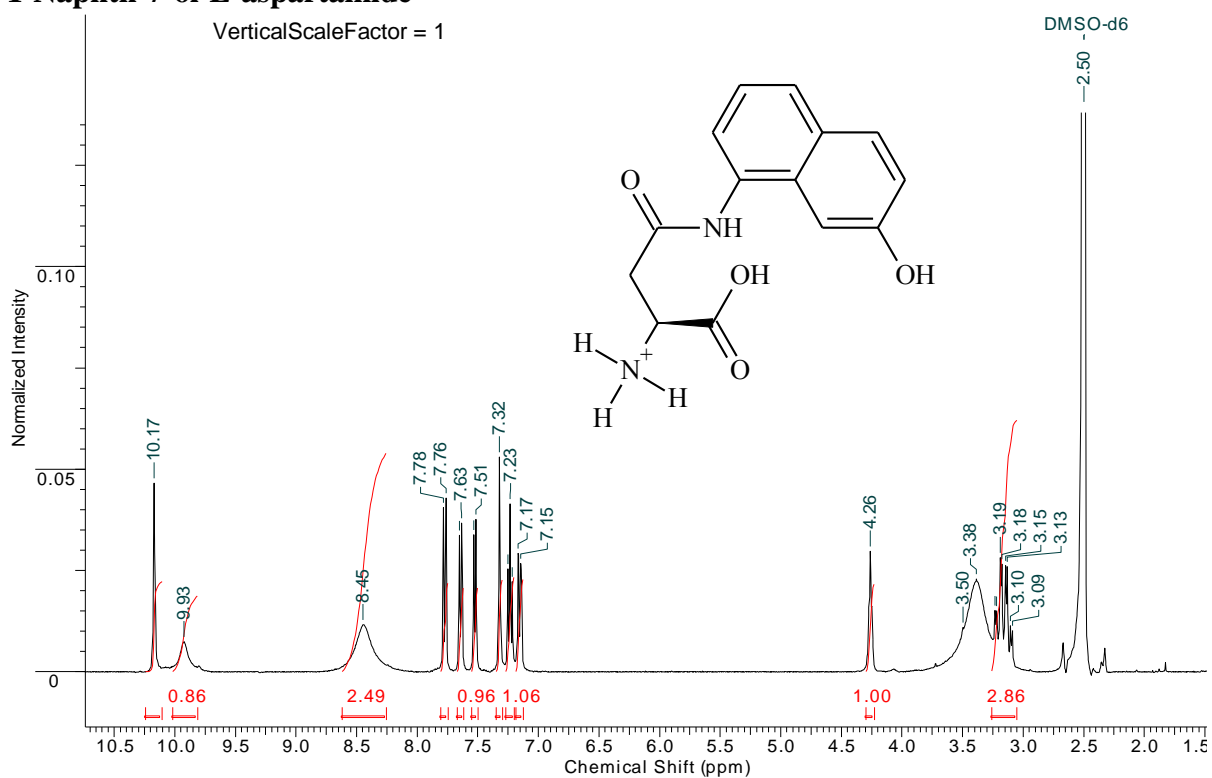
Appendix A: NMR spectra of final product β -aryl-aspartamides & α -aryl-amide aspartates

p-Chloro-phenyl-L-aspartamide



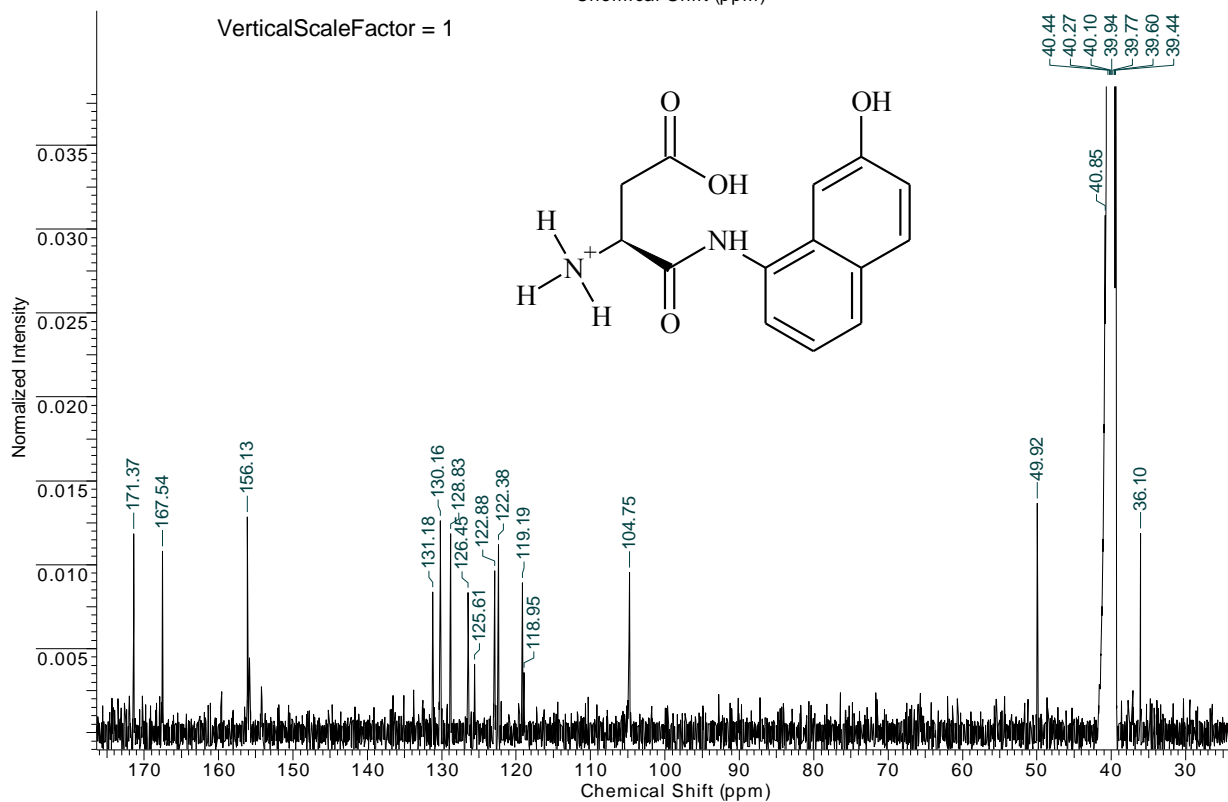
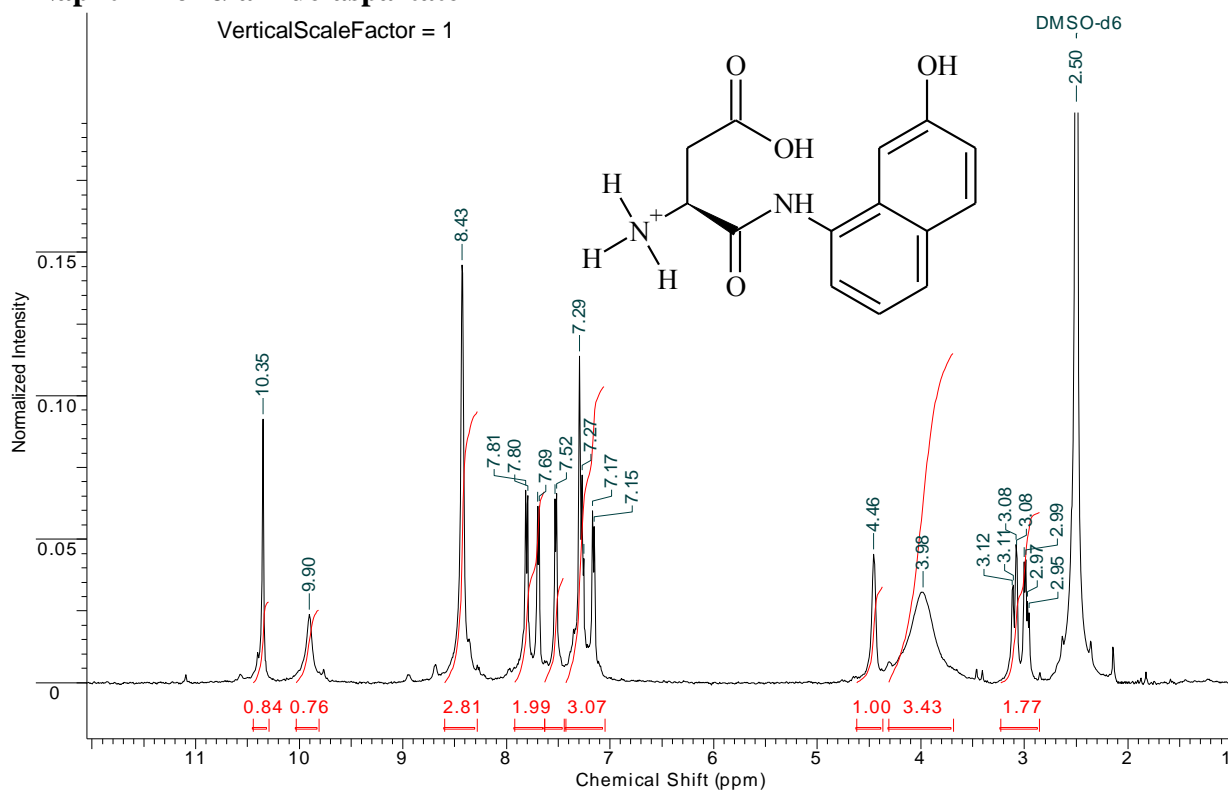
Appendix A: NMR spectra of final product β -aryl-aspartamides & α -aryl-amide aspartates

1-Naphth-7-ol-L-aspartamide



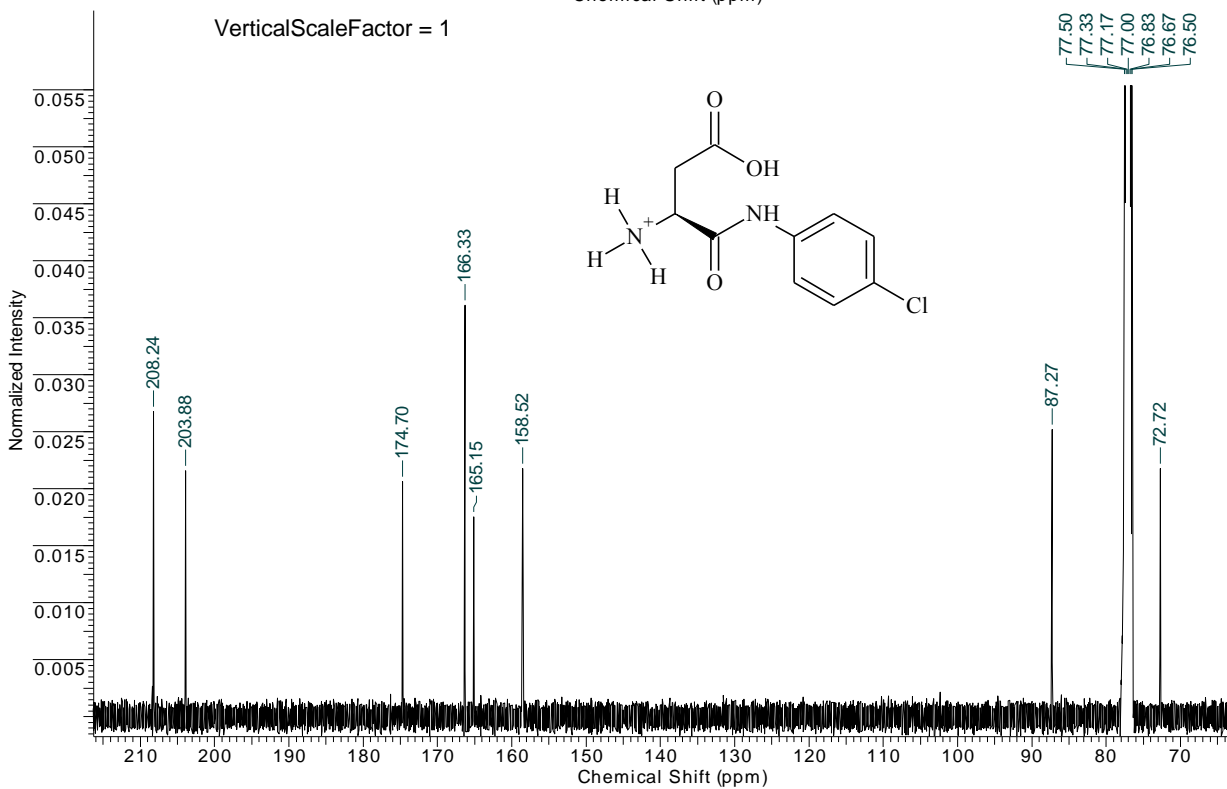
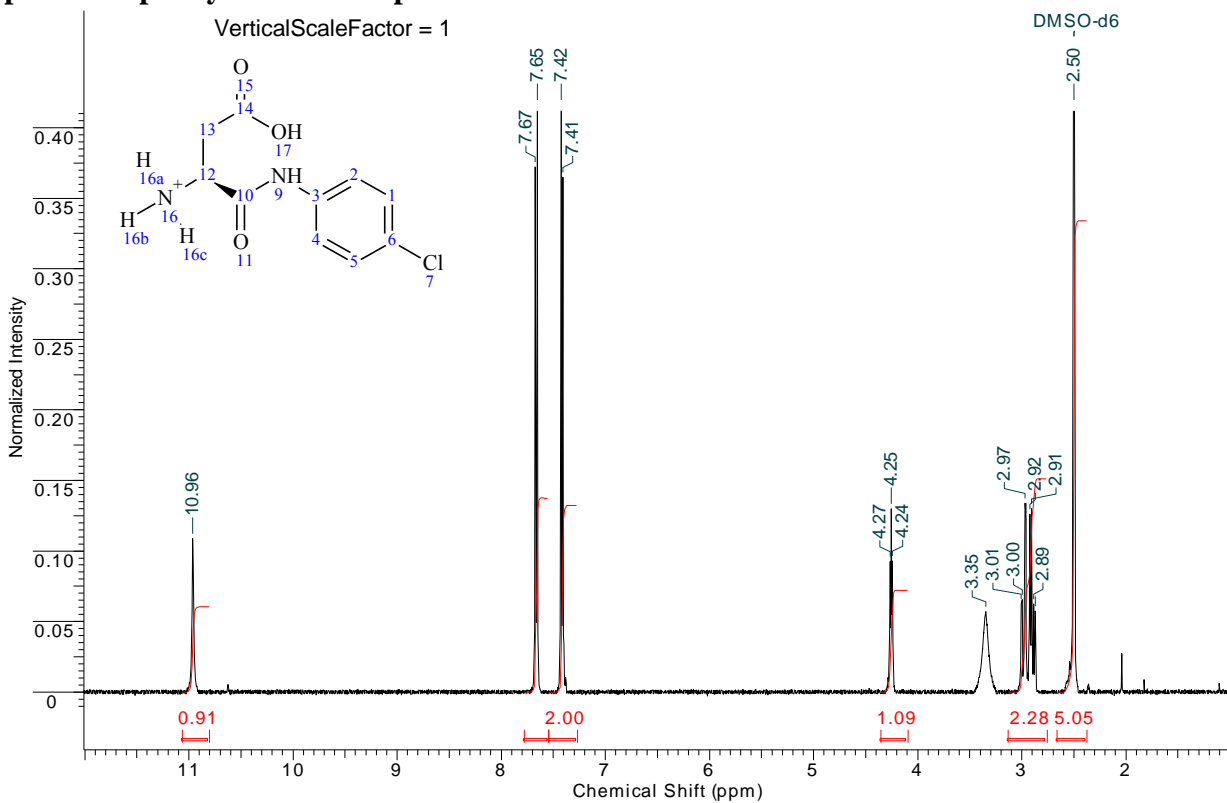
Appendix A: NMR spectra of final product β -aryl-aspartamides & α -aryl-amide-aspartates

1-Naphth-7-ol- α -amide-aspartate



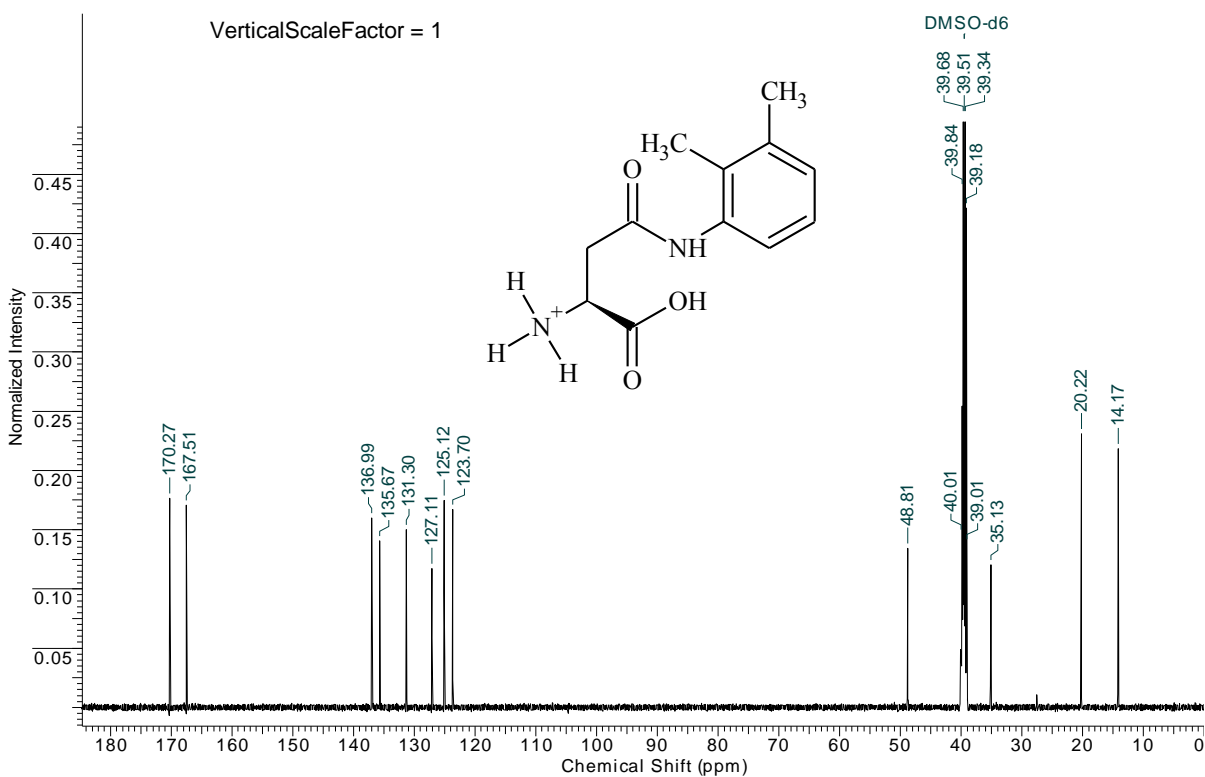
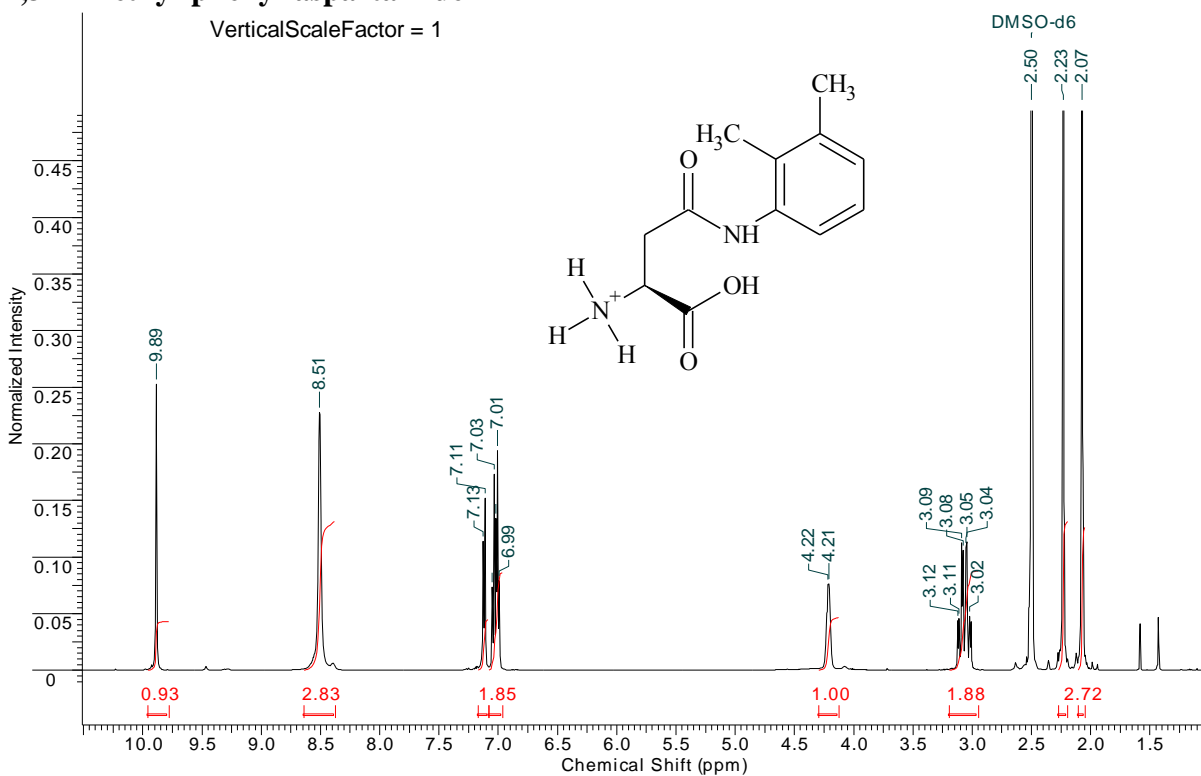
Appendix A: NMR spectra of final product β -aryl-aspartamides & α -aryl-amide aspartates

p-Chloro-phenyl- α -amide-aspartate



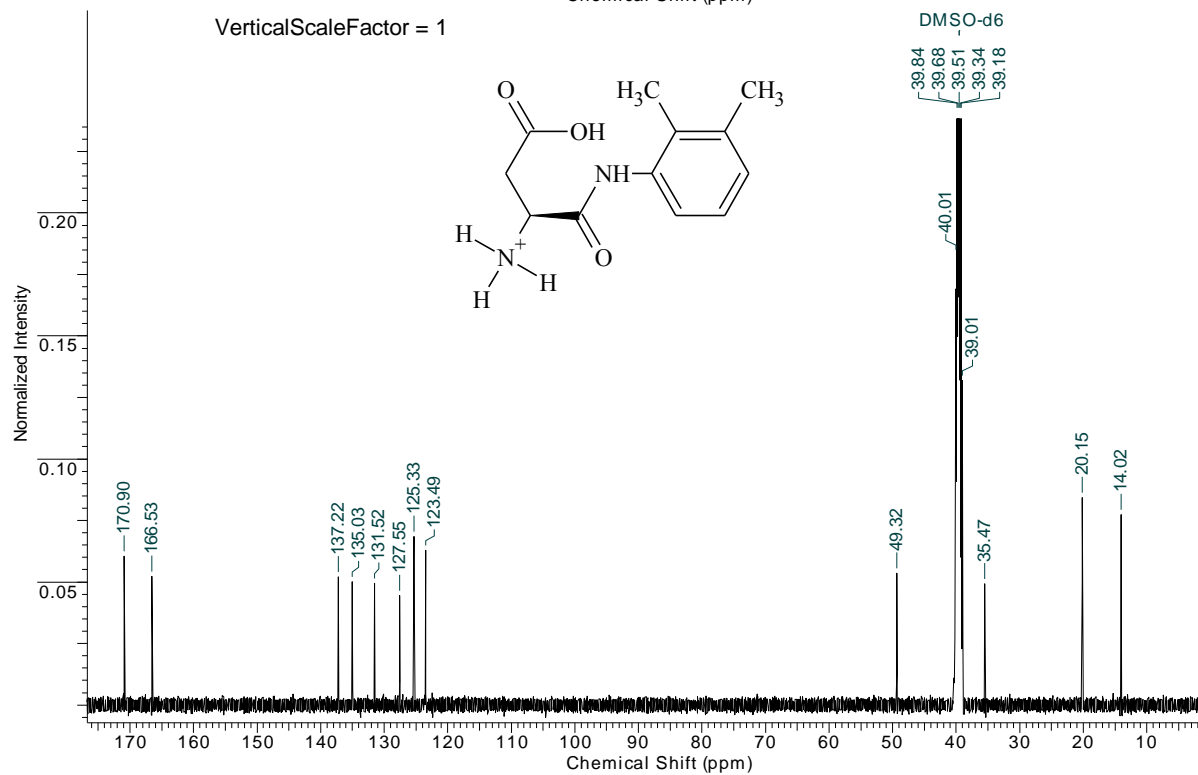
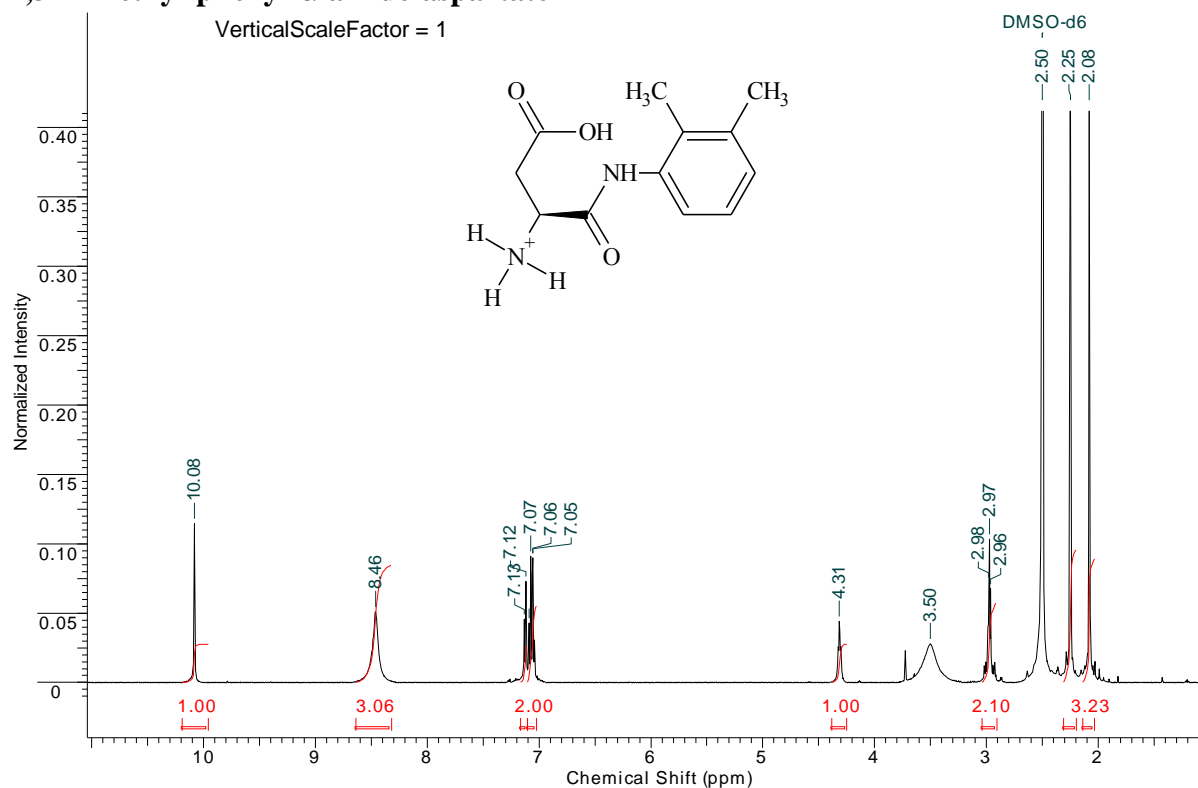
Appendix A: NMR spectra of final product β -aryl-aspartamides & α -aryl-amide aspartates

2,3-Dimethyl-phenyl-aspartamide



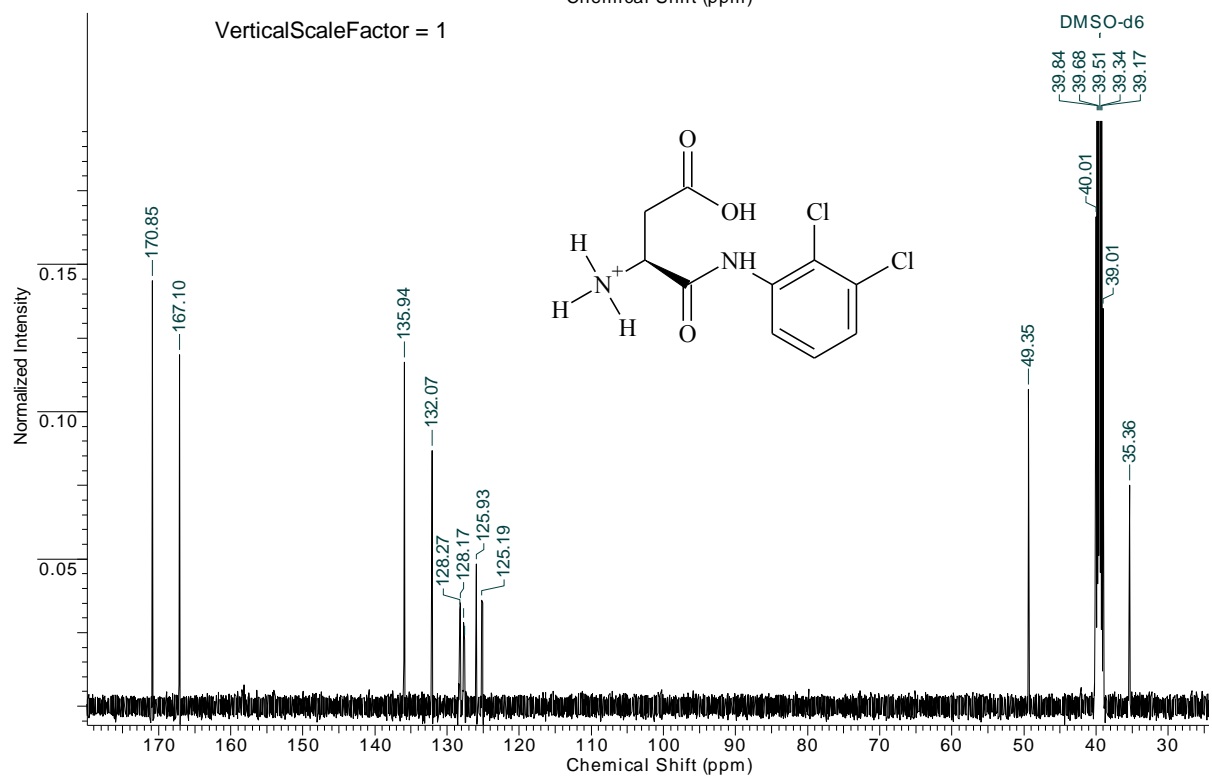
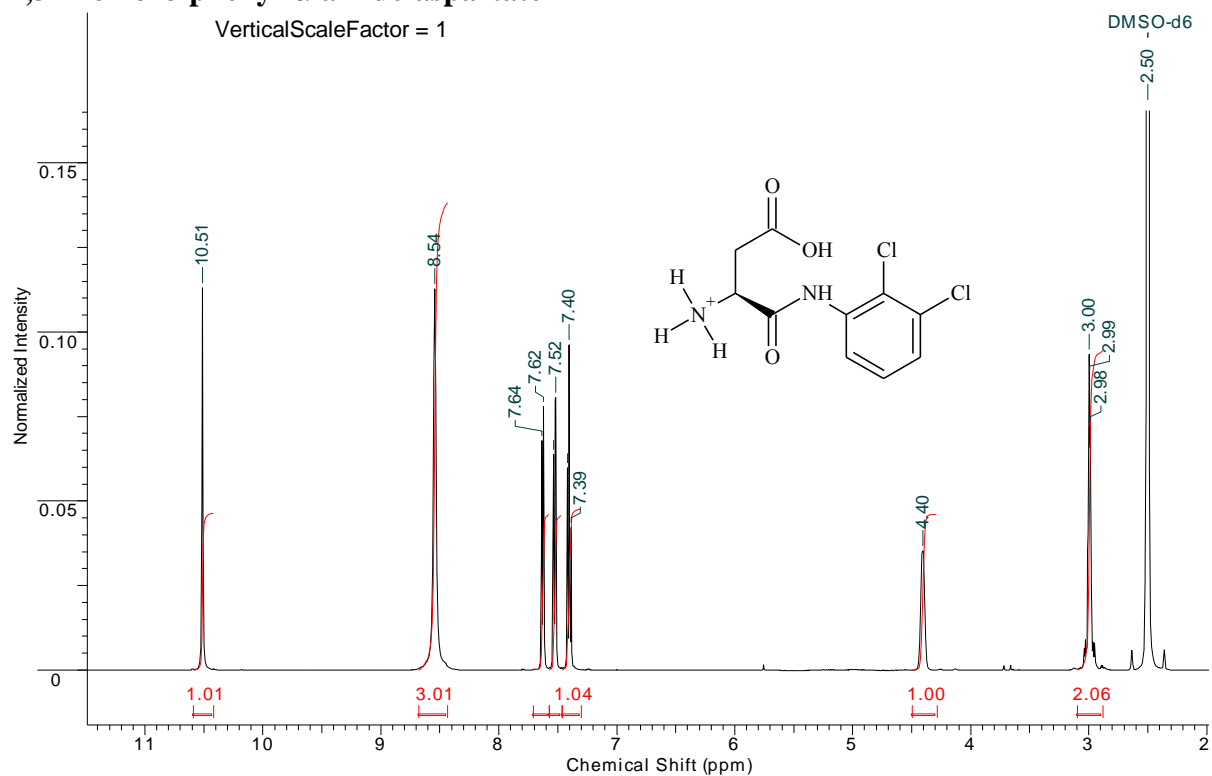
Appendix A: NMR spectra of final product β -aryl-aspartamides & α -aryl-amide aspartates

2,3-Dimethyl-phenyl- α -amide-aspartate



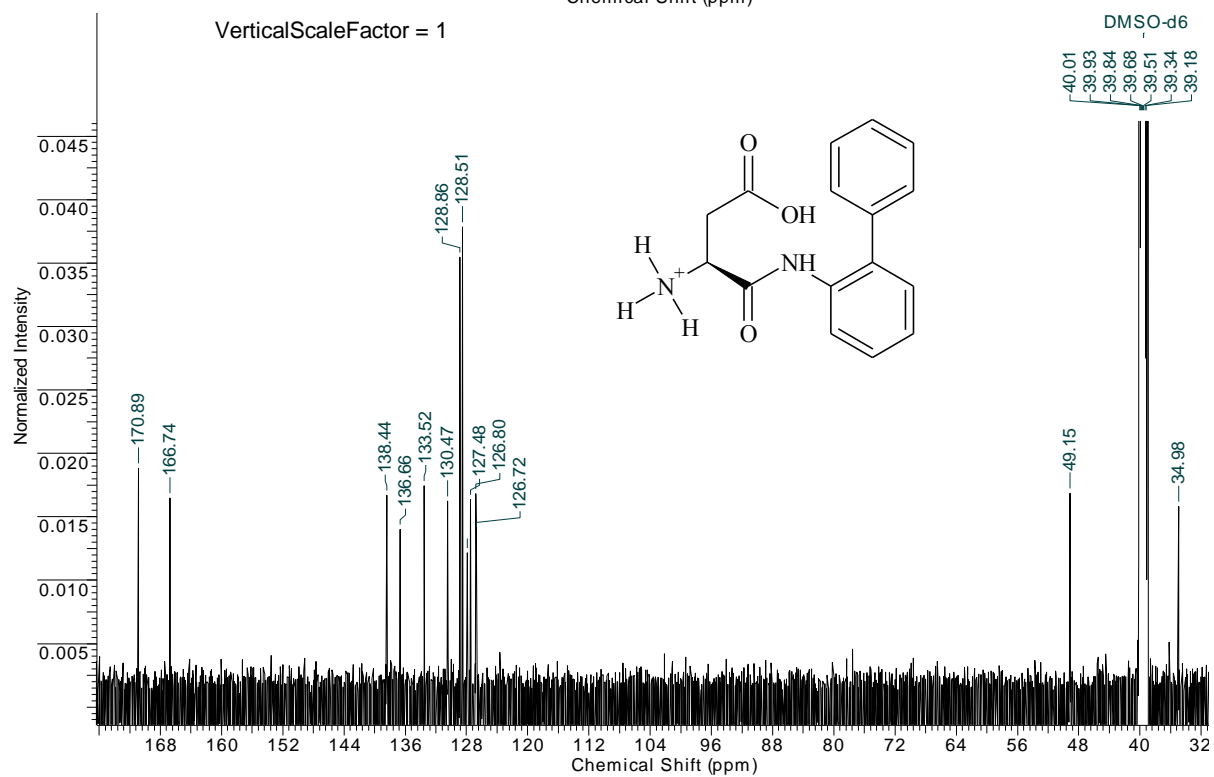
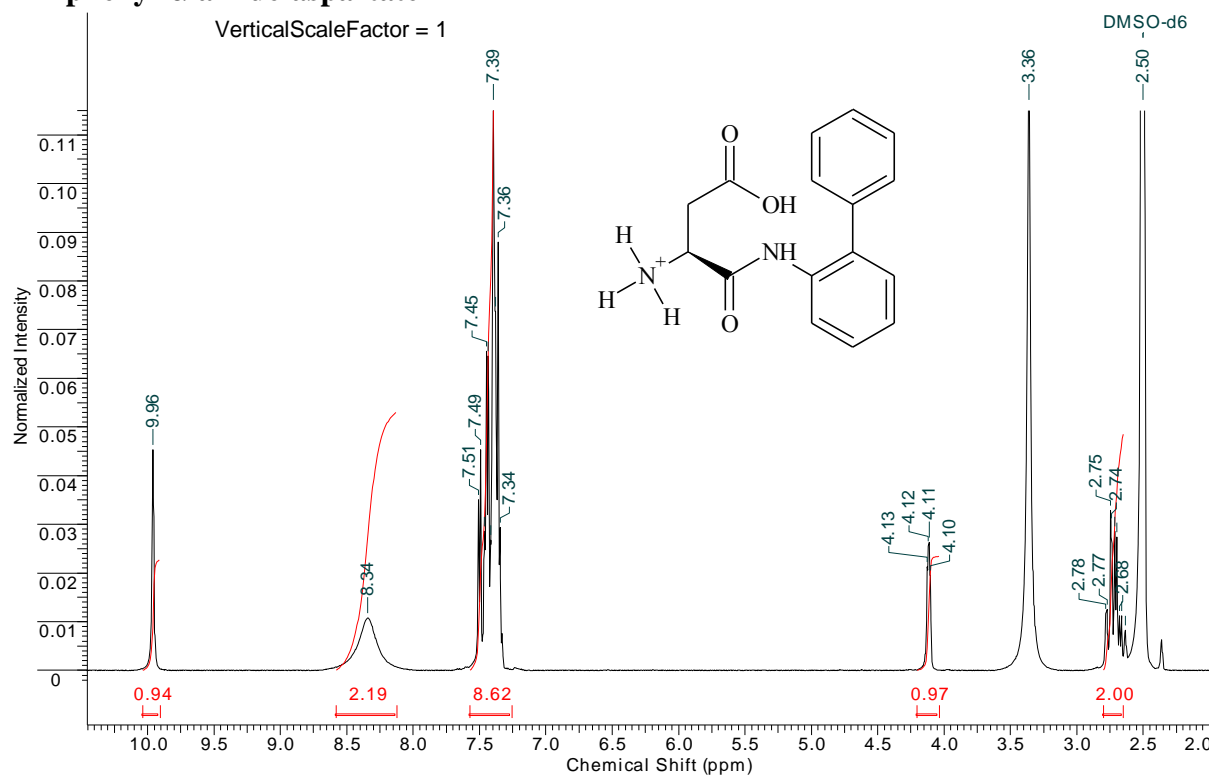
Appendix A: NMR spectra of final product β -aryl-aspartamides & α -aryl-amide aspartates

2,3-Dichloro-phenyl- α -amide-aspartate



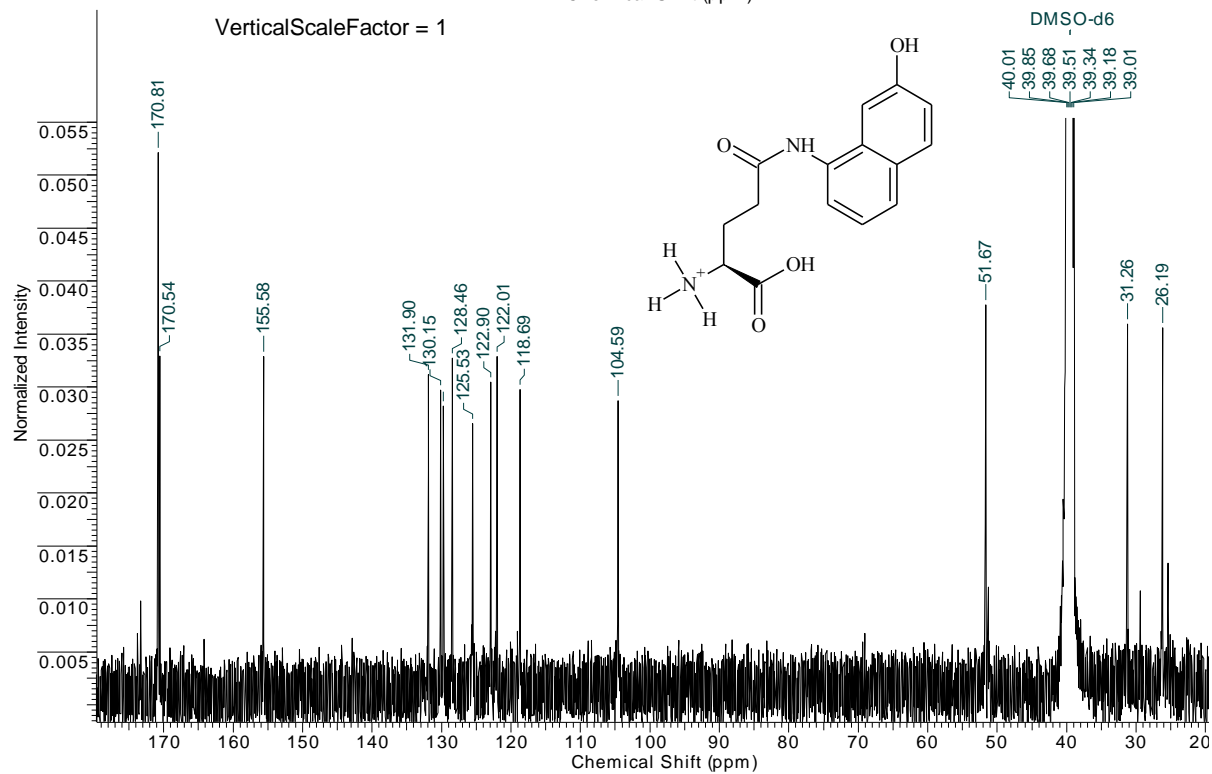
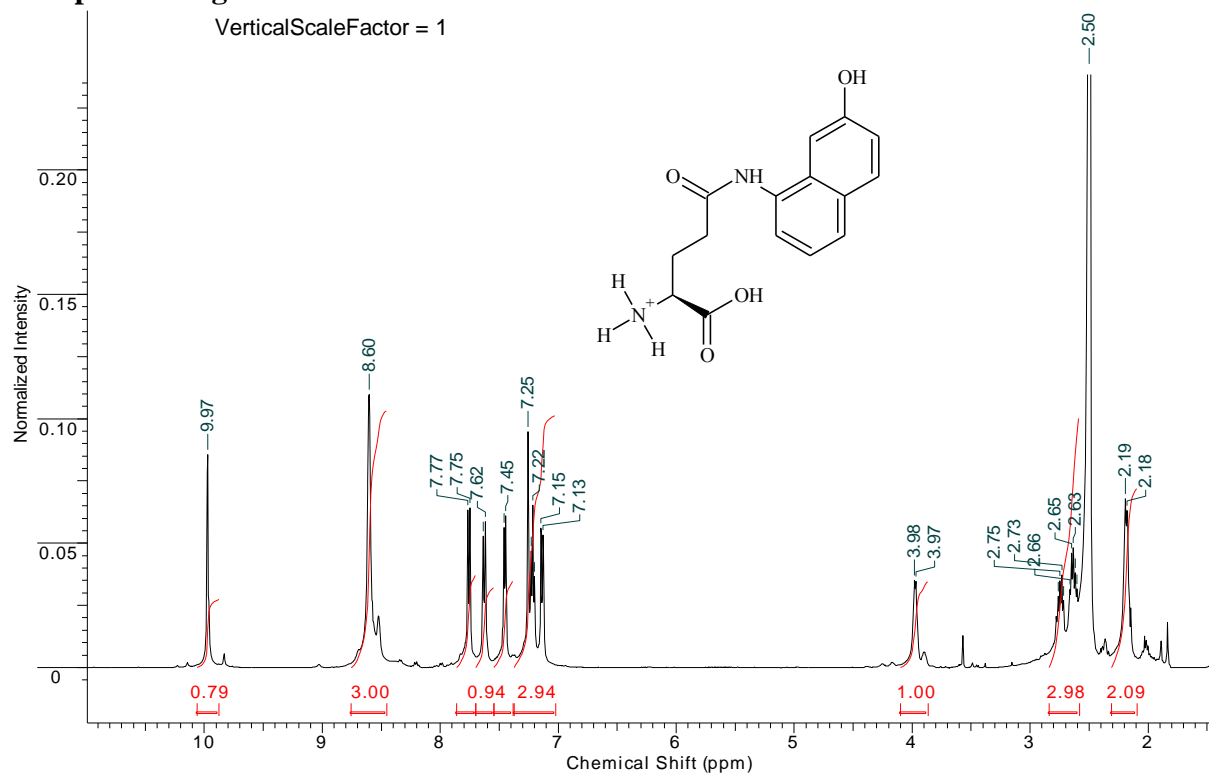
Appendix A: NMR spectra of final product β -aryl-aspartamides & α -aryl-amide-aspartates

1-Biphenyl- α -amide-aspartate



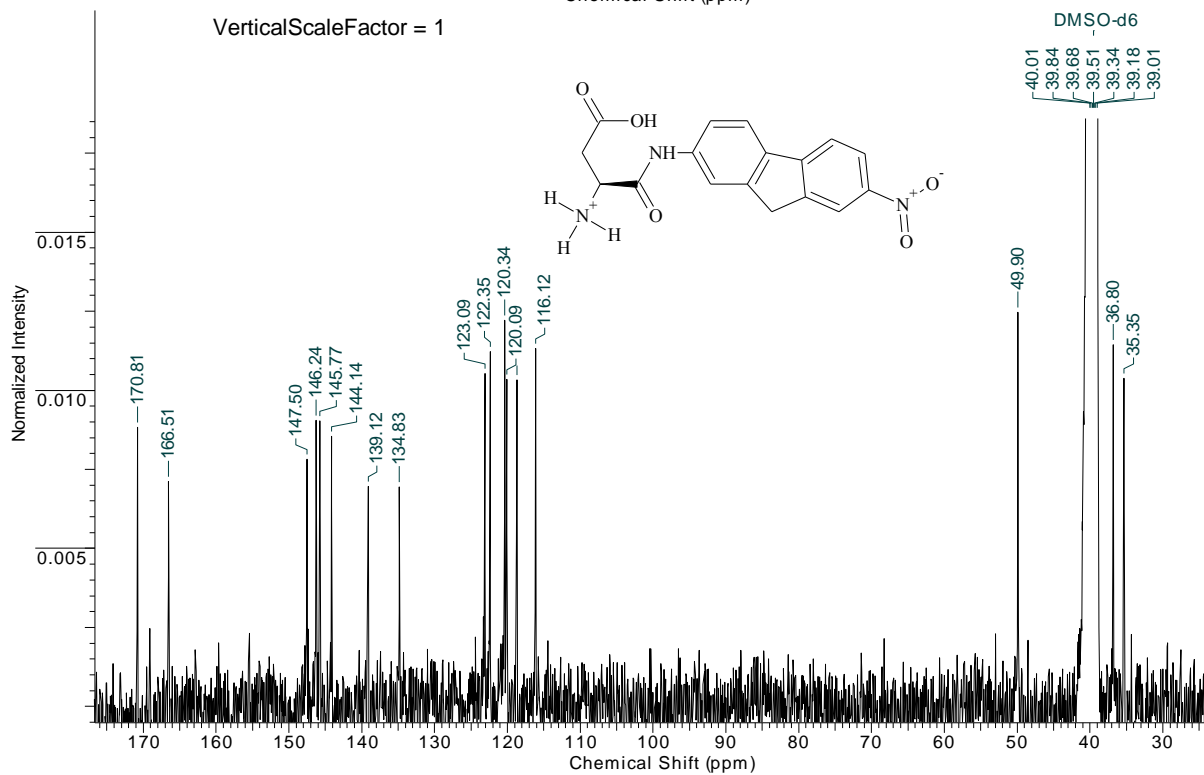
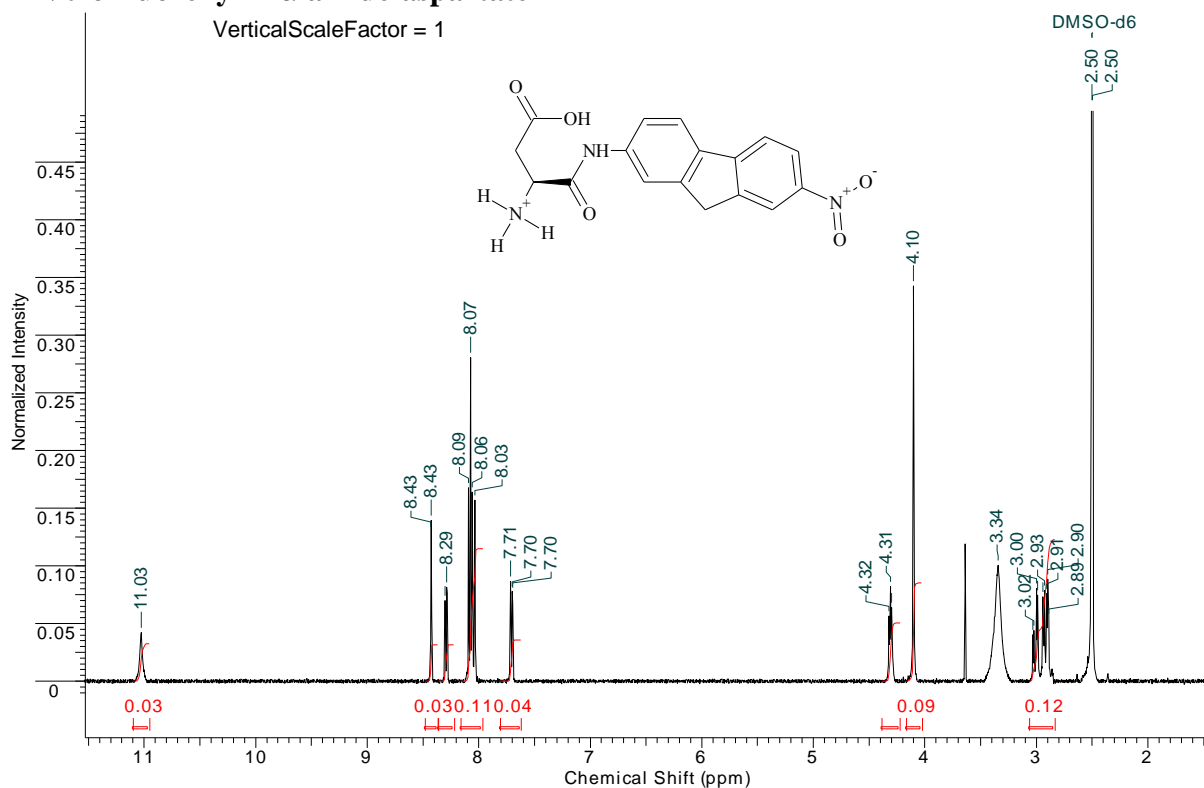
Appendix A: NMR spectra of final product β -aryl-aspartamides & α -aryl-amide aspartates

1-Naphth-7-ol-glutamide



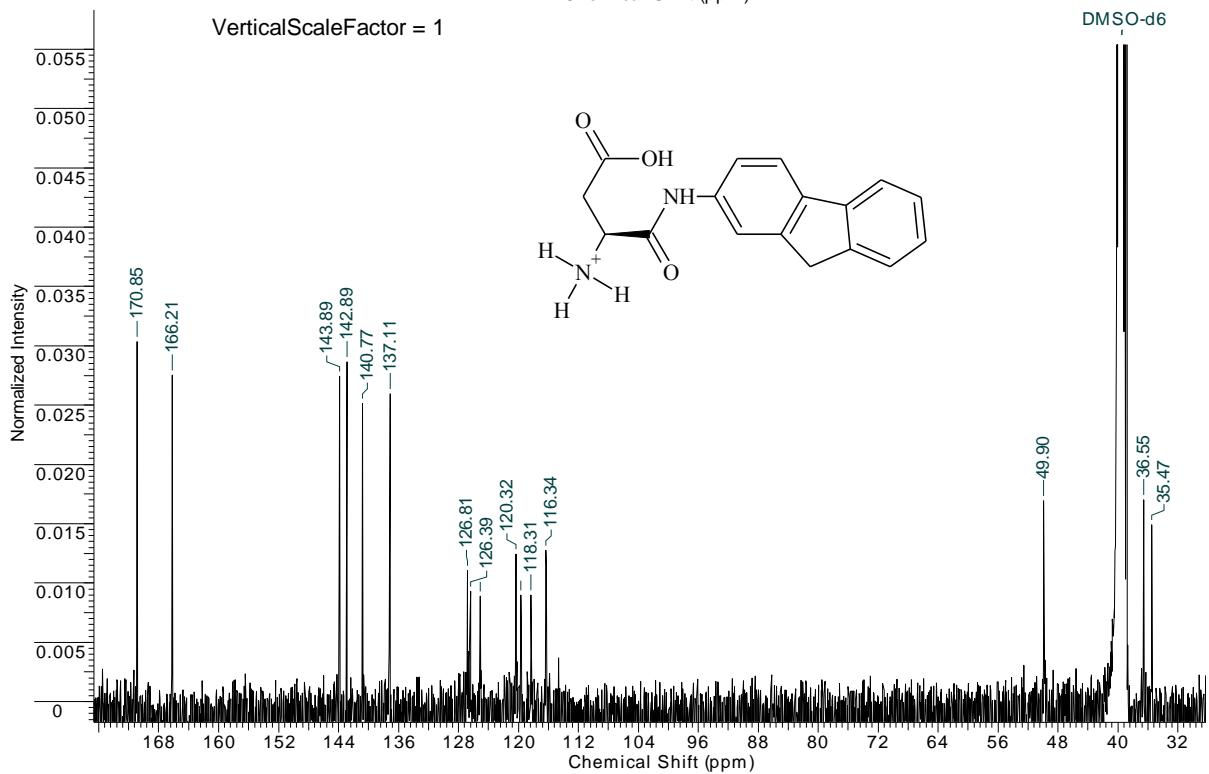
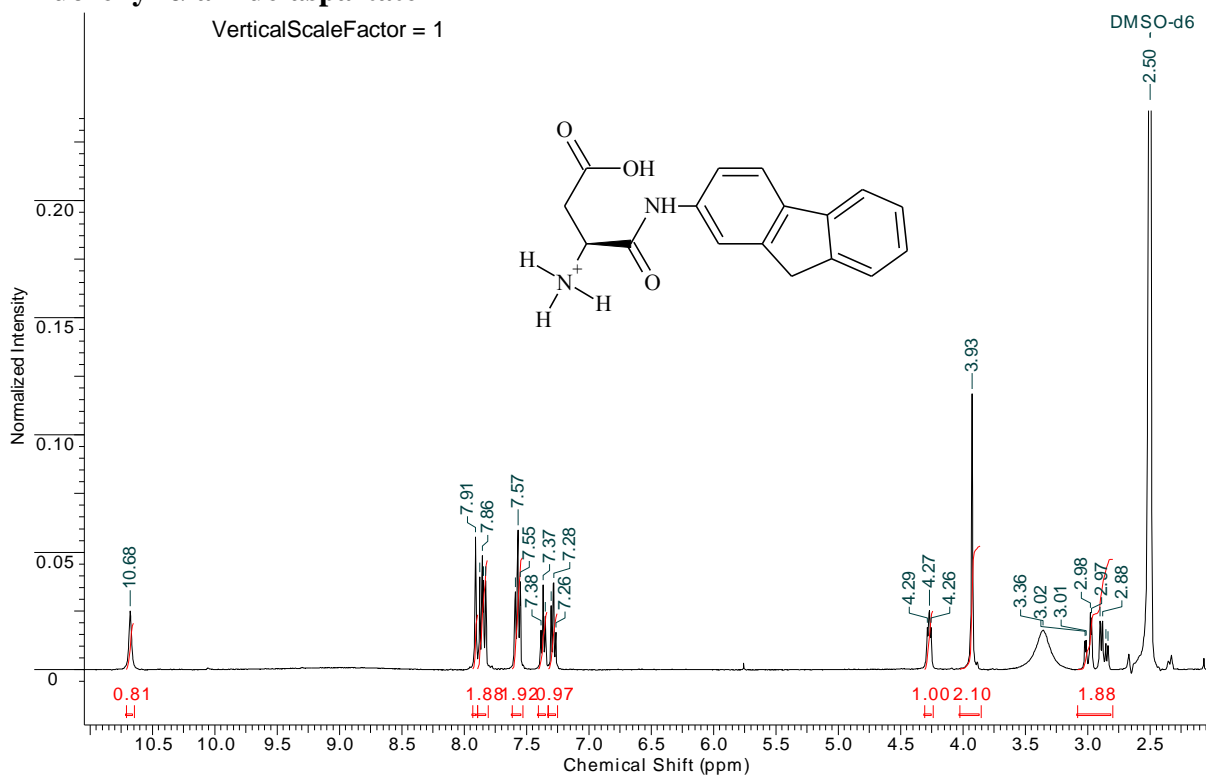
Appendix A: NMR spectra of final product β -aryl-aspartamides & α -aryl-amide aspartates

7-Nitro-fluorenyl-2- α -amide-aspartate



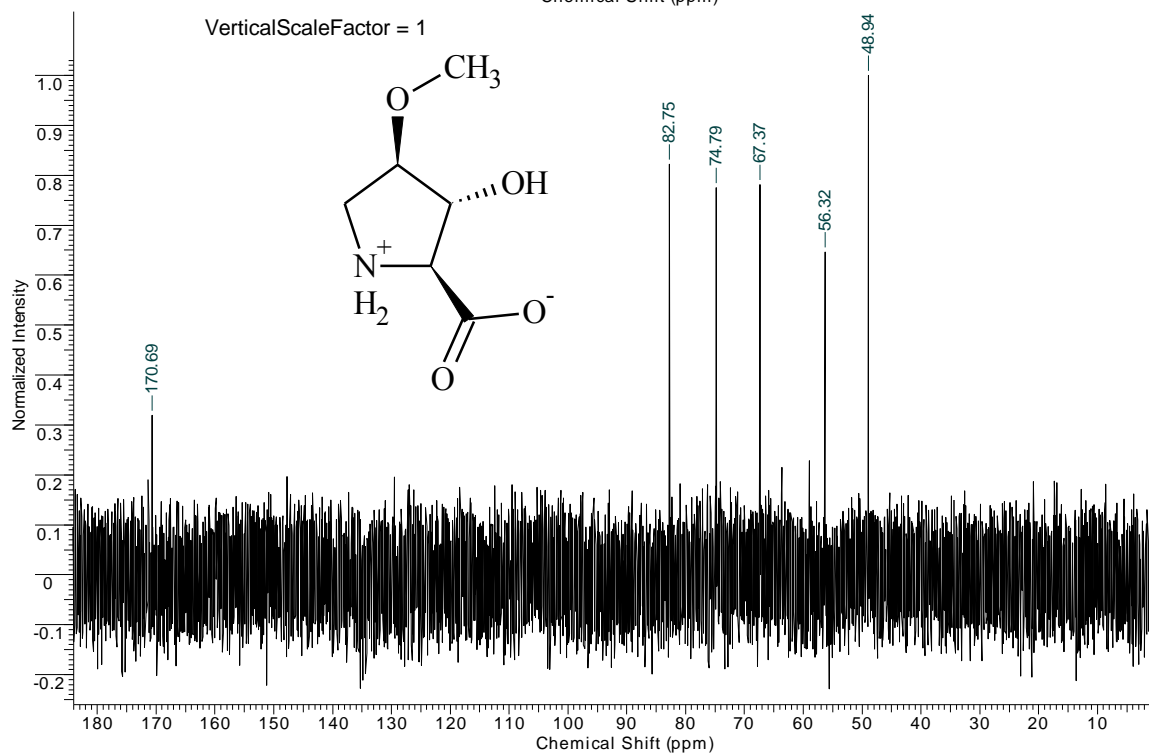
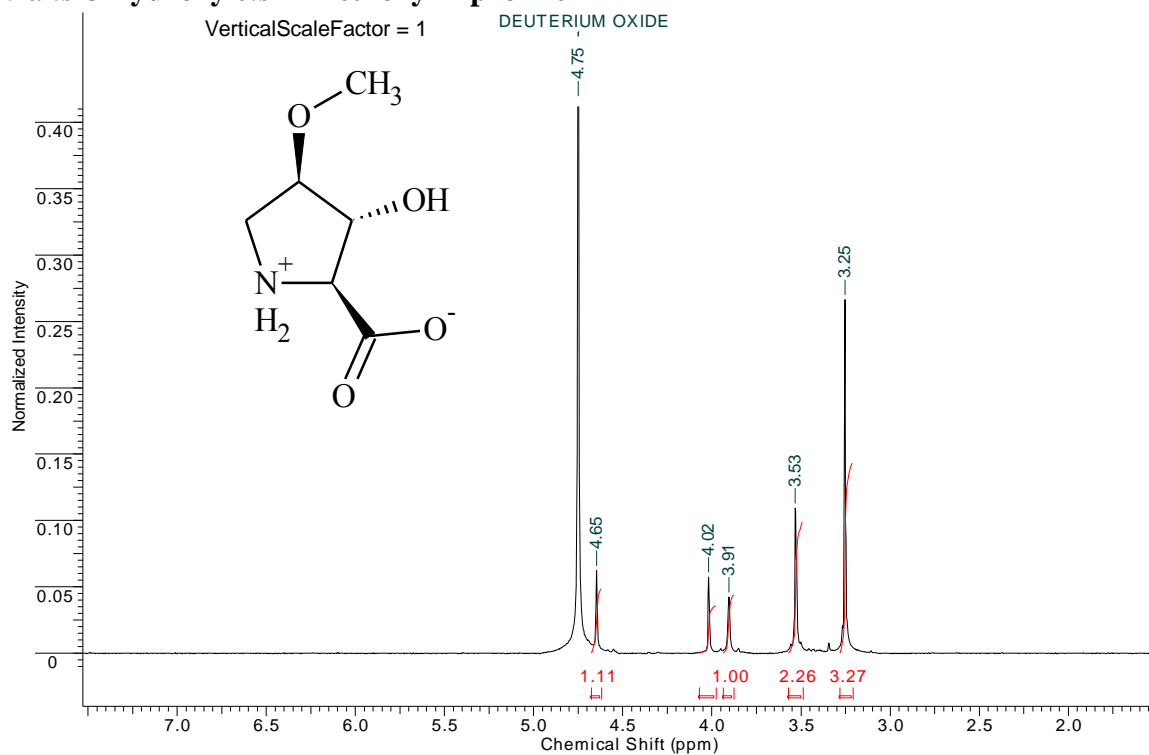
Appendix A: NMR spectra of final product β -aryl-aspartamides & α -aryl-amide aspartates

2-fluorenyl- α -amide-aspartate



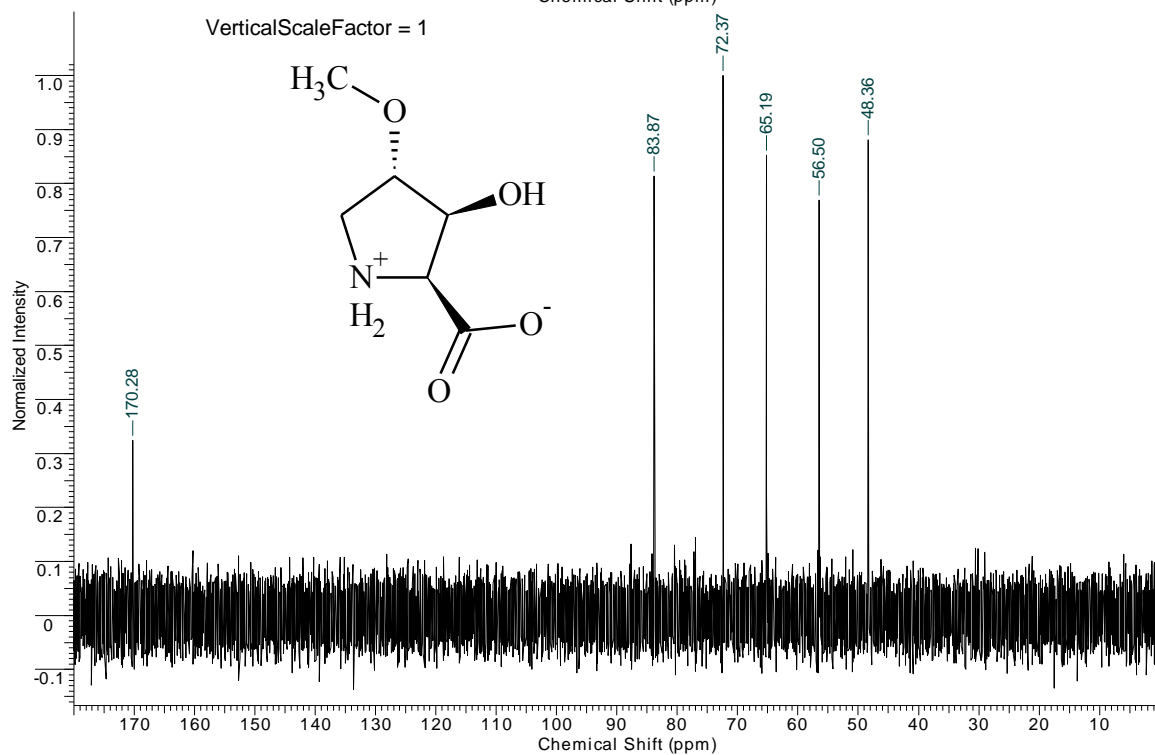
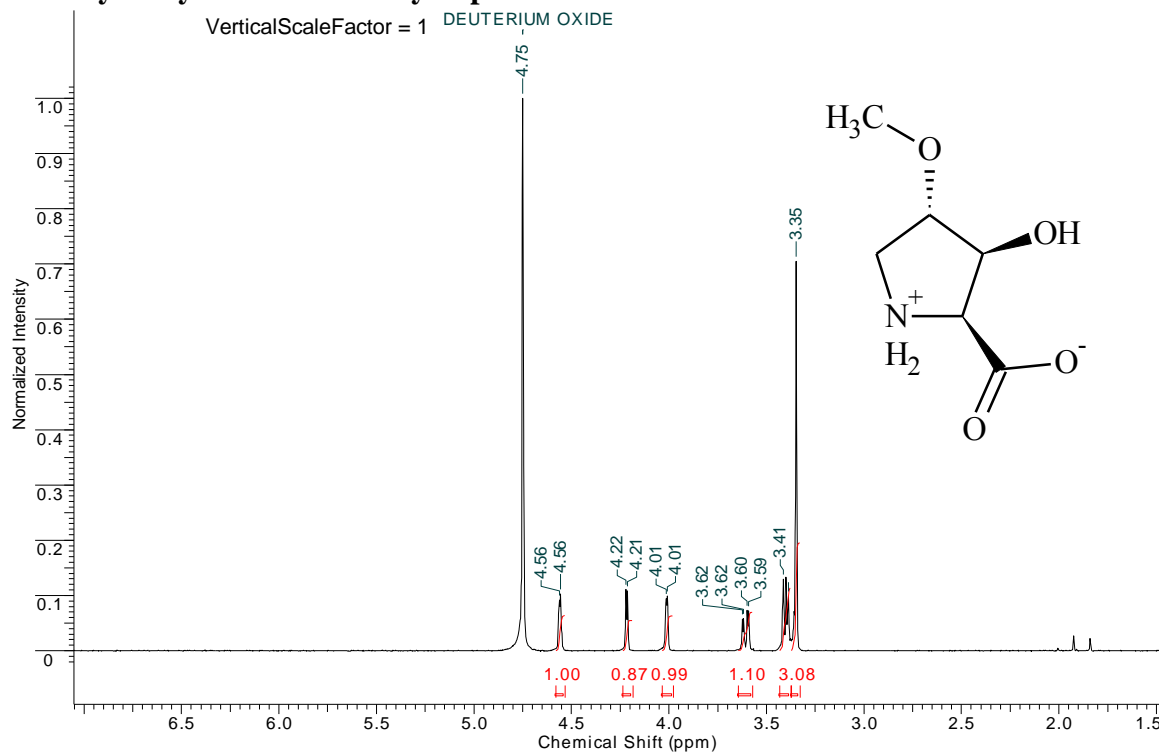
Appendix B: NMR spectra of hydroxy-L-proline derivatives

***trans*-3-hydroxy-*cis*-4-methoxy-L-proline**



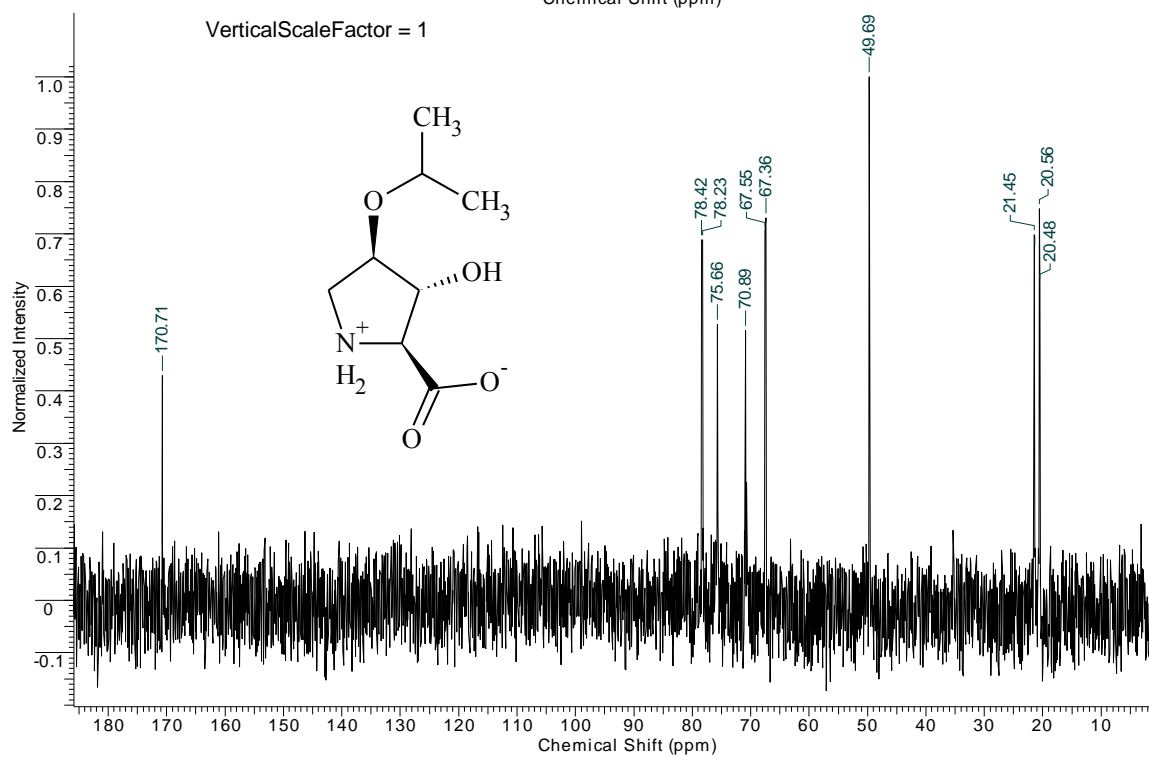
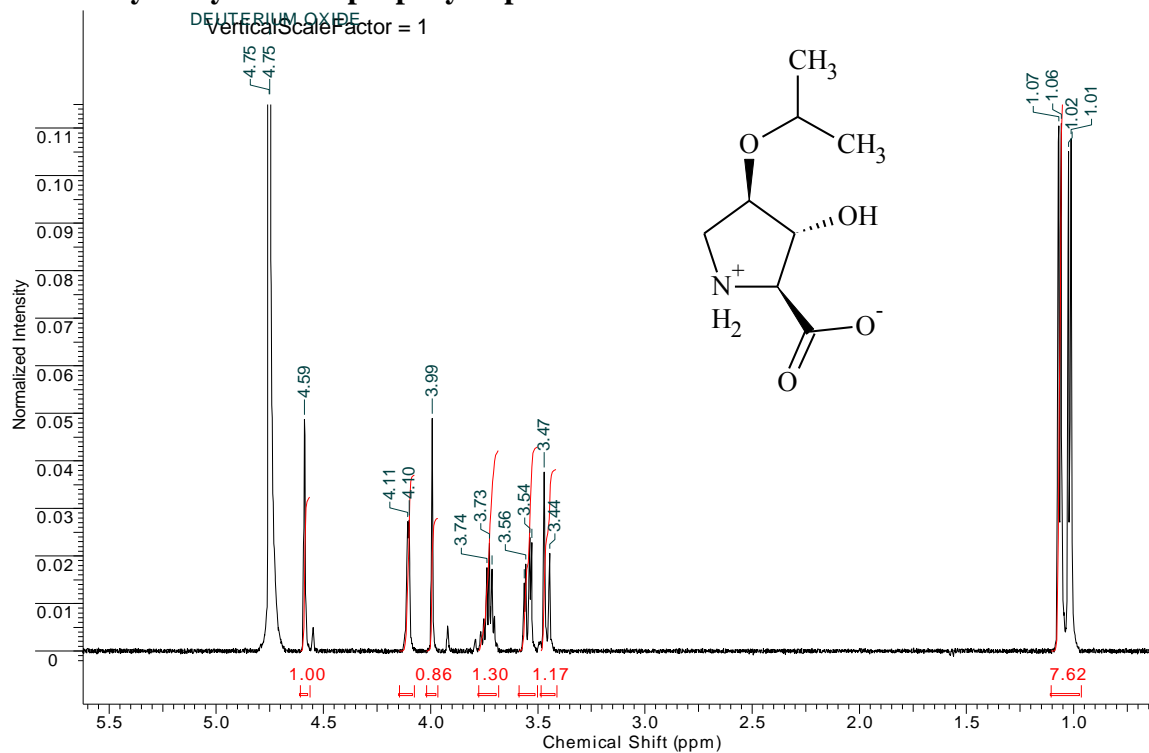
Appendix B: NMR spectra of hydroxy-L-proline derivatives

***cis*-3-hydroxy-*trans*-4-methoxy-L-proline**



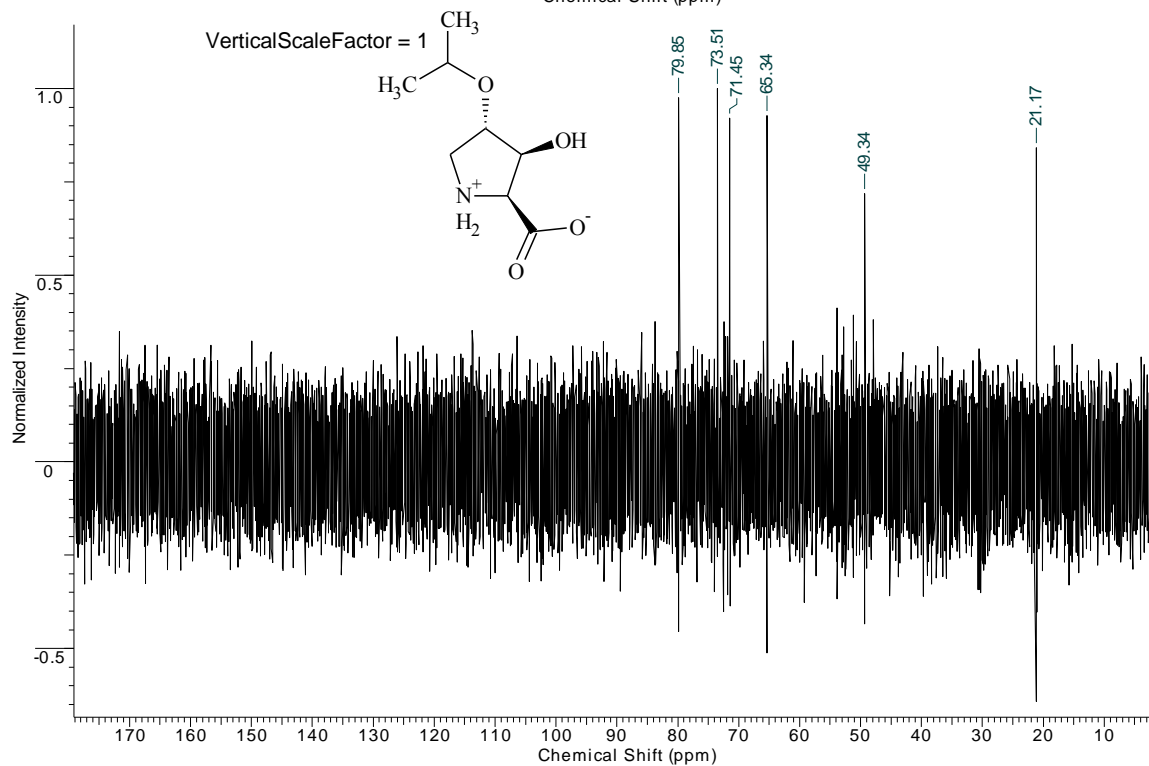
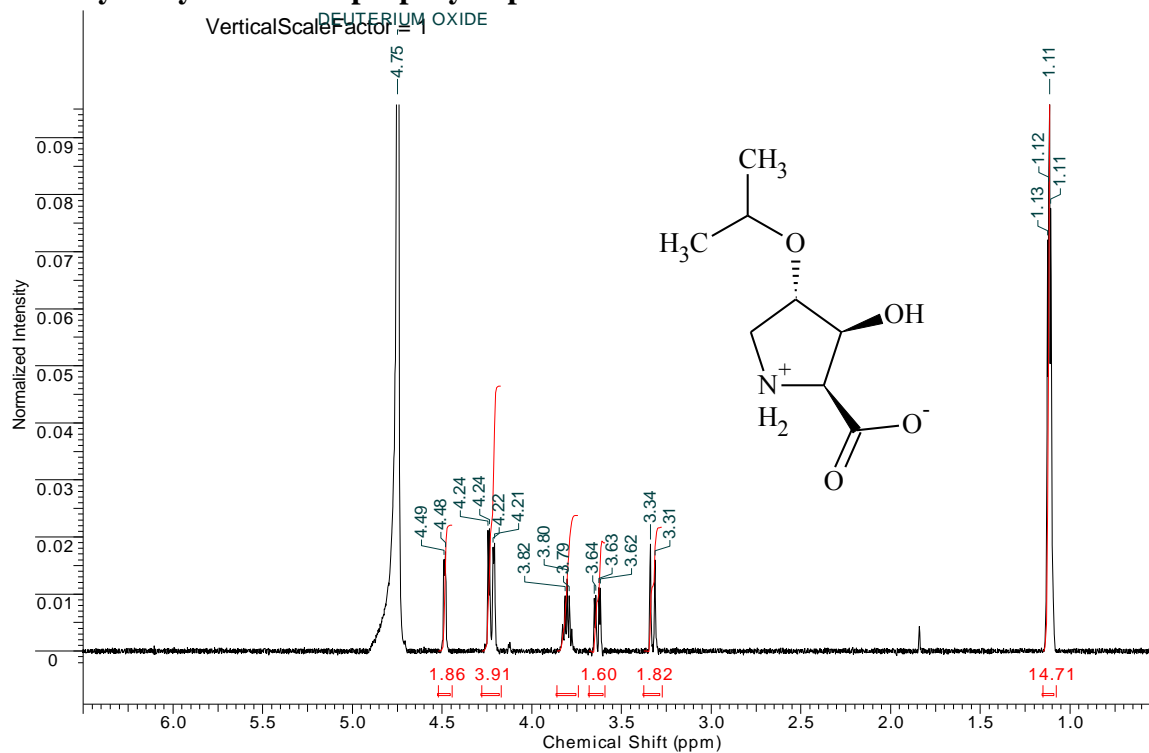
Appendix B: NMR spectra of hydroxy-L-proline derivatives

***trans*-3-hydroxy-*cis*-4-isopropoxy-L-proline**



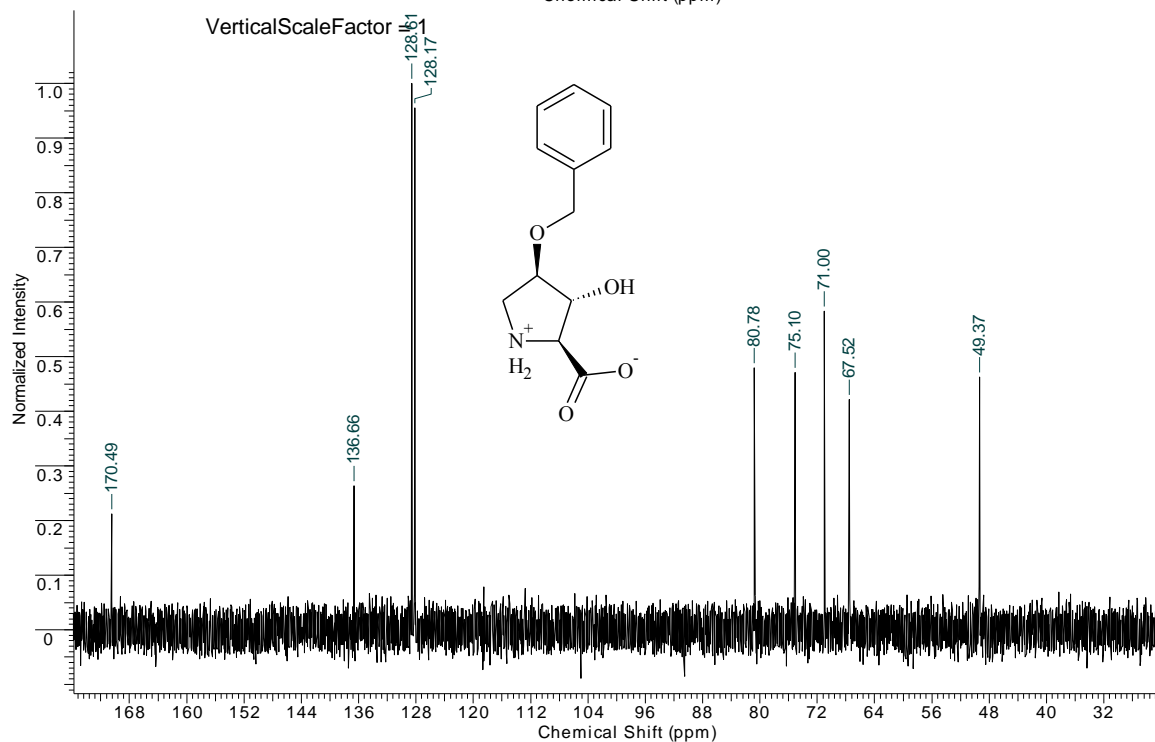
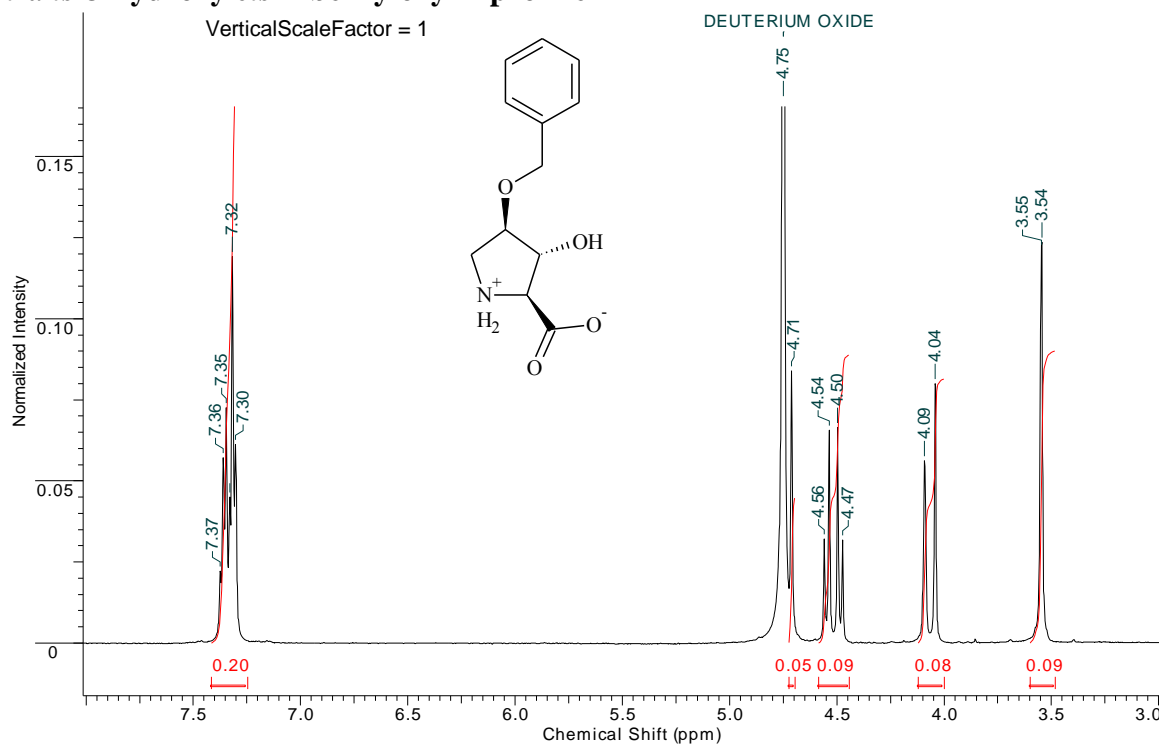
Appendix B: NMR spectra of hydroxy-L-proline derivatives

cis-3-hydroxy-trans-4-isopropoxy-L-proline



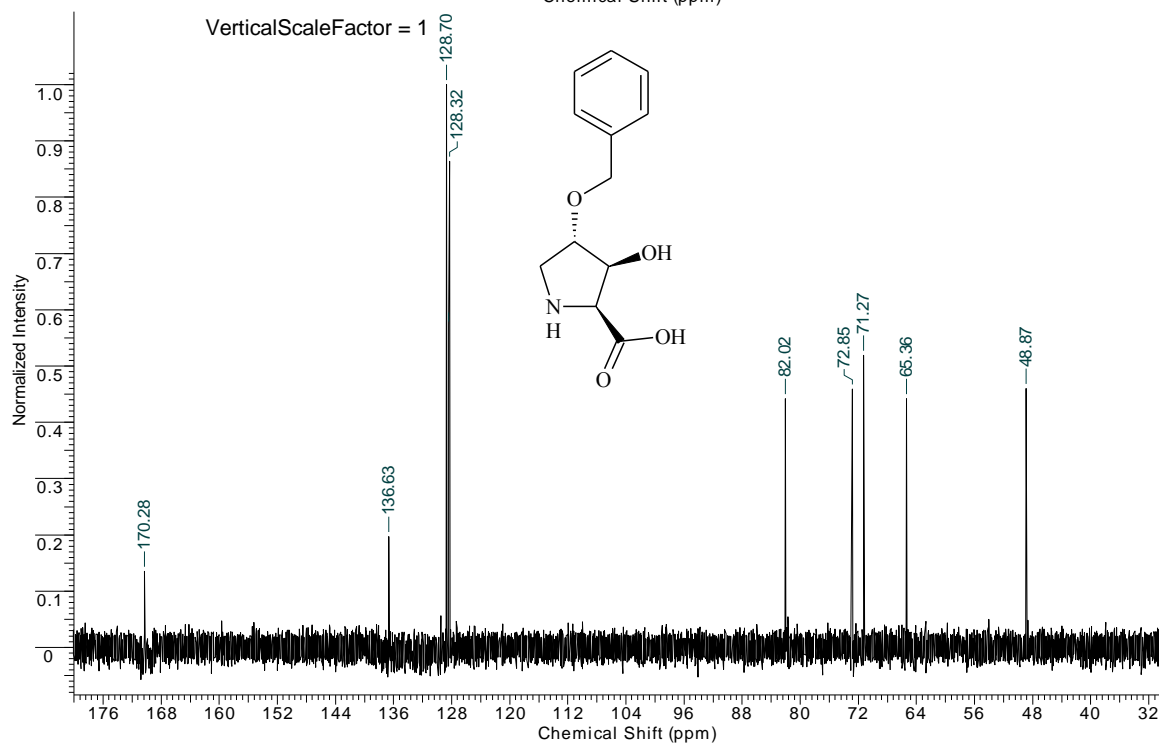
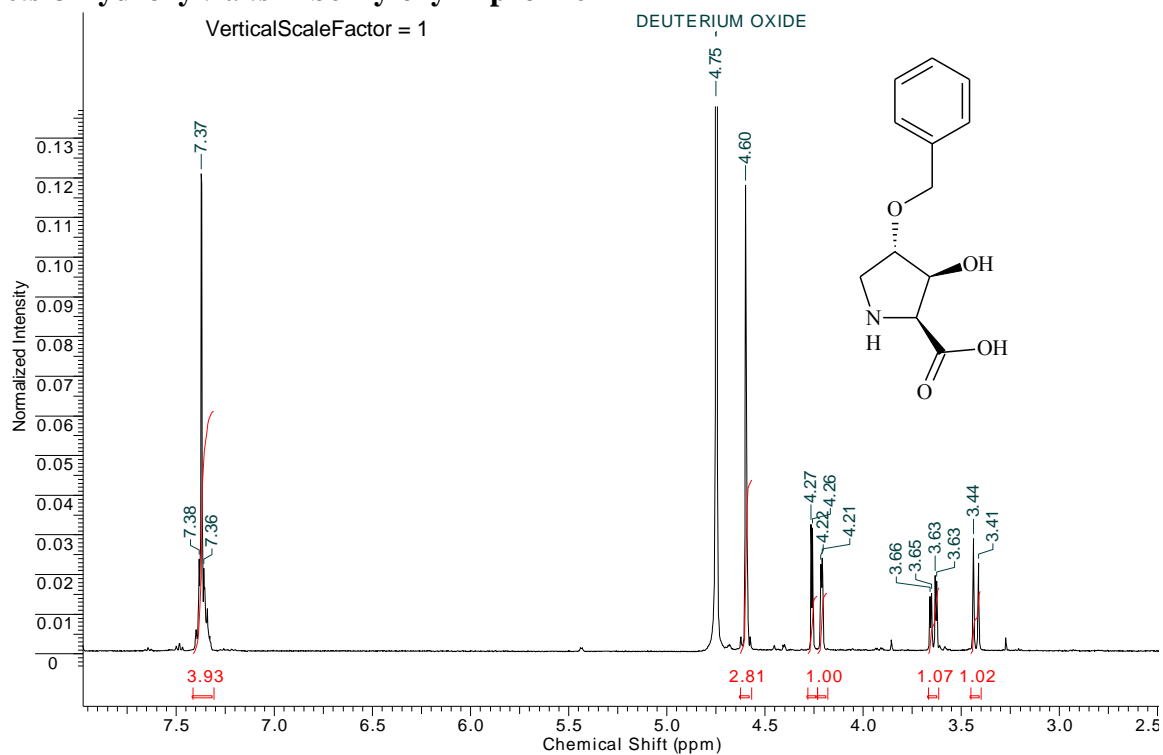
Appendix B: NMR spectra of hydroxy-L-proline derivatives

***trans*-3-hydroxy-*cis*-4-benzyloxy-L-proline**



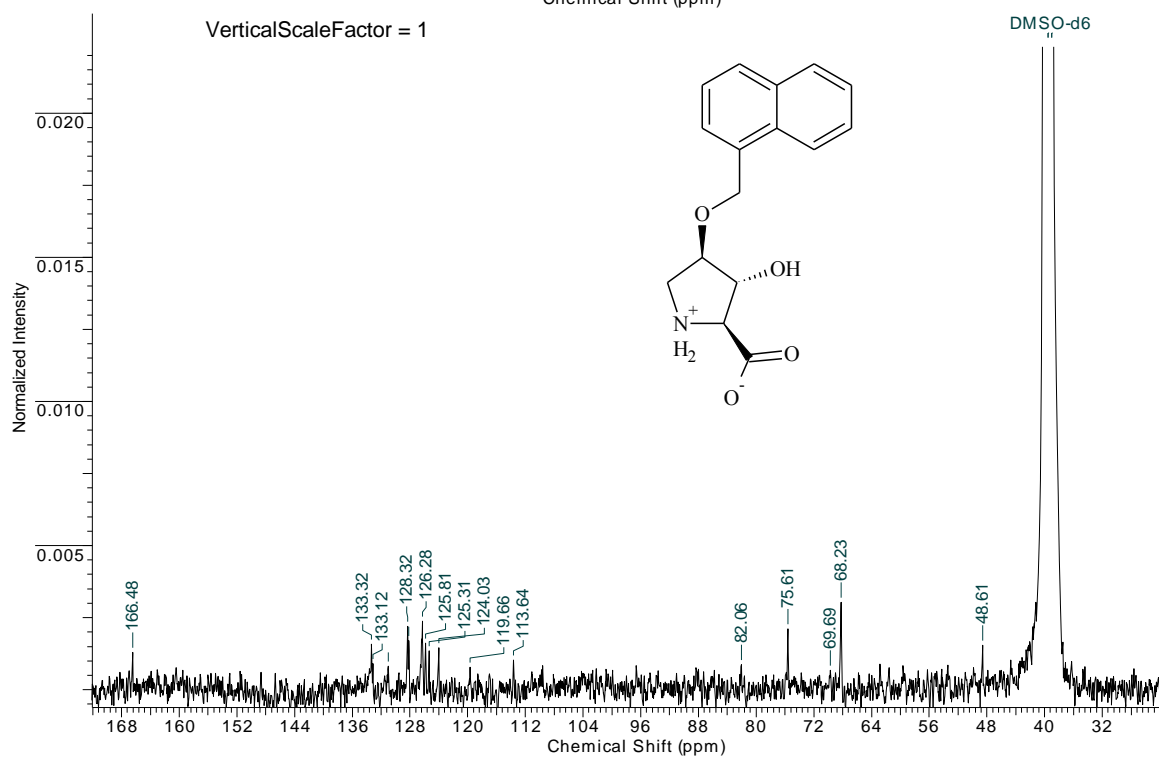
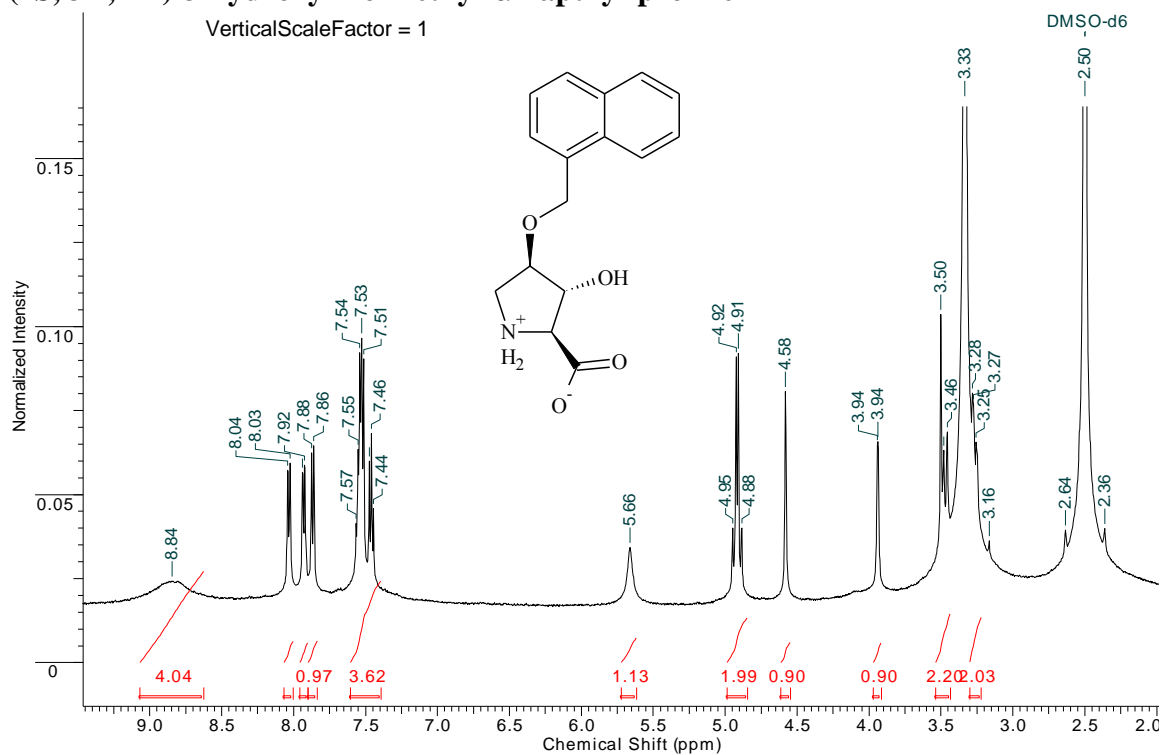
Appendix B: NMR spectra of hydroxy-L-proline derivatives

***cis*-3-hydroxy-*trans*-4-benzyloxy-L-proline**



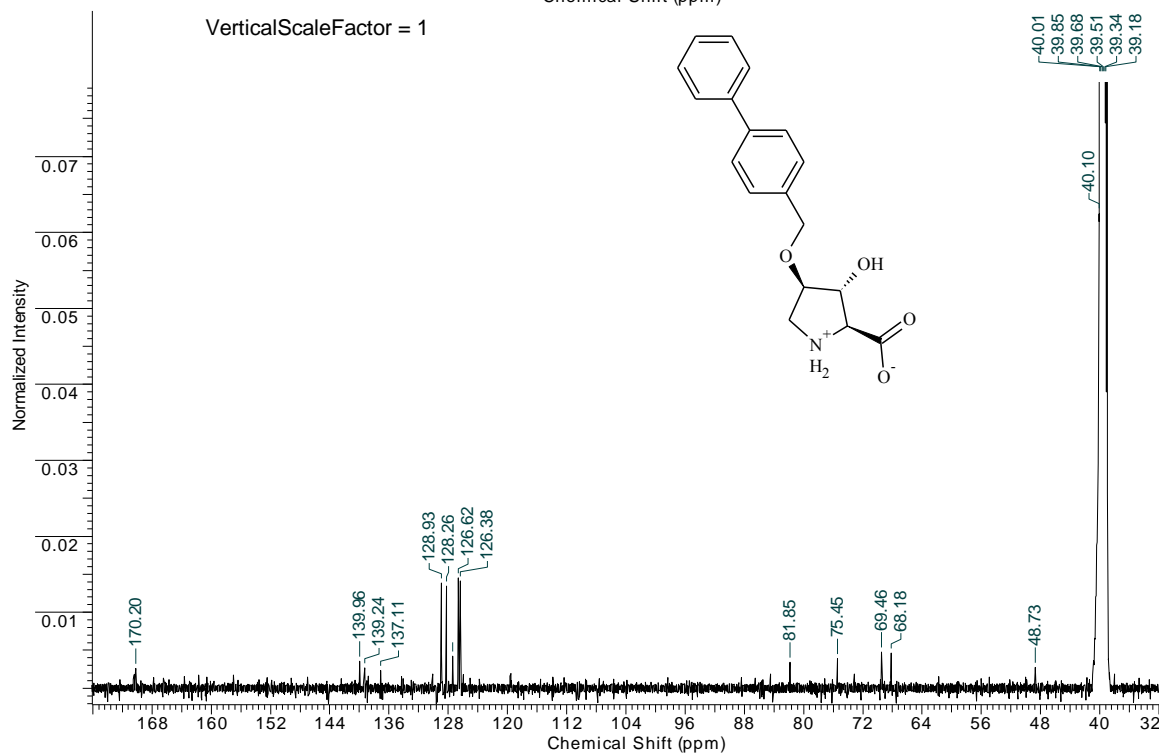
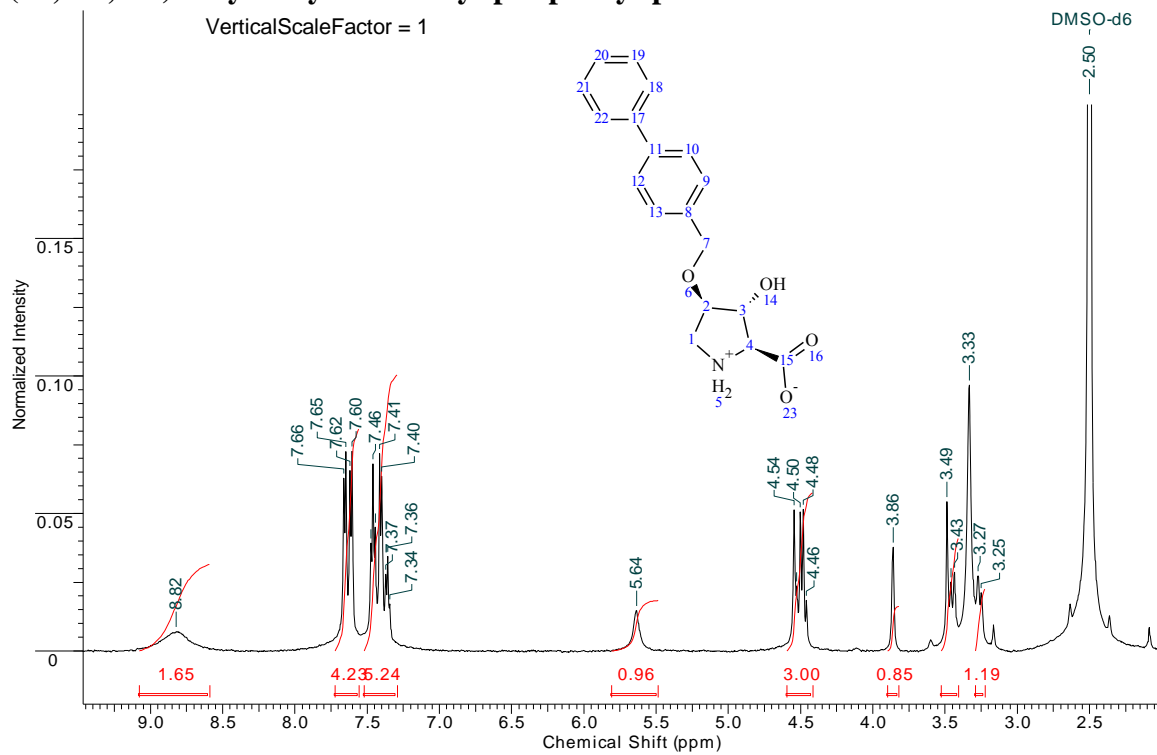
Appendix B: NMR spectra of hydroxy-L-proline derivatives

(2S, 3R, 4R)-3-hydroxy-4-o-methyl- α -naphthyl-proline



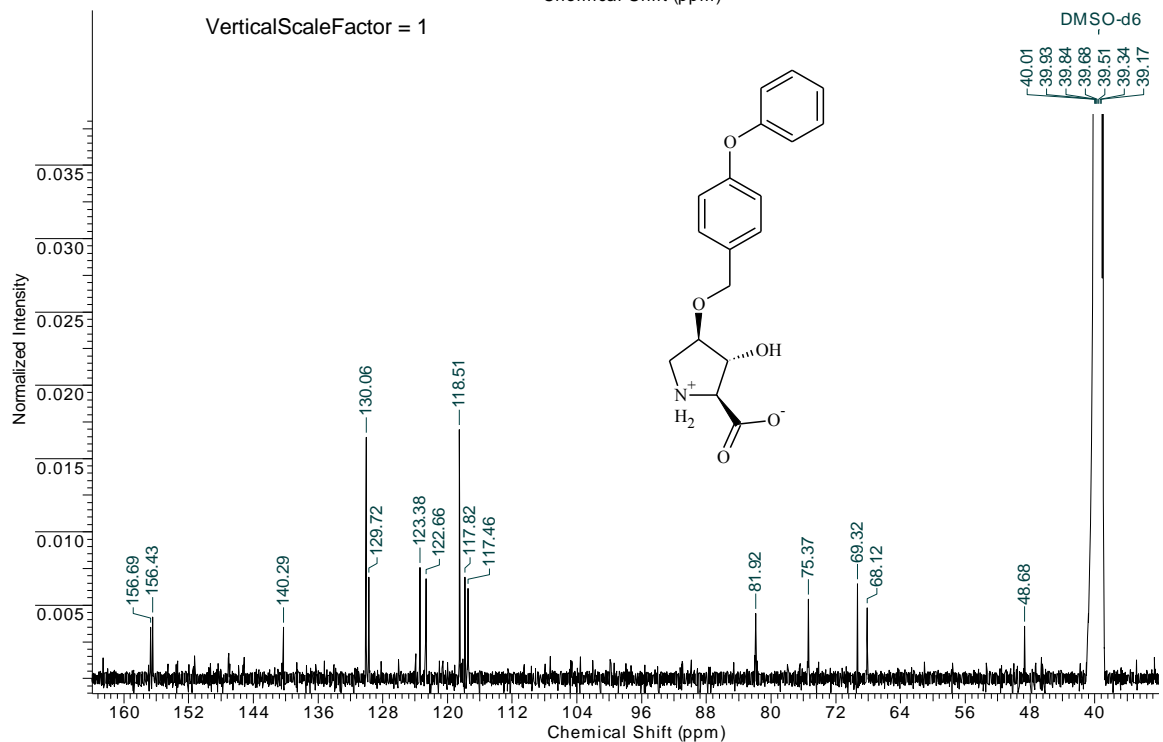
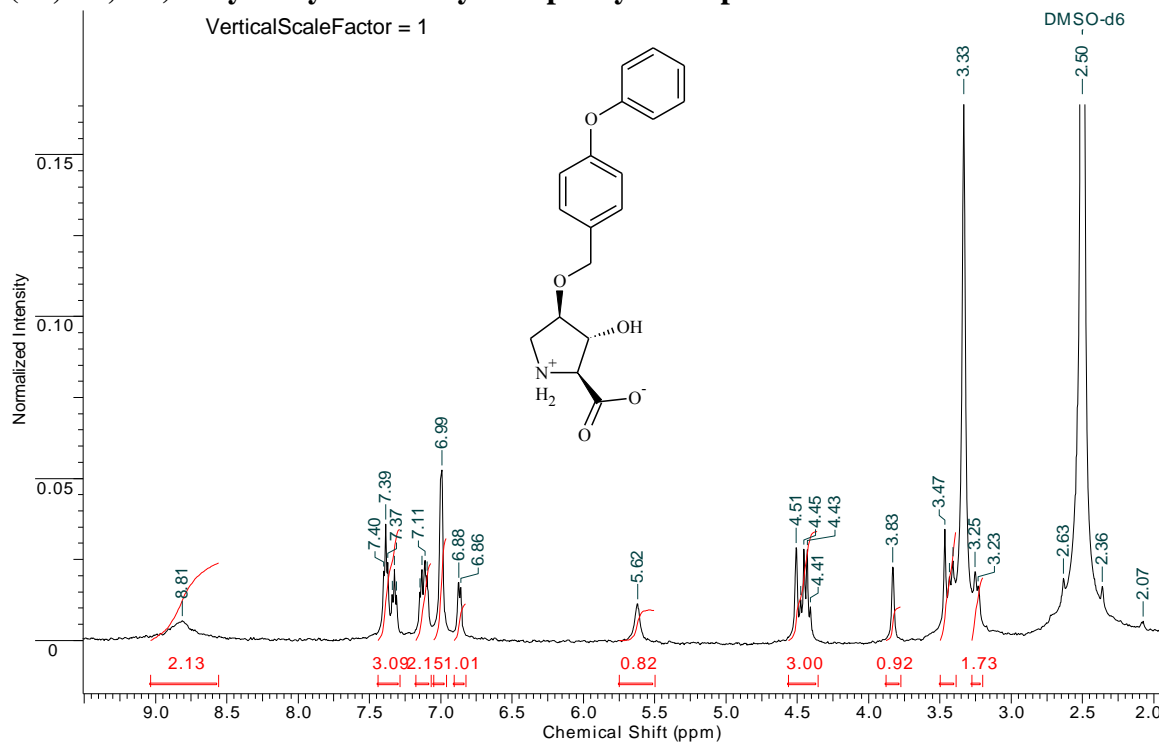
Appendix B: NMR spectra of hydroxy-L-proline derivatives

(2S, 3R, 4R)-3-hydroxy-4-o-methyl-p-biphenyl-proline



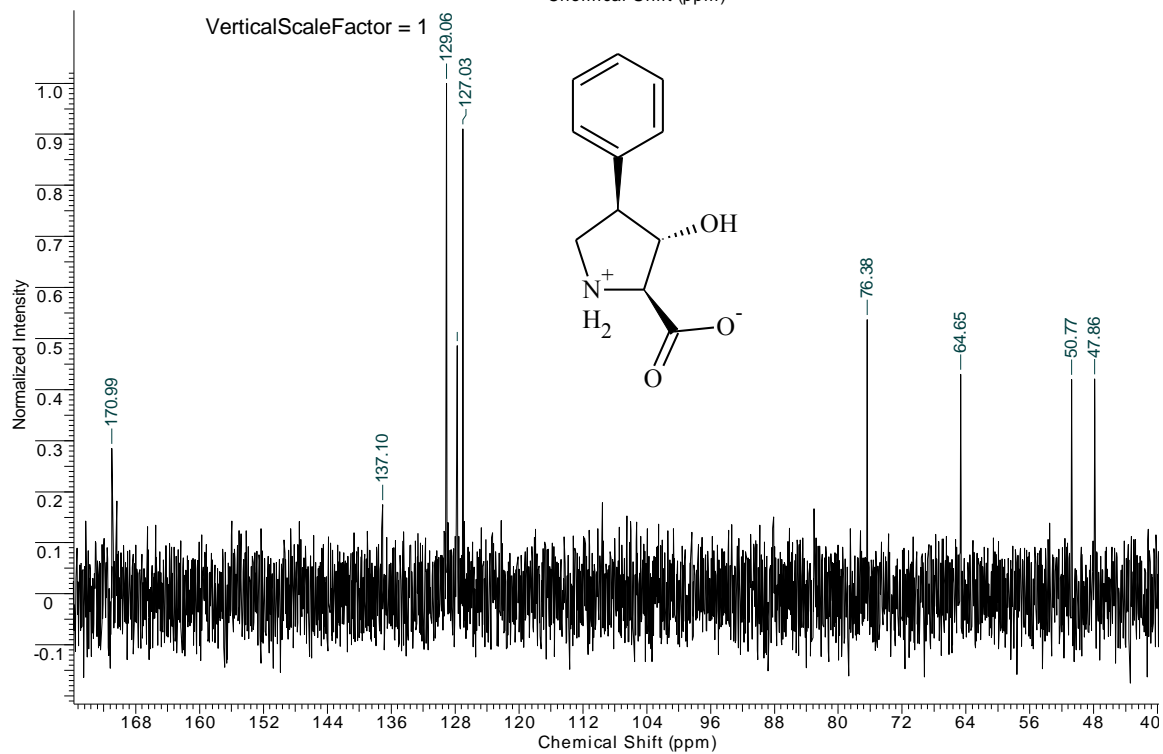
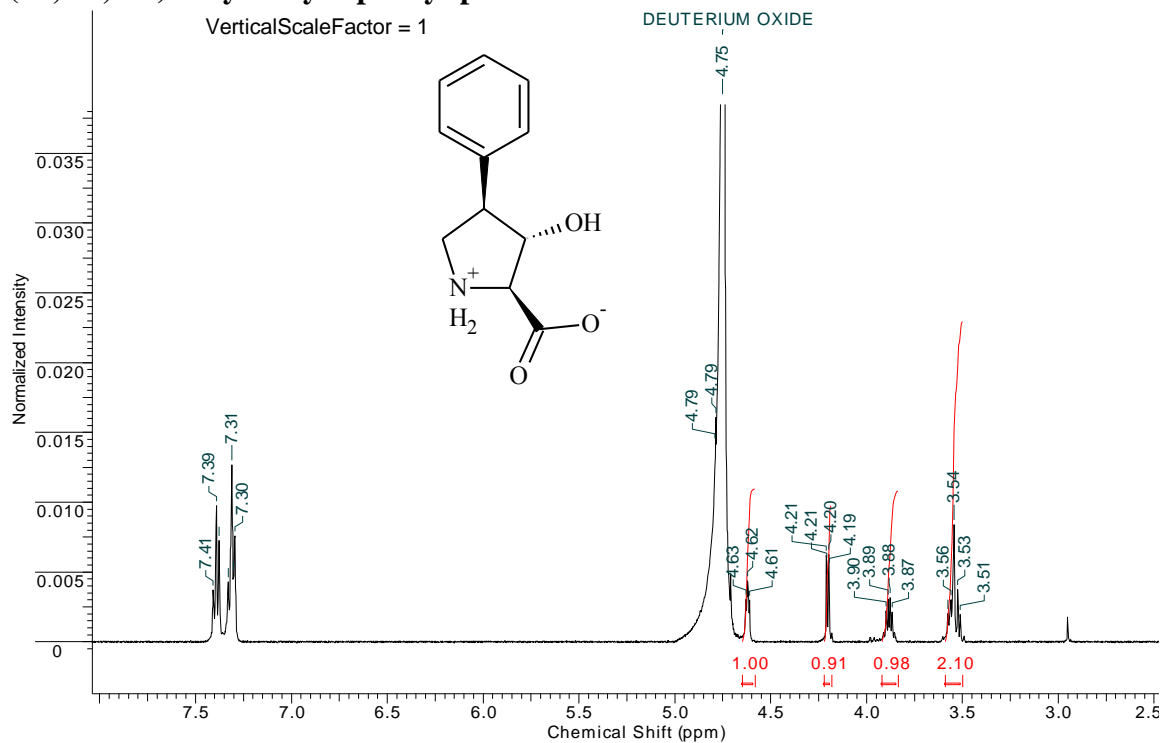
Appendix B: NMR spectra of hydroxy-L-proline derivatives

(2S, 3R, 4R)-3-hydroxy-4-o-methyl-3-biphenylether-proline

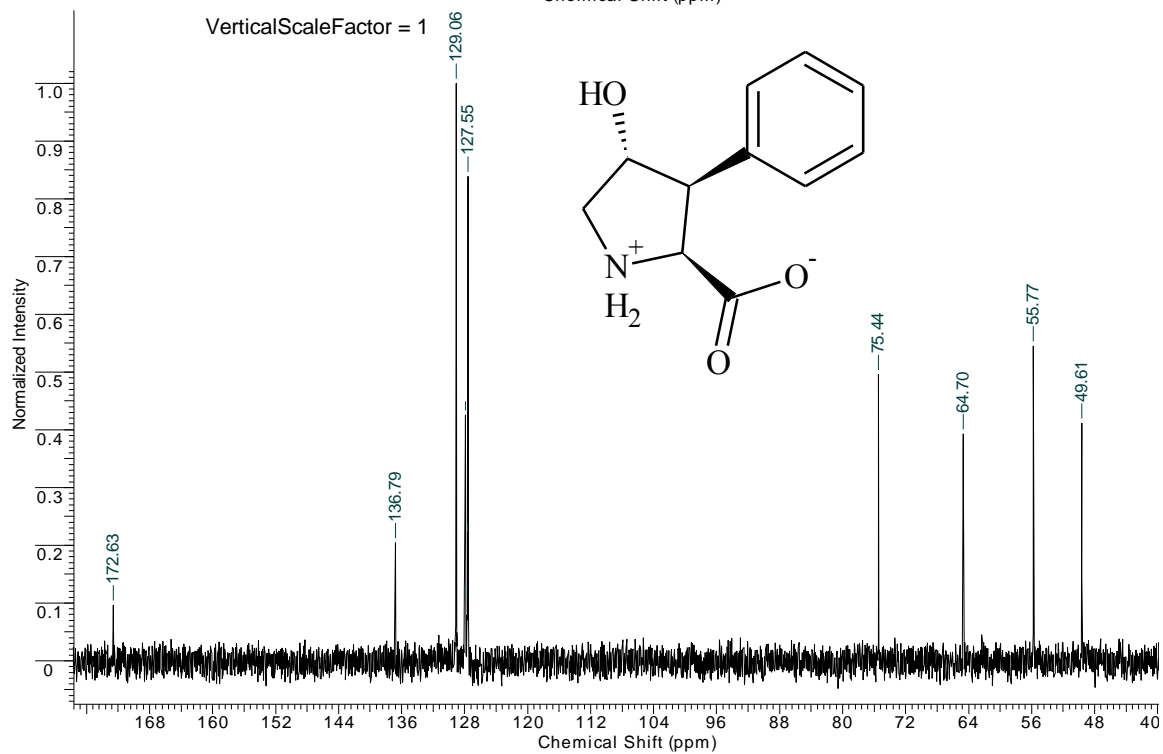
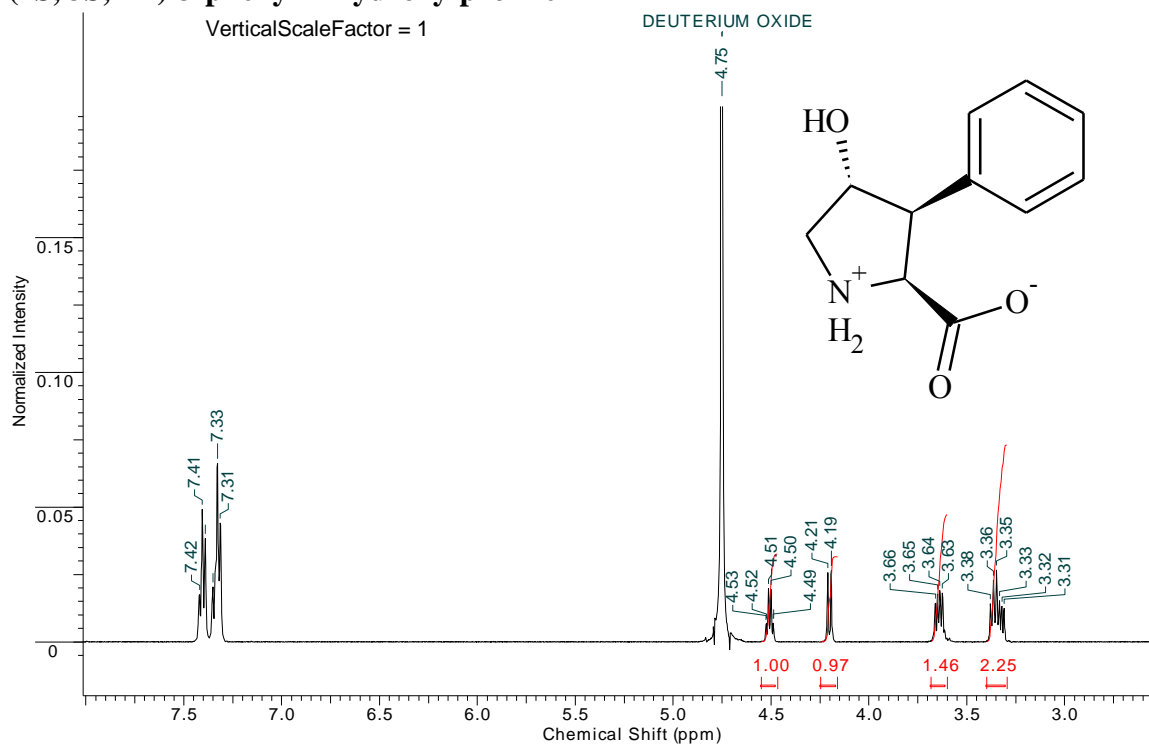


Appendix B: NMR spectra of hydroxy-L-proline derivatives

(2S, 3S, 4R)-3-hydroxy-4-phenyl-proline

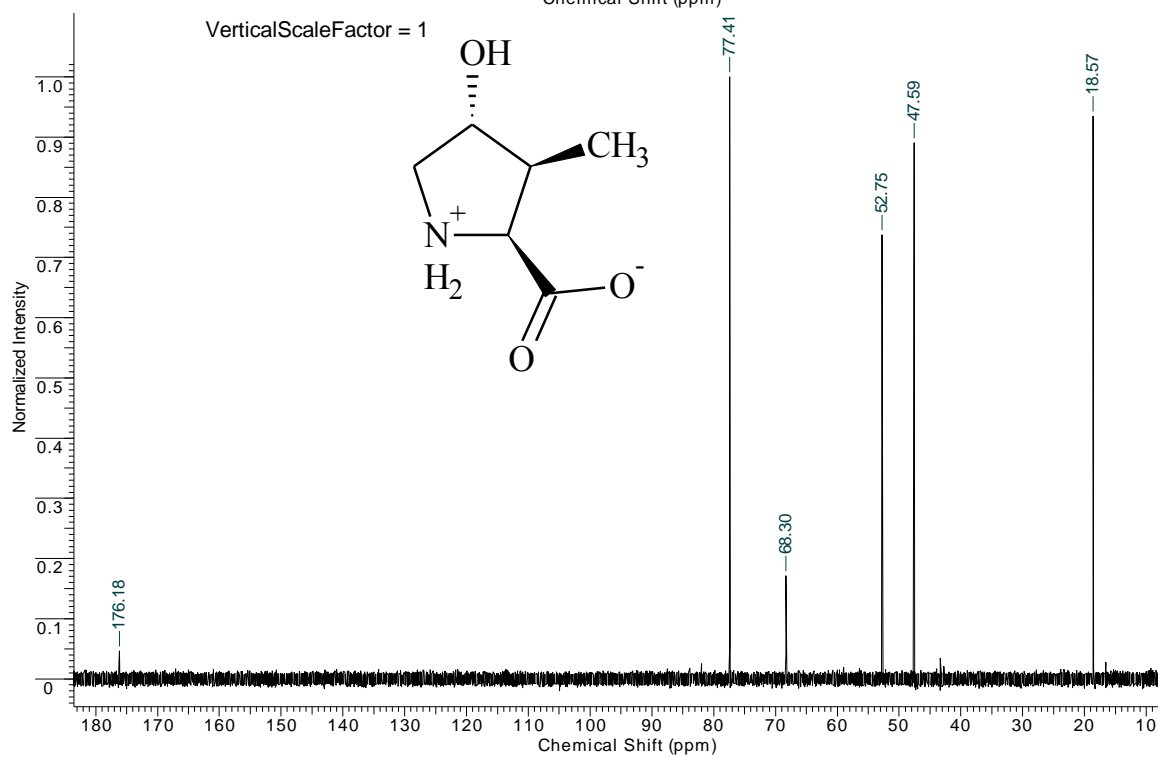
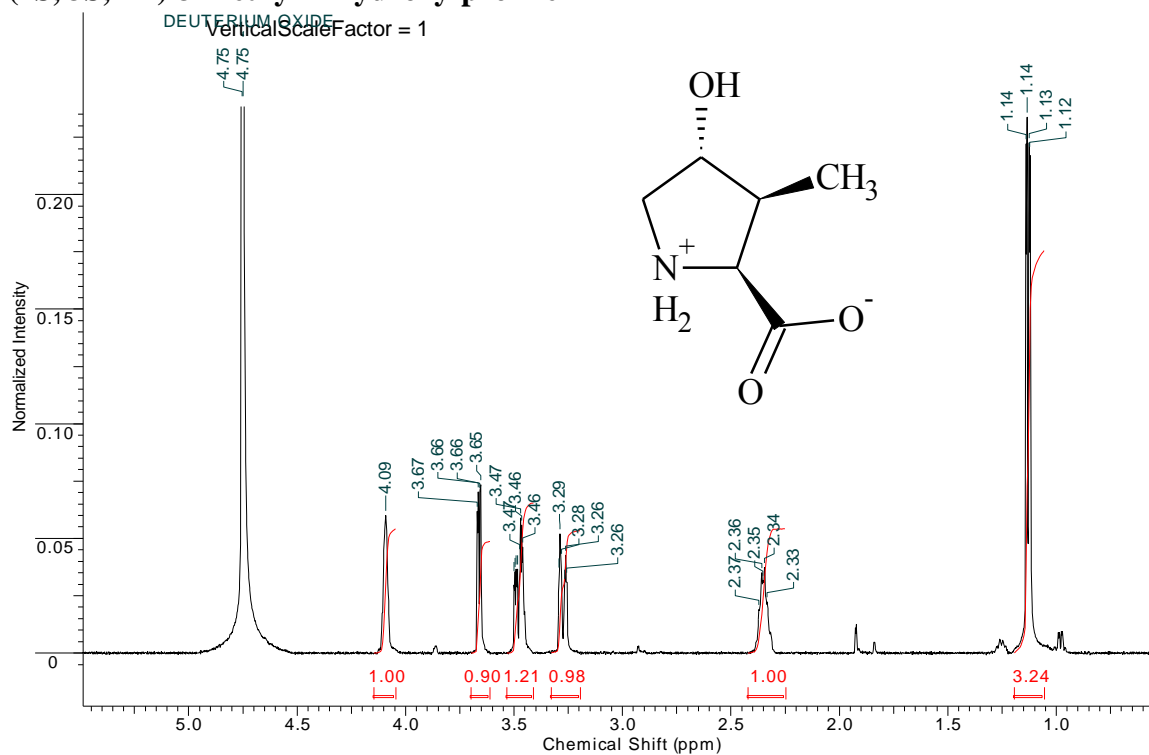


(2S, 3S, 4R)-3-phenyl-4-hydroxy-proline

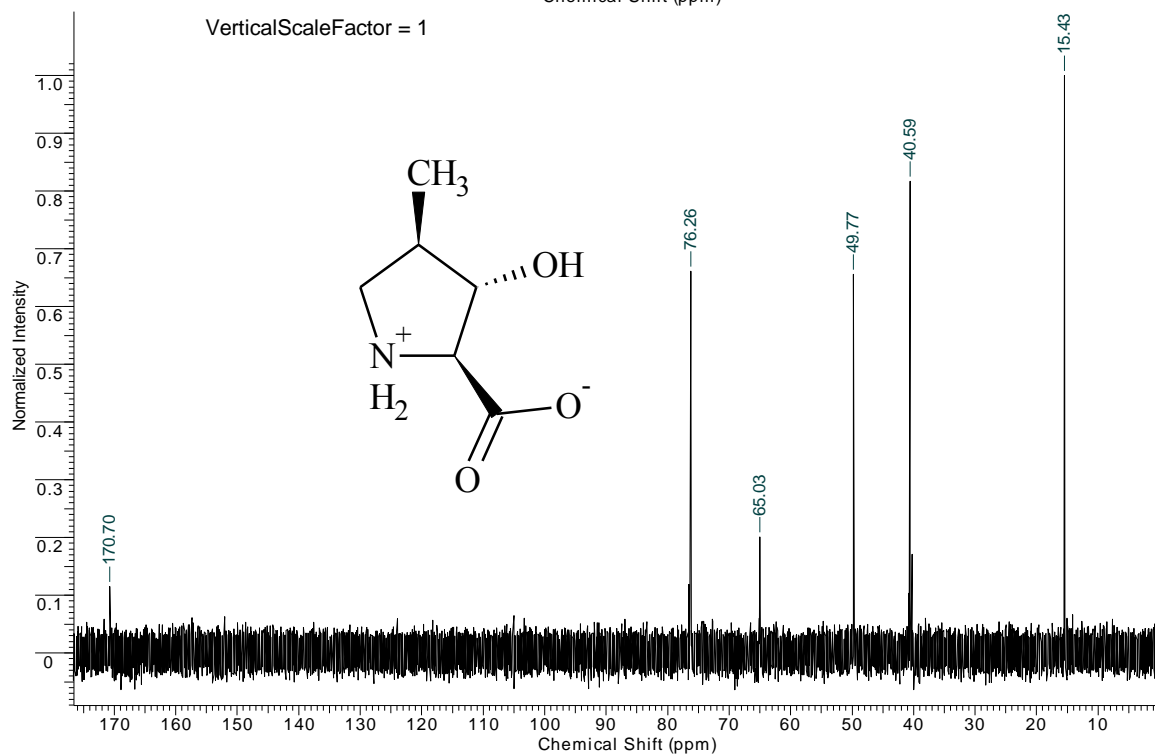
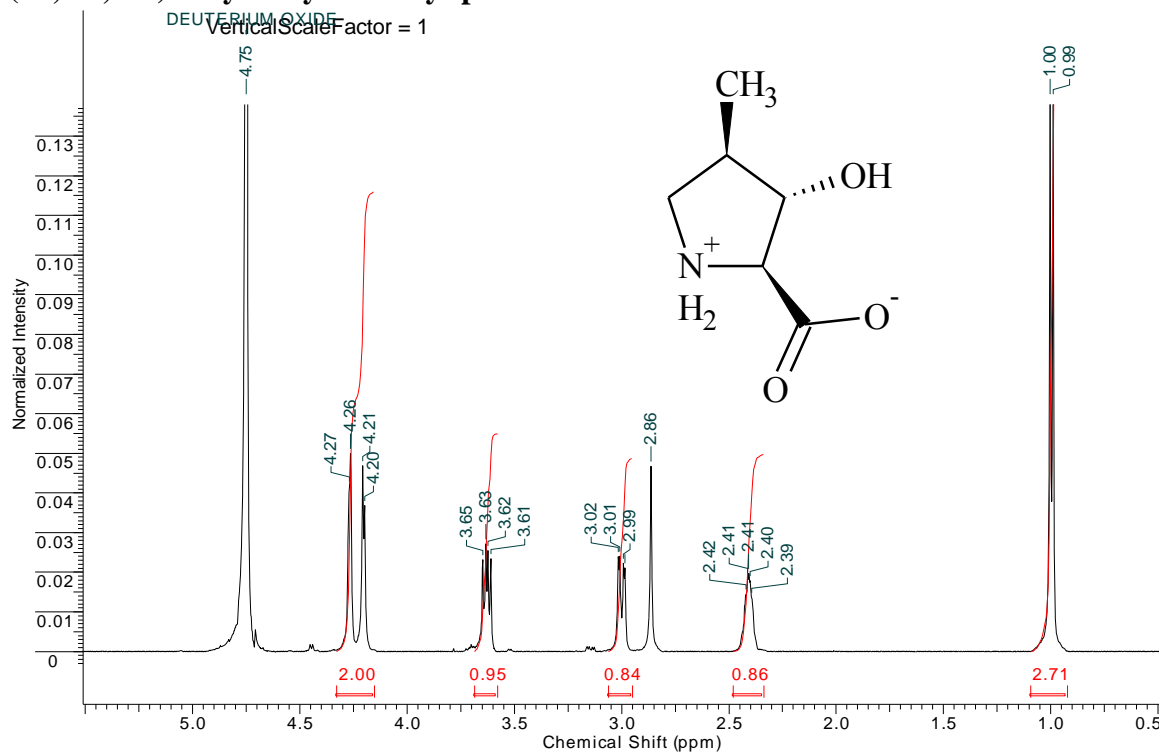


Appendix B: NMR spectra of hydroxy-L-proline derivatives

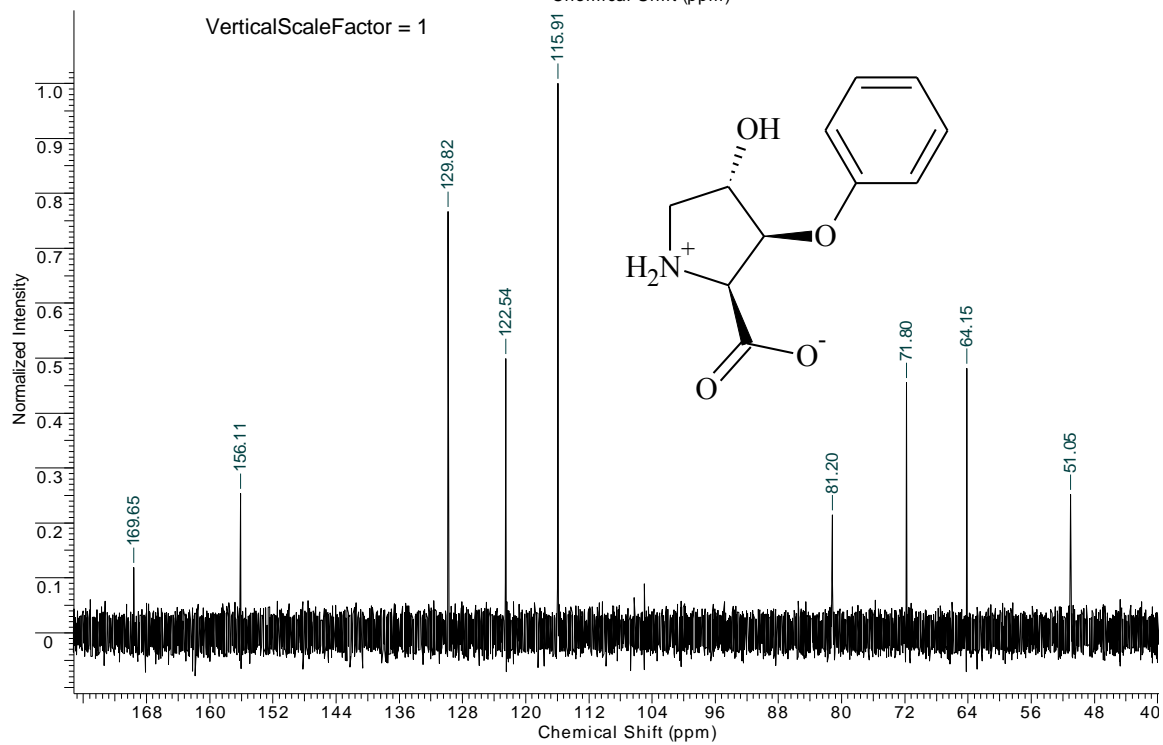
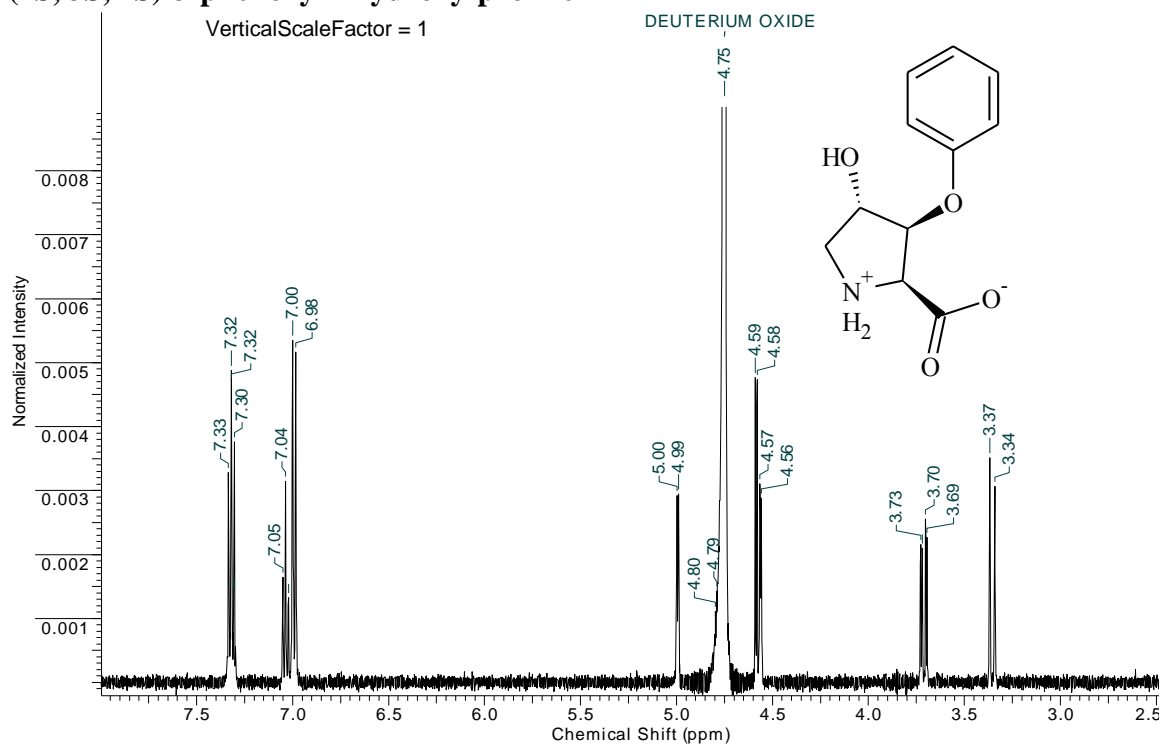
(2S, 3S, 4R)-3-methyl-4-hydroxy-proline



(2S, 3S, 4R)-3-hydroxy-4-methyl-proline

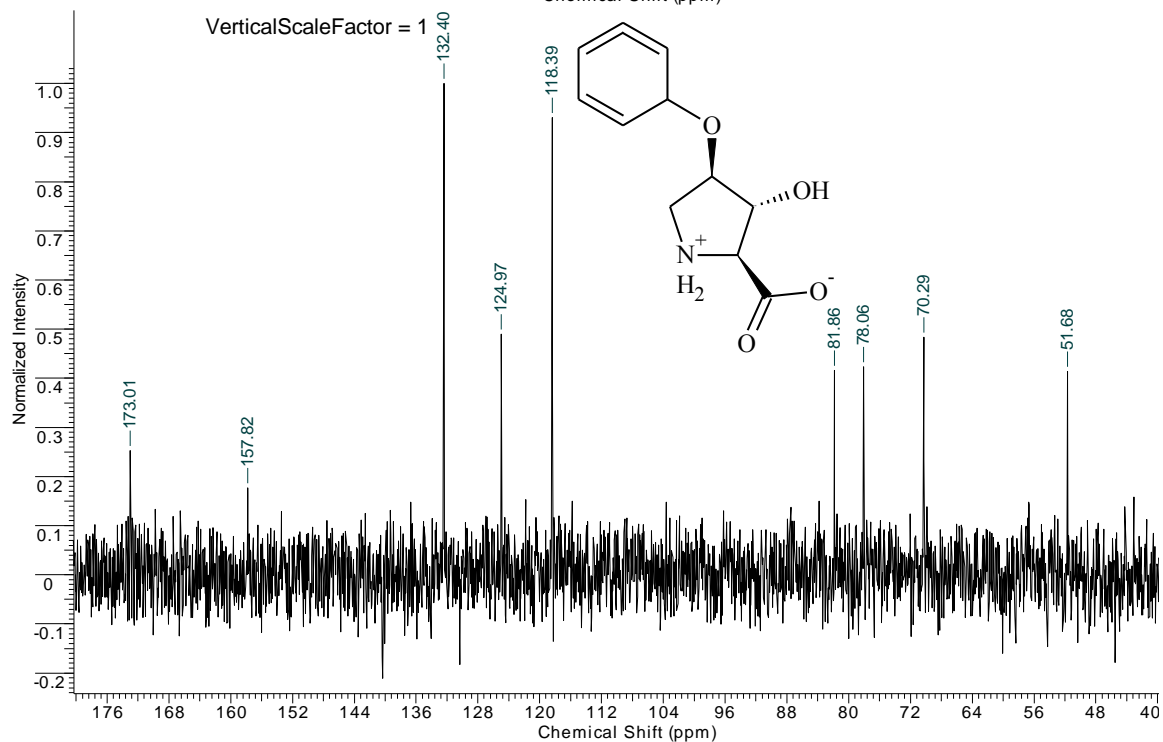
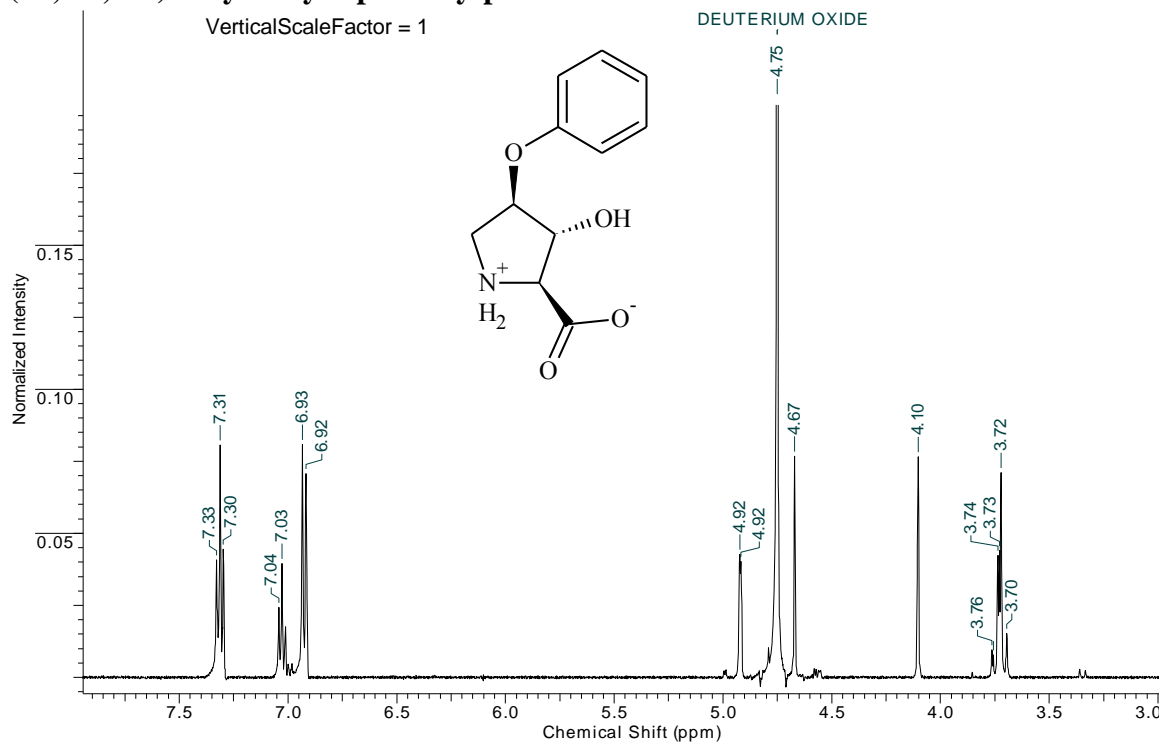


(2S, 3S, 4S)-3-phenoxy-4-hydroxy-proline



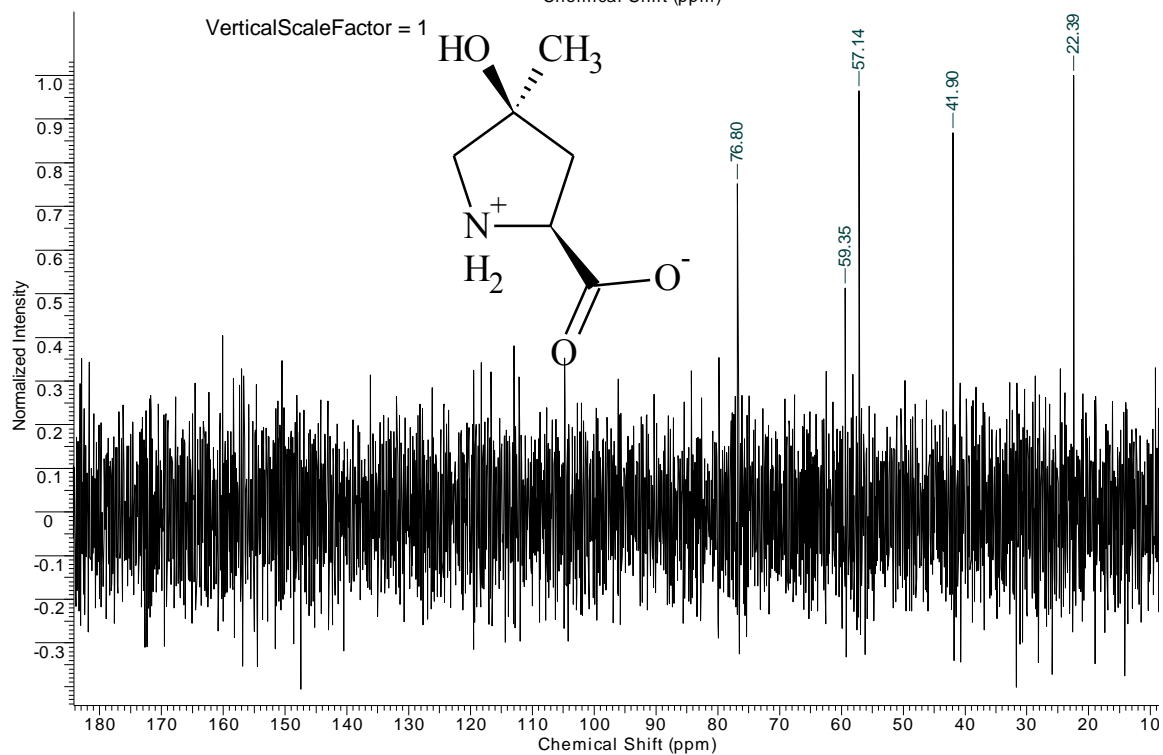
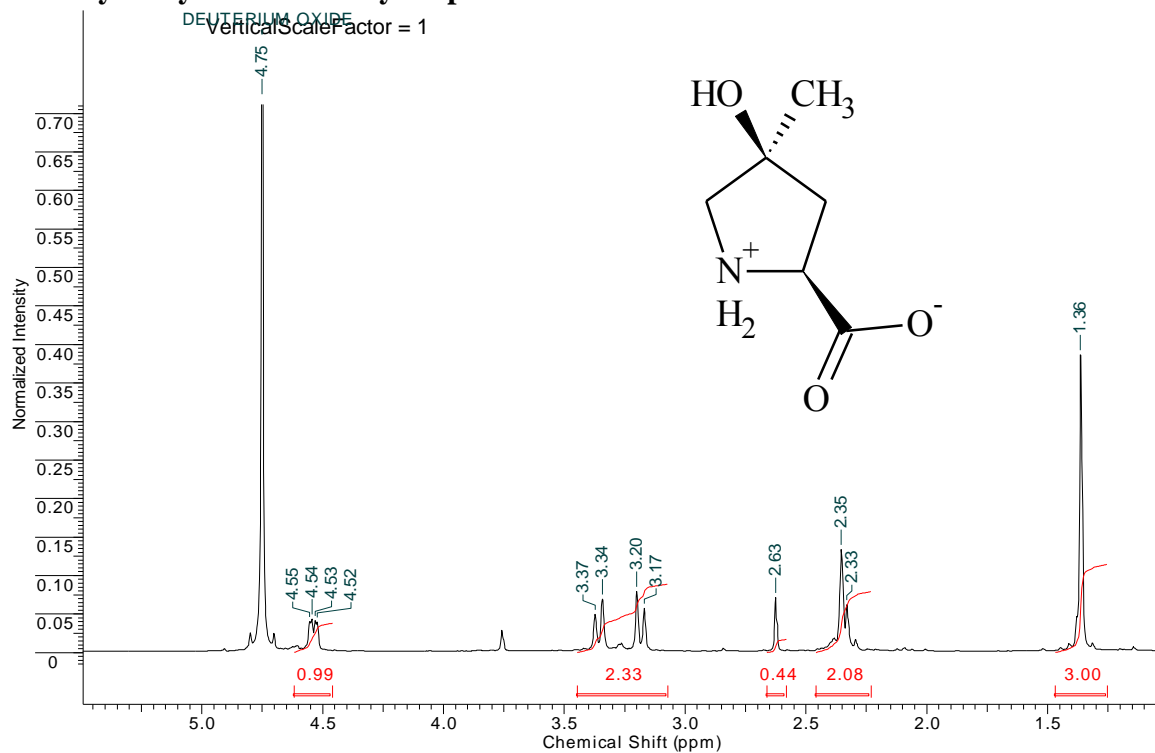
Appendix B: NMR spectra of hydroxy-L-proline derivatives

(2S, 3S, 4R)-3-hydroxy-4-phenoxy-proline



Appendix B: NMR spectra of hydroxy-L-proline derivatives

cis-4-hydroxy-trans-4-methyl-L-proline



Appendix B: NMR spectra of hydroxy-L-proline derivatives

cis-4-methyl-trans-4-hydroxy-L-proline

